THE UNIVERSITY OF CHICAGO

FURTHER CONTRIBUTIONS TO THE STUDY OF NEOCORTICAL ORIGINS: INPUT CELLS, IT CELLS, AND THE ALLIGATOR DORSAL TELENCEPHALON

A DISSERTATION SUBMITTED TO
THE FACULTY OF THE DIVISION OF THE BIOLOGICAL SCIENCES
AND THE PRITZKER SCHOOL OF MEDICINE
IN CANDIDACY FOR THE DEGREE OF
DOCTOR OF PHILOSOPHY

COMMITTEE ON DEVELOPMENT, REGENERATION, AND STEM CELL BIOLOGY

BY

STEVEN DANIEL BRISCOE

CHICAGO, ILLINOIS

DECEMBER 2017

Copyright © 2017 by Steven D. Briscoe

All rights reserved

TABLE OF CONTENTS

LIST OF FIGURES

CHAPTER 5

LIST OF TABLES

ACKNOWLEDGEMENTS

I first thank my thesis advisor, Cliff Ragsdale, for his mentorship and guidance. His vast scholarship, rigorous scientific approach, and knack for identifying interesting questions have considerably shaped my own intellectual development. I am thankful for the opportunity he provided for me to explore my interests in comparative neuroscience.

I thank members of my thesis committee: Elizabeth Grove, Chip Ferguson, and Robert Ho. Thank you for your expertise, suggestions, and encouragement.

I am grateful for members of the Ragsdale lab past and present, including Jennifer Dugas-Ford, Joanna Rowell, Carrie Albertin, and Yan Wang. Jennifer and Joanna performed the excellent comparative studies that laid the foundation for my thesis research. I especially thank Joanna and Carrie for crucial early contributions to my project. Without their generous help, this thesis, at least in its present form, would not exist. I also thank Stavroula Assimacopoulos for years of invaluable technical assistance, reagents, and advice.

I thank my parents Dan and Dana Briscoe, for raising a difficult little scientist who preferred to question everything. Thanks for letting me run rampant through the Island Lake wilds collecting frogs, salamanders, and turtles. Thanks for encouraging my curiosity and for always prodding me onto the right path when I was discouraged or astray.

I thank my wife, the incomparable Tanya “TanTan” Shpigel. Thanks for supporting me through the strenuous weeks of writing this thesis (and for fixing it!). Thanks for believing in me, for joining me on our alligator adventure, and for all of the adventures to come.

ABSTRACT

The six-layered neocortex is a neuroanatomical hallmark of all extant mammals. The massively enlarged human neocortex is thought to be largely responsible for the cognitive and behavioral abilities that set us apart from other animals. The evolution of this important structure is thus an enduring source of interest for neuroscientists and nonscientists alike. The brains of reptiles and birds, the closest living relatives of mammals, completely lack a morphologically defined neocortex. It has therefore been extremely challenging to determine whether reptiles and birds possess any brain structures that share an evolutionary relationship with the neocortex through common descent with modification.

Harvey Karten first proposed that the dorsal telencephalon (DT) of reptiles and birds contains cells homologous to neocortical neurons found in particular layers. These conserved cell types include "input" cells found in neocortical layer 4 (L4) and "output" cells located in neocortical L5. In birds, these cells are found in clustered neuronal aggregates, or nuclei, that bear little morphological resemblance to neocortical layers. The Ragsdale laboratory previously tested Karten's cell-type homology hypothesis in comparative molecular studies. They found that the input and output cells of mammals, birds, and reptiles share specific expression of molecular marker genes. These findings support the hypothesis of cell-type homology and suggest that the last common ancestor of amniotes had input and output cells in its DT. Over evolutionary time, these cell types were reorganized into very different structures in extant amniote groups.

I took advantage of the unique nuclear morphology of avian DT for an unbiased, forward RNAseq search for genes that are conserved across amniote DT cell types. For these experiments, embryonic day 14 tissue from seven distinct districts was harvested from the DT of the chicken (*Gallus gallus*). I first sought to identify novel marker genes for avian DT input

nuclei. Markers specific to input nuclei were tested for conservation in mouse neocortical L4. In addition to the previously known gene *RORB*, three additional transcription factors—*RORA, NR0B1,* and *SATB1*—were found to be enriched in avian DT input nuclei as well as in mouse neocortical L4. In contrast, almost all non-transcription factor molecules were found to be divergent in their expression patterns. These results strengthen the case for homology of DT input cells and identify a candidate gene regulatory network for DT input cell identity. In contrast, the extensive molecular expression differences between chick and mouse DT input territories may contribute to the massive divergence in their DT architectures.

Guided by the observation that transcription factor genes are likely to be conserved at the cell-type level, I tested whether the avian mesopallium, an enigmatic DT structure, shares homology with any cell population in mammalian neocortex. Five transcription factor genes were identified that are highly enriched in both the chicken mesopallium and mouse neocortical intratelencephalic (IT) neurons, cell populations that were known to share extensive connectional similarities. I propose the novel hypothesis that IT cells are ancestral to amniotes and function in a conserved circuitry with input and output cells.

These molecular findings on input cells and IT cells were extended to a reptile, the American alligator (*Alligator mississippiensis*). Transcription factor marker genes for input and IT cells were found to be expressed in both the crocodilian dorsal ventricular ridge and the cerebral cortex. I identified a clear reptilian mesopallium. The surprising finding that neocortical cell-type homologs are organized into neocortex-like layers in the alligator dorsal cortex indicates a previously unappreciated cellular and architectural complexity to reptile cerebral cortex.

CHAPTER 1

The neocortex quandary

INTRODUCTION

The neocortex is by far the largest structure in the human brain. The massive, intricately folded human neocortex expands over and completely dominates all subcortical structures (Figure 1.1, Ncx). To most nonspecialists, the neocortex may as well be synonymous with the "human brain." The neocortex is necessary for all human-specific cognitive and behavioral abilities including language, problem solving, and fine motor control. It is roughly three times larger than the neocortex of chimpanzees, our closest nonhuman relatives (Blinkov and Glezer 1968, Stephan et al. 1981). With around 16 billion neurons (Herculano-Houzel et al. 2015, Herculano-Houzel 2016), 176,000 kilometers of myelinated axons (Marner et al. 2003), and up to a quadrillion synapses (Silbereis et al. 2016, Sousa et al. 2017), the human neocortex is among the most complex anatomical entities known in biology. Somehow, and over a great period of time, this remarkable computational device that harbors our perceptions, emotions, and ambitions arose through the purely mechanistic means of evolution by natural and sexual selection (Darwin 1859, Darwin 1871).

The evolutionary origin of the neocortex is the longest standing and most controversial problem in evolutionary neuroscience (Striedter 2005, Dugas-Ford and Ragsdale 2015). A neocortex is present in the brain of every extant mammal and appears to have essentially the same fundamental six-layered architecture. We must look outside of mammals to the brains of birds and other reptiles to understand how the neocortex arose. Unfortunately, the corresponding part of the brain in nonmammals is completely divergent in its morphology. To make matters even more difficult, we cannot assume that the structures present in any nonmammalian brain are

primitive. In other words, we cannot assume that mammals evolved from animals with a reptile-like or bird-like brain organization. Rather, all living animals are perched at the tips of branches on the tree of life. The intermediate forms connecting them, the animals within the branches, are gone with no fossil traces of their internal brain organizations. The only available course of action is to compare the brains of extant animals to identity shared features and then infer the contents and structure of the brain in their last common ancestor.

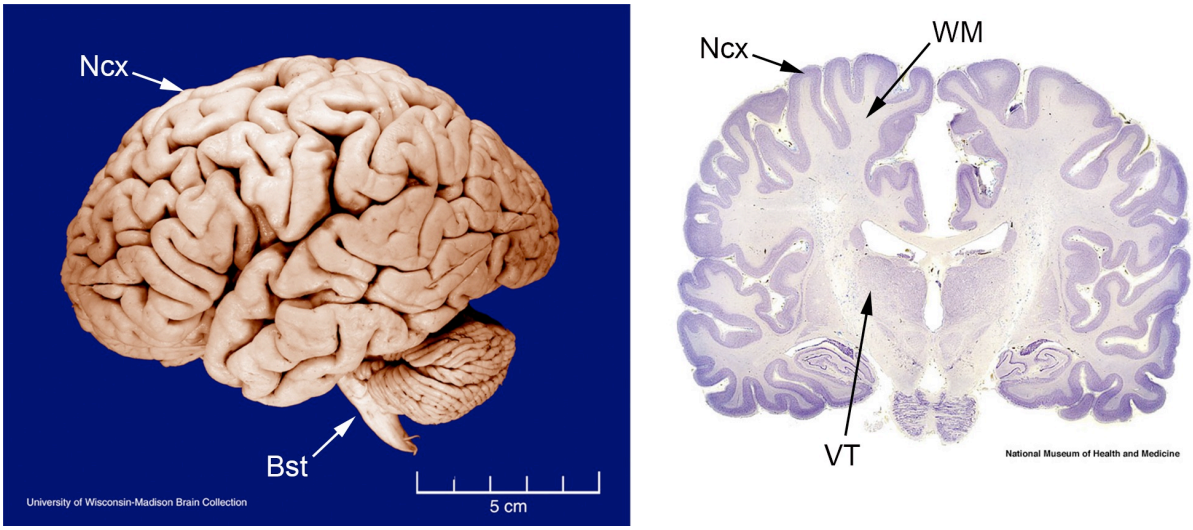

Figure 1.1 The human neocortex
The neocortex is the largest part of the human brain. Left: Lateral view of a whole human brain. Anterior is to the left. Right: Coronal cross section through the human brain. Neurons of the neocortex are contained in the outer, blue-stained "rind" of the brain. The internal white matter contains mostly axonal projections. The neocortex engulfs most other brain parts, excluding the cerebellum and the base of the brainstem. Images modified from www.brainmuseum.org. Abbreviations: Bst, brainstem; Ncx, neocortex; VT, ventral telencephalon; WM, white matter.

Comparative anatomy of the amniote dorsal telencephalon

If we want to find homologs of the neocortex in nonmammals, how do we know where to look? We know not to look in the legs, or in the gut, but rather somewhere in the brain. However, if nothing in the nonmammalian brain resembles the neocortex, selecting the right components for comparison is a nontrivial challenge. In fact, this very challenge is at the heart of debate on neocortex evolution. The problem of selecting components for comparison will be

discussed in more depth in Chapter 6. I begin by considering the embryonic origins of brain structures. The process of vertebrate nervous system developmental regionalization is highly conserved and the recognition of shared embryonic divisions across species forms the basis of comparisons of adult structures, such as the neocortex (Nieuwenhuys et al. 1998).

A brief summary of vertebrate nervous system development

The vertebrate central nervous system develops along the dorsal side of the animal (Kandel 2013, Gilbert and Barresi 2016). Neural tissue is first specified from ectoderm, early in embryogenesis, to produce the neural plate. The neural plate folds up and seals at its dorsal margins to form a hollow neural tube. The internal cavity of the neural tube persists into adulthood as the ventricular system of the brain. Three primary brain vesicles form at the anterior end of the neural tube: the prosencephalon (forebrain), mesencephalon (midbrain), and rhombencephalon (hindbrain). These three primary vesicles together form the brain, while the posterior neural tube gives rise to the spinal cord. Two secondary brain vesicles, the telencephala, bulge out from either side of the prosencephalon. Each telencephalon gives rise to a cerebral hemisphere with a dorsal and ventral division. The mammalian neocortex is a dorsal telencephalon derivative.

The neocortex is a cortex, which is defined by neuroanatomists as a multilayered neuronal structure at the surface of the brain (Nauta and Feirtag 1986). Within a cortex, the principal neurons possess an apical dendrite that points to the brain surface and spans the cortical layers in order to interact with different cell and axon populations. Cortices usually have an outer molecular layer, or a layer consisting primarily of axons, dendrites, and synapses. There are multiple types of cortex in most vertebrate brains, including the cerebellum, optic tectum, hippocampus, olfactory cortex, and olfactory bulb (Nieuwenhuys et al. 1998, Butler and Hodos

2005). The neocortex is defined as a six-layered cortex in the dorsal telencephalon (DT) and, by this definition, only mammals have a neocortex (Figure 1.2a, nctx). Nonmammals have a DT and if they possess neocortical homologs we should expect to find them in the adult territories derived from the DT.

The mammalian neocortex, the reptile dorsal cortex, the avian Wulst, and the DVR

The most important structural and organizational features of the mammalian neocortex are its tangential divisions into areas and its stacked cellular layers. The ability of the neocortex to process information depends largely on these properties. Neocortical areas, for instance, are organized into a complex hierarchy that allows sensory information to be processed and integrated in stages (Nieuwenhuys et al. 2008). Peripheral sensory information is first targeted to primary sensory areas after relays in the dorsal thalamus: visual information to primary visual cortex in the posterior pole of the occipital lobe, auditory information to primary auditory cortex in the temporal lobe, and somatosensory information to primary somatosensory cortex in the parietal lobe. Sensory information then proceeds to higher-order, or associational, areas in temporal, parietal, and frontal cortex. Highly processed information from frontal and other areas feeds into primary motor cortex, which executes volitional behaviors through its connections to motor neurons in the spinal cord.

Neocortical layers serve to organize the incoming and outgoing connections of areas. Layers are defined by the collection of neural cell types present, and every neocortical area has the same basic set of six cortical layers. However, there are substantial area-specific variations on layer properties. Sensory information from the thalamus enters the neocortex through synapses onto neurons in layer 4. These neurons send short axons to local-circuit and long-distance excitatory neurons in the upper layers, layers 2 and 3. These upper layer neurons can

send short axons down to layer 5, to other neocortical areas within the same hemisphere, or across the corpus callosum to the other cerebral hemisphere. Further complexities of upper layer and related neurons will be discussed in Chapter 4. Layer 5 neurons send long axons out of the telencephalon to brainstem and spinal cord, while layer 6 neurons project back to the thalamus. Layer 1 is the molecular layer. The primary sensory areas possess a highly developed layer 4 but a relatively small layer 5. Primary motor cortex, in contrast, has a reduced layer 4 but a thick layer 5 with massive motor output neurons.

The DT of reptiles and birds, our closest nonmammalian relatives, is organized quite differently from the mammalian neocortex. Reptiles have a DT cortex, though it contains only three layers and is therefore not a neocortex. The reptile cortex is usually referred to as the dorsal cortex (Figure 1.2b, dctx) (Ulinski 1990a). Below the dorsal cortex, the reptile DT contains a second, very different, structure called the dorsal ventricular ridge (DVR) (Figure 1.2b, DVR) (Ulinski 1983). The DVR does not contain cortical layers. Instead, neurons are typically distributed throughout the DVR and are packed into clusters referred to as nuclei. In some reptiles including turtles, the DVR forms a protrusion into the ventricle (Figure 1.2b).

Birds, as descendants of archosaur reptiles, possess a DT much more similar to the typical reptilian organization than to that of mammals. Birds have a large, cell-dense DVR that contains a number of nuclei (Figure 1.2c,d, DVR) (Reiner et al. 2004a). The mesopallium (Figure 1.2c, M), a dorsal division, is stacked atop an intermediate territory called the nidopallium (Figure 1.2d, N). The arcopallium, another large DVR territory, is located in posterior DVR (Figure 1.2d, A). Birds appear to have replaced the reptilian dorsal cortex with another nuclear territory, the Wulst (Figure 1.2c, W). This structure forms a bump on the dorsal DT surface; Wulst is the German translation for “bulge.”

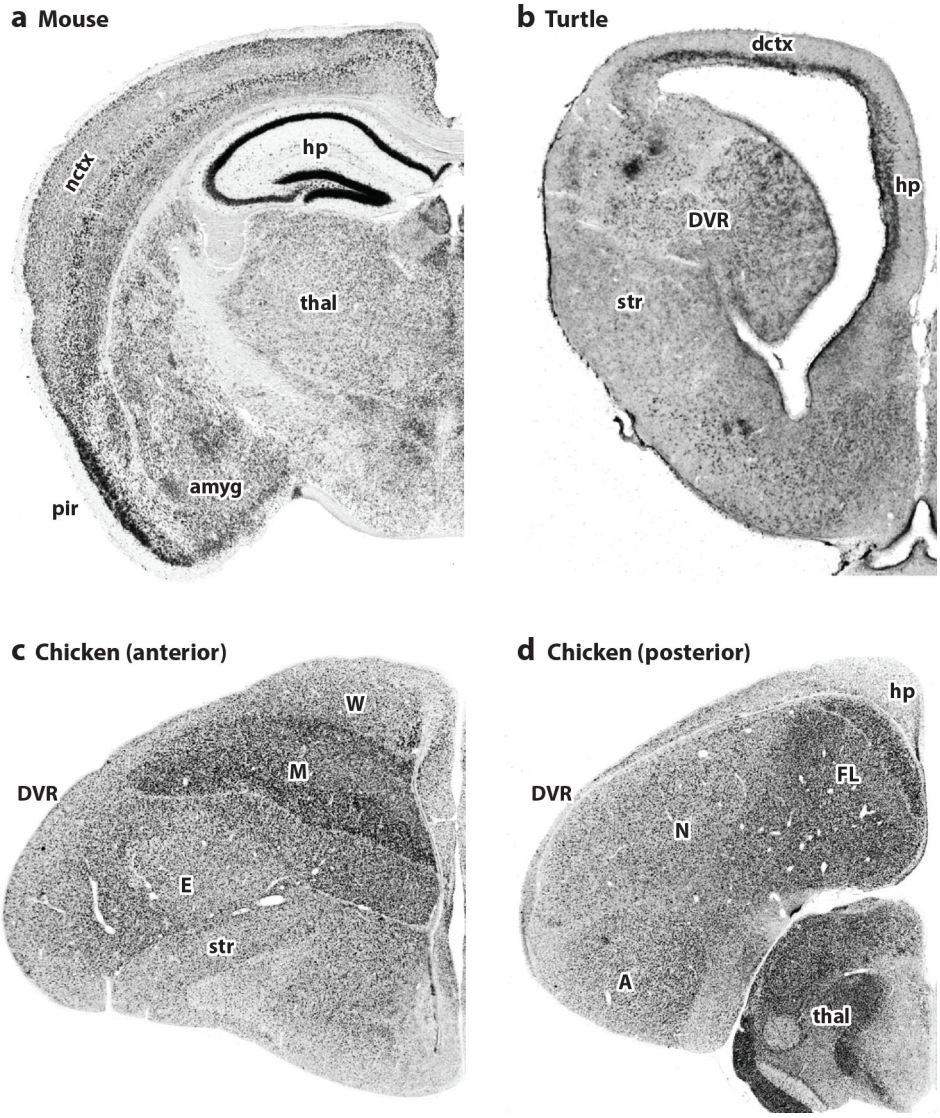

Figure 1.2 Comparative anatomy of the amniote telencephalon
Only mammals have a neocortex. Coronal cross sections through the brain of a mammal, reptile, and bird are shown. Medial is to the right. **(a)** Mouse telencephalon. The neocortex is a smooth, layered structure in mouse dorsal telencephalon. **(b)** Turtle telencephalon. Reptiles have a three-layered dorsal cortex and a DVR instead of a neocortex in their dorsal telencephalon. **(c)** Chicken telencephalon, anterior. Birds have a Wulst and a DVR instead of a neocortex in their dorsal telencephalon. **(d)** Chicken telencephalon, posterior. nctx, neocortex. pir, piriform cortex. amyg, amygdala. thal, thalamus. Abbreviations: hp, hippocampus; str, striatum; DVR, dorsal ventricular ridge; dctx, dorsal cortex; E, entopallium; M, mesopallium; W, Wulst; A, arcopallium; N, nidopallium; FL, Field L. Figure reproduced, with permission, from Dugas-Ford and Ragsdale 2015.

Even a cursory glance at the DT structures in mammals, non-avian reptiles, and birds (together, the amniotes) reveals that their organizations are greatly divergent. All of these

animals evolved from a common ancestor that lived approximately 320 million years ago. The amniote last common ancestor (LCA) had a DT with some set of neural cell types organized into unknown structures, and this DT was adapted into the very different morphologies present today. The nature of this process has stimulated a rich history of fervent debate (Edinger et al. 1899, Holmgren 1925, Ariëns Kappers et al. 1936, Karten 1969, Bruce and Neary 1995, Puelles 2001, Butler et al. 2011, Dugas-Ford et al. 2012).

Camps of researchers disagree on which features in the reptile DT and bird DT are homologous to which features of the mammalian neocortex. Some hold that the reptile dorsal cortex and avian Wulst are homologous as structures to the neocortex, while the DVR is homologous to nuclei in the mammalian claustrum and amygdala (Figure 1.2a, amyg) (Bruce and Neary 1995, Striedter 1997, Cheung et al. 2007, Puelles et al. 2016b). Others suggest that reptile dorsal cortex and avian Wulst are homologous as structures to dorsal neocortex, while DVR is homologous to lateral neocortex (Butler et al. 2011). Erich Jarvis and his collaborators suggested that layers of the mammalian neocortex are homologous to particular nuclei in both the avian Wulst and the DVR (Jarvis et al. 2013).

A more nuanced version of the layers-to-nuclei idea, originated by Harvey Karten (1969), proposes that classes of neocortical cell types are homologous as cell types to cells organized into nuclei in the Wulst and DVR (Karten 1969, Karten 1997, Dugas-Ford et al. 2012, Reiner 2013, Dugas-Ford and Ragsdale 2015, Karten 2015). This idea differs from the layers-to-nuclei idea of Jarvis et al. (2013) because although neocortical cell types are typically found in a particular layer, layers are highly heterogeneous structures containing multiple distinct cell types. The cell-type homology hypothesis will be explored throughout the remainder of this thesis. The

most prominent current alternative view, which compares the DVR to mammalian amygdala, will be assessed in Chapter 6.

This thesis is about cell-type homology, yet cell type is a deceptively difficult concept to define. Cells of the nervous system are incredibly complex entities with numerous properties by which one can potentially denote cell-type categories. These properties can include location in the nervous system, axon and dendrite morphology, physiological and firing properties, neurotransmitter usage, and other molecular traits. Some properties may be necessary to define a cell type, but they may not be sufficient because they are characteristic of multiple cell types. Indeed, it is debatable whether a cell type is a real thing at all, or only exists insofar as we define it. At the very least, a definition of cell type should be useful. It should not focus on transient cell type properties like state-dependent transcriptional profiles, but should rather rely on stable characteristics. I recognize cell types by properties that are not only ontologically stable, but are also stable across phylogeny. For dorsal telencephalon cell types, major connectional properties like input from thalamus and long-distance projections to brainstem targets are phylogenetically stable (Dugas-Ford et al. 2012, Dugas-Ford and Ragsdale 2015). As will be demonstrated in the following chapters, these connectional characteristics are accompanied by highly conserved transcription factor expression profiles.

The Karten hypothesis of cell-type homologies

The most well supported hypothesis of neocortex origins proposes a homology between specific classes of cell types found in both the mammalian neocortex and in the avian DT. Mammals and birds share striking similarities in the organization of four ascending sensory pathways to DT, despite the massive differences in DT gross morphology (Dugas-Ford and Ragsdale 2015). In mammals, two distinct visual pathways target separate neocortical areas: a

tectofugal channel that passes through the midbrain and a lemniscal channel that does not. These two pathways target the middle layer of the neocortex, layer 4 (L4), in the tectorecipient and primary visual cortices, respectively (Figure 1.3, V_T and V1 in mammals). An auditory sensory channel targets primary auditory cortex L4 (Figure 1.3, A1) and a somatosensory channel targets primary somatosensory cortex L4 (Figure 1.3, S1).

Decades of connectional studies from multiple groups have worked out the details of ascending sensory pathways in the avian brain (Reiner et al. 2004a). A lemniscal visual pathway targets the posterior interstitial nucleus of the hyperpallium apicale (IHA) in avian Wulst, while a tectofugal visual pathway targets the entopallium, a nucleus in the DVR (Figure 1.3, IHA post and E in birds) (Karten and Hodos 1970, Karten et al. 1973, Krutzfeldt and Wild 2004, Krutzfeldt and Wild 2005). An auditory pathway targets a separate DVR nucleus named Field L (Figure 1.3, Field L) (Karten 1968). Finally, a somatosensory pathway originating in spinal cord targets the anterior part of IHA (Figure 1.3, IHA ant) (Wild 1989, Wild 1997).

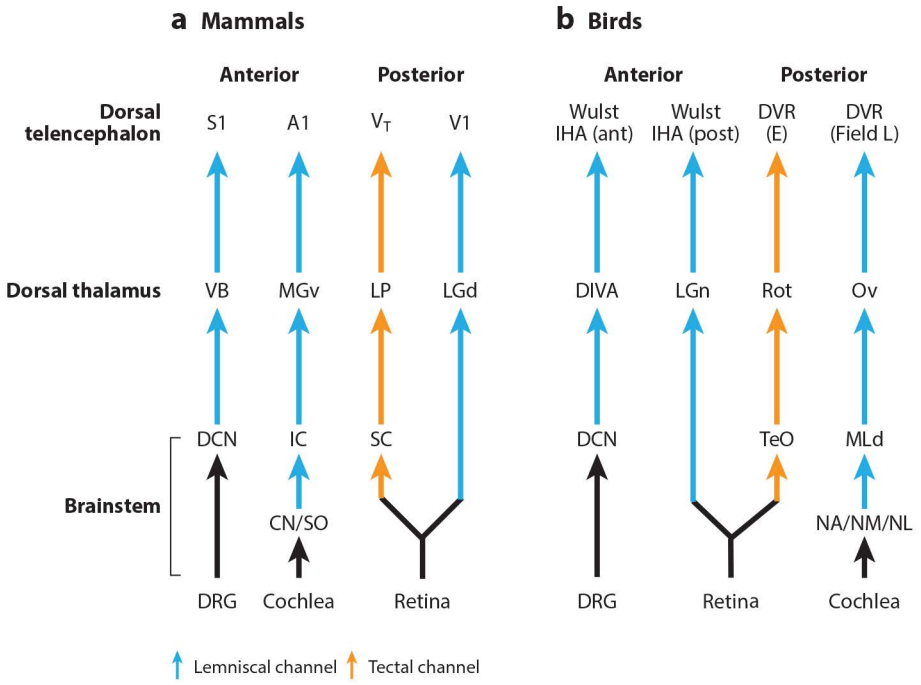

Figure 1.3 Ascending sensory pathways in mammals and birds
Unimodal sensory pathways to the dorsal telencephalon are strikingly similar across **(a)** mammals and **(b)** birds. In both groups, lemniscal (blue) visual, somatosensory, and auditory pathways target discrete DT territories. Both groups also share a tectofugal (orange) visual pathway distinct from the lemniscal visual pathway. The mammalian visual tectal channel contains two parallel streams: one passing through LP (or medial pulvinar), and the other through caudal pulvinar. Abbreviations: A1, primary auditory cortex; ant, anterior; CN, cochlear nuclei; DCN, dorsal column nuclei; DIVA, dorsal intermediate ventral anterior nucleus; DRG, dorsal root ganglia; DVR, dorsal ventricular ridge; E, entopallium; IC, inferior colliculus; IHA, interstitial part of the hyperpallium apicale; LGd, dorsal division of the lateral geniculate nucleus; LGn, lateral geniculate nucleus; LP, lateral posterior nucleus of the thalamus; MGv, ventral division of the medial geniculate nucleus; MLd, nucleus mesencephalicus lateralis, pars dorsalis; NA, nucleus angularis; NL, nucleus laminaris; NM, nucleus magnocellularis; Ov, nucleus ovoidalis; post, posterior; Rot, nucleus rotundus; S1, primary somatosensory cortex; SC, superior colliculus; SO, superior olive; TeO, optic tectum; V1, primary visual cortex; VB, ventrobasal nucleus of the thalamus; VT, tectorecipient visual cortex. Figure reproduced, with permission, from Dugas-Ford and Ragsdale 2015.

These four pathways are very similar in that they all include relays in the dorsal thalamus, and they all ultimately target spatially segregated cell populations in the mammalian neocortex or in the avian DT. The neuroanatomist Harvey Karten first noted that it would be unparsimonious to presume that these sensory pathways to DT had arisen independently in mammals and birds—it is much more likely that they were inherited from the amniote LCA, in

which they were already developed. The proposed homology of the ascending sensory pathways to DT has been referred to as the weak Karten hypothesis (Dugas-Ford and Ragsdale 2015). Karten went a crucial step further and suggested that not only are the sensory channels homologous, but the DT cell types that receive sensory input from thalamus are homologous at the cell-type level (Karten 1969). Specifically, Karten proposed that the sensory "input" cells located in L4 of primary sensory neocortical areas are homologous, as cell types, to the input cells located in the avian IHA, entopallium, and Field L—the strong Karten hypothesis (Dugas-Ford and Ragsdale 2015).

This idea was soon expanded to include homology of another major DT cell type, the brainstem-projecting "output" cells. Neurons located in both the avian hyperpallium apicale (HA, in the Wulst) and the arcopallium (in the DVR) were discovered that extend long axons to motor-related nuclei in the brainstem (Zeier and Karten 1971, Wild and Williams 2000). Karten proposed that the avian DT output cells are homologous to the mammalian output neurons located in neocortical L5.

The Karten hypothesis of cell-type homologies was based on just one character trait of neurons: their fiber connections. As such, other authors frequently dismissed the connectional similarities as convergence. Instead, these authors emphasized that the location and the nuclear architecture of the avian DVR indicates homology to the mammalian amygdala (Striedter 1997, Puelles 2001, Striedter 2005). More types of evidence are necessary to resolve these different interpretations of homology. If input and output cells are homologous, they may share additional conserved character features. In particular, input and output cells may share expression of cell-type-specific genes necessary for their development, function, and identity.

The Ragsdale laboratory tested this prediction with comparative molecular studies. They first identified from the literature neocortex L4/input and L5/output marker genes conserved across mammals (Rowell et al. 2010), then tested where avian orthologs of these genes are expressed in DT. The conserved neocortical L4 markers *KCHN5* and *RORB* were found to be highly enriched in avian IHA, E, and Field L, as predicted by the Karten hypothesis (Dugas-Ford et al. 2012) (Figure 1.4a–d). Conserved L5 markers, including *ER81* (*ETV1*) and *PCP4,* were found to be expressed in the avian output nuclei HA and arcopallium (Figure 1.4e–h) (Dugas-Ford et al. 2012). If character features are conserved across mammals and birds, the same features should be present in reptiles. Input cell markers were found in anterior, visual-recipient turtle dorsal cortex, while output cell markers were found in posterior turtle dorsal cortex. These gene expression data provided compelling support for Karten's cell-type homology hypothesis.

The connectional and gene expression data together support a model in which the amniote LCA had input and output cells located in its DT (Figure 1.5). Input cells received unimodal ascending sensory information from dorsal thalamus and they expressed *KCNH5* and *RORB*. Output cells sent projections to the brainstem and expressed at least six conserved output neuron marker genes (Dugas-Ford et al. 2012). Over evolutionary time, these cell types independently came to be organized into neocortical layers in mammals, cortical fields in turtles, and nuclei of the avian Wulst and DVR.

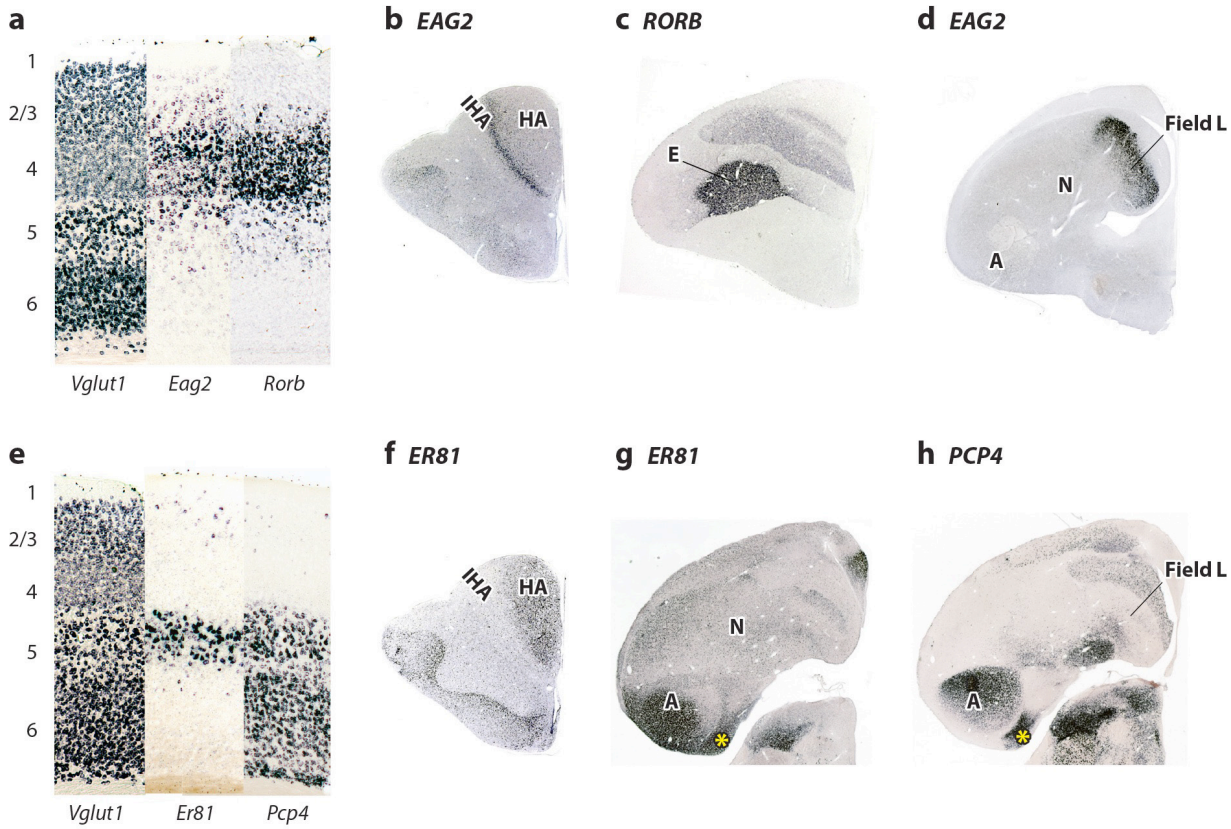

Figure 1.4 A molecular test of the cell-type homology hypothesis
Gene expression evidence strongly supports homology of DT input and output cells. Molecular markers of neocortex layer 4 input cells, **(a)** *Eag2* and *Rorb*, are strongly expressed in avian input nuclei **(b)** IHA, **(c)** entopallium, and **(d)** Field L. Molecular markers of neocortical deep layer output neurons, including **(e)** *Er81* (or *Etv1*) and *Pcp4*, are expressed in the avian output nuclei **(f)** HA and **(g, h)** arcopallium. Abbreviations: HA, hyperpallium apicale; IHA, interstitial nucleus of the hyperpallium apicale; E, entopallium; A, arcopallium. N, nidopallium. Figure reproduced, with permission, from Dugas-Ford and Ragsdale 2015.

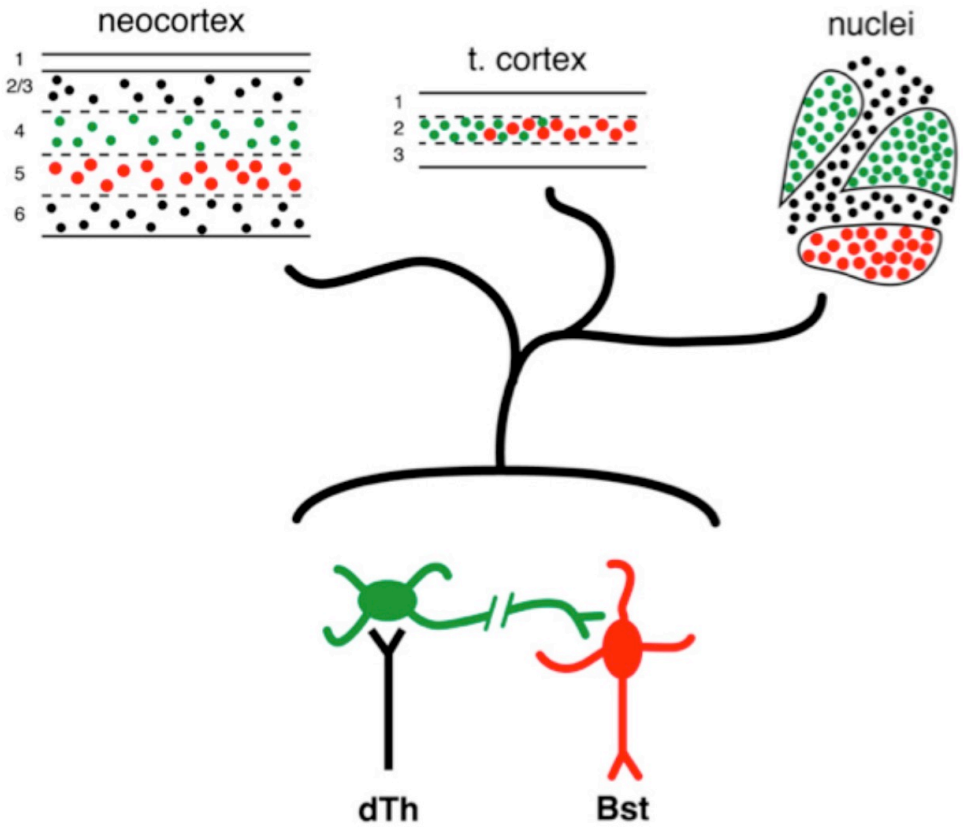

Figure 1.5 Evolution of neocortical input and output cells
The last common ancestor of amniotes had input (green) and output (red) cells in its dorsal telencephalon. Input cells received sensory information from the dorsal thalamus (dTh), while output cells extended axons out of the telencephalon to brainstem (Bst) targets. Input and output cells are organized into cortical layers in mammalian neocortex, are partially segregated into cortical fields in the turtle dorsal cortex, and are clustered into nuclei in the avian Wulst and DVR. Figure reproduced, with permission, from Dugas-Ford et al. 2012.

AIMS AND RESULTS

Homology of amniote DT input cells is supported by similarities in ascending sensory pathways as well as the conserved expression of two input cell-specific marker genes. Commentaries following the demonstration of conserved marker gene expression argued, however implausibly, that these similarities can (still) be explained by convergent evolution (Belgard et al. 2013, Medina et al. 2013, Puelles et al. 2016b). While I disagree with this

conclusion, an argument for homology of amniote DT input cells would certainly be strengthened by the identification of additional conserved input marker genes (Rowell 2013).

The mammalian L4 marker genes *Kcnh5* and *Rorb* were identified serendipitously and then studied in birds. To expand upon these findings, I performed an unbiased forward search for novel input cell marker genes using an RNA sequencing approach (Chapter 3). I first sought to identify all transcripts selectively enriched in late-embryonic chicken DT input nuclei. Next, I tested whether mouse orthologs of chicken input marker genes are expressed in the neocortex. Marker genes expressed in mouse neocortical L4, as well as in chicken DT input nuclei, are most parsimoniously interpreted as conserved features. Three novel, conserved input cell transcription factors were identified—*RORA, NR0B1,* and *SATB1*—which provide additional support for Karten's cell-type homology hypothesis. In contrast, and perhaps unsurprisingly, I found that nearly all non-transcription factor genes isolated were highly divergent in their expression patterns across mammals and birds. As I will discuss, these findings are fully consistent with cell-type homology and with emerging views on the nature of cell-type evolution in metazoans.

The mammalian neocortex and the avian DT contain many cell populations in addition to input and output cells. The evolutionary origins and relationships of these cell types are unknown. In particular, the avian DVR contains two vast territories, the nidopallium and the mesopallium, which are neither input nor output in their connectivity (Chapter 4). Instead, they form associational connections within the telencephalon and are implicated in avian cognitive abilities (Atoji and Wild 2009, Atoji and Wild 2012). I applied the lessons from the input cell comparative study to test whether mesopallium and nidopallium are homologous to any cell populations in the neocortex. I used an RNA sequencing approach to identify transcription factors selectively enriched in the mesopallium and nidopallium. Six mesopallium-enriched

transcription factors were identified, and five of these were expressed in the mammalian neocortex. These gene expression data suggest that neocortical intratelencephalic (IT) neurons—which are neither input nor output, but instead form connections within the telencephalon—are homologous at the cell-type level to the avian mesopallium. This finding leads to the conclusion that a third core DT cell type, the IT cell, was present in the amniote LCA. By contrast, my data suggest that the bulk of the nidopallium is a major nonmammalian DT innovation with little similarity to any neocortical structure or cell type.

Reptiles are a diverse and evolutionarily important group whose brains remain underexplored using modern molecular techniques. Our understanding of the molecular organization of reptile DT lags well behind that of mammals and birds, as there has not been a detailed molecular study of any reptile brain. I chose the American alligator, *Alligator mississippiensis*, as a model reptile species (Chapter 5). The alligator is exquisitely suited to comparative studies for several reasons. Crocodilians are the closest living relatives to birds and possess a large DVR. Ascending sensory pathways to the crocodilian DT are well described by the tracing studies of Michael Pritz (Pritz 1974b, Pritz 1975, Pritz and Northcutt 1977, Pritz and Northcutt 1980). Alligators are therefore an attractive reptile outgroup for the input cell study. I found that four input cell-specific markers are expressed in the previously described alligator input cell nuclei, affirming the predictive value of the cell-type homology hypothesis. In addition, I identified a crocodilian DVR mesopallium based on the selective expression of five IT- and mesopallium-specific transcription factors. Alligators are likely to be of great interest for future comparative studies of the vertebrate brain.

The comparative molecular studies presented in Chapters 3, 4, and 5 strengthen the homology argument for input cells and introduce a new conserved DT cell type, the IT neuron.

An important future research direction is to identify the molecular and developmental mechanisms that differentially organize conserved DT cell types in mammals, reptiles, and birds. In Chapter 6, I present a model of the evolutionary transformations underlying extant amniote DT organizations. Specifically, I propose a model for the structure of the DT in the amniote LCA and describe how this ancestral DT may have been adapted into the neocortex, DVR, dorsal cortex, and Wulst. Finally, I argue that the dorsal telencephala of mammals, reptiles, and birds represent distinct "DT types" that differ substantially in their developmental construction. The DT types may have arisen to meet the changing behavioral needs of amniote ancestors amidst great evolutionary transitions.

CHAPTER 2

Materials and methods

Animals

Embryonic and postnatal CD-1 mice (*Mus musculus*) were provided by the University of Chicago Transgenic Facility. Postnatal day zero (P0) begins on the day of birth.

Embryonic and hatchling chickens were raised from fertilized White Leghorn chicken (*Gallus gallus*) eggs purchased from Sunnyside Hatchery (Beaver Dam, Wisconsin). These eggs were incubated at 38°C with 90% relative humidity in a Model 1502 circulated air incubator (GQF Manufacturing Company, Savannah, Georgia). Eggs were manually rotated 180° three times per day for the first four days of incubation to promote viability. Embryonic day zero (E0) begins at the start of incubation, post-hatching day zero (P0) on the day of hatching.

Adult, wild-caught starlings (*Sturnus vulgaris*) were provided by the laboratory of D. Margoliash at the University of Chicago.

Adult red-eared slider turtles (*Trachemys scripta elegans*) were purchased from Kons Scientific (Germantown, Wisconsin).

Fertilized alligator (*Alligator mississippiensis*) eggs were provided by Ruth Elsey and colleagues at the Rockefeller Wildlife Refuge (Grand Chenier, Louisiana). Alligator eggs were transported by car in maternally provided nesting material in moistened, perforated Styrofoam boxes. Eggs were subsequently transferred to the GQF incubator where they were incubated at 30°C and 90% relative humidity. Embryos were staged according to the criteria of Ferguson (Ferguson 1985). I only studied stage 25 animals, which are defined as resembling “a miniature version of a hatchling, with a considerable volume of external yolk and a large umbilical region”

(Ferguson 1985). Stage 25 typically corresponds to sixty days after egg laying and one week before hatching.

The sex of the chickens, starlings, turtles, and alligators was not determined.

All animal procedures were reviewed and approved by the University of Chicago Institutional Animal Care and Use Committee (IACUC).

Tissue collection and preparation

Gravid mice were sacrificed by carbon dioxide inhalation followed by cervical dislocation prior to the collection of embryos. Harvested mouse embryos were dissected in phosphate-buffered saline (PBS) (Sigma-Aldrich) and fixed by immersion in 4% paraformaldehyde in PBS (PFA) (Sigma-Aldrich) at 4°C. Postnatal mice were anesthetized with a lethal overdose of pentobarbital (120 mg/kg) delivered as Euthasol, and perfused transcardially with 5–10 mL of PFA.

Embryonic chicken brains up to E14 and stage 25 alligator brains were collected by decapitation, dissection, and immersion fixation in 4°C PFA. Late embryonic and hatchling chickens, adult starlings, and adult turtles were anesthetized with Euthasol deeply and perfused prior to tissue collection.

I established that brain tissue can remain in PFA at 4°C for up to a year without obvious effects on in situ hybridization signal strength. All fixed brain tissue was cryogenically protected by equilibration in 30% sucrose/PBS (without paraformaldehyde) overnight at 4°C before sectioning. Sucrose-saturated brains were mounted on a freezing sledge microtome (Leica SM2000R) and sections were cut at a thickness of 20–24 microns. Sections were collected in diethyl pyrocarbonate (DEPC, Sigma-Aldrich) treated PBS (D-PBS). They were then mounted onto Superfrost Plus slides (Fisher Scientific) and dried for 20 minutes at room temperature in a

fume hood before further processing for in situ hybridization. Whenever possible, tissue was sliced, mounted, and processed in a single day for maximal in situ hybridization signal.

cDNA preparation

Dissected brain tissue of all species was flash-frozen on dry ice and stored at −80°C, or was used immediately for RNA extraction. Tissue was homogenized with a pestle and RNA was extracted with Trizol Reagent (Invitrogen) following manufacturer instructions. RNA was either stored at −80°C in RNase-free water (Sigma) or used immediately for cDNA synthesis using the SuperScript III 1st strand cDNA kit (Fisher Scientific) following manufacturer instructions. cDNA was diluted in RNase-free water and stored at −20°C.

Molecular cloning

For all species examined, EST sequence was readily available from the National Center for Biotechnology Information (NCBI). I designed polymerase chain reaction (PCR) primers using deposited sequence and Primer3 online software (bioinfo.ut.ee/primer3-0.4.0/). When possible, I selected primers yielding a product of 1000–1200 nucleotides from predicted protein coding regions. PCR reaction mixtures comprised standard reagents and concentrations (1x polymerase buffer, 0.75mM $MgCl_2$, 200 μM dNTP, 0.2 μM primers, 1.25 units Taq DNA polymerase per 50 μL solution). PCR reactions were performed using a RoboCycler Gradient 40 (Stratagene). Reaction solutions were initially heated to 94°C for 5 minutes, followed by 40 cycles of 94°C for 1 minute, 50–55°C for 1 minute, and 72°C for 1 minute per kilobase of product length. A final elongation step was performed at 72°C for 10 minutes. 53°C was most frequently used as the annealing temperature, but it was varied slightly to 50°C or 55°C as needed. PCR product length was estimated by running 5 μl of the 50 μl reaction solution on a 1%

agarose gel alongside a DNA ladder. When necessary, target DNA bands were gel-purified using a Zymoclean Gel DNA Recovery Kit (Zymo Research). PCR products were ligated into the pGEM-T Easy Vector (Promega) for 1–7 days at 4°C then transformed into DH5α competent cells at 42°C for 30 seconds. Transformed cells were plated on ampicillin-positive LB agar plates with X-Gal (Goldbio) for blue/white selection and incubated overnight at 37°C. Plates were then stored at 4°C for 1–4 days to allow for any blue-colored colonies to darken. White colonies were picked and miniprepped using PureLink Quick Plasmid DNA Miniprep Kits (Invitrogen). Plasmids were sequenced with a T7 primer at the on-campus UC Comprehensive Cancer Center DNA Sequencing Facility. cDNA sequences were analyzed using BLAST (NCBI) and annotated using A Plasmid Editor software (ApE, M. Wayne Davis). Plasmids with the intended cDNA targets were stored at −20°C. Primers used for cDNA synthesis are described in Tables 2.1–2.5. In these tables, the forward primer is listed above the reverse primer for each gene.

Table 2.1 PCR primers for chicken cDNA isolation

Chicken cDNAs	Forward Primer	Reverse Primer
ABLIM2	ACAGATTAGATGGCAACACG	TATTGATAGAGCACACCAAGC
ADARB2	TTCACTTCCTCTACTCACAGC	CAGCGATAAACTATGACAAGC
ADPRHL1	TCACAGATTACTGGTGTTTGG	CCTTTCAGACTAACTCTCAGC
ALDH1A2	GGCAGTTCTTGCTACTATGG	TGCTCTTCTGCACTATGTGG
ANKFN1	GATCTGAAGTGGGTACTTAGG	TTCTCTGACATGATTTAGCC
ANOS1	AGCTGATAGTGAATGTTCTGG	GTCCAGTGATGTTACCTTCC
ANTXR1	AAACCAAGAAACAGAAGTGC	ACAACCTGAAATGACTCTCC
ASTN2	CCCTTTACTATCAGATCAATGC	CTCGTCATACTTGATGTCTCC
BCAS1	AGGAGATAGATGACTGCAACC	CACTTCCTTACCTTACATACCC
BCL11A	GTAAAGAAGAGCCCAGCAGC	CACTCTTGAACTTGGCCACC
BCL11B	(from J. Dugas-Ford)	
BET3L	ACGGTATAACCTGACACATACG	GCATATCTTACCATCCATGC
BETA-KERATIN	GATCCAACTCCATTCCTAGAC	ATAGCAGGGGAAGATTTACAC
BHLHE40	AGGATACCGAACTGAAATACG	ACAACACAGAATAGGGAAAGG
BRINP2	ATATGGGACACACTTCTTGC	CGTAGTAGATTGTCTCGTTGG
BTBD11	GAGGAAGAGTACACAGAAGAGC	GGCAAGATTATACCACTTTAGG

Table 2.1, continued

Chicken cDNAs	Forward Primer	Reverse Primer
C11ORF87	TCTCTTAACCCTGTCTTACCC	AATTCGTAGCTTCTCACACC
C14ORF79	TGAGTGTTCTGGAATAGATGC	CATTGACTCTACCTGTCTTACC
C19ORF35	TCACCTTTAGGAAAGAACAGC	TATGGCATGTAAAGAGTCTGG
CASQ1	TGAGATGATTGAGTACGATGG	ACATCTTCGATCCACTCCTC
CDH6	GAACTTACCATTGCTTCTGG	CTGTGTGTCCTTGTCTGTGG
CHL1	CATACACCAATTACCAGTTCC	CACACATCAGTCCAATAAACC
CHN2	GAACAGACCAAAGTATTACGG	ACTTGGAATAGGTGTCATAGG
CHRM5	ATGAACCTCTTAGTCATCAGC	CACATAGCATAGCCAATATCC
CPNE7	CTCAAATATGGGAAGTTTGC	ATCAGCAGGATGAAGTATTGC
CPNE9	ATGGACACCTTCTCCAAGTC	TTGTTGTTCAGAGGGAACTG
CRABP1	ACCTGGAAGATGAGGAGCAG	CCATTGCAAATGACAACTAC
CRHBP	AGGAGAGAAGTTTCCTAGTTCC	CACACTAACATTGGATTTCCTC
CTGF	GAGGAGAACATCAAGAAAGG	ACCAAAGCATTACACATAGGC
CUX1	(from J. Rowell)	
DACH1	GCTATGTCCAACTACCATGC	CCTGAGACTATCTGTTGAAGC
DACH2	GAACCACCTCAATACAATAGC	CATGCTACAAATCCTGTTCC
DCBLD1	CTCTCTGCTGTTCTCTCTGC	CTCTGTATGTTCTCCATTTCG
DIRAS2	ACTTTCAGAGAGAGCTACATCC	GGATACAAACTTCAGTCATTCC
DISP2	GTATGGAGGAATGTAGAGAGC	GAAGTAGGTGAATCTGAAGG
DRD5	ACAGGTACTGGGCTATTTCC	AAACCATTTGGAGTGAAAGG
EMX1	TTTGAGAAGAACCATTACGTG	ACGCAGTAACACACACTACAG
ESRRG	ACATTGATTCTAGCTGTTCG	GTGACAAACTCTTCTTTCTCC
FEZF2	(from J. Dugas-Ford)	
FGF14	TTATTTCAGACTCCCTATCTGC	CAAATACCTTCAGTTCAGTGC
FMOD	TGTTTGATCTGGGATCTAGG	CACCTTGAAATAGTCATCAGG
FNDC5	CACACATTTACAAGCAGACC	AGAAGATGGTTGGATTTACC
FOSL2	AGTAGATATGCCAGGATCAGG	CCATAATAACCTCCAGCAATG
FOXP1	CATGATTCCAACAGAACTGC	CTCTTGTTCATCCACTGTCC
GABRE	GCACAGAGGAGTATGATTACG	CACCAGGTAGTTGAGTGTAGC
GAD1	GATCCAATACAGGAGATTGC	CTGCTGACAATAAACAAGACC
GPC3	GAGGATGGAGGAGAAGTACC	TCAGCTTCGTAATCAGTTCC
GRP17	CCAGACAACATTTACTACACTGC	GCTTGTAGAGGTACAGAAGAAGC
GPR26	AGAGAGAAAGAGAGTGCTATTCG	CCATGTCTTCTTGTACTGATTCC
GRM4	AGTACCAACTGGATGAGTTCC	GTTGCTGTAGCTGACGTAGG
GRTP1	CCAGATGACTTTGATTACGC	GTGCCAGAGTTAATACAATACG

Table 2.1, continued

Chicken cDNAs	Forward Primer	Reverse Primer
HS3ST4	TGTGAATCATCCTTAGAGACC	GTTTGTTCCATAGCTTCTACC
HTR1E	ACTGAGAAGATGCTTGTTACC	GTTCTCTACACCTGATGAGC
HTR7	ACTATCTCATCGTCTCTCTGG	TAGTTTCCGGTTGATATTCC
ID2	GTACAACATGAACGACTGCTAC	CCATTTCTGCCACTATACAAG
IL17RA	CAGTCCCTAAACAGAGAGAGC	GTGATGGCTAGTATTTGTTGC
JPH1	GATATGGATGTACCATGTTTCC	GCAGTTACGGTATATTGTTTCC
KCNF1	GTCAGTCACTTTGCAGTAAGC	AGTGGAGTTTATTTGGAGAGG
KCNG2	ATAACTGGTTGAGTTTGTGC	TTTAGCTCACTGTAGGAACG
KCNH5	(from J. Dugas-Ford)	
KEL	CAATCCAGTTCTATCGTTCC	TGGTATCAGTCAAACACTTCC
KLHL2	CAGAAGAGAAGGTATTTGAAGC	AAGTCTGTCCTTATGAAAGTGG
KLHL4	CTGAAACAATGTCAGTATCTGG	TAGGAGATGGTACTTCATAGCC
LBH	ACTTTGACTGTTACTGCAAGC	CACTGATAATCCACACTGTCC
LINGO3	AAGCAATAATGATCCACACC	ATCACACTTCCAAAACATGG
LRFN2	AAGGGTCTACTATTTGTACCG	ATGTGAAAGTCCCATAATCC
LRRC3C	GTTGGGACTCGATATGAAAC	TCCCTTAAACAAACACTCCTC
LYPD6B	GTATGGATGGAGTTCAGAGG	TCTGAGTTAGGTGCTCAACC
MBP	CACTCTGCTTCATAACCTAACC	CTTCTACTGGACACATAGATGC
MEIS2	CAAGGAGCAGCATATAGTCC	TCTTCTGAGTGATGAGAGACC
MKRN3	TTACCTCCGCCTACTACATC	GATAACTCCATTCCCAGAAG
MMP1	TAGAGCAATATGTCTTCACACC	TATTCTTCTGTGGAATCTAGGC
MOXD1	GATAAGAGCATAACGGAGAGC	GTACTGGATGCGACATATACC
MPPED1	CGCTATTAGAGAAGTGGAACC	TACTGAACACTGGGTTACTGG
MYOM2	ATGATTCTGCTACCTATTCAGC	CCAGTCCTCTGTATCTACTTCC
NDNF	ACCCTGAATTACCTTATGATCC	ACCATCTACACTCAGAGAAAGG
NHLH2	ATGTCAGCTCGTTAGAAAGG	AGATAGGAGATGTAGCAGATGG
NOV	GTGTTACCAACAGAAATCAGC	TCAGCTATCAATCTCCTATGC
NR2F2	(from J. Rowell)	
NR0B1	CACCTAGAGACGGTGGAGAG	GAATAGCCAGTTGACTTTGG
NR4A2	TTAAGGTGGAAGACATTCAG	AGATGTCGATGTTCATGTTC
NR4A3	GTGCTTCATAGACTTCAGTGC	ACTTCTCACTTGGTTTCTTCC
NRXN3	TGTGACATTCAAGACTAAGAGC	TTATCTGTTACCAAGGAGAAGG
NTNG2	CCAACTACTACTGGAGACAGG	ATGTGTGGATAAGACACTGC
NTSR1	AGCTCTACAACTTCATCTGG	GTTTAGACTCCACGAAATGC
OPRK1	GAATACCTGATGAACTCTTGG	CCACAGCTCTCTTTATCTAGC

Table 2.1, continued

Chicken cDNAs	Forward Primer	Reverse Primer
P2RY8	ACATTCAGAGGAATCACTGG	TGCACTTCTACTTCTTATCAGC
PAX6	TGTACCAACGATAACATACCC	CTTGAACTGGAACTGACACTC
PDE1A	CCATGTCTTTGATTCTACACG	TTGTTAGGTGTCTTGAGTTCC
PKIB	GAAGTATCATCATCCAAAGC	GTCACATCCATCTACTTATCC
PLCH2	TCATGGAAGTTCTGATGTACC	CTGGTTATCGTCTGTATCAGC
PLK2	GTCAGAGGAACTTTAGGAAGC	TCTTTAACACACACAGGAAGC
PLP1	TCCAAGAACTACCAGGACTACG	AACTCCTCCAGGCTTTAATAGG
PMP2	TATATGAAAGAACTGGGAGTGG	GACCATTTACACAGACAAGAGC
PPP1R17	TATCTTCAAGTGCTTCTCTGC	AAGGTAAGCACAAAGCTATCC
PPP3CB	GAGTCTATGATGCTTGTATGG	AGTGAGTAAACCAGAAGTTGG
PROKR2	GGAGCAAGATGAACATAACC	GTCTACCTCTTCTGTGACTGG
PVALB	CTATCAGACAAAGAGACAAAGG	GAATGTCAGCAGTAGCATCC
RALY	CTGAGGAACAGAAACAGTCC	AAGGAACAAGATGAGAAAGG
RAP1GDS1L	GCAAGTATTAGCACACCTTTACC	ACTATTACAACACCTCGTCAACC
RBFOX1	TGTTGGTGCAGTTTATAGTCC	ATATGATAGTTGGTGCAGTGG
RGS20	AATCAGGAAGAAGAGAGAGC	TACTTTGGGTCATAGTGTGG
ROBO2	GCTACTATGCTTTCTGATGG	TCTGTTATTCCTTCCCTACG
RORA	ACACCAACGTACAATATCACC	ATGAAGTCGTACAATGTCTGG
RORB	(from J. Dugas-Ford)	
ROS1	ATCCTTTACCAACTCTTCTCG	AAAGTGCAACTCTACCCTACC
RPS6KA2	TGACAAGAGCAAGAGAGACC	ATGCTGTACTTCTGCTAGTTCC
RSPO3	AAAGAGATGTCAGAAGGAAGG	CACTGTACCACTGTTCAGACC
RXFP1	AGGAAGACCAAACTGAGTACC	TGAGCCTTAGATTACACAAGC
RXFP3	AGCTATGTGTAAGATTGTCTCC	CCATCTCAGTAGTGTTGCTC
SATB1	AGACTTGCCTCCTGAACAATGG	CGTGGTGCTTGAGATAATACCG
SATB2	(from J. Rowell)	
SCNN1A	CTGTTGAGGCTGTAGTGACC	GAGAAGGTGTATGCTGTTAGG
SCRT2	AGGAGGAGTACAGCGATCC	CTAGTTCCCTATTGCACAGC
SEC14L1	TAGAAGCCTACAATGAAACC	CAAAGAACTGGAAATACTCG
SFRP2	GAGCAAGACCATCTACAAGC	CAGGTTAGGTTAGCCACTAGG
SLC10A7	CCCTTACTCATCTATCATCC	TACTTCACTCATAACCCAAGC
SLC25A47	TATGACACCCAGTGAAGTAGC	TACACAAAACCCTTGATTCC
SLC35F4	CACAGGAATCGTAATGATGG	TTAAGCATACAAGGAGTGAGG
SLITRK3	TAAATTGAGGGTCCTTATCC	GAAGTACAGGTAATGCAAGC
SOX2	GATCCAAGTGTGGTTTTGG	TATGTGATAGAGGGAGTGTGC

Table 2.1, continued

Chicken cDNAs	Chicken cDNAs	Chicken cDNAs
STC2	GAGGTCCAATTCATCTATGG	AACCGAGTATCTTCTTTCTCC
STK31	AGCATTAGAATAGGAGCTTGG	AATTACACTGCACACCTAACG
SULF1	TCACTCCCAGCTATAATTACG	GTTGACCTATAGCATCAGTGC
SYT10	AAGTCTGTGGATTCTGATGG	CCAGTGAGTTATTGGTTTACG
TFAP2D	CCACTAACCACCAGTACACC	AATGTCTCTGGATGTCAAGG
TLE4	CTTCTCTTGCTGTAGTGATGG	GAGGTCTTATCCAAGAACAGG
TMEM132E	AACCTATGACTATGACCACGTTC	TAGACACAGTGGTGGGTAACTTC
TMEM196	GTGCTCTCACAAAGAAGTCG	CACTGTTCATTTACACTCTGC
TPBG	CACTACAGGTATGAGATCAACG	GGACTGCTTTGTATTTATGAGC
TRPC4	GGAATAAACAAGCATACAGC	CAATCTAAAGGTGGACAAGG
VGLL2	AGAAACTCGCCTTGTACTCC	TTCACACCACTGAAATAACC
SLC17A6	TCAATAACAGCACCATACACC	AAGAAGAGTTGCTTCCATACC
WWOX	GATTTACTCCTCCATTCATCG	GGATGGAAATACCACTTAACC
ZDHHC2	CTGTCTTCTCTCTTTGGATACC	AGTGTGAGTCTACCTGAAAAGC

Table 2.2 PCR primers for starling cDNA isolation

Starling cDNAs	Forward Primer	Reverse Primer
BCL11A	AGACCTTCAAGTTTCAGAGC	CACAGTACTCACAAGTGTCG
KCNH5	TGCACCTATAAGAAATGAGC	GTCATGGTAAAGTAGAGAGAGG
FOXP1	GATTAAAGTCTCCCAAGAGG	GTTGTATTTGTCCGAGTACC

Table 2.3 PCR primers for mouse cDNA isolation

Mouse cDNAs	Forward Primer	Reverse Primer
Aldh1a2	AGTAACCTGAAGAGAGTGACC	AGAAGGCGATAGATACATGAC
Bcl11a	AACAACAGAGGTAATGGAAGC	CACTCAACAACCAACTAGAGC
Crabp1	CAGTTCTACATCAAGACATCC	CTGGTACAATCATGCAAATG
Dach1 3' coding	AGTCAGATGAACCACCTTAGC	ACAAACATTCTCAGTCTCTGG
Dach1 UTR	TTTCATTCCAAACTGGTAGC	GCTGAACCAAACACTAATGC
Dach2 5' coding	AAGAGAGAGAGAGAGAGTCAGC	ATCAGTCCTGGTGATAAGAGG
Dach2 3' coding	ACTCCAACAGGTATCACAGC	GTAGCTTGTTTAAGTGCTTGC
Dach2 UTR	AGGCTAAGAGAAAACTTCAGG	AAAGCCAAGCAGAAATGAG
Dcbld1	CCTAGAGACGACCTCACTTAC	TGAGTATAAGCACGTATGCAG
Emx1	(from lab of E. Grove)	

Table 2.3, continued

Mouse cDNAs	Forward Primer	Reverse Primer
Esrrg	TCTGCGTACATAGTCAATACC	CAGGTATCATCTAATCCTTGG
Fezf2	(from J. Rowell)	
Fndc5	AGGTGTTATAGCTCTCTTCTGC	TTTGATGATGTTCACAGAGG
Foxp1	GAAGTCTACAGAACCCAAAGC	CAATGCACAGAGTACAAATCC
Gabre	CATCCTGAGCAACTATGACC	GTTATCCAGACGATAAACATGG
Grm4	CTTGCACCTCAGAATAGAGC	AAGAGGATGATGTAGACTTTGG
Grtp1	GCCCTGGATACTACCATCG	ACTCTGTCACAAAGTCCCC
Id2	GTCTGCTCTACAACATGAACG	CACTGGTTGTCTGAAATAAAGC
Kcng2	GTGATGACAGTACACGTTCG	TTGGTTACAGTAGATCCTTGC
Klhl4	GCAACTGAGAGAAGACACC	ATCCATCGTGACCTCCAACCGC
Lingo3	GGGTAACGACACTTATTTCG	AGACACAGGTCACAATGAGC
Mkrn3	ATAACTGTCGCTACTCTCACG	ACTCACTAGGAATGACAAAGC
Nhlh2	CTCCTATCTCAACCATGTCC	ATAGTGAAGGGCTAGTGTTGC
Nr0b1	GCAGCATCCTCTACAATCTAC	CACAAGAAGCCAGTATGGAG
Plk2	TAACGACACACACAATAAGG	CAGAGGAATTGTATTCGTACC
Ppp1r17	AGACGACATACTAGGCAAGC	GAGTTGGACTCTCAAGATAGG
Prokr2	GAGCTGTGTAGCTGTCTAAGC	TAGAGTTGGATACCATGAACC
Rora	CTAATATGCAAGGTGTCTACG	AGCTAAACTTGTGTTTCTGG
Rorb	(from J. Rowell)	
Satb1	AAGGAAGTTGGAAGGACAGG	CTCAGGGAGTGTTCAGTTGC
Satb2	(from J. Rowell)	
Sec14L1	CGACTACATCAAGAGATACTTGG	AGAATCTGATATGCAAAGAATGG
Slc25a47	ATGACACAGTTAGAGGAGTGTCG	CCACAGAAACATTTATTAACAGC
Slc35f4	GATTCTTCTGCTCCTATTCTTG	TCCTCACTCTTCTTCTCCTTC
Stk31	AACATCAGTATTCGCTTTGG	ATAGCCCTTTAAGAGAACTGG
Sulf1	CATAACCACAATGTCTACACC	TCCACTAGGAATGTATCACG
Tmem196	GGATTAGCTGTCTTCTCTGG	GACTAAGCTACAACATTTCTGG
Tpbg	(from lab of E. Grove)	
Trpc4	TGATGAACTCCTTGTATCTGG	TTGCTTAGGTTATGTCTCTCG
Vgll2	CCTACTTCCAGGGGGACATCAG	GGCAGGGTGCTACTTCCTAAAGAC
Wnt11	TGGAAACGAAGTGTAAATGC	ATTTCTGTAACTCCCACATCC
Zdhhc2	TACTACGCCTACGCCATCC	GGAACAGCCATCACCTTG

Table 2.4 PCR primers for turtle cDNA isolation

Turtle cDNA	Forward Primer	Reverse Primer
SATB1	TCTGAACTATCCCAACAAGG	CTGAGGAAGACTGAGGAACC

Table 2.5 PCR primers for alligator cDNA isolation

Alligator cDNAs	Forward Primer	Reverse Primer
BCL11A	TATCCCACAATTCATCTTCC	GGTGGACTAGAGGTGTTTCC
BCLL1B	ACAAATGTCAACTCTGTGACC	TAGACCTCTTTCCCTATCTGG
BHLHE40	CTTTAGGTCACTTGGAGAAGG	CACACTCTGCTTAGTCTTTGG
CACHA1H	TATCTGGACCTGTTCATTACG	GAATACTGTGCTGGCTATACG
CADP2	GTTTGTAGCGAAAGAAATGG	AACGAGCACAGTATTCATCC
CHAT	AGAGAGAAGTCTGGAAACTGG	CTGAGGAGGTCTCTTTACAGC
CHN2	CACTGGTGTGAATACTGTGC	ACCTTTCTGCTTCTCTAGCC
CUX1	CTGTGAGCGAGATACTAGCC	CTTTGACCTGACGAGTTAGC
CUX2	GGGACAAAGTGAACTACTCG	GAGTGATGCTACCTCTCTGG
DACH1	TATTATGCCACATTCTGTCC	CCTTGTATTGTCCTTTCAGC
DACH2	TCATCAACACTTTCATCTCG	AGAGCTGGACACACTACTGC
DLX5	CTCAACCCCTACCAGTACC	GCAATAAGTTACATGCACAAGC
KCNH1	TTTAGTCCCTTACAATGTCTCC	TTCACTTCTAGCACAGTAGCC
KCNH5	GCTTGGATCTGATATTCTTCC	GTGACATTATTCCAGTCTTCC
ELAVL4	ACAGTAGAAACTGCCCTTCC	CTGTCTCCTAAACGGTATCC
EMX1	ACCAGAAGAAGAAAGGTTCC	AGCTGTTGACGACCTACG
EOMES	CAACATGCAAGGTAACAAGG	GAGTCGTCTTCTCTTACAAGC
ETV1	AGTCCATTCAAGACAACAGC	GCAGACCATAGGAGTAATGC
FEZF2	GCCCTCTACTACTTCAACTACC	CAGAACTCGCAGACGAAGG
FMOD	CTGAGGTATCTTCCCTTCG	GAAAGACAAGGTTGAGAACG
FOXP1	TGTATGGACATGGTGTATGC	ATGGTTCTTCTTTGACATGC
GAD1	TCAAATAAGGATGGTGATGG	CCATTGTTGTACCTGACTCC
GRIK3	TTAGACCTAGAGCCATACCG	GTGAAGAACCACCAGATACC
GRM4	AGAGGAAGAAGCTAGTGAAGG	AGAGAACTTGTTGGACATGG
ID2	ACCCTAAATACAGACATCAGC	CACTAGGAAACTGAACACTGG
KAL1	ATGTGGTACAAAGGAGATGG	TTCCTGAACAATGAAAGAGG
LHX2	CCTTAACGGACTTGACTAACC	TGCCTCTCAAATTATTCACC
LHX6	GACACCATGATCGAGAACC	AGAAGTCACAGCCTTAGTTCC
LHX9	AGTGCTGTGAATGTAAACTGG	CTGGCTGATACTTCAATAAGG
NEFM	CAACCATCAGTCACAATATCC	CTCTACCTTCTTAGTGGACACC

Table 2.5, continued

Alligator cDNAs	Forward Primer	Reverse Primer
NHLH2	CGACAAGAAGCTGTCCAAG	TTCCCCAAGGCTTAGCTC
NKX2.1	AGGAAAGCTACAAGAAAGTGG	GCAAAGTAGAACAAGACATGG
NR0B1	AGCATCCTCTACCACATCC	GGCCTAAAGAATAGTTCAGC
NR2F1	GATATGGCAATGGTAGTTAGC	ACGAAACACTTCTTGCTAGG
NR2F2	CGAGAGAGAGAAACAAACTGC	ATTTAAGAAACCACCAGACC
PCP4	TGGAAAGATCCCTATACTGC	GGTGAGTTACAGAAGAAGTGG
PPP1R1B	AGAGAAGAGACAGAGACAGAGC	GAAAGTCCTGGAGATACATGG
PROKR1	ACCCAGAATATCAACTTTGC	TCAACCTCTTCTGTGACTGG
PROX1	GGTCAGATAACGAGATGTCC	GATGAGCTGAGAGGTAATGC
RORA	ACTCCAACAGAAGATTCAGC	AGTACCATCCAAACCTCTCC
RORB	GAATGCAAGAATTACAGTTGG	GAGCGTGTTCACTATATCTGG
RSPO3	AGTGGATACTACGGAACACG	GCTCTTGAGAAATGTTGTCC
SATB1	TGAACGAGATCGAATTTACC	TGTACTTGGGTAGGTCAAGC
SATB2	CATCCCTAGAGCTATCAAACC	GTATTGCTTTCTGCGTTACC
SCRT2	CTATGAGACGGACAAGAAGC	GTGGAGGTACGACTTGAGG
SLC17A6	CGTTGTAACTTGGGAGTAGC	GGACTAAAGCAGCAATAAGG
SLC32A1	CTGTCTTTACGAGGAGAACG	TGCAGATACCACCTATAACG
SLC35F4	TCTGTTGTTGAGGATTCTGC	GAGTCTGTGATGTCTTCTGC
SULF1	CAGTAGTGCCTCAGATAGTGC	AAAGTCAGTTAGCACAACAGG
SULF2	AGAGACCAGTCAATAGGTTCC	ATGTAGCTGGAGAGAGAGAGG
TAC1	ACGAGGATGTGAACTACTGG	CCAGACTATGAAATGAAGACC
ZBTB20	GCTACAGTGACATTGAAATCC	CTGTCTGGCGTAAATAGAGC

Single-color section in situ hybridization (ISH)

RNA probe template preparation. 75 µg of miniprepped plasmid DNA were linearized by overnight restriction digestion, standardly by *SacII* or *Spe1* enzymes (New England Biolabs). Other enzymes were chosen as needed in order to avoid internal cDNA cut sites. 1 µl of 100 µl total restriction digest was run on an agarose gel beside its corresponding circular miniprep to confirm complete digestion. Digested DNA was treated with 5 µl 10% SDS (Bio-Rad) and 5 µl proteinase K (Roche) for 15 minutes at 37°C, phenol/chloroform (Acros Organics) extracted, and ethanol precipitated. The dried DNA pellet was resuspended in 10 µl of Sigma water.

DIG-conjugated antisense RNA probe synthesis. RNA transcription reactions comprised 4 µl water, 4 µl 10x bovine serum albumin, 2 µl 10x transcription buffer, 2 µl 10x DIG-labeling nucleotide mix (Roche), 2 µl Protector RNase inhibitor (Roche), 2 µl DTT, 2 µl template DNA, and 2 µl of RNA polymerase T7/SP6 (New England Biolabs). The transcription reaction was carried out overnight at 37°C. A white cloud or pellet of RNA should be apparent after incubation. The reaction solution was treated with 4 µl of RNase-free DNase (Roche) for 1 hour at 37°C. RNA was purified with two consecutive ethanol/LiCl precipitations and suspended in 100 µl of formamide (Sigma-Aldrich). RNA in formamide was heated at 50°C for 15 minutes to remove secondary structure before being imaged on a 1% agarose gel with ethidium bromide. RNA probes were judged acceptable if one or more bright, tight bands were visible on the gel.

Pre-hybridization tissue processing. Completely dried slides bearing brain sections were post-fixed in PFA for 15 minutes at room temperature and rinsed three times with D-PBS. Tissue was then treated with proteinase K (Roche) in incubation buffer (1.5 µl stock proteinase K per 20 ml 100 mM Tris-HCL pH8.0, 50 mM EDTA pH 8.0) for 30 minutes at 37°C. Digested tissue was fixed in PFA for 15 minutes, rinsed three times with D-PBS, and transferred to 5-slot slide mailers (Evergreen Scientific) containing 15 ml hybridization solution (50% formamide, 5x SSC, 1% SDS, 0.25 grams yeast RNA [Roche], and 0.1 grams heparin sulfate [Alfa aesar] per 500 ml). Slides can be stored in hybridization solution at −20°C indefinitely before continuing the in situ hybridization protocol.

Hybridization and antibody binding. Slides in hybridization solution were heated in a 73°C Isotemp 210 water bath (Fisher Scientific) for 30 minutes. Hybridization solution was then decanted into a 50 ml conical tube (Denville Scientific), mixed with 95 µl antisense RNA probe reaction, and returned to the slide mailer for an overnight incubation at 73°C. The next day, RNA

solution was decanted into a 50 ml conical and stored at −20°C for up to 3 total uses. Slides were washed three times for one hour each at 73°C in preheated Solution X (50% formamide, 2x SSC, 1% SDS). After the first wash, slides were consolidated into as few mailers as possible in order to conserve reagents. This does not result in any obvious cross-contamination of probe signals. Following Solution X washes, slides were washed briefly three times in TBST (A 10x TBS stock was first prepared with 250 ml Tris-HCl pH 7.5, 80 g NaCl, 2 g KCl per 1 L. This was then diluted and combined with 10 ml Tween for 1 L of 1X TBST). Slides were then blocked for 1 hr in 10% lamb serum (Invitrogen) in TBST at room temperature.

Hybridized complexes of antisense probe/target mRNA were detected with anti-DIG Fab fragments conjugated to the colorigenic enzyme alkaline phosphatase (Roche). The antibody-enzyme conjugate was preadsorbed with chick embryo powder/1% lamb serum in TBST, then diluted to 1:5000 in TBST/1% lamb serum (3 µl of antibody per 15 ml of TBST/1% lamb serum per mailer). Antibody solution was poured into slide mailers and antibody binding was carried out for 2 hours at room temperature on a rocker. Antibody solution was decanted and stored at 4°C for up to 3 total uses. Unbound antibody was removed by washing slides three times for 15 min in TBST. Slides were then briefly washed once in NTMT (100 mM Tris-HCl pH 9.5, 100 mM NaCl, 50 mM $MgCl_2$, 1% Tween).

Color reaction. Antibody/mRNA was detected using phosphatase histochemistry. 5-bromo-4-chloro-3-indolyl phosphate (BCIP, Denville Scientific) stocks were produced by diluting 50 mg powder per 1 ml 100% dimethyl formamide (DMF, Acros Organics). The formazan nitro blue tetrazolium (NBT, Denville Scientific) stock was produced by mixing 100 mg powder in 1 ml 70% DMF in water. Color reagent stocks were stored at −20°C. Slides were incubated in 4 µl BCIP and 4 µl NBT stock per 1 ml NTMT at room temperature for 1–7 days.

For best results, post-hybridization washes through to the color reaction were typically done in a single day. Color reaction solution was replenished every day for the duration of color development. The length of color reaction depended on several factors including length of probe used and abundance of target mRNA in the tissue. Highly expressed target genes can develop a clear signal in minutes, while low-abundance target genes may require 5 days of incubation to be visible. Following the color reaction, slides were washed twice in Stop TE (10 mM Tris-HCl pH 7.5, 10 mM EDTA pH 8.0) then once more ranging from 2 hours to overnight. Slides were then washed overnight in TBST, then fixed overnight in 10% Formalin (Fisher Scientific) in PBS. Slides were rinsed in PBS, dried, dehydrated in an ethanol series, soaked in Histoclear (National Diagnostics) and coverslipped using Eukitt mounting medium (Sigma-Aldrich) and Fisher Scientific microscope cover glass.

Single-color whole mount ISH

Whole brains were dissected from chick embryos in PBS, then fixed overnight in PFA at 4°C. Tissue was washed in PTW (1% Tween in PBS) two times for five minutes each at room temperature. Tissue was then dehydrated in 25%, 50%, 75% and 100% MeOH in PTW for ten minutes each, followed by overnight incubation in 100% MeOH at −20°C. Tissue was rehydrated in 75%, 50%, and 25% MeOH in PTW for five minutes each, then washed in PTW twice for five minutes each. Tissue was incubated in 6% hydrogen peroxide in PTW for 60 minutes at room temperature on a rocker, then washed two times in PTW for five minutes each. Tissue was incubated in detergent mix three times for 30 minutes each at room temperature, post-fixed in 1% Tween in PFA for 20 minutes, washed twice in PTW for five minutes each, then stored in glass scintillation vials with 5 ml of hybridization solution at −20°C.

Tissue was hybridized overnight at 73°C with 33 µl of the 100 µl RNA transcription solution, prepared as described above. Tissue was washed in preheated Solution X four times for 30 minutes each. TBST was then added, which causes tissue to settle to the bottom of the vial, and washed three more times in TBST for five minutes each. Tissue was blocked in 10% lamb serum in TBST for two hours at room temperature. Incubation solution was then replaced with five ml 1% lamb serum in TBST. Antibody solution was prepared as described above. One µl of antibody was added to each five ml scintillation vial (as opposed to the three µl added to a 15 ml slide mailer) and tissue was incubated overnight at 4°C on a rocker.

Tissue was washed in TBST three times for five minutes each, five times for 60 minutes each, and overnight at room temperature. Color reaction was then performed as described above.

In ovo electroporation

Transgene overexpression was accomplished using in ovo electroporation of embryonic chicken telencephalon (Agarwala et al. 2001, Hasan et al. 2010). Chicken eggs for electroporation were incubated on their sides and rotated regularly. Eggs were set in the incubator on the evening of receipt and electroporated in the morning 4 days later; electroporated eggs were therefore E3.5 or HH23, an ideal stage due to size and accessibility of the telencephalon. The day before electroporation, 4 ml of albumin were extracted from the eggs by producing a small hole in the pointed end of the egg and inserting a needle attached to a syringe. The day of electroporation, a small window was cut into the egg directly above the presumed location of the embryo. Four drops of Ringer's solution (9 g NaCl, 0.42 g KCl, and 0.16 g $CaCl_2$ per 1 L water) were deposited on the embryo for hydration.

Borosilicate Glass Capillaries (World Precision Instruments, Inc) were tapered by a Model P-97 Flaming/Brown micropipette puller (Sutter Instrument Co.), and their tips were

manually cut open to a width of 40 μm. Gene expression plasmids were prepared using an Origene Maxiprep System, phenol/chloroform extraction, ethanol precipitation, and resuspension in 100 μl TE buffer (Origene) for a concentration of approximately 5–15 μg DNA per μl TE. The electroporation mix comprised one or more plasmids at a final concentration of 1–2 μg per plasmid per μl TE with 0.02% Fast Green dye. The electroporation mix was back-filled into the open glass capillary using a PV830 Pneumatic PicoPump (UPI). Expression vectors employed are described in Table 2.6.

The filled capillary was inserted into the right telencephalon of the chick embryo and electroporation mix was injected until green dye filled the lateral ventricle. A negative electrode (made from 0.025 mm tungsten wire) was then inserted into the right telencephalon and a positive electrode (0.063 mm platinum wire) was positioned outside but very close to the neuroepithelium. Precisely localizing the site of electroporation is difficult, but the positive electrode can be shifted anteriorly or posteriorly for consistent differences. A Model 2100 Isolated Pulse Stimulator (A-M systems) was used to generate an electrical field by delivering three 25 millisecond pulses of 9 V each with an inter-pulse period of 1 second. The appearance of bubbles along both electrodes indicates a successful pulse delivery. For more restricted electroporation sites, 1–2 pulses were delivered. The electric field thus generated drives DNA from the ventricle into neural progenitor cells. Both electrodes were dipped into 5M NaOH and wiped with a Kimwipe (Kimtech Science) after each animal was electroporated in order to remove any crusty biomatter. Eggs were then sealed with Scotch packing tape and returned to the incubator. Because the electroporation mix always included a fluorescent reporter molecule, embryos could be examined the next morning using a Leica Fluo III fluorescent microscope to screen for successfully electroporated animals. Eggs displaying reported fluorescence were then

given 4 drops of Ringer's solution, sealed with Parafilm "M" Laboratory Film (Pechiney Plastic Packaging), and returned to the incubator for another 10 days (to E14).

Table 2.6 Expression plasmids used

Construct Name	Contents
CDV-hypbase	PiggyBac construct with CAGGS promoter, B globin poly A, amp resistance
PBXW-sfGFP	minimal PiggyBac ITRs flank expression cassette, CAGGS promoter, superfolder GFP, woodchuck posttranscriptional regulatory element (WPRE)

Plasmids were kindly provided by T. Sanders.

RNA sequencing and analysis

Embryonic day 14 chicken brains were dissected out whole then sliced into 300 μm thick sections using a McIlwain Tissue Chopper (The Mickle Laboratory Engineering Company). Nuclei were dissected from sections in D-PBS using forceps and transferred to RNAlater (Life Technologies) where they were stored overnight at 4°C. Dr. J. Rowell identified and dissected the chick nuclei. Dr. C. Albertin extracted the RNA using Trizol Reagent, suspended in nuclease-free water, and submitted to the University of Chicago Functional Genomics Core Facility for Illumina 100 base pair paired-end directional sequencing (Wang et al. 2009). Raw reads were quality trimmed using Trimmomatic (Bolger et al. 2014), digitally normalized using Trinity (McCorrison et al. 2014), and assembled de novo using Trinity (Haas et al. 2013). Raw reads were then mapped onto assembled transcripts using bioconductR (Trapnell et al. 2012) to generate abundance estimates in fragments per kilobase of transcript per million mapped reads (FPKM). FPKM allows for direct comparisons across samples by controlling for length of transcript (longer transcripts generate more reads) and for total numbers of reads per sample. In order to identify transcripts enriched in particular nuclei (or combinations of nuclei), I performed differential expression analysis using High-Low Ordering of Like Transcripts (HOLT). HOLT is

a series of sequential pairwise comparisons of transcript abundance that progressively filters reads to those enriched in particular samples. For instance, in order to identify transcripts enriched in samples A and B compared with samples C and D, I performed the following operations (order does not matter and comparison value can be varied for stringency): A/C > 2.5, A/D > 2.5, B/C > 2.5, B/D > 2.5. The filtered transcript list was ordered by abundance in a chosen sample to identify the most highly expressed and differentially expressed candidate genes. Transcripts were annotated using BLASTN and BLASTX (NCBI) searches.

Microscope and image analysis

Images of brain sections were captured using either a Leica Fluo III microscope or a Zeiss Axioskop 40, a mounted AxioCam HRc color camera (Zeiss), and AxioVision software (version 4.8, Zeiss). Images were cropped and corrected for brightness using Photoshop CS6 (Adobe Systems).

Anatomical nomenclature

Abbreviations used for all species in all parts of the text are listed in Table 2.7.

Table 2.7 Abbreviations for anatomical nomenclature

Chicken (*Gallus gallus*)	
Starling (*Sturnus vulgaris*)	
A	Arcopallium
Bas	Nucleus basorostralis
CDLCo	Caudodorsolat pallium, core
Cpi	Piriform cortex
DT	Dorsal telencephalon
DVR	Dorsal ventricular ridge
E	Entopallium
HA	Hyperpallium apicale
Hp	Hippocampus
IHA	Interstitial nucleus of the HA
L	Field L
M	Mesopallium
Md	Dorsal mesopallium
Mv	Ventral mesopallium
MVL	Ventrolateral mesopallium
N	Nidopallium
VT	Ventral telencephalon
W	Wulst

Mouse (*Mus musculus*)	
CA	Cornu ammonis
Cpi	Piriform cortex
DG	Dentate gyrus
L1	Ncx layer 1
L2	Ncx layer 2
L3	Ncx layer 3
L4	Ncx layer 4
L5	Ncx layer 5
L6	Ncx layer 6
Ncx	Neocortex
Sub	Subiculum
VT	Ventral telencephalon
WM	White matter

Alligator (*Alligator mississippiensis*)	
Turtle (*Trachemys scripta elegans*)	
A	Arcopallium
Adl	Dorsolateral arcopallium
Adm	Dorsomedial arcopallium
Av	Ventral arcopallium
Bas	Nucleus basorostralis
D	Area D
DC	Dorsal cortex
DCl	Lateral dorsal cortex
DCm	Medial dorsal cortex
DT	Dorsal telencephalon
DVR	Dorsal ventricular ridge
E	Entopallium
GP	Globus pallidus
Hy	Hypothalamus
L	Field L
L1	Dorsal cortex layer 1
L2	Dorsal cortex layer 2
L2a	Dorsal cortex layer 2a
L2b	Dorsal cortex layer 2b
L3	Dorsal cortex layer 3
LC	Lateral cortex
M	Mesopallium
mb	mesopallial bridge
MC	Medial cortex
MCi	Intermediate medial cortex
MCl	Lateral medial cortex
MCm	Medial medial cortex
N	Nidopallium
NR	Nucleus reuniens
OB	Olfactory bulb
Rt	Nucleus rotundus
St	Striatum
VT	Ventral telencephalon

CHAPTER 3

An evolution-based search for neocortical layer 4 genes

ABSTRACT

A fundamental function of the dorsal telencephalon (DT) in all vertebrates is the receipt and integration of external sensory information. In mammals, the DT features a six-layered neocortex. Visual, auditory, and somatosensory information is first targeted to layer 4 (L4) of neocortical primary sensory areas. In birds, however, sensory information reaches the DT through several large nuclei that could hardly be more different from neocortical L4 in their morphology. Molecular and connectional evidence suggests that these primary sensory input cells are homologous at the level of cell type across mammals and birds: in addition to their similarities in functional connectivity, they selectively express the well-established L4 marker genes *RORB* and *KCNH5*. We took advantage of the nuclear morphology of the chicken DT by dissecting and transcriptionally profiling sensory input nuclei as a forward search for new marker genes. This screen yielded three transcription factors, *SATB1*, *NR0B1*, and *RORA*, that are enriched in chicken sensory input territories and mouse neocortical L4. In contrast, and consistent with the great differences in DT anatomy, most non-transcription factor genes that are highly enriched in avian input nuclei are not enriched in mouse L4. These gene expression data lend further support for input cell-type homology and identify a candidate gene regulatory network for DT input cell identity. These findings accord with the emerging view that character identities, such as the amniote DT input cell, are determined by a conserved gene regulatory network of transcription factors, whereas character states, such as the differential spatial organizations of input cells, are produced by distinct molecular programs.

INTRODUCTION

The integration of sensory information from multiple distinct modalities is fundamental to animal behavior. Peripheral sensory organs are specialized to collect distinct types of information: eyes for light, ears for sound, surface receptors for touch, and so on. These types of information must eventually be assembled in the brain to produce representations of external objects and events that guide adaptive behaviors. The dorsal telencephalon (DT) is believed to perform such sensory-integrative functions in mammals, reptiles, and birds (together, the amniotes) (Ulinski 1983, Nieuwenhuys et al. 1998). Despite this basic functional similarity, the gross morphology of the DT greatly diverges across amniotes and other vertebrate groups. Only in mammals does the DT contain a six-layered neocortex. Birds, in contrast, have a nuclear DT lacking any multilayered cortical structure. Whether the avian DT is in some feature homologous to the mammalian neocortex is among the most controversial problems in evolutionary neuroscience (Striedter 2005). Similarities in the construction of amniote DT sensory pathways may offer a partial solution.

It is a common organizational feature in amniotes that visual, auditory, and somatosensory information accesses the DT through spatially segregated, unimodal input cell populations. In mammals, these input DT cell populations are found in neocortical layer 4 (L4) of primary sensory areas. Lorente de Nó described thalamic afferents in the neocortex of Golgi-stained rodent tissue. He distinguished “specific” thalamic axon arborizations most prominent in L4 from “unspecific” arborizations spanning multiple layers. He suggested that the specific class of afferents arose from specific sensory thalamic nuclei (Lorente de Nó 1922, Lorente de Nó 1938). Herkenham tested this concept with extensive anterograde tracing experiments in rodent

thalamus. His experiments established that sensory-specific thalamic relay nuclei projected densely to L4 granule cells of corresponding primary sensory cortices (Herkenham 1980).

Numerous lines of evidence converge to suggest that neocortical input cells are an essential and universally conserved cell type in mammals. Von Economo categorized human neocortical areas into five cytoarchitectonic types. Type 5 "heterotypical" cortex is notable for the presence of densely packed granule cells, especially in L4 (Economo and Triarhou 2009). Using similar cytoarchitectonic criteria, Brodmann found similar areas in nearly every mammal examined (Brodmann 2006). Flechsig studied the development of myelination in the human neocortex. He identified "primordial areas" that myelinated first, and these early myelinating areas were nearly equivalent to Von Economo's type 5 cortex (Flechsig 1901). It is now known that Von Economo's type 5 cortex and Flechsig's primordial areas correspond to primary visual, auditory, and somatosensory areas in the human neocortex. Decades of anatomical, physiological, and behavioral studies since have established that all mammals possess a set of primary sensory areas organized in roughly the same topological pattern (Krubitzer 2007). The last common ancestor of all extant mammals must surely have had these primary sensory areas, and they received sensory input to L4 granule cells from specific thalamic nuclei.

Outside of mammals, however, the evolutionarily origin of primary sensory input cells is less clear. Birds do not have a multilayered cortex in their DT, and thus do not have "areas" in the sense used to describe the neocortex. Birds instead have two large DT nuclear complexes: the Wulst and the dorsal ventricular ridge (DVR) (Ulinski 1983, Reiner et al. 2004a). Both the Wulst and the DVR contain spatially segregated input nuclei that are targets of unimodal sensory information channels from the thalamus. The ascending sensory pathways from thalamus to DT in birds strongly resemble mammalian thalamocortical projections.

The avian Wulst contains sensory input cells in the interstitial nucleus of the hyperpallium apicale (IHA) (Reiner et al. 2004a), with the anterior IHA receiving somatosensory information and the posterior IHA receiving visual information (Karten et al. 1973, Funke 1989b, Funke 1989a, Korzeniewska and Gunturkun 1990, Wild 1997). The IHA sensory targets are topologically similar to mammalian primary somatosensory and visual areas, as primary somatosensory cortex is located anterior to primary visual cortex (Medina and Reiner 2000). In some large-brained and visually oriented birds, such as owls, the Wulst is significantly developed and contains a dense band of granule cells in the IHA (Karten 1969).

The avian DVR, located ventrolateral to the Wulst, contains two separate nuclei that receive sensory information: Field L and entopallium. Field L is a dense nucleus of granule cells in posterior DVR that receives auditory information following relays in the brainstem cochlear nuclei (Boord 1965), the midbrain nucleus mesencephali lateralis (Papez 1936, Karten 1967), and the thalamic nucleus ovoidalis (Karten 1968). The avian auditory pathway resembles the mammalian pathway from the cochlear nuclei, to midbrain inferior colliculus, to the ventral division of the thalamic medial geniculate nucleus, to the primary auditory area in posterolateral neocortex.

Birds and mammals have a second, tectofugal, visual pathway distinct from the lemniscal visual pathway. In birds, visual information travels from the retina to superficial layers of the midbrain optic tectum (Cowan et al. 1961), to the thalamic nucleus rotundus (Karten and Revzin 1966), to the entopallium (E) in central DVR (Karten and Hodos 1970). Similarly, the mammalian visual tectofugal pathway comprises a projection from the retina to midbrain superior colliculus, to the thalamic nucleus lateralis posterior (Altman and Carpenter 1961,

Tarlov and Moore 1966), to the "circumstriate" cortex adjacent to primary visual cortex (or striate cortex) (Diamond et al. 1970).

There are, therefore, four separate sensory pathways apparently shared between mammals and birds—lemniscal somatosensory, lemniscal visual, tectofugal visual, and lemniscal auditory—that reach dedicated DT input territories. In the mid-20th century, most anatomists considered the avian DVR homologous to mammalian striatum in ventral telencephalon (Ariëns Kappers et al. 1936). This view implies the independent evolution of the auditory and tectofugal visual sensory pathways in mammals and birds, or at least a dramatic change to their telencephalic targets. Harvey Karten argued against the independent and unparsimonious genesis of "massive quantities of specific sensory neuronal populations in the telencephalon, without precedence or correspondence" (Karten 1969). He suggested instead that, despite the great divergence in gross morphology, the primary sensory input cells of mammalian neocortex and avian DT are homologous as cell types. In this view, the four major ascending sensory pathways arose once in evolution, but the DT input cell populations underwent independent structural reorganizations into layers in mammals and nuclei in birds.

The Ragsdale laboratory predicted that if DT sensory input cells are homologous across amniotes, they should share expression of conserved marker genes that reflect their common ancestry. They first established that the ion channel gene *Kcnh5* and the transcription factor *Rorb* are conserved markers of mammalian neocortical L4 in comparative studies of mouse and ferret (Rowell et al. 2010). Gene expression studies were then extended to two avian species, the chicken and the zebra finch. *KCNH5* and *RORB* are strongly enriched in the input nuclei IHA (in the Wulst), and E and Field L (in the DVR), of both species (Dugas-Ford et al. 2012). They further showed that both *KCNH5* and *RORB* are expressed in a visual input part of the turtle

cortex (Dugas-Ford et al. 2012). The gene expression data gathered from five distantly related representatives of mammals, reptiles, and birds harmonizes with connectional anatomy to strongly support a single origin of DT sensory input cells at least as early as the last common ancestor of amniotes.

Currently, there are only two known marker genes specifically expressed in amniote DT input cells. The full extent of molecular conservation is not well understood. Do mammalian and avian DT input cells require the same collection of genes to establish connections with thalamic axons? Do they require the same transcription factors to regulate input cell-specific genes, or to repress alternate cell identities? In order to answer these questions, it is necessary to identify novel input cell marker genes and to compare their expression across multiple species.

In this study, I took advantage of the substantial differences between mammalian neocortical L4 and the avian DT input nuclei, namely that the DVR input nuclei E and Field L are large, circumscribed nuclei segregated from other DT cell types. Entopallium, Field L, and five other DT territories from embryonic day 14 (E14) chicken embryos were dissected, and I sequenced their mRNA content. Using a bioinformatics approach called the HOLT method, I identified transcripts selectively enriched in chicken input nuclei. I tested whether mouse orthologs of chicken input cell marker genes are expressed in neocortical L4 toward the following ends: 1) the identification of additional conserved input cell marker genes would further support Karten's hypothesis of conserved cell types; 2) conserved marker genes of amniote DT input cells are likely to perform essential functions; 3) conserved transcription factors, in particular, would be attractive candidate input cell determinants; and 4) genes expressed in divergent, species-specific patterns may contribute to the substantial architectural differences inherent in neocortex and avian DT organization. I identified three additional

transcription factors that are enriched in mouse and chicken DT input cells: *SATB1*, *NR0B1*, and *RORA*. These genes, in combination with *RORB*, may form a conserved gene regulatory network for input cell type identity. I found that most of the non-transcription factor genes examined were expressed in divergent patterns.

RESULTS

Dissection strategy and the HOLT method

At E14, chicken DT input nuclei are well formed with distinct nuclear morphologies. I predicted that nuclei at this stage would express differentiation markers, and would possibly also maintain expression of early cell-type determinants. The entopallium (Figure 3.1c, E) and Field L (Figure 3.1d, L) were collected from E14 chicken telencephalon as representative input cell populations. In addition, five outgroup cell populations were collected: hyperpallium apicale (Figure 3.1a, HA), rostral mesopallium (Figure 3.1a, M), nucleus basorostralis (Figure 3.1b, Bas), caudal nidopallium (Figure 3.1e, N), and arcopallium (Figure 3.1e, A). The Wulst input population, IHA, is a thin band of *KCNH5*(+) cells at the ventral edge of HA (Figure 3.1a,b). IHA tissue was not collected. Ragsdale laboratory alumnus Dr. Joanna Rowell performed all tissue dissections.

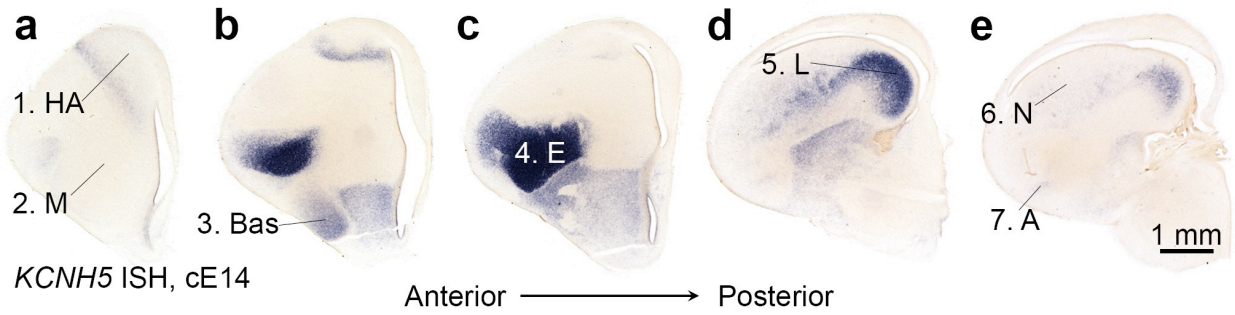

Figure 3.1 Embryonic day 14 chicken dorsal telencephalon territories harvested for RNAseq
In situ hybridization for the conserved input cell marker *KCNH5* on E14 chicken telencephalon. Five coronal sections from a single cerebral hemisphere are shown in anterior to posterior sequence. Sections are oriented with medial to the right. The seven indicated cell populations were collected from E14 telencephalon: **(a)** 1. Hyperpallium apicale (HA), 2. Mesopallium (M), **(b)** 3. Nucleus basorostralis (Bas), **(c)** 4. Entopallium (E), **(d)** 5. Field L (L), **(e)** 6. Nidopallium (N), and 7. Arcopallium (A). RNA was purified from these cell populations and submitted for sequencing.

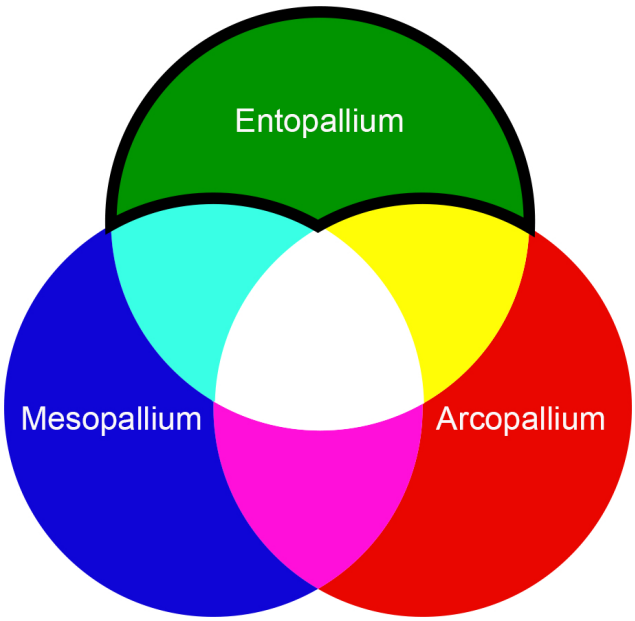

Figure 3.2 Idealized representation of target entopallium-specific transcripts
Entopallium (green) is a dorsal telencephalon sensory input nucleus. Arcopallium (red) is a dorsal telencephalon motor output nucleus. Mesopallium (blue) is neither input nor output, but instead forms intratelencephalic association connections. Transcripts presumably exist that are expressed in any combination of these three fundamental neuronal types. My goal is to identify transcripts expressed in input cells, but not output or association cells (bold black line around green area). I designed the HOLT method to identify these transcripts.

HA and arcopallium form long-distance "output" projections to brainstem and spinal cord, and express marker genes of mammalian neocortical L5 output neurons (Dugas-Ford et al. 2012). M and N are neither input nor output, but instead form a variety of intratelencephalic association connections (Atoji and Wild 2009, Atoji and Wild 2012). It is unknown whether M and N have mammalian homologs. Bas is an input-like territory, but receives sensory information directly from the main trigeminal sensory nucleus of the hindbrain rather than from the thalamus (Reiner et al. 2004a). I sought to identify transcripts specifically expressed in input cell populations, but are excluded from output and association cell populations (Figure 3.2, green area with bold outline).

To identify differentially expressed transcripts, I developed the High-to-Low Ordering of Like Transcripts (HOLT) method. HOLT uses serial pair-wise comparisons of transcript abundance to progressively filter candidate genes. Beginning with a list of all transcripts and their read counts for each sample (in units of fragments per kilobase of transcript per million mapped reads, FPKM), I first selected those transcripts expressed at 2.5 fold or greater levels in E compared with M. Many genes expressed across DT territories such as *VGLUT2*, GABAergic interneuron markers, pan-glial, and pan-neuronal genes will be removed by this first HOLT filter. This operation reduced 356,804 total transcripts to 75,823 (Table 3.1). From these transcripts, I selected those that are also enriched in E in comparison with A by 2.5 fold or greater. This operation reduced 75,823 transcripts to 29,062 (Table 3.1). The vast majority of these twice-filtered candidates are expressed at levels too low to detect with in situ hybridization (ISH). For the final HOLT filter, I ordered transcripts in descending levels of expression in the input nucleus E and selected only coding transcripts expressed at 5 FPKM levels or greater. Exploratory experiments established that 5 FPKM is near the lower limit of ISH detectability.

Table 3.1 Progressive HOLT filters for entopallium-enriched transcripts

Sequential HOLT Filters	# of Transcripts
1) All Transcripts	356804
2) Entopallium/Mesopallium ≥ 2.5	75823
3) Entopallium/Arcopallium ≥ 2.5	29062
4) Abundance ≥ 5 FPKM, Coding	70

I first selected transcripts enriched in E compared to M by 2.5 fold. From these, I selected transcripts enriched in E compared to A by 2.5 fold. Then, I ranked transcripts in descending order of expression and selected coding transcripts expressed at 5 FPKM or greater.

The HOLT approach resulted in 70 candidate genes, which are listed in Table 3.2. FPKM values for E, M, A, L, and Bas samples are shown. It is notable that this relatively simple approach is sufficient to identify numerous highly specific marker genes (see below). However, the appropriate values for comparison cutoffs in any HOLT screen must be empirically established. I found that a HOLT value of 3-fold enrichment excluded specific markers (was too stringent), and a value of 2 yielded many non-specific markers (was too permissive). This approach recovered *KCNH5*, one of two previously known input cell-specific markers (Table 3.2, #11). The other known marker, *RORB*, was not recovered due to high levels of expression in the mesopallium at E14. *RORB* and its paralogue *RORA* are noted at the bottom of Table 3.2.

Table 3.2 Entopallium HOLT candidates

The 70 most abundant entopallium-specific genes are listed by descending levels of expression. The transcription factor genes *RORB* and *RORA* were not recovered by the HOLT method but are included at the bottom of the list. Expression values for each transcript, in each sample, are shown in units of FPKM.

Rank	Gene	E	M	A	L	Bas
1	*SATB1*	226.87	37.19	40.60	75.05	51.42
2	*ANOS1*	188.43	8.62	11.48	57.98	20.24
3	*CRABP1*	175.31	26.41	51.78	145.78	788.21
4	*DCBLD1*	163.14	22.15	37.45	116.74	75.37
5	*SEC14L1*	157.01	41.27	57.14	135.85	68.36
6	*ALDH1A2*	94.04	14.63	15.96	16.49	111.52
7	*ABLIM2*	92.24	20.28	26.43	29.33	59.08
8	*LINGO3*	90.19	19.08	31.51	87.37	40.17

Table 3.2, continued

Rank	Gene	E	M	A	L	Bas
9	*C11ORF87*	85.34	22.95	26.83	59.03	109.24
10	*GABRE*	78.00	20.66	18.73	28.43	15.29
11	*KCNH5/EAG2*	64.49	3.06	12.34	20.14	12.39
12	*MBP*	61.14	9.25	13.27	5.03	38.62
13	*PPP1R17*	58.02	5.55	6.49	9.21	3.70
14	*KLHL4*	51.78	12.41	14.00	3.74	17.14
15	*SULF1*	49.54	8.18	2.79	9.50	7.38
16	*GPC3*	47.48	6.70	3.88	10.61	30.31
17	*CTGF*	41.88	12.27	11.18	24.49	13.76
18	*VSTM2L*	39.53	7.89	10.84	24.31	19.82
19	*CRHBP*	38.23	4.29	9.97	5.12	22.85
20	*TMEM196*	37.97	2.23	9.68	13.25	3.75
21	*IL17RA*	36.65	1.52	6.04	14.05	7.45
22	*DIRAS2*	35.33	1.79	8.26	5.94	14.59
23	*SLC25A47*	34.49	11.29	9.63	10.22	4.69
24	*CDH6*	33.85	6.71	10.18	13.64	6.71
25	*DACH1*	32.75	8.00	9.28	11.23	7.44
26	*TPBG*	32.67	10.04	7.26	5.54	25.36
27	*MOXD1*	31.75	2.39	4.75	0.51	5.42
28	*PMP2*	30.01	2.91	3.49	0.42	14.68
29	*PLK2*	28.14	5.24	6.81	7.46	14.44
30	*NR0B1*	27.32	3.46	4.75	5.24	2.97
31	*FNDC5*	22.82	5.64	7.35	8.39	14.01
32	*JPH1*	21.24	4.24	6.52	8.03	4.07
33	*LYPD6B*	20.71	3.73	7.58	12.90	10.80
34	*ASTN2*	20.10	6.46	3.09	6.85	8.26
35	*SFRP2*	18.56	2.36	2.74	2.05	14.20
36	*STK31*	18.48	2.25	6.40	14.33	1.80
37	*GRTP1*	17.97	4.37	6.07	4.71	5.24
38	*BRINP2*	16.48	5.18	6.19	2.68	9.02
39	*CPNE9*	16.45	3.04	6.53	3.52	5.75
40	*TMEM132E*	16.11	5.40	5.34	4.94	38.84
41	*NDNF*	15.54	2.72	2.48	1.80	13.34
42	*ROBO2*	15.04	3.47	5.55	12.09	13.61
43	*ROS1*	14.89	0.06	1.21	2.20	0.52
44	*BCAS1*	14.34	3.46	4.86	1.88	14.83
45	*MYOM2*	13.40	0.77	4.64	0.35	16.00
46	*ESRRG*	13.20	4.06	4.95	6.32	5.71

Table 3.2, continued

Rank	Gene	E	M	A	L	Bas
47	*SCRT2*	13.13	4.41	4.11	12.56	8.93
48	*RPS6KA2*	13.10	1.78	2.75	1.74	1.62
49	*PLP1*	13.00	3.83	5.07	3.16	11.03
50	*ZDHHC2*	12.76	3.87	4.75	5.48	4.20
51	*TRAPPC3L*	12.45	0.53	2.62	0.50	0.77
52	*KLHL2*	11.41	2.51	4.53	4.28	6.51
53	*WWOX*	11.17	3.14	2.35	3.61	4.86
54	*SLC35F4*	10.94	0.80	1.52	1.35	2.65
55	*GPR26*	10.66	1.18	2.13	0.72	1.82
56	*SLC18A3*	9.43	1.32	3.31	1.30	0.95
57	*IL1RAP*	7.68	1.58	2.92	2.08	2.80
58	*WNT11*	7.64	1.59	1.13	1.53	1.39
59	*C14ORF79*	7.58	0.89	1.27	1.25	0.33
60	*P2RY8*	7.13	0.00	1.26	4.63	0.83
61	*FGF14*	7.00	0.49	2.16	1.92	1.56
62	*NRXN3*	6.69	0.36	2.31	2.04	4.23
63	*GPR17*	6.66	1.22	1.88	0.76	5.02
64	*PCP4L1*	6.39	0.44	2.49	2.03	4.22
65	*C19ORF35*	6.18	0.53	2.27	4.70	1.63
66	*RAP1GDS1*	5.98	0.62	1.74	0.44	0.81
67	*MKRN3*	5.89	0.00	0.00	1.07	0.76
68	*MMP1*	5.79	0.29	0.36	0.07	0.37
69	*VGLL2*	5.21	0.03	0.20	2.20	0.08
70	*PLCH2*	5.09	0.67	0.54	1.03	1.06
-	*RORB*	2.99	4.60	2.01	3.17	2.39
-	*RORA*	4.38	1.25	3.25	4.45	2.44

Gene ontology analysis using PANTHER domain identification (Mi et al. 2017) demonstrates a wide diversity of protein classes. There is no apparent enrichment for any type of molecule defined either structurally (Figure 3.3) or by function in a biological pathway (not shown).

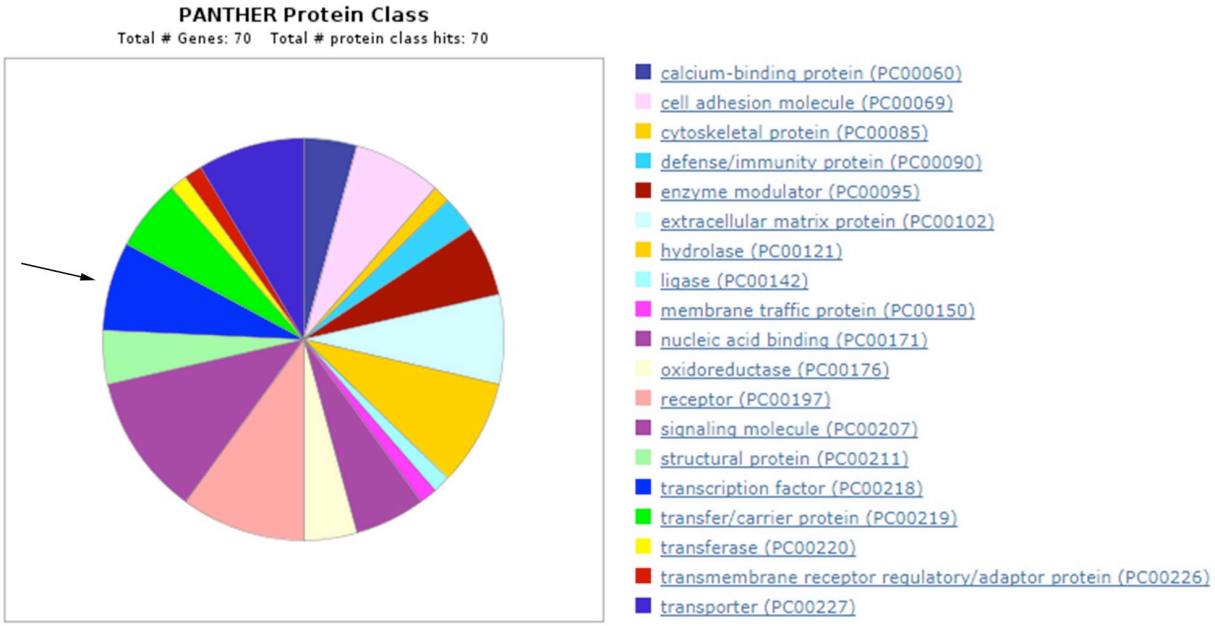

Figure 3.3 Gene ontology analysis of entopallium HOLT candidate genes
Entopallium HOLT candidate genes shown in Table 3.2 were analyzed using the online PANTHER resource (pantherdb.org). Pie chart at left shows the breakdown into protein classes. Colored wedges correspond to colored key at right. The entopallium-specific genes are a diverse group not particularly enriched for any protein molecule class (e.g. transcription factors, **arrow**), gene family (e.g. solute carriers), or biological function (e.g. axon guidance).

Expression patterns of entopallium HOLT candidates

I PCR-amplified cDNAs and performed ISH for HOLT candidates in Table 3.2 to determine whether the selective expression predicted bioinformatically could be confirmed histologically. Candidates were tested at E14 and at E19, E20, or postnatal day zero (P0). Chicks are precocial and fairly mature at hatching, so I predicted that expression patterns at these later stages would reflect adult-like expression. To my knowledge, only candidates #2 *ANOS1* and #11 *KCNH5* were previously described in chicken telencephalon (Soussi-Yanicostas et al. 1996, Dugas-Ford et al. 2012). I failed to recover cDNA fragments for 5 out of 70 candidate genes: #18 *VSTM2L*, #32 *JPH1*, #56 *SLC18A3*, #57 *IL1RAP*, and #64 *PCP4L1*. An additional 9 candidates were examined, but were not detected by ISH and may be RNAseq false positives: #7 *ABLIM2*, #21 *IL17RA*, #33 *LYPD6B*, #51 *BET3L*, #53 *WWOX*, #60 *P2RY8*, #66 *RAP1GDS1L*, #68 *MMP1*,

and #70 *PLCH2.* The remaining 56 candidate genes proved to be enriched in E and in some instances with great specificity.

SATB1

Candidate #1: Special AT-rich sequence binding protein 1 (*SATB1*) is the most highly expressed entopallium-enriched gene. It belongs to the CUT class of homeobox factors, a relatively small family including *CUX1, CUX2,* and *SATB2,* all of which are expressed in neocortex (Britanova et al. 2005, Szemes et al. 2006, Cubelos et al. 2010, Huang et al. 2011, Cubelos et al. 2015). The canonical SATB1 isoform contains 763 amino acids comprising an N-terminal oligomerisation domain, two matrix attachment regions (MAR), two DNA-binding CUT domains, and a C-terminal DNA-binding homeodomain. SATB1 performs numerous essential biological functions by regulating gene expression, chromatin looping, nucleosome positioning, and histone acetylation (Yasui et al. 2002, Cai et al. 2003, Cai et al. 2006, Yamasaki et al. 2007, Kohwi-Shigematsu et al. 2012). Previous studies reported *Satb1* expression throughout the mouse nervous system, including expression in neocortex (Huang et al. 2011, Balamotis et al. 2012).

At P0, chicken *SATB1* was intensely expressed in the input nuclei IHA (Figure 3.4a,b), E (Figure 3.4b), and Field L (Figure 3.4c). Expression was also found in cells scattered throughout HA, M, and N, but enrichment in input nuclei was clear. Adjoining sections from the same telencephalon are labeled with the previously characterized input cell marker *KCNH5* (Figure 3.4d,e,f). I conclude that *SATB1* labels the same cell populations identified by *KCNH5* staining, plus additional non-input cell types. Both genes were also found to be strongly expressed in Bas (Figure 3.4b,e).

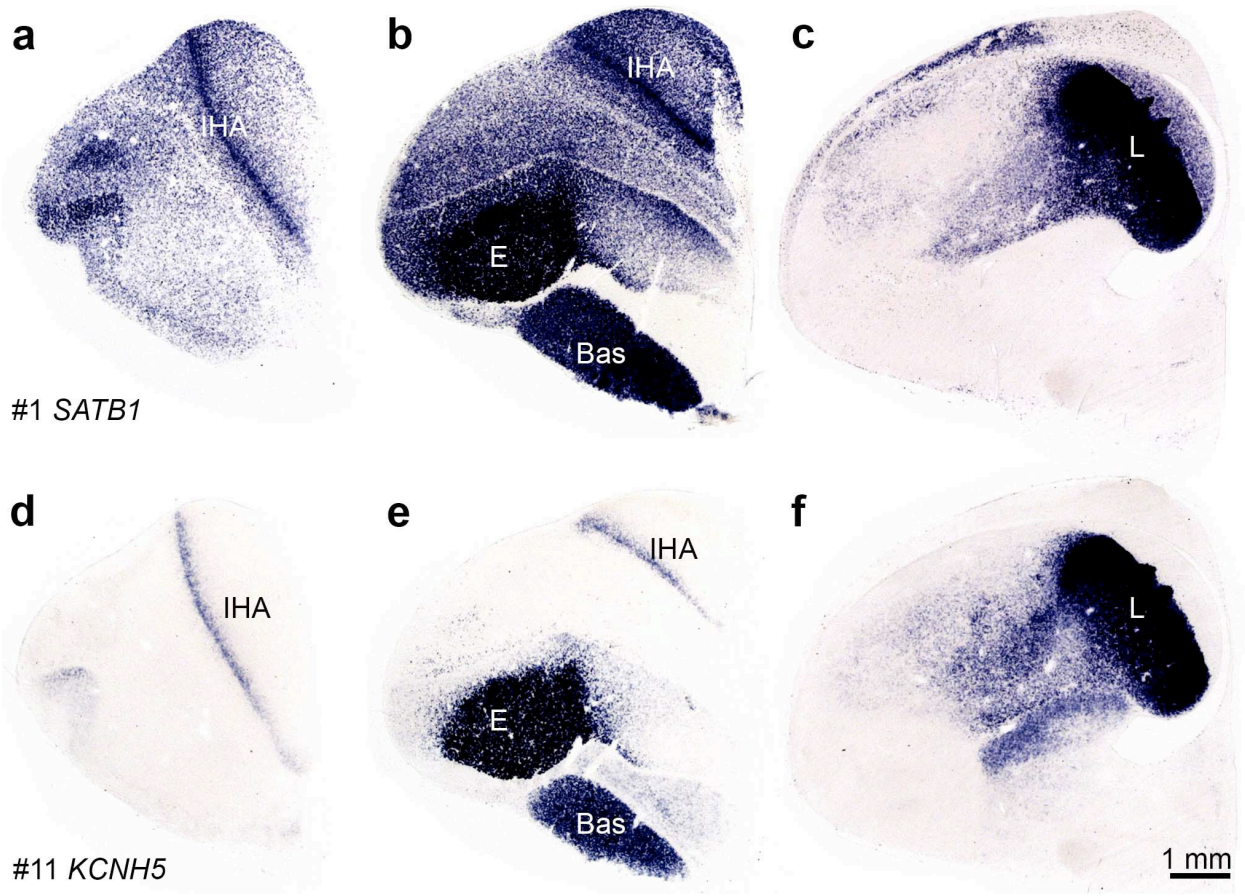

Figure 3.4 Candidate #1, Chicken *SATB1*, is enriched in dorsal telencephalon input territories
In situ hybridization for novel candidate **(a–c)** *SATB1* and known input marker **(d–f)** *KCNH5* on coronal sections from a single postnatal day zero telencephalon. Sections in **a** and **d** are most anterior, **c** and **f** are most posterior. Rows of sections are serially adjoining. *SATB1*, like *KCNH5*, is strongly enriched in the input nuclei **(a, b)** IHA, **(b)** E and Bas, and **(c)** L.

Other chicken candidates

Gene expression patterns for 20 additional entopallium HOLT candidates are shown in Figures 3.5 through 3.9. Each gene is presented at three anterior-posterior levels to show input nuclei labeled by that particular gene. All brains are from E14 chicken, except for #26 *TPBG* (Figure 3.8b) and #54 *SLC35F4* (Figure 3.9c), which are shown at P0.

Every gene expression pattern shown is unique. All 20 genes were found to be expressed in E, though there were substantial variations in labeling patterns. #26 *TPBG* (Figure 3.8b) and #53 *SLC35F4* (Figure 3.9c) were very specific in E, with sharp external borders. Other genes

extended their expression into the nidopallium surrounding E. Examples included #4 *DCBLD1* (Figure 3.5c) and #9 *C11ORF87* (Figure 3.6c). #8 *LINGO3* was more strongly expressed in external than in internal E (Figure 3.6b).

The HOLT approach was designed to detect E-enriched genes and did not filter according to Field L expression levels. Surprisingly, every E-enriched gene was also expressed in Field L. Marker genes of E and Field L often included a prominent bridge-like expression domain that reflects continuity of E with Field L in the anteroposterior axis (e.g. 3.6b, third section) (see also Dugas-Ford et al. 2012). Other differences in the morphology of Field L expression patterns across experiments were likely due to variations in level and plane of the section shown.

The receptor tyrosine kinase #43 *ROS1* (Figure 3.9a) and transcriptional regulator #69 *VGLL2* (Figure 3.9d) were both found to be expressed in a similar pattern. They were highly specific to both E and Field L, and at anterior levels they may label cells migrating into E. *ROS1*, *VGLL2*, and *DCBLD1* (Figure 3.5c) are chromosomally adjacent, a synteny conserved at least from humans to sharks (UCSC Genome Browser, https://genome.ucsc.edu/) (data not shown). This was the only example I found of chromosomal correspondence with input gene expression.

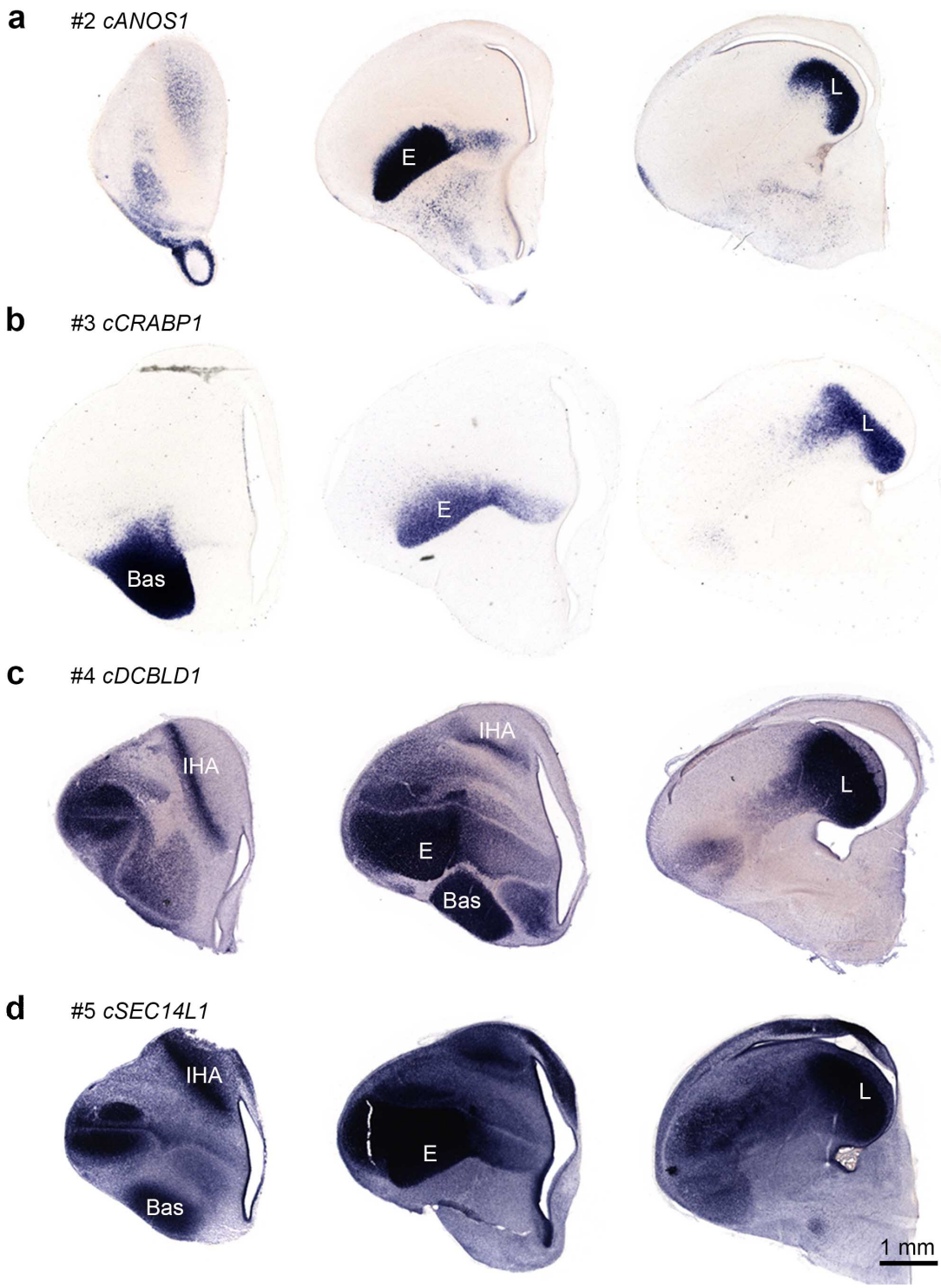

Figure 3.5 Novel chicken dorsal telencephalon input cell markers: Part 1
In situ hybridization for the entopallium HOLT candidates **(a)** #2 ANOS1, **(b)** #3 CRABP1, **(c)** #4 DCBLD1, and **(d)** #5 SEC14L1. Three sections arranged in anterior to posterior sequence are shown for each marker. Levels are not necessarily equivalent for each gene. All sections are from E14 telencephalon. The interstitial nucleus of the HA (IHA), nucleus basorostralis (Bas), entopallium (E), and Field L (L) are labeled.

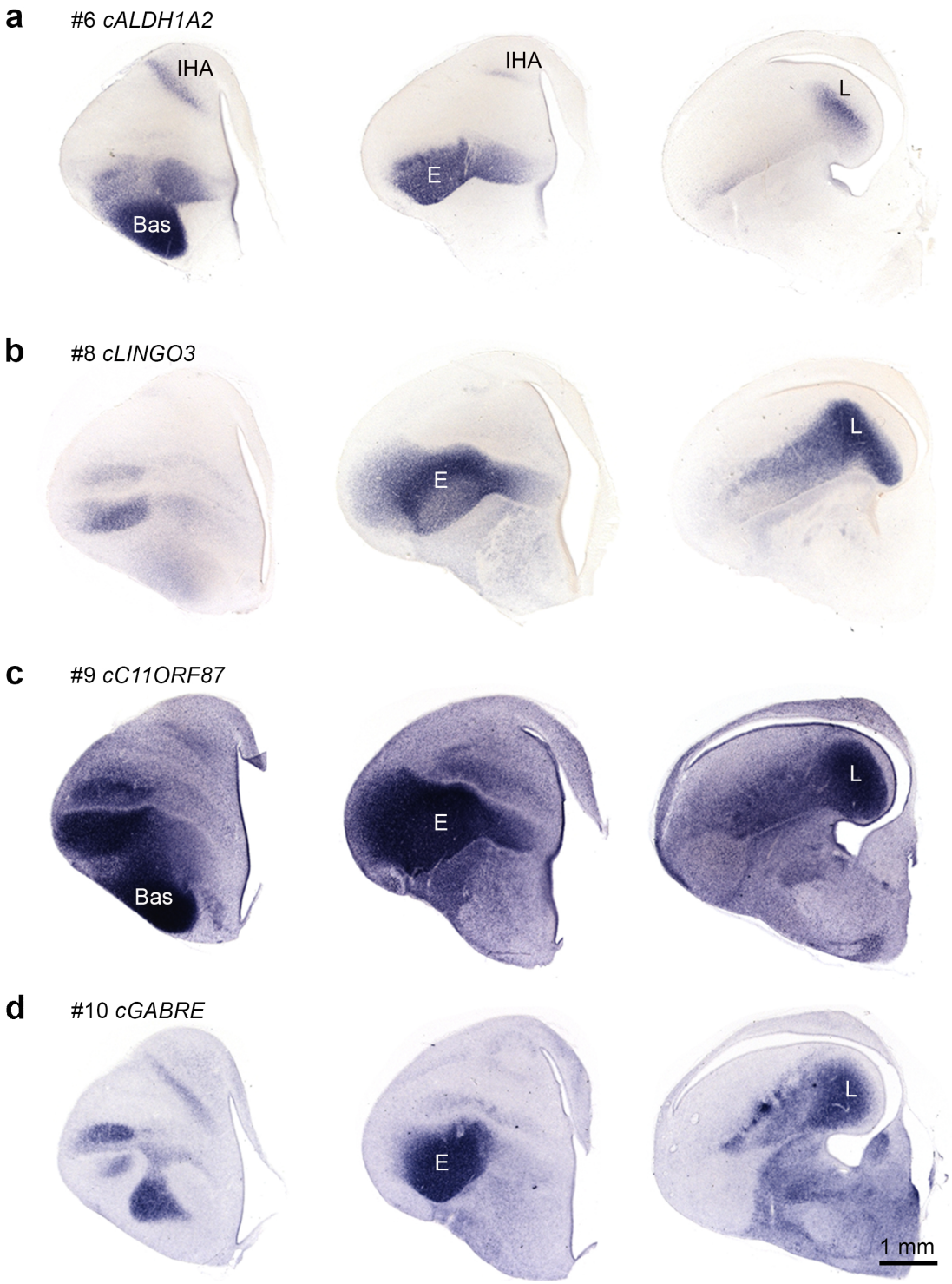

Figure 3.6 Novel chicken dorsal telencephalon input cell markers: Part 2
In situ hybridization for the entopallium HOLT candidates **(a)** #6 *ALDH1A2*, **(b)** #8 *LINGO3*, **(c)** #9 *C11ORF87*, and **(d)** #10 *GABRE*. Three sections arranged in anterior to posterior sequence are shown for each marker. Levels are not necessarily equivalent for each gene. All sections are from E14 telencephalon. The interstitial nucleus of the HA (IHA), nucleus basorostralis (Bas), entopallium (E), and Field L (L) are labeled.

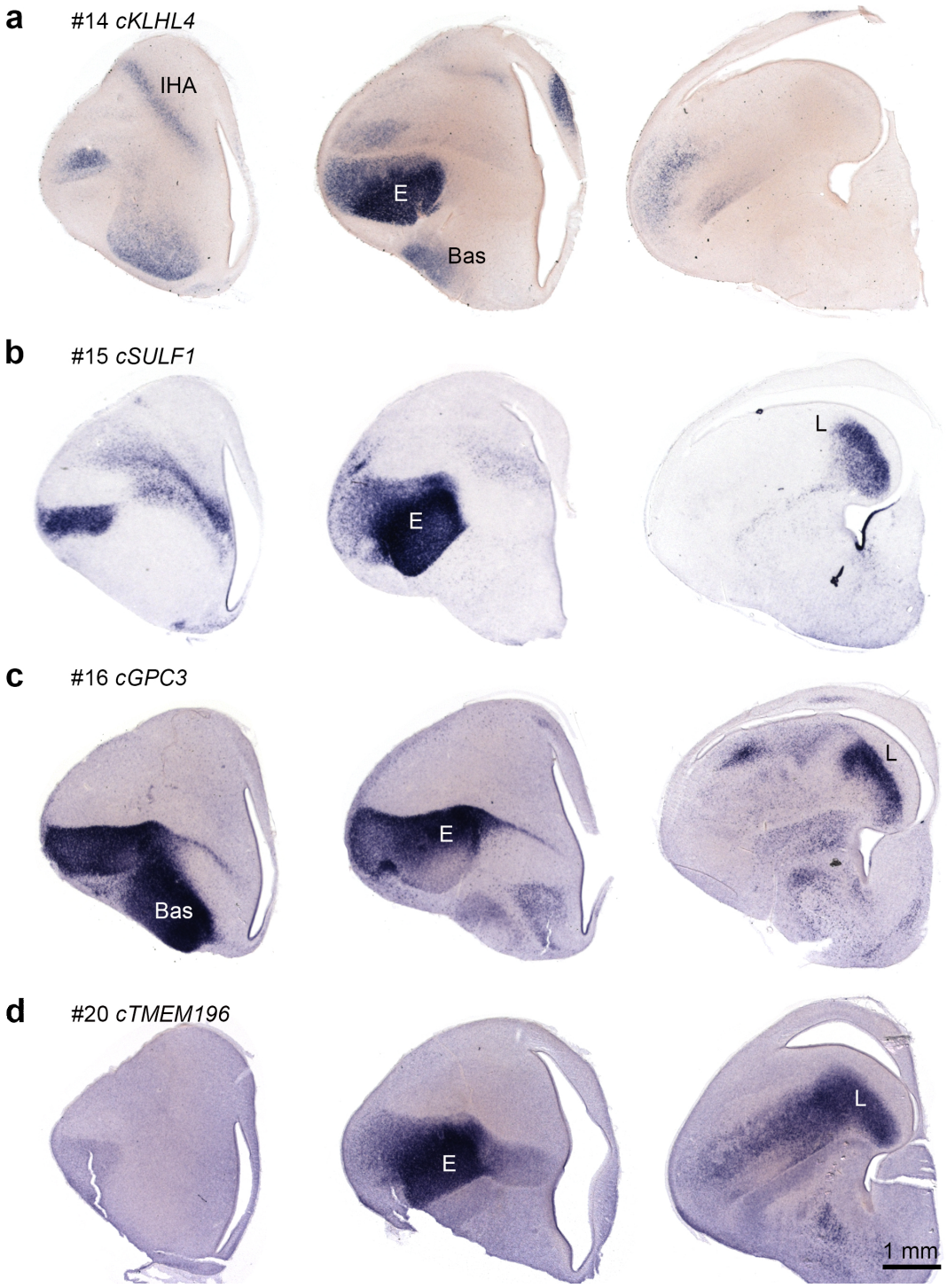

Figure 3.7 Novel chicken dorsal telencephalon input cell markers: Part 3
In situ hybridization for the entopallium HOLT candidates **(a)** #14 *KLHL4*, **(b)** #15 *SULF1*, **(c)** #16 *GPC3*, and **(d)** #20 *TMEM196*. *KLHL4* more strongly labels Field L at E20 (not shown). Three sections arranged in anterior to posterior sequence are shown for each marker. Levels are not necessarily equivalent for each gene. All sections are from E14 telencephalon. The interstitial nucleus of the HA (IHA), nucleus basorostralis (Bas), entopallium (E), and Field L (L) are labeled.

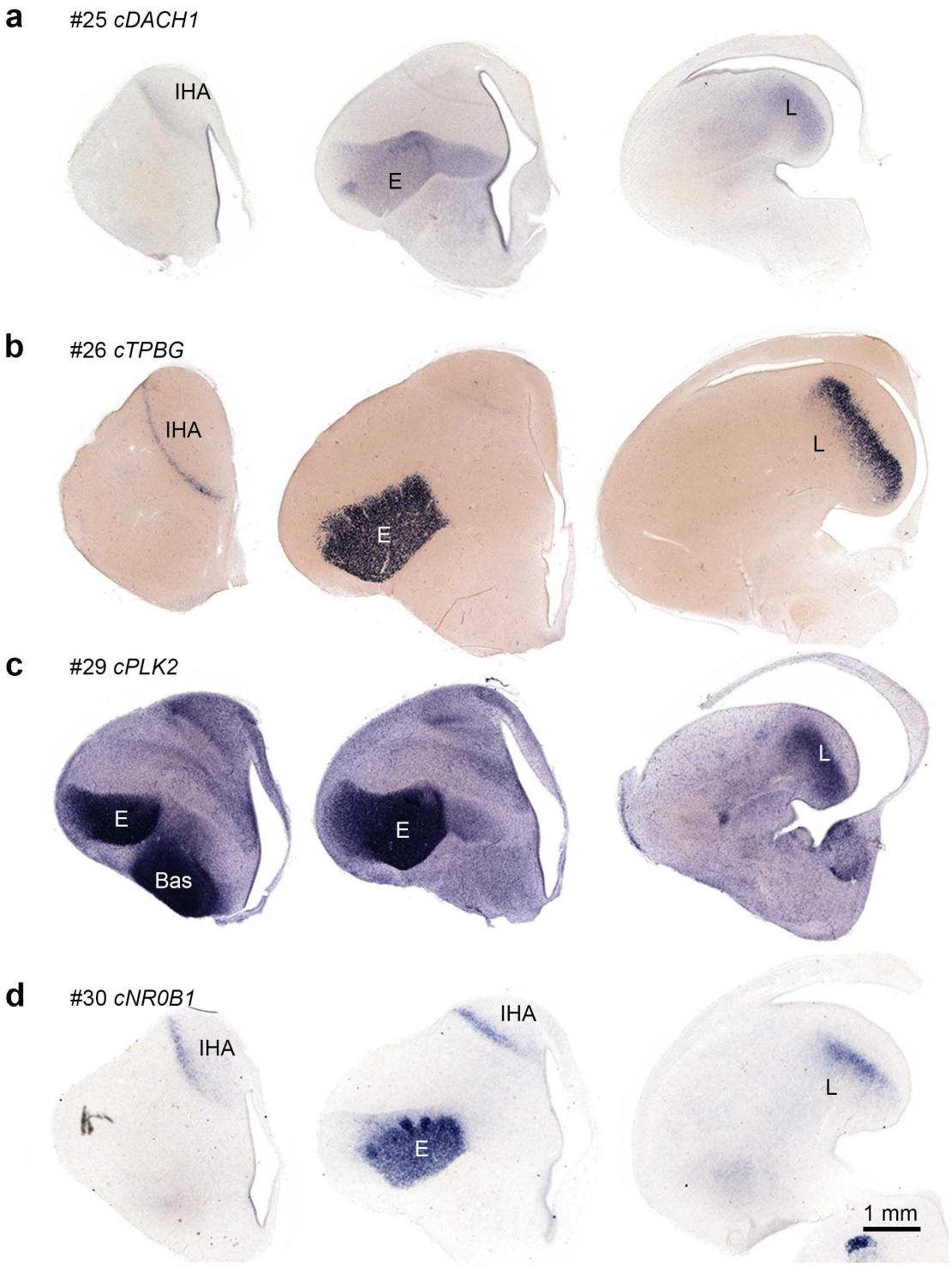

Figure 3.8 Novel chicken dorsal telencephalon input cell markers: Part 4
In situ hybridization for the entopallium HOLT candidates **(a)** #25 *DACH1*, **(b)** #26 *TPBG*, **(c)** #29 *PLK2* (**c**), and **(d)** #30 *NR0B1*. Three sections arranged in anterior to posterior sequence are shown for each marker. Levels are not necessarily equivalent for each gene. All sections are from E14 telencephalon, except for *TPBG,* which is shown at P0. The interstitial nucleus of the HA (IHA), nucleus basorostralis (Bas), entopallium (E), and Field L (L) are labeled.

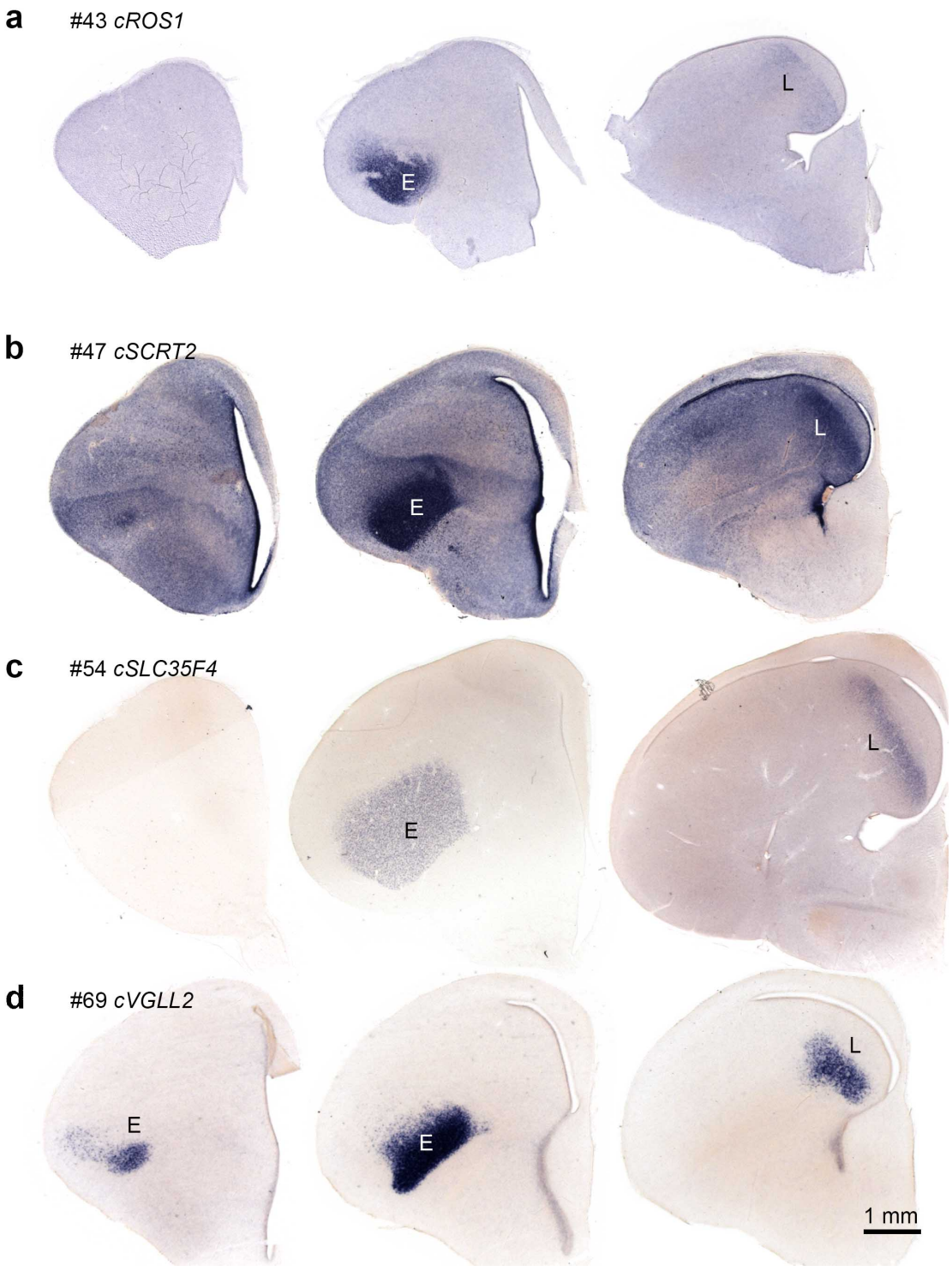

Figure 3.9 Novel chicken dorsal telencephalon input cell markers: Part 5
(Above) In situ hybridization for the entopallium HOLT candidates **(a)** #43 *ROS1*, **(b)** #47 *SCRT2*, **(c)** #54 *SLC35F4*, and **(d)** #69 *VGLL2*. Three sections arranged in anterior to posterior sequence are shown for each marker. Levels are not necessarily equivalent for each gene. All sections are from E14 telencephalon, except for *SLC35F4*, which is shown at P0. Entopallium (E) and Field L (L) are labeled.

Expression patterns occasionally included IHA, Bas, or both. Genes expressed in all four input nuclei (IHA, E, Field L, and Bas) included #1 *SATB1* (Figure 3.4a–c), #4 *DCBLD1* (Figure 3.5c), #5 *SEC14L1* (Figure 3.5d), #6 *ALDH1A2* (Figure 3.6a), #11 *KCNH5* (Figure 3.4d–f), #20 *TMEM196* (at E20, not shown), #25 *DACH1* (Figure 3.8a, Bas not shown), #26 *TPBG* (Figure 3.8b, Bas not shown), and #30 *NR0B1* (Figure 3.8d, Bas not shown). Genes such as these, with expression in multiple sensory input nuclei, are particularly interesting candidates for cross-species tests of input cell gene expression conservation.

SATB1 **is a conserved marker of dorsal telencephalon input cells in amniotes**

SATB1 is the most highly expressed input nucleus marker gene. It is present in four chicken DT sensory input nuclei and is likely to perform essential biological functions. I tested whether reptile and mammal DT input cells express *SATB1* orthologs. I tested for expression in adult turtle and in postnatal day 7 (P7) mouse neocortex, a stage roughly corresponding to the maturity of an E20 chicken telencephalon.

Turtles, like other reptiles, have a three-layered dorsal cortex. Excitatory pyramidal cells are most abundant in the middle, principal cellular layer. Anterior dorsal cortex in the turtle receives lemniscal visual information from the thalamus (Desan 1988, Ulinski 1990a), and the Ragsdale lab previously established the cells in this input region express the input cell markers *KCNH5* and *RORB* (Dugas-Ford et al. 2012). If *SATB1* is a conserved marker of input cells, I would expect to find turtle *SATB1* expression in anterior dorsal cortex. ISH experiments on adult red-eared slider (*Trachemys scripta elegans*) telencephalon confirmed this prediction: *SATB1* was strongly expressed in anterior dorsal cortex (Figure 3.10a, DC), but was expressed weakly in posterior dorsal cortex (Figure 3.10b). Labeling was restricted to the middle pyramidal cell layer, likely corresponding to excitatory cells (Figure 3.10c) (Connors and Kriegstein 1986).

Turtles have a second, tectofugal, visual projection from thalamic nucleus rotundus to an anterolateral DVR territory (Hall and Ebner 1970b, Hall and Ebner 1970a). The turtle DVR visual-recipient territory is referred to as the dorsal area (D) (Balaban 1978) and expresses the conserved input cell markers *KCNH5* and *RORB* (Dugas-Ford et al. 2012). Turtle D is likely homologous to the avian E. I established that turtle D expresses *SATB1* (Figure 3.10a, D). A higher power view demonstrates small, scattered clusters of *SATB1*(+) cells in turtle D (Figure 3.10d).

I confirmed strong expression of *Satb1* in mouse neocortex. *Satb1* expression was found in every neocortical layer, but *Satb1*(+) cells were particularly dense in L4 (Figure 3.10e). The rodent somatosensory whisker barrels are prominent L4 structures that form within the first postnatal week (Erzurumlu and Kind 2001, Jabaudon et al. 2012). Each blob-like barrel represents a population of L4 sensory input cells condensed around thalamocortical axons conveying sensory information from a single facial whisker. The barrels are useful cytoarchitectonic features for ascertaining L4 gene expression. A higher power view shows the dense *Satb1*(+) barrels in primary somatosensory cortex (S1) (Figure 3.10f).

Satb1 was also found to be expressed in a thin band of L4 cells across the neocortex, including primary motor cortex (Figure 3.10e, thin stripe in L4 medial to S1 whisker barrels). Consistent with this observation, previous studies reported L4-like gene expression and physiological properties in motor cortex (Rowell et al. 2010, Yamawaki et al. 2014). Many *Satb1*(+) cells scattered throughout L2/3, L5, and L6 are likely ventral telencephalon-derived inhibitory interneurons (Close et al. 2012, Denaxa et al. 2012), although some may be excitatory neurons as well. It is unknown whether any reptile or bird inhibitory interneurons express *SATB1*.

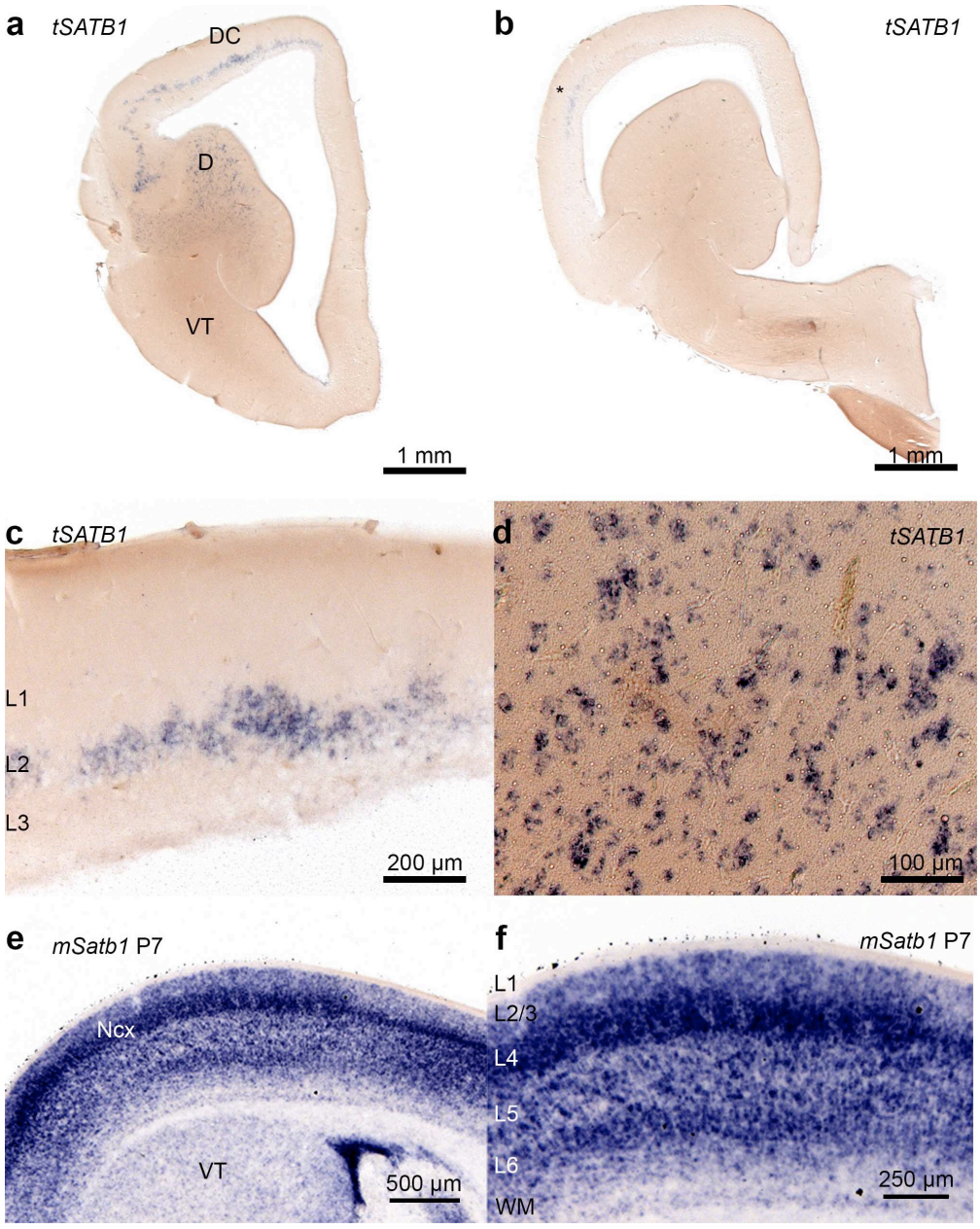

Figure 3.10 Turtle *SATB1* and mouse *Satb1* are expressed in input cells
In situ hybridization for turtle *SATB1* on **(a–d)** adult tissue and **(e, f)** mouse *Satb1* on P7 tissue. Reptiles have a three-layered dorsal cortex (DC) that receives lemniscal visual input to the middle layer (L2) in anterior regions. **(a, c)** This visual input area expresses *SATB1*. (**b**, asterisk**)** *SATB1* expression extends posteriorly and gradually thins to a narrow domain of weak expression. Turtles also have a tectofugal visual pathway that terminates in area D (D) of the dorsal ventricular ridge. **(a, d)** Visual area D expresses *SATB1*. **(e)** Mouse neocortex expresses *Satb1* in cells of every neocortical layer. **(f)** *mSatb1* expression is particularly strong in somatosensory whisker barrels in L4. Expression in other layers is probably attributable to inhibitory interneurons. Turtle and mouse ventral telencephalon (VT), turtle dorsal cortex layers (L1–L3), mouse neocortex (Ncx), mouse neocortex layers (L1–L6), and mouse neocortex white matter (wm) are labeled.

The transcription factors *NR0B1* and *RORA* are conserved input cell markers

NR0B1

Nuclear receptor subfamily 0 group B member 1 (*NR0B1*, or *DAX1*) is an unusual member of the steroid/hormone nuclear receptor superfamily. It is an orphan receptor containing a ligand binding domain, but lacks the DNA binding domain characteristic of most other family members. It binds to a variety of hormone receptors and forms homodimers with itself. It is transcriptionally regulated by and often co-expressed with *NR5A1* (or *SF-1*) (Achermann et al. 2001, Patel et al. 2001, Hoyle et al. 2002, Park et al. 2005).

At E14, I found that chicken *NR0B1* was expressed in the input nuclei IHA, E, Field L (Figure 3.8d) and Bas (not shown). At this stage, it is one of the most specific marker genes I identified. However, it appeared to be more evenly expressed throughout nidopallium by E20 (not shown).

Mouse *Nr0b1* is expressed at fairly low levels and it proved difficult to obtain high quality ISHs for this gene. It did not strongly label the S1 whisker barrels at P7. Instead, I found labeling in a dense L4 band immediately lateral to the barrels (Figure 3.11a). *Nr0b1* was probably absent from L5/6, but was expressed weakly in L2/3 (Figure 3.11a).

Nr0b1 expression and function require further characterization. Interestingly, chicken *NR0B1* contains 263 amino acids while mouse *Nr0b1* contains 472. My comparative analysis of NR0B1 sequence from mammals, reptiles, birds, amphibians, and fish indicated that eutherian mammals acquired an N-terminus NR0B1 expansion (it is absent from the monotreme platypus, *Ornithorhynchus anatinus*, and the marsupial koala, *Phascolarctos cinereus*. Data not shown.). This expansion contains four repeated nuclear receptor-binding domains involved in dimerization with NR5A1 (NCBI). A mouse *Nr5a1*-Cre line drives expression specifically in

neocortical L4 (Harris et al. 2014). Unfortunately, I was unable to isolate mouse *Nr5a1* cDNA to verify L4 expression. Chicken *NR5A1* is completely absent from the transcriptome data for any sample. Future studies should test whether neocortical *Nr5a1* expression is a mammalian novelty, and whether the eutherian-specific *Nr0b1* domain is functionally important in neocortex development. As *Nr0b1* and *Nr5a1* also regulate gonadal development, the expanded *Nr0b1* domain may also contribute to eutherian-specific reproductive biology. Interestingly, *Nr0b1* was relocated from an autosome to the X-chromosome in eutherian mammals, concomitant with its acquisition of the novel N-terminus domain (Stickels et al. 2015).

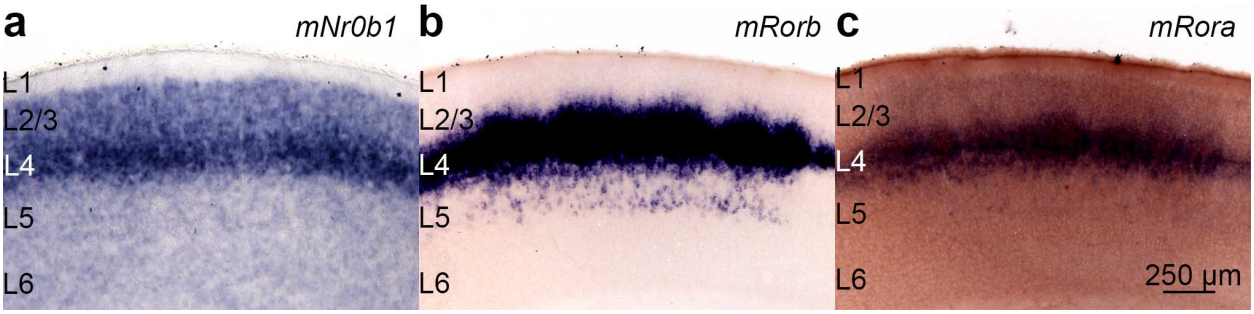

Figure 3.11 Mouse *Nr0b1* and *Rora* are expressed in neocortical layer 4
In situ hybridization for the mouse transcription factor genes **(a)** *Nr0b1*, **(b)** *Rorb*, and **(c)** *Rora*. *Rorb* and *Rora* sections are serially adjoining and thus depict approximately equivalent location in the neocortex. **(a)** *Nr0b1* does not strongly label the S1 whisker barrels, but does label L4 immediately lateral to the barrels. **(b)** *Rorb* and **(c)** *Rora* label the L4 barrels and scattered cells in L5. *Rorb* is expressed at significantly higher levels than *Rora*.

RORA

RAR related orphan receptor A (*RORA, NR1F1, RZRA*) is a representative nuclear receptor containing DNA-binding and ligand-binding domains. It is closely related to *RORB* (Jetten et al. 2001), and has well-characterized roles in the development of cerebellar Purkinje cells and in transcriptional regulation of the circadian clock (Dussault et al. 1998, Sato et al. 2004, Akashi and Takumi 2005, Boukhtouche et al. 2006a, Boukhtouche et al. 2006b, Chen et al. 2013b). Gene association studies identify human *RORA* as a risk locus for neuropsychiatric

conditions including autism and post-traumatic stress disorder (Sarachana et al. 2011, Logue et al. 2013, Devanna and Vernes 2014, Hu et al. 2015, Lowe et al. 2015).

Expression of *Rora* in mouse neocortical L4 was previously reported (Nakagawa and O'Leary 2003). ISHs on adjoining sections through P7 mouse telencephalon show that *Rora* is expressed in a nearly identical pattern to *Rorb*, although at far lower levels (Figure 3.11b,c). S1 whisker barrels are pictured, but both *Rorb* and *Rora* label L4 across the neocortex (not shown). *RORA* also appears to be strongly expressed in marmoset neocortical L4 (Riken Marmoset Gene Atlas, https://gene-atlas.bminds.brain.riken.jp/).

Chicken *RORA* was not identified by the HOLT method. ISH experiments performed at E14 (not shown) showed *RORA* is expressed at very low levels in input nuclei, as reflected by the low FPKM values in Table 3.2. However, *RORA* was robustly expressed at P0 (Figure 3.12a–c). ISHs on adjacent sections demonstrated that both *RORA* and *RORB* were expressed in similar patterns in IHA, E, Field L, and Bas (Figure 3.12).

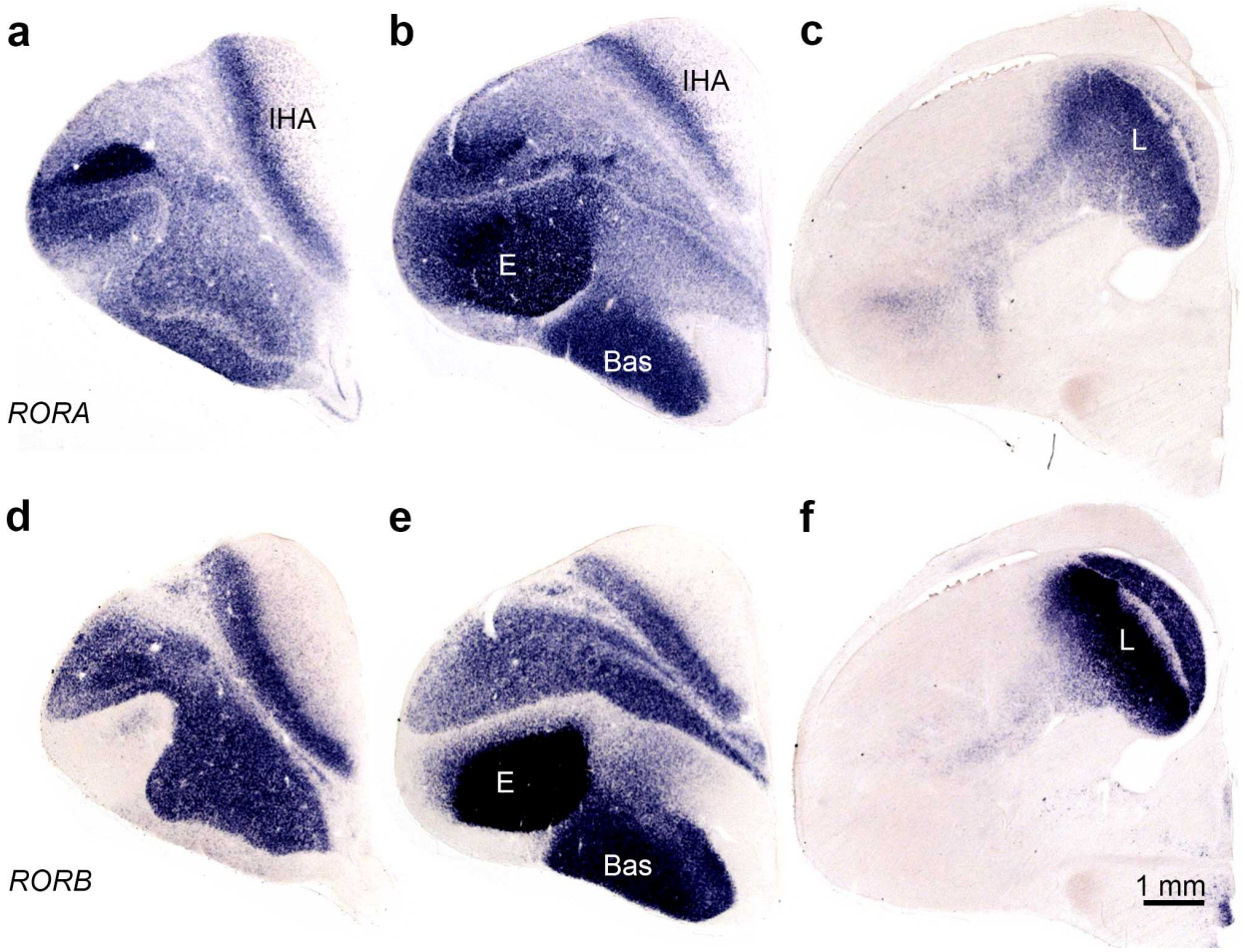

Figure 3.12 Chicken *RORA* is strongly expressed in dorsal telencephalon input territories at posthatch day zero
In situ hybridization for **(a–c)** novel candidate *RORA* and **(d–f)** known input marker *RORB* on coronal sections from a single posthatch day zero telencephalon. Sections in **a** and **d** are most anterior, **c** and **f** are most posterior. Rows of sections are serially adjoining. *RORA*, like *RORB*, is strongly enriched in the input nuclei **(a, b)** IHA, **(b)** E and Bas, and **(c)** L.

Expression patterns of other mouse orthologs

I chose 22 additional ISH-validated chicken input markers for analysis in mouse neocortex: #3 *CRABP1*, #4 *DCBLD1*, #5 *SEC14L1*, #6 *ALDH1A2*, #8 *LINGO3*, #10 *GABRE*, #13 *PPP1R17*, #14 *KLHL4*, #15 *SULF1*, #20 *TMEM196*, #23 *SLC25A47*, #25 *DACH1*, #26 *TPBG*, #29 *PLK2*, #31 *FNDC5*, #36 *STK31*, #37 *GRTP1*, #46 *ESRRG*, #50 *ZDHHC2*, #54 *SLC35F4*, #67 *MKRN3*, and #59 *VGLL2*. I found no neocortical expression for five of the mouse

orthologs: #4 *Dcbld1*, #10 *Gabre*, #13 *Ppp1r17*, #36 *Stk31*, and #69 *Vgll2*. #2 *Anos1* is absent from mouse and rat genomes. The remaining expression patterns are highly variable.

Six sample expression patterns are shown in Figure 3.13 to demonstrate the diversity of results. *Sec14l1* (Figure 3.13a) and *Plk2* (Figure 3.13e) were found to be expressed strongly in all neocortical layers. *Aldh1a2* was possibly expressed in meninges outside of the neocortex (Figure 3.13b). *Tmem196* was expressed in outer L2 and L6 (Figure 3.13c). Chicken *TPBG* was very specific to all input nuclei (Figure 3.8b), but mouse *Tpbg* was expressed in a complex multilayered pattern (Figure 3.13d).

The only non-transcription factor, L4-specific mouse ortholog I identified is *Slc35f4*. It was expressed at low levels, but labeling in S1 whisker barrels is clear (Figure 3.13f). No telencephalic expression domains were detected outside of neocortical L4. *Slc35f4* is a member of the solute carrier family and contains 10 helical transmembrane domains. Nothing is known with respect to the subcellular localization or function of this gene, but one previous study reported expression in the human brain (Nishimura et al. 2009).

The cassette-like expression of *ROS1*, *VGLL2*, and *DCBLD1* I found in chicken does not appear to be conserved in mouse, despite conserved chromosomal synteny. I was unable to isolate *Ros1* cDNA from mouse. *Vgll2* was absent from the neocortex at the developmental stages I examined (data for E18.6, P0, P4, and P6 not shown). *Dcbld2*, however, is expressed in mouse neocortical L4 (Allen Brain Atlas, http://www.brain-map.org/). Future studies should examine *DCBLD1* and *DCBLD2* expression in other species and test whether they can functionally substitute for one another. Chicken and mouse *DCBLD2* appear to share little synteny (UCSC genome browser).

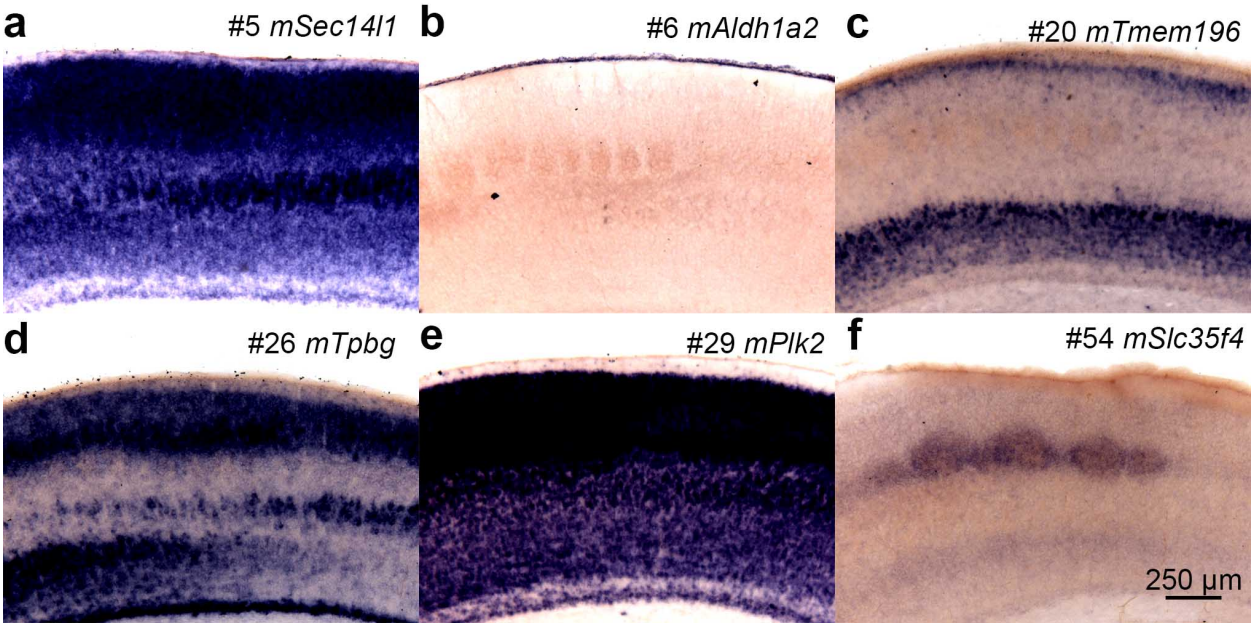

Figure 3.13 Mouse orthologs of chicken input markers are expressed in highly divergent patterns

In situ hybridization for six representative mouse orthologs of chicken input cell marker genes. Mouse orthologs are expressed in highly variable patterns: (**a)** #5 *Sec14l1* and **(e)** #29 *Plk2* are expressed in all neocortical layers. **(b)** #6 *Aldh1a2* is expressed outside of neocortex proper in the meninges. **(c)** #20 *Tmem196* is expressed in outer L2 and L6. **(d)** #26 *Tpbg* is expressed in L2/3, and opposing gradients in L5 and L6. **(f)** *Slc35f4* is expressed very specifically in L4 at low levels. Blob-like *Slc35f4*(+) structures are the S1 whisker barrels.

DISCUSSION

In this study, I report a forward RNAseq screen for novel, conserved marker genes of amniote DT sensory input cells. I identified, in an unbiased way, the 70 most highly expressed coding transcripts enriched in chicken E. In situ hybridization experiments established that many of these genes are expressed in E (and Field L), with others additionally expressed in IHA and Bas. I tested whether these marker genes are selectively expressed in mouse neocortical L4.

The most important finding was the conserved expression of *SATB1* and *RORA* in input cells. *SATB1* conservation is supported by gene expression experiments in chicken, mouse, and turtle. *RORA* conservation is supported by gene expression experiments in chicken, mouse, and

marmoset. Both *SATB1* and *RORA* are expressed in multiple characterized input cell populations in the alligator DT (Chapter 5). These data provide compelling additional molecular support for input cell homology in amniotes by increasing two conserved input cell marker genes to four.

I also found that *NR0B1* and *SLC35F4* are expressed in chicken and mouse DT input cells. These expression patterns may provide additional evidence for cell type homology, but convergence remains a plausible alternative explanation until additional outgroup species are examined. Alligator *NR0B1* was not detected by ISH, and alligator *SLC35F4* is restricted to the ventricular zone at late embryonic stages (data not shown).

The regulatory architecture of input cell genes

The diversity of gene expression patterns observed in this study is striking. Every novel marker shown in Figures 3.5 through Figure 3.9 is unique in some way, as are the many HOLT candidates not shown. This theme will be echoed in the expression patterns of mesopallium marker genes in Chapter 4. Even the conserved input marker genes *KCNH5*, *RORB*, *RORA*, and *SATB1* differ from one another and every non-conserved gene. It follows that expression of each gene in the telencephalon is controlled by a unique combination of transcriptional regulators and DNA cis-regulatory elements.

It is possible to divide total expression patterns into a collection of expression motifs. I define motifs as subdomains of expression reproducibly observed in the patterns of multiple genes. E and Field L are clear examples of motifs present in many gene expression patterns. Motifs, in turn, may be subserved by modular cis-regulatory elements, or enhancers. Evolutionary mixing of mobile enhancers at gene loci is a key mechanism by which gene expression patterns evolve (Davidson 2006).

The HOLT method I used in this study was directed toward detecting E-enriched transcripts, but I did not identify any E-unique transcripts. Instead, E and Field L expression motifs co-occurred in every instance. This may imply that a common enhancer element always drives expression in both input nuclei. For other genes, this enhancer may be joined by Bas or IHA enhancers to direct expression in some combination of input nuclei. A bioinformatics approach may be able to identify conserved regulatory sequences present at loci of multiple input marker genes. By comparing loci of all IHA-expressed genes with those excluded from IHA, one may uncover an IHA enhancer. If such enhancers exist for conserved input genes, they could be tested for conservation of function in mammals and birds. A similar approach was used to support homology of tetrapod digits and fish fin rays on the basis of conserved Hox gene enhancer function (Gehrke and Shubin 2016, Nakamura et al. 2016).

E and Field L differ from one another in location, morphology, and connections. It is unknown how these differences are produced given extensive shared gene expression. Genes that differentiate E and Field L may not be specific to either, but may instead appear in broad anterior or posterior domains. Such genes would not be identified by the present approach. A pairwise comparison of E and Field L transcriptomes may, however, uncover these hypothetical genes.

An interesting question for future research is whether multiple different enhancer elements can give rise to a common expression motif. Is the E expression motif of different marker genes regulated by common or by different mechanisms? The possibilities lie at two extremes. The first possibility is that every E-specific gene is regulated by an independent collection of signals and transcription factors. The second is that every E-specific gene is regulated by a single primary determinant transcription factor.

High-level regulatory genes, referred to as terminal selector genes, have been identified for multiple neuron classes in the nematode worm *C. elegans* (Hobert 2008, Hobert 2011, Hobert 2016). The transcription factor UNC-3, for example, is expressed in cholinergic motor neurons and directly controls a battery of motor neuron-specific effector genes (Kratsios et al. 2011). Mouse *Fezf2* is believed to act as a selector-like gene by specifying neocortical L5 output neurons during normal development, and is sufficient to do so in multiple ectopic contexts (Molyneaux et al. 2005, Rouaux and Arlotta 2010, Amamoto and Arlotta 2013, De la Rossa et al. 2013, Rouaux and Arlotta 2013, Arlotta and Hobert 2015). The diverse and complex expression patterns I observed suggest that regulation of input cell identity falls somewhere between the two extremes. I characterized four transcription factors that may together control input cell identity.

Cell-type homology and character identity networks

Characters found in different organisms are homologous if they are derived from the same character in their last common ancestor. Any type of character, at any hierarchical level of organization, can potentially have homologs in other species. Characters can be organs, sensory pathways, cell types, macromolecular complexes, and genes. The only requirements are similarity and historical continuity linking homologs to a common antecedent. Harvey Karten proposed that DT primary sensory input cells in neocortical L4 and avian Wulst and DVR are homologous at the level of cell type (Karten 1969). He argued that the similar types of connections these cells made could not be explained by independent evolution.

A character, such as a DT input cell, must be an independent unit of evolution that can develop and evolve separately from other parts of the organism. It must be able to express a collection of genes that allows for developmental differentiation. This collection of expressed genes may also undergo evolutionary change without changing the fundamental identity of the

character (e.g. input cell). A major finding of molecular evolutionary biology is that homologous cell type characters often express conserved transcription factors that permit differential gene expression during development and evolution (Wagner 2007, Arendt 2008, Carroll 2008, Shubin et al. 2009). For example, cartilage-synthesizing chondrocytes of protostomes and deuterostomes share expression of homologous Sox-family transcription factors (Tarazona et al. 2016). These factors may together comprise a "character identity network" (ChIN) that specifies cellular identity (Wagner 2007, Wagner 2014). The ChIN serves to recreate the character in successive generations, thereby underlying the historical continuity necessary for homology.

Homologs are the same thing in different organisms, but they are also different. This apparent paradox can be resolved by invoking the concepts "character" and "character state" (Fitch 2000). A character is the fundamentally similar thing compared across species. The forelimbs of whales and bats are homologous characters ("forelimb"). However, they take on very different character states: the whale forelimb is adapted into a paddle for swimming, while the character state of the bat forelimb is a wing. A DT input cell is a character that exists in different character states in mammals and birds: a cortical layer or a collection of nuclei, respectively. The character and character states of DT input cells may be reflected in the gene expression patterns observed in this study. Specifically, a conserved network of transcription factors may specify the DT input cell character, while differences in character states arise from the substantial divergence in effector genes.

Gene expression patterns are invisible to natural selection. Animals are selected for based on whether their behaviors facilitate survival and reproduction. Natural selection preserved the behaviorally essential ascending sensory projections to DT in mammals and birds. I propose that a conserved ChIN likely including RORA, RORB, NR0B1, and SATB1 transcription factors was

indirectly selected for because it is necessary for the development of DT cells that receive sensory input from thalamus and participate in DT circuitry (Figure 3.14). While loss of any of these transcription factors from the ChIN may compromise input cell development, downstream target genes can be lost or gained. It may be that the vast majority of target genes downstream of the input cell ChIN differ between mouse and chicken. The extensive differences I observed are fully compatible with homology of the input cell character, and should perhaps even be expected when comparing such dramatically different character states.

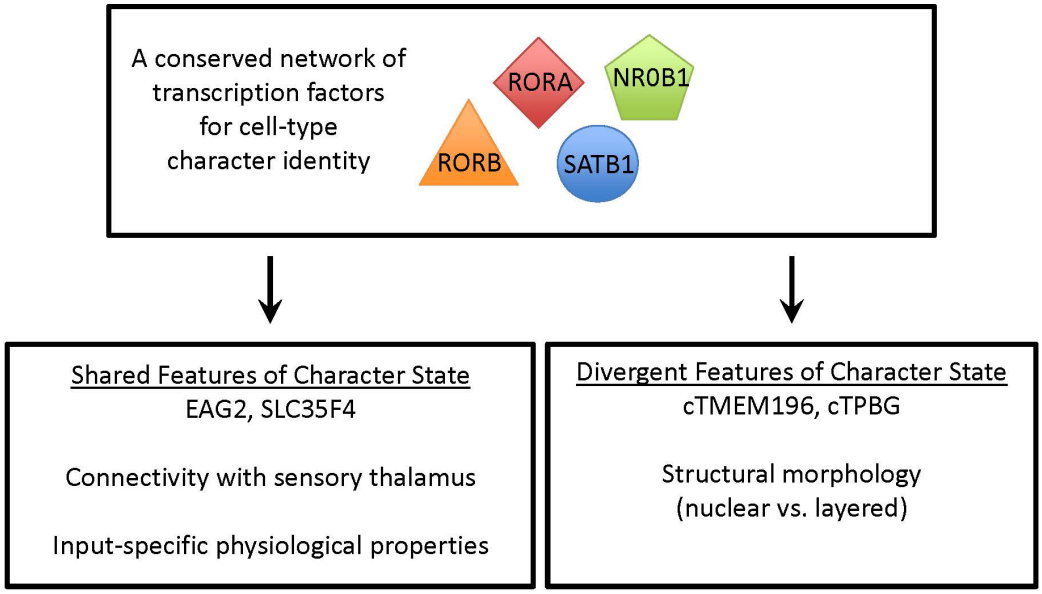

Figure 3.14 Character identity network (ChIN) model of input cell evolution
The last common ancestor of amniotes had DT input cells expressing at least four specific transcription factors: RORA, RORB, NR0B1, and SATB1. Expression of these transcription factors in DT input cells is highly conserved in multiple independent descendant lineages. I hypothesize these factors together form a gene regulatory network (GRN), or character identity network (ChIN), for input cell identity. The input cell ChIN may control the expression of effector genes that mediate the development and function of input cells. Some of these effector genes and functions may be conserved, like expression of KCNH5 and SLC35F4, connectivity with thalamus, and perhaps physiological characteristics of mature input cells. The ChIN may also control species-specific input cell characteristics. Divergence in target effector genes may contribute to species-specific anatomy, like organization of cells into layers versus nuclei.

Molecular manipulation studies are necessary in mouse and chicken to test whether any part of the proposed ChIN is necessary for regulation of DT input cell-type identity. *Rorb* was shown to regulate the clustering of whisker barrels found in L4 of the primary somatosensory

cortex (Jabaudon et al. 2012), but *RORB* has not been functionally tested in the chicken. *Satb1* is a particularly attractive candidate for gene manipulation experiments. *Satb1* is closely related to *Satb2*, which has well-studied roles in the development of mammalian neocortical callosal projection neurons (Alcamo et al. 2008, Britanova et al. 2008). Genetic studies have shown *Satb1* promotes the maturation of ventral telencephalon-derived inhibitory interneurons (Close et al. 2012, Denaxa et al. 2012). *Satb1* and *Satb2* have antagonistic functions in embryonic stem cells, raising the interesting possibility that they may regulate alternate cell fates in the telencephalon (Savarese et al. 2009). They are ancient and highly conserved genes, and their *Drosophila* ortholog *Defective proventriculus* (*Dve*) has multiple essential developmental functions (Shirai et al. 2007, Minami et al. 2012, Kiritooshi et al. 2014).

The transcription factor genes *RORA* and *RORB* were not recovered by the present experimental approach despite their enrichment in DT input nuclei. There may be other undetected transcription factors that work in combination with the input cell ChIN but are not restricted to input nuclei. My HOLT screen would have missed these factors. Additionally, there may be early acting but transiently expressed input cell determinants, or very late acting factors, which would not have been present in the E14 samples. Future studies should harvest tissue at earlier and later developmental stages. The novel marker genes described in this study could provide a genetic access point to DT input cells for fluorescence activated cell sorting (FACS) purification approaches.

CHAPTER 4

Comparative analysis of avian telencephalic association territories

ABSTRACT

The avian dorsal telencephalon has two vast territories, the nidopallium and the mesopallium, both of which have been shown to contribute substantially to higher cognitive functions. From their connections, these territories have been proposed as equivalent to mammalian neocortical layers 2/3 or various neocortical association areas, but whether these are analogies or homologies by descent is unknown. I investigated the molecular profiles of the mesopallium and nidopallium with RNA sequencing. Gene expression experiments show that the mesopallium, but not the nidopallium, shares a putative gene regulatory network with the intratelencephalic class of neocortical neurons, which are found in neocortical layers 2, 3, 5, and 6. Together with previous studies, these findings indicate that all major excitatory cell types of mammalian neocortical circuits—the layer 4 input neurons, the deep layer output neurons, and the multilayer intratelencephalic neurons—were present in the last common ancestor of birds and mammals.

INTRODUCTION

Examples of impressive cognitive abilities are relatively scarce in the animal world, despite a vast diversity of animal forms, behaviors, and nervous system anatomies (Roth 2015). The most familiar varieties of cognition are found in mammals. Elephants display sophisticated social structures, empathic behavior, and tool use (Bates et al. 2008). Aquatic mammals including sea lions and cetaceans (dolphins and whales) are similarly gifted (Marino 2004). Mammalian intelligence is invariably associated with the presence of a large and complex

neocortex, which is by far the largest structure of the human brain (Lui et al. 2011, Molnar and Pollen 2014) and attains astonishing proportions and folding complexity in elephants and cetaceans (Jacobs et al. 2011, Butti et al. 2015).

Less familiar are the cognitive abilities of birds, which went underappreciated and misinterpreted until the mid-20th century (Ariëns Kappers et al. 1936, Reiner et al. 2004a, Striedter 2005). Birds have large brains relative to body size, and avian brains are packed with neurons at a density greater than that of the primate brain (Iwaniuk et al. 2005, Olkowicz et al. 2016). Large, cell-dense brains likely allow some birds to perform cognitively demanding tasks with skill rivaling that of primates (Balakhonov and Rose 2017): they manufacture and use tools to solve problems (Weir et al. 2002, Auersperg et al. 2012), can recognize themselves in a mirror (Prior et al. 2008), and can communicate vocally (Pepperberg 1999, Jarvis 2004).

Birds are not mammals, but are instead descendants of archosaur reptiles, a group including living crocodilians and extinct dinosaurs (Zhang et al. 2014, Brusatte et al. 2015). Neither birds nor reptiles possess a six-layered neocortex, the neuroanatomical hallmark of all extant mammals. In place of a laminar structure, the bird dorsal telencephalon (DT) contains nuclear territories of clustered neuronal cell bodies. The DT is organized into two main subdivisions: the Wulst and the dorsal ventricular ridge (DVR) (Reiner et al. 2004b). The DVR is subdivided into mesopallium, nidopallium, and arcopallium (Reiner et al. 2004a, Jarvis et al. 2013). Whether any of these bird DT territories is homologous to neocortex is a longstanding problem in evolutionary neuroscience (Dugas-Ford and Ragsdale 2015), though it is clear that bird intelligence does not require a laminated neocortex (Kirsch et al. 2008).

Bird intelligence may, however, arise from neural circuitry fundamentally similar to that of the neocortex. The bird DT, like the neocortex, receives unimodal visual, auditory, and

somatosensory input from dorsal thalamic axons (Figure 4.1, green territories and black axons). The targets of ascending sensory information in the bird are clearly delimited nuclei, whereas the neocortex receives sensory information primarily through neocortical layer 4 (L4). Information output from the bird DT arises from cells in the arcopallium (A) and the hyperpallium apicale (HA) (Figure 4.1, red) that project to brainstem motor centers, and are functionally similar to the subcortical projection neurons of neocortical L5. These cross-species similarities in functional connectivity led Harvey Karten to propose that input and output neurons of mammals and birds are homologous at the cell-type level (Karten 1969). Work from the Ragsdale laboratory provided strong support for the cell-type homology hypothesis by demonstrating input and output cells express conserved molecular marker genes: input cells are enriched for expression of *KCNH5*, *RORB*, *RORA*, and *SATB1* (Chapter 3), while output cells express other markers including *FEZF2*, *CACNA1H*, and *SULF2* (Rowell et al. 2010, Dugas-Ford et al. 2012). It is likely that input and output cells, along with their characteristic connectivity and gene expression patterns, were inherited from the last common ancestor (LCA) of amniotes.

Most of the bird DT is neither strictly input nor output in terms of function and connectivity. Two large territories, the nidopallium and the mesopallium, extend across the anteroposterior and mediolateral extent of the bird DT. These territories are not the targets of primary sensory information, and their axonal projections do not leave the telencephalon (Atoji and Wild 2009, Atoji and Wild 2012). Their functions can be described as associational: they contribute to the integration of multiple sensory modalities and perform higher-order information processing.

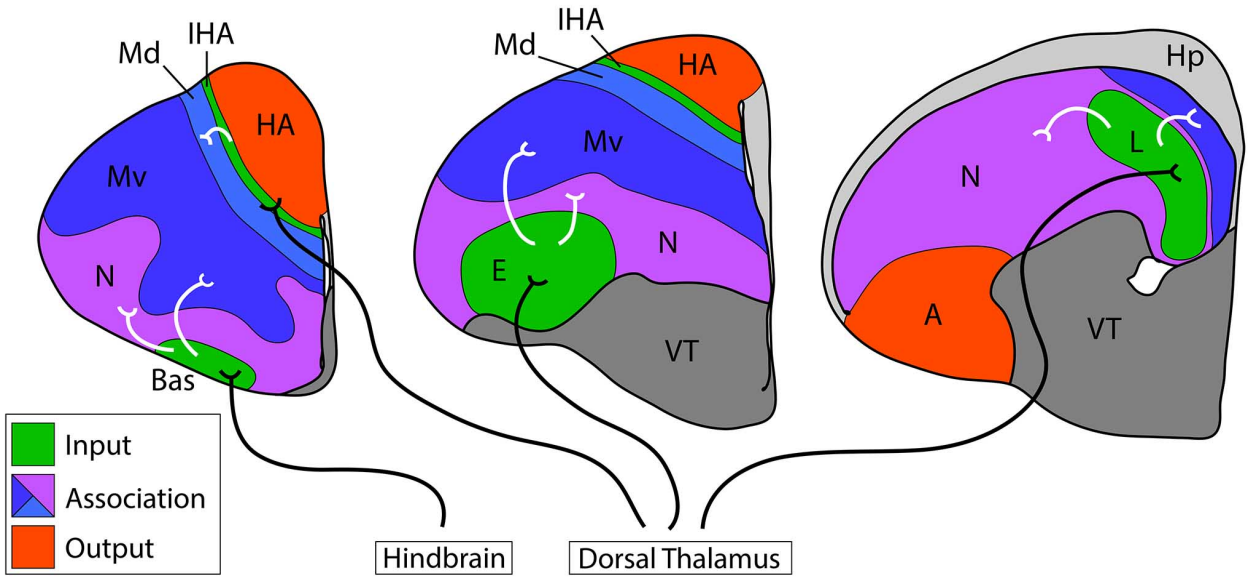

Figure 4.1 Connectional anatomy of the avian dorsal telencephalon
Three sections through chick telencephalon are shown in series. Primary input cell populations are shaded in green. The entopallium (E) receives visual information from the dorsal thalamus. Field L (L) receives auditory information from the dorsal thalamus. The interstitial nucleus of the hyperpallium apicale (IHA), located in the Wulst, receives visual and somatosensory information from the dorsal thalamus. The unusual nucleus basorostralis (Bas) receives trigeminal somatosensory information directly from the hindbrain without a thalamic synapse, but this nucleus expresses markers of input cell identity and is categorized with other input populations. Sensory information input pathways are represented by black axons. The dorsal mesopallium (Md) of the Wulst (light blue), ventral mesopallium (Mv) of the dorsal ventricular ridge (dark blue), and nidopallium (N, purple) receive secondary sensory information from primary input populations, represented by white axons. Output populations are red. Other dorsal telencephalon territories are light gray (e.g., hippocampus, Hp) and the ventral telencephalon is dark grey.

Mesopallium

The mesopallium was classically called the hyperstriatum ventrale and has long been considered a DVR structure (Ariëns Kappers et al. 1936). It appears at far anterior levels of the DVR, with its ventral border at the nidopallium and dorsal border at the Wulst, and gradually retreats towards the ventricle medially in the posterior DVR (Figure 4.1, dark blue). Ventral Wulst was classically divided into hyperpallium densocellulare (HD) and hyperpallium intercalatum (HI), but recent molecular studies show that ventral Wulst expresses many genes characteristic of the DVR mesopallium (Chen et al. 2013a, Jarvis et al. 2013). These studies suggest the mesopallium has a bi-partite organization, with a dorsal mesopallium (Md) in the

Wulst (Figure 4.1, light blue) abutting a ventral mesopallium (Mv) in the DVR (Figure 4.1, dark blue).

Md and Mv are similar in that they form a link between primary input and other DT cell populations. Mv receives afferents from the DVR input territories nucleus basorostralis (Bas) (Veenman and Gottschaldt 1986, Dubbeldam and Visser 1987), the entopallium (E) (Krutzfeldt and Wild 2004, Krutzfeldt and Wild 2005), and Field L (L) (Bonke et al. 1979, Atoji and Wild 2012) (Figure 4.1, white axons into Mv). Mv sends efferents to the arcopallium and nidopallium, especially to the caudal nidopallium (Figure 4.1, purple in third section) (Atoji and Wild 2012). Md receives afferents from the interstitial nucleus of the hyperpallium apicale (IHA), the primary Wulst input population (Nakamori et al. 2010). Efferent connections of Md are poorly understood, partly as a result of inconsistent use of nomenclature for ventral Wulst.

Nidopallium

The nidopallium, formerly called the neostriatum (Reiner et al. 2004a), is a heterogeneous structure with connectional similarities to the mesopallium. It is defined as the territory above the striatum, with the mesopallium at its dorsal border. It gradually displaces the mesopallium in posterior DVR until it occupies most of the cerebral wall (Figure 4.1, purple). At posterior levels it forms a border with the arcopallium ventrally (Figure 4.1, A in red). The nidopallium contains both input and associational cell populations. The input nuclei Bas, E, and Field L are embedded within the nidopallium as subnuclei. The remainder of the nidopallium, however, does not receive direct primary sensory input but instead receives secondary information from Bas (Veenman and Gottschaldt 1986, Dubbeldam and Visser 1987), E (Krutzfeldt and Wild 2004, Krutzfeldt and Wild 2005), and Field L (Brauth and McHale 1988).

Its caudal division is heavily interconnected with the mesopallium and projects to the nearby arcopallium (Atoji and Wild 2009).

The mesopallium and nidopallium are believed to contribute substantially to avian cognition, learning, and memory (Salzen et al. 1975, Salzen et al. 1979, Horn 1985, Johnson and Horn 1987). Their proportions are striking already in the relatively small-brained and basally branching chicken, and they are expanded and elaborated in large-brained birds including parrots and owls (Karten et al. 1973, Jarvis and Mello 2000). This expansion is analogous to neocortical expansion of association areas in large-brained mammals. Specifically, as the neocortex expands through phylogeny, not all neocortical areas expand equally. Rather, associative areas, or those areas intercalated between primary sensory and motor areas, come to occupy increasing proportions of total cortical surface area (Nieuwenhuys et al. 2008). Likewise, mesopallium and nidopallium enlarge to a greater extent than primary sensory input nuclei such as E (Rehkamper et al. 1991). Selective expansion of associative telencephalic territories may represent a common mechanism for the evolution of higher cognitive functions in birds and mammals.

Homology hypotheses

Numerous homologies of the mesopallium and nidopallium have been proposed based on differing criteria. One group of researchers argues the mesopallium is homologous to temporal neocortex based on their similar positions in lateral DT (Karten 1997, Reiner et al. 2005, Butler et al. 2011). A second view proposes the mesopallium is homologous to neocortical L2/3 neurons based on shared intratelencephalic connections and gene expression (Suzuki and Hirata 2012, Suzuki et al. 2012, Suzuki and Hirata 2013). These two camps both compare the mesopallium to neocortex, but the former view suggests the homology is to areas, while the second compares the mesopallium to layers. Other researchers note the nidopallium and

mesopallium are nuclear territories in ventral DT, adjacent the ventral telencephalon. They argue the nidopallium and mesopallium are not comparable to neocortex at all, but are instead homologous to subcortical nuclei in the piriform lobe. Bruce and Neary suggest both nidopallium and mesopallium are homologous to amygdala (Bruce and Neary 1995). Puelles and colleagues most recently claim the nidopallium is homologous to amygdala and the mesopallium is homologous to the claustrum (Puelles et al. 2016a).

Arguments of homology based on morphology, topology, and connections have brought this debate to a stalemate. I interrogated the molecular profiles of mesopallium and nidopallium with RNA sequencing and in situ hybridization. I found that the mesopallium is a coherent territory with shared molecular properties, and provide extensive additional evidence for the division of mesopallium into a DVR sector (Mv) and Wulst sector (Md) abutting the IHA. I identified six transcription factors highly enriched in Md and Mv and further show that five of these transcription factors are expressed by mouse neocortical intratelencephalic (IT) neuronal populations. I propose mesopallium is homologous to IT cells, found in multiple neocortical layers and areas, rather than to any particular neocortical area or layer. Fate mapping experiments in the chicken demonstrate mesopallium IT cells arise from a fate-restricted territory in anterodorsal telencephalon, a developmental mechanism quite distinct from the columnar, sequential specification of cells in the neocortex.

The nidopallium, despite superficial connectional similarities to mesopallium, has a distinct molecular profile. I failed to identify any additional transcription factor markers of this territory beyond the single previously known gene *DACH2* (Szele et al. 2002). I show that mouse *Dach2* is expressed in a cryptic cell population in L5 requiring further study. I suggest

nidopallium is a heterogeneous mixture of molecularly distinct cell types, and may not be homologous to any single cell type or structure in the mammalian DT.

RESULTS

HOLT analysis of the mesopallium transcriptome

In order to test whether the mammalian DT contains homologues of avian DT association territories, I first set out to establish a panel of molecular markers for chicken mesopallium and nidopallium. Marker genes can then be used to test for homology in mammalian DT. Tissue was collected from seven territories in E14 chicken DT: rostral mesopallium (M); caudal nidopallium (N); the input populations E, Field L, and Bas; and the output populations HA and A (see Figure 3.1). Purified RNAs from these tissues were submitted for Illumina RNA sequencing. Reads were assembled using Trinity software.

To identify genes restricted to mesopallium and nidopallium, I employed the HOLT (High-to-Low Ordering of Like Transcripts) method. In each case, I found that one or two pair-wise comparisons of gene expression abundance were sufficient to identify marker genes. For mesopallium, I first selected only those transcripts expressed at 2.5 fold greater fragments per kilobase of transcript per million mapped (FPKM) values in M compared to A. This filtered 356,804 total transcripts to 38,922 (Table 4.1). From these transcripts, I selected those that are expressed at 2.5 fold greater levels in M compared to E. This operation resulted in 26,764 transcripts. To identify genes expressed at high levels, I ranked transcripts in descending order of expression in M and selected only those transcripts expressed at 5 FPKM or higher. I determined that 5 FPKM is around the threshold of detection by ISH (data not shown). The vast majority of total transcripts are expressed below 5 FPKM and are likely undetectable by in situ hybridization

(ISH). To perform comparative gene expression across species, it is necessary to identify homologous transcripts. I filtered out all non-coding transcripts, as these are more likely to diverge across species. These cumulative filters resulted in a final number of 78 highly expressed coding transcripts enriched in the M compared to input and output cell populations (Table 4.1).

Table 4.1 Progressive HOLT filters for mesopallium-enriched transcripts

Sequential Filters	# of Transcripts
1) All Transcripts	356,804
2) Mesopallium/Arcopallium ≥ 2.5	38,922
3) Mesopallium/Entopallium ≥ 2.5	26,764
4) Abundance ≥ 5 FPKM, Coding	78

I first selected transcripts enriched in M compared to A by 2.5 fold. From these, I selected transcripts enriched in M compared to E by 2.5 fold. Then, I ranked transcripts in descending order of expression and selected coding transcripts expressed at 5 FPKM or greater.

The top 78 mesopallium HOLT candidates are ordered by FPKM value in Table 4.2, with transcriptional regulators in bold. The experimental approach recovered 9 previously examined genes. #4 *SATB2* was described by the Hirata group (Suzuki et al. 2012). This important transcription factor will be examined in detail later. #5 *CCK* was described by Atoji and Karim (Atoji and Karim 2014). While highly expressed in the mesopallium, it is found throughout much of the DT and does not resolve mesopallium homology as the authors suggest (data not shown). #8 *GRM4*, #11 *FOXP1*, #17 *CADPS2*, #21 *GRIK3*, and #28 *SCUBE1* were described by the Jarvis group, and all of these genes are largely restricted to mesopallium (Jarvis et al. 2013). #48 *DRD5* was first described by Sun and Reiner (then referred to as "D1B") and may represent the first known molecular marker of the mesopallium (Sun and Reiner 2000, Reiner et al. 2004a). #54 *NR4A2* was described by Puelles and colleagues (Puelles et al. 2016a, Watson and Puelles 2017). They refer to this gene as a mesopallium marker, but it is expressed in only a small part of mesopallium in addition to other DT territories. One known mesopallium marker gene, *EMX1*,

was not recovered from this screen due to its expression in the arcopallium but is included at the bottom of Table 4.2 (Fernandez et al. 1998). The remaining 69 genes are novel candidates.

Table 4.2 Mesopallium HOLT candidates

The 78 most abundant mesopallium-specific genes are listed by descending levels of expression. Transcriptional regulator genes are bolded. *EMX1* was not recovered by the HOLT method but is included at the bottom of the list.

Rank	Gene	M	A	E	N
1	*MPPED1*	151.10	52.63	37.79	44.92
2	*CHL1*	122.39	47.00	40.31	41.88
3	***ID2***	119.20	39.97	29.90	25.74
4	***SATB2***	85.02	8.94	17.31	10.42
5	*CCK*	83.60	7.06	3.43	5.03
6	*RSPO3*	73.26	7.77	13.07	7.58
7	***NHLH2***	69.82	13.42	6.72	4.44
8	*GRM4*	68.87	27.08	20.09	33.79
9	*PROKR2*	67.55	3.57	11.90	4.63
10	*PHF24*	63.29	17.23	20.71	22.67
11	***FOXP1***	55.39	10.53	10.95	13.07
12	*PVALB*	53.53	16.21	19.97	21.24
13	***BCL11A***	50.33	11.49	9.33	15.74
14	*PDE1A*	49.64	18.30	19.56	17.65
15	*KEL*	42.43	13.00	9.18	23.18
16	*RGS20*	39.90	8.06	9.96	9.36
17	*CADPS2*	36.88	9.59	6.36	6.99
18	*KIT*	33.68	6.87	4.98	3.08
19	*HS3ST4*	33.28	4.26	10.70	5.96
20	*NTSR1*	32.73	7.67	10.47	8.43
21	*GRIK3*	30.35	8.15	11.12	10.18
22	*CHN2*	30.32	7.80	9.66	7.19
23	*OPRL1*	29.92	10.73	8.55	9.68
24	*ADARB2*	29.12	10.05	6.11	10.03
25	*NPNT*	28.97	9.71	6.56	8.05
26	*OPRK1*	26.99	4.06	4.25	4.73
27	***TFAP2D***	25.92	6.55	10.27	7.00
28	*SCUBE1*	21.86	6.52	8.17	5.71
29	*KCNJ5*	20.74	6.11	7.66	5.37
30	*ANTXR1*	18.76	1.67	4.65	2.82
31	*BTBD11*	16.86	3.99	3.90	1.61
32	*SEMA3C*	16.43	3.80	0.75	2.40

Table 4.2, continued

Rank	Gene	M	A	E	N
33	***TLE4***	16.17	6.34	5.36	6.48
34	***PKIB***	15.27	3.82	4.75	4.57
35	*KCTD4*	15.08	4.92	4.04	2.55
36	*CRLS1*	13.86	4.84	0.87	2.01
37	*CLMN*	13.78	5.33	3.13	3.49
38	*RXFP3*	13.18	0.78	1.37	1.19
39	*SAMD14*	12.08	4.00	4.33	10.69
40	***BHLHE40***	11.72	3.57	3.10	4.01
41	***FOSL2***	11.60	2.17	0.26	1.17
42	*DRD5*	11.27	1.43	2.46	3.37
43	*LRFN2*	10.91	3.02	2.02	3.08
44	*NTNG2*	10.74	2.11	1.62	1.44
45	***ATOH8***	9.86	3.04	3.72	2.79
46	*HTR1E*	9.39	2.53	1.61	2.06
47	*VIP*	9.29	3.63	1.48	1.75
48	*H1FX*	9.28	3.64	1.37	5.33
49	*TBXAS1*	9.27	2.38	2.72	2.30
50	*COL9A1*	9.08	2.79	3.43	3.13
51	*FDX1*	8.61	3.21	3.09	8.25
52	***NR4A3***	8.57	3.18	0.67	2.28
53	*SLC2A9*	8.49	2.26	3.30	2.22
54	***NR4A2***	8.24	1.86	0.27	0.68
55	*SLITRK3*	8.24	0.70	1.17	1.26
56	*AAR2*	8.10	1.99	1.13	3.11
57	*IFFO1*	7.92	3.16	2.14	3.92
58	*OPN1SW*	7.91	1.22	1.96	3.26
59	*KL*	7.84	0.76	0.73	0.40
60	*ABHD14B*	7.46	2.94	1.54	4.90
61	*KCNF1*	7.33	2.10	2.17	2.23
62	*GAP43*	7.16	2.86	1.93	6.10
63	*PRKCQ*	7.15	2.15	1.47	1.23
64	*F8A3*	6.27	2.21	2.31	3.48
65	*IFITM10*	6.24	1.33	1.74	2.58
66	*MANBAL*	6.05	1.45	1.63	0.87
67	*EXOSC6*	5.96	1.91	1.61	2.56
68	*ASIP*	5.95	1.65	2.11	0.99
69	*PPID*	5.83	1.55	1.75	3.40
70	*C14H16ORF73*	5.76	0.68	1.50	0.58
71	*FAM198B*	5.73	2.01	1.02	2.31

Table 4.2, continued

Rank	Gene	M	A	E	N
72	*TANC1*	5.70	2.23	1.49	2.41
73	*TCP10*	5.63	0.37	0.55	0.33
74	*APELA*	5.54	2.17	0.77	0.67
75	*SAMD11*	5.44	1.75	1.30	0.26
76	*EFNA2*	5.37	0.83	2.04	1.84
77	*RBFOX1*	5.28	1.86	1.63	7.77
78	*ADAMTSL1*	5.09	1.42	1.41	1.65
-	***EMX1***	12.08	12.34	8.79	7.99

A gene enriched in the mesopallium is not necessarily an exclusive marker gene for mesopallium, as it may have additional expression domains that complicate interpretation. Additionally, many genes identified by HOLT may be false positives. I next set out to validate additional candidate genes with ISH.

Mesopallium comparative analysis

Expression patterns of mesopallium marker genes

In situ hybridization expression patterns for a selection of mesopallium HOLT candidates are shown in Figures 4.2 and 4.3. Gene expression patterns for #8 *GRM4* (Figure 4.2a) and #42 *DRD5* (Figure 4.3f) were previously described (Sun and Reiner 2000, Jarvis et al. 2013), but the other 16 genes shown are novel. All sections shown are taken from a similar anteroposterior level midway through the telencephalon. While every expression pattern is unique, the gene patterns presented also share important similarities.

The candidates shown have a clear boundary of expression at the mesopallial lamina (LaM), a cell-poor zone separating the mesopallium from the ventrally adjacent nidopallium (Reiner et al. 2004a). Most, but not all, marker genes identify two delineable territories: a thicker ventral district and a thinner dorsal one. Comparison with published *DRD5* expression patterns identifies these two territories as Mv and Md (then referred to as HVd and HVv) (Sun and Reiner

2000). These two territories are separated by a thin cell-poor zone that may correspond to the lamina frontalis superior (LFS). The LFS was previously described in the avian nomenclature paper as the zone separating the DVR mesopallium from the HD in the Wulst (Reiner et al. 2004a). In some cases, the Md also has a sharp dorsal border possibly corresponding to the lamina frontalis suprema (LFM) (Figures 4.2h and 4.3c). The LFM was previously defined as separating the HD from HI above it (Reiner et al. 2004a), but see below for further discussion of HD and HI. At rostral levels, the lateral boundary of Md and Mv is the pial surface of the brain (Figure 4.3c). More posteriorly, an expression-free zone that includes parts of the area corticoidea dorsolateralis (CDL) intercalates between the mesopallium and the telencephalic surface (Figures 4.2f and 4.3e) (Reiner et al. 2004a).

Additional heterogeneities in the mesopallium are evident. A dense, ovoid nucleus in lateral Mv was found to be selectively enriched (Figure 4.3h) or impoverished (Figure 4.3b, d) for mesopallium marker gene expression. This nucleus was referred to as MVL by Krutzfeldt and Wild (2005) and is a major target of entopallium projections. Mesopallium markers frequently show gradations in expression within Mv, suggesting further anatomical subdivisions requiring future study. Some mesopallium markers identify a very small nucleus near the posterior end of Md, which can be seen most clearly in Figure 4.3i. This nucleus appears to correspond to the CDLCo of Puelles (Puelles 2007) and may participate in avian navigation sense (Mouritsen et al. 2005, Wu and Dickman 2011). It is presently unclear how this nucleus relates to the mesopallium in the absence of connectional and developmental data.

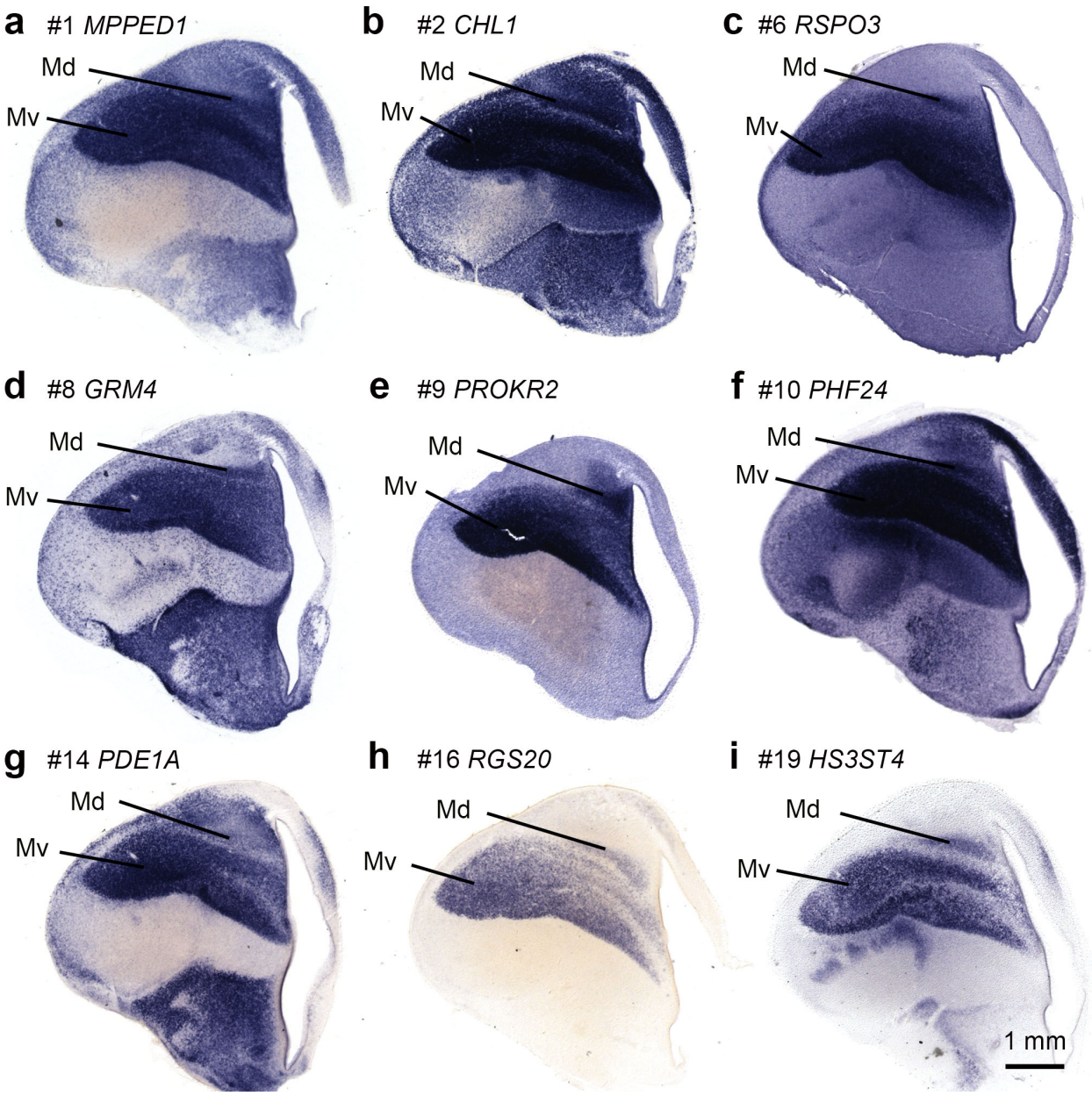

Figure 4.2 Mesopallium marker genes: Part 1
In situ hybridizations for the indicated genes on coronal sections from E14 chicken telencephalon. Numbers refer to the gene list in Table 4.2. All genes shown in **a** though **i** are expressed in a dorsal (Md) domain and a ventral (Mv) domain.

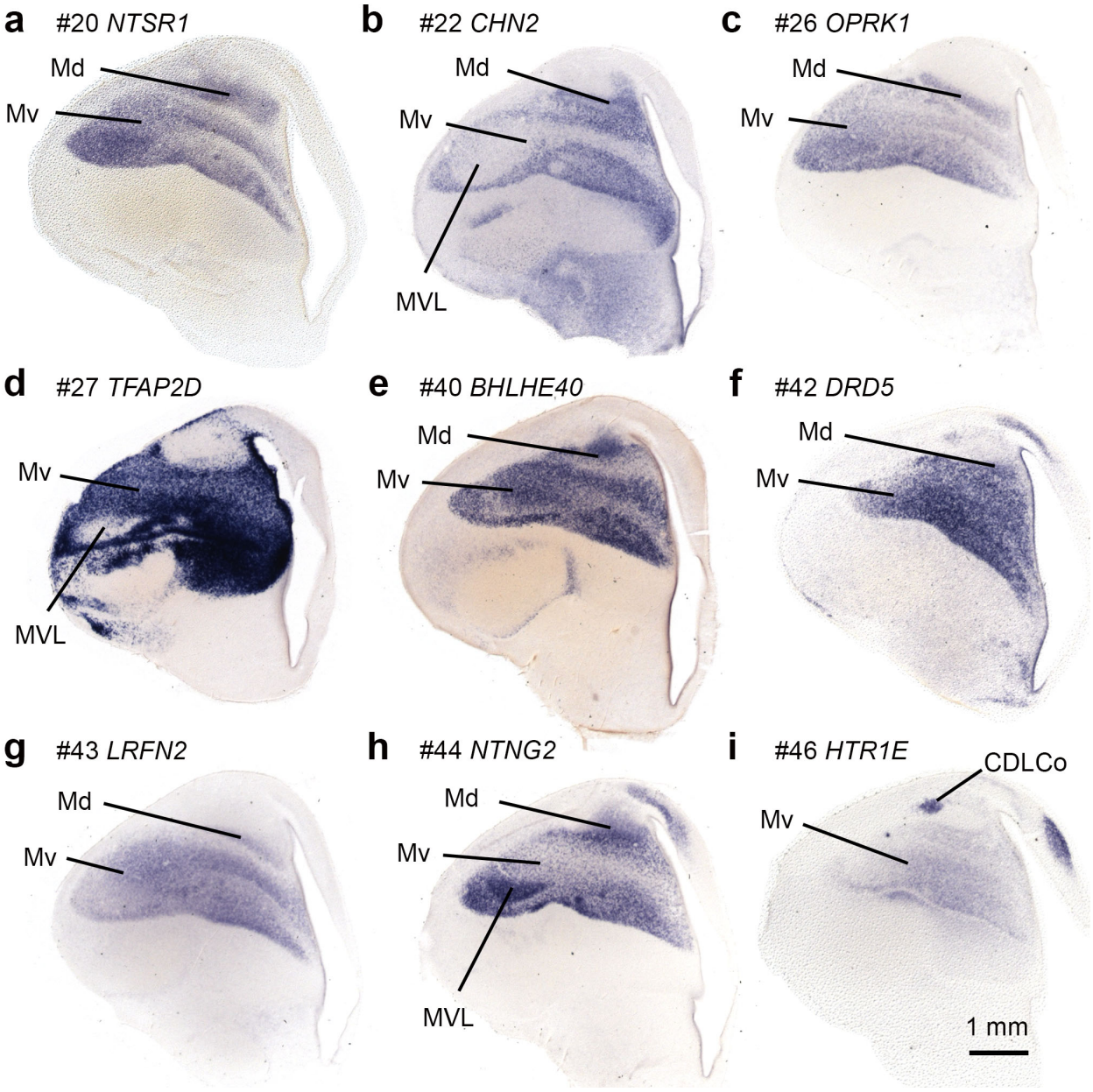

Figure 4.3 Mesopallium marker genes: Part 2
In situ hybridizations for the indicated genes on coronal sections from E14 chicken telencephalon. Numbers refer to the gene list in Table 4.2. All genes shown in **a** though **h** are expressed in a dorsal Md domain and a ventral Mv domain. **(i)** *HTR1E* strongly labels a small dorsal nucleus (not labeled). Other genes either **(h)** positively or **(b, d)** negatively label the MVL nucleus within Mv.

These gene expression data establish that the mesopallium is a coherent molecular territory with sharp borders. It has dorsal (Md) and ventral (Mv) divisions that share extensive similarity in gene expression. Indeed, none of the mesopallium HOLT candidates examined proved to be selective markers of either the Md or Mv singularly. Moreover, both Md and Mv have been shown to form intratelencephalic connections, and lack primary sensory input and long output projections (Atoji and Wild 2012). These data prompt the hypothesis that the mesopallium, like the input and output nuclei of the avian DT, is dominated by a unique class of excitatory neurons.

Novel marker gene NHLH2 illuminates mesopallium organization

Expression of the transcription factor gene *NHLH2* (#7) is particularly informative about the molecular complexity and structure of the chick mesopallium. A conspicuous zone of weak expression separates Md from parts of Mv. MVL can also be identified as a zone free of *NHLH2* expression in lateral Mv (Figures 4.4f–i and 4.5a,b).

In the posthatch day zero (P0) chicken, Md appears at a slightly more rostral level than Mv (Figure 4.4a,). At this age, an inflection point in the curvature of the brain surface is apparent in dorsolateral DT. This landmark is called the vallecula (Edinger 1903), and defines the boundary between the Wulst dorsally and the DVR ventrally. The vallecula is marked by an asterisk in Figures 4.4 through 4.6: it is first seen at the level in Figure 4.4b and cannot be discerned posterior to the level shown in Figure 4.5h. At the most anterior levels of mesopallium, Md is contained entirely within the Wulst as defined by the bulge dorsal to the vallecula. Mv, by contrast, is a DVR territory. The Md gradually retreats medially, thins out toward posterior DVR, and disappears a short distance posterior to the end of the vallecula (Figure 4.6d,e).

Mv, located ventral to the vallecula, contains several differentiated zones at its rostral and middle levels. A thin, dense band of cells in central Mv first appears at the level in Figure 4.4g and can be followed through Figure 4.6a. This band appears to have been identified by specific expression of *CBLN2* and called MDd (dorsal mesopallium, dorsal band) by Reiner (Reiner et al. 2011). This interpretation is inconsistent with my designation of the band as a part of Mv. Importantly, it also differs from an earlier interpretation by Sun and Reiner (Sun and Reiner 2000), thus underscoring the importance of standardizing the confusing and inconsistently applied nomenclature for mesopallium and Wulst. At the level shown in Figure 4.6b, the band appears to fuse with the remainder of Mv, and continues posteriorly beyond Md to terminate in posterior DVR. It is clear from this series that posterior mesopallium is the caudal part of Mv.

The *NHLH2*-rich central band of Mv is set off from Md by a *NHLH2*-poor zone, indicating the presence of at least three major zones in Mv: a dorsal *NHLH2*(−) zone, a dense *NHLH2*(+) central zone, and a larger and more complex ventral Mv which includes the MVL nucleus. To understand the function of these divisions, it is essential that future anatomical studies combine gene expression with tracing experiments.

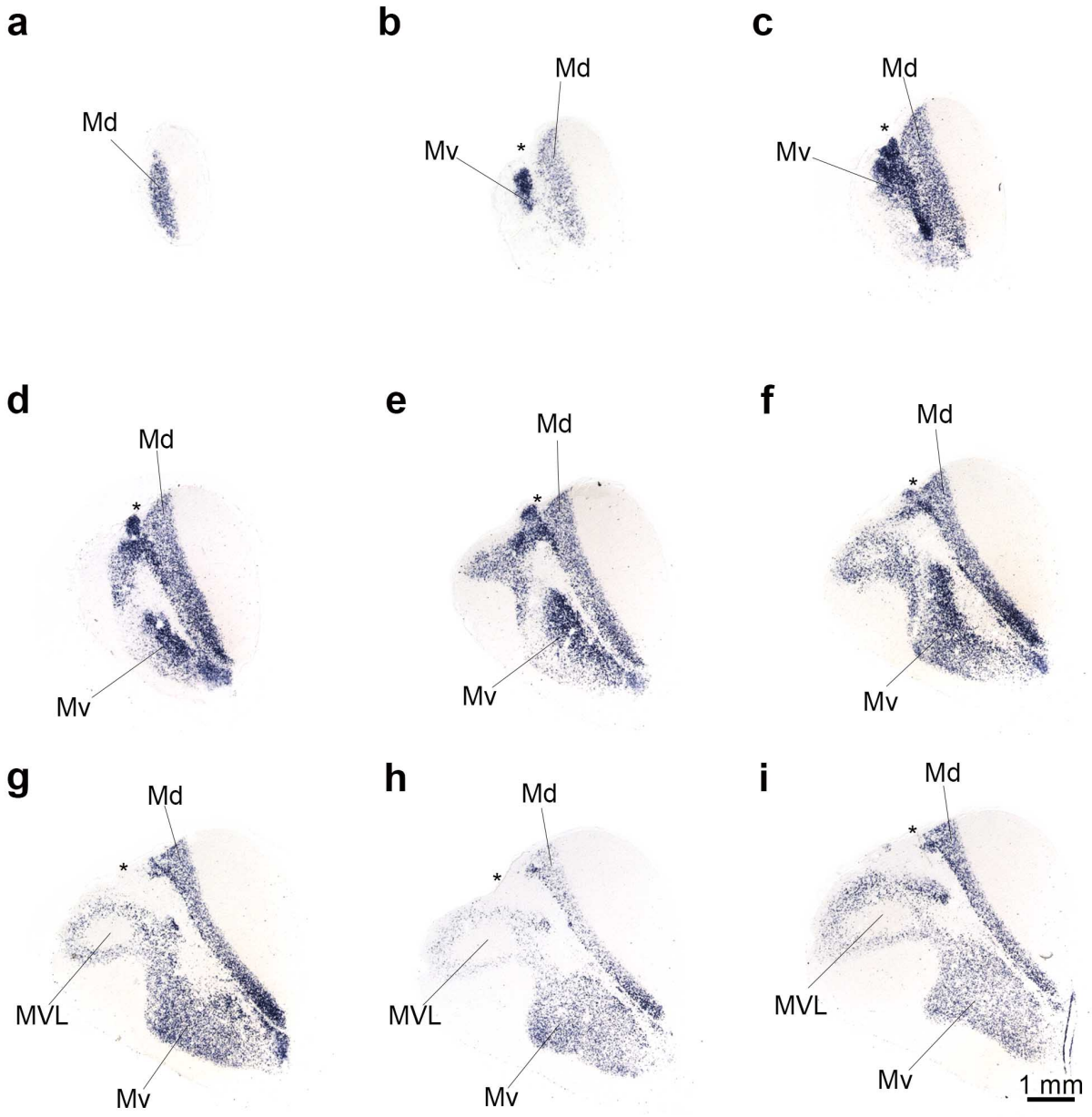

Figure 4.4 *NHLH2* series: Part 1
In situ hybridization for mesopallium candidate #7 *NHLH2* on coronal sections from a single P0 chicken telencephalon. Dorsal mesopallium (Md), ventral mesopallium (Mv), and MVL are labeled. An asterisk notes the location of the vallecula.

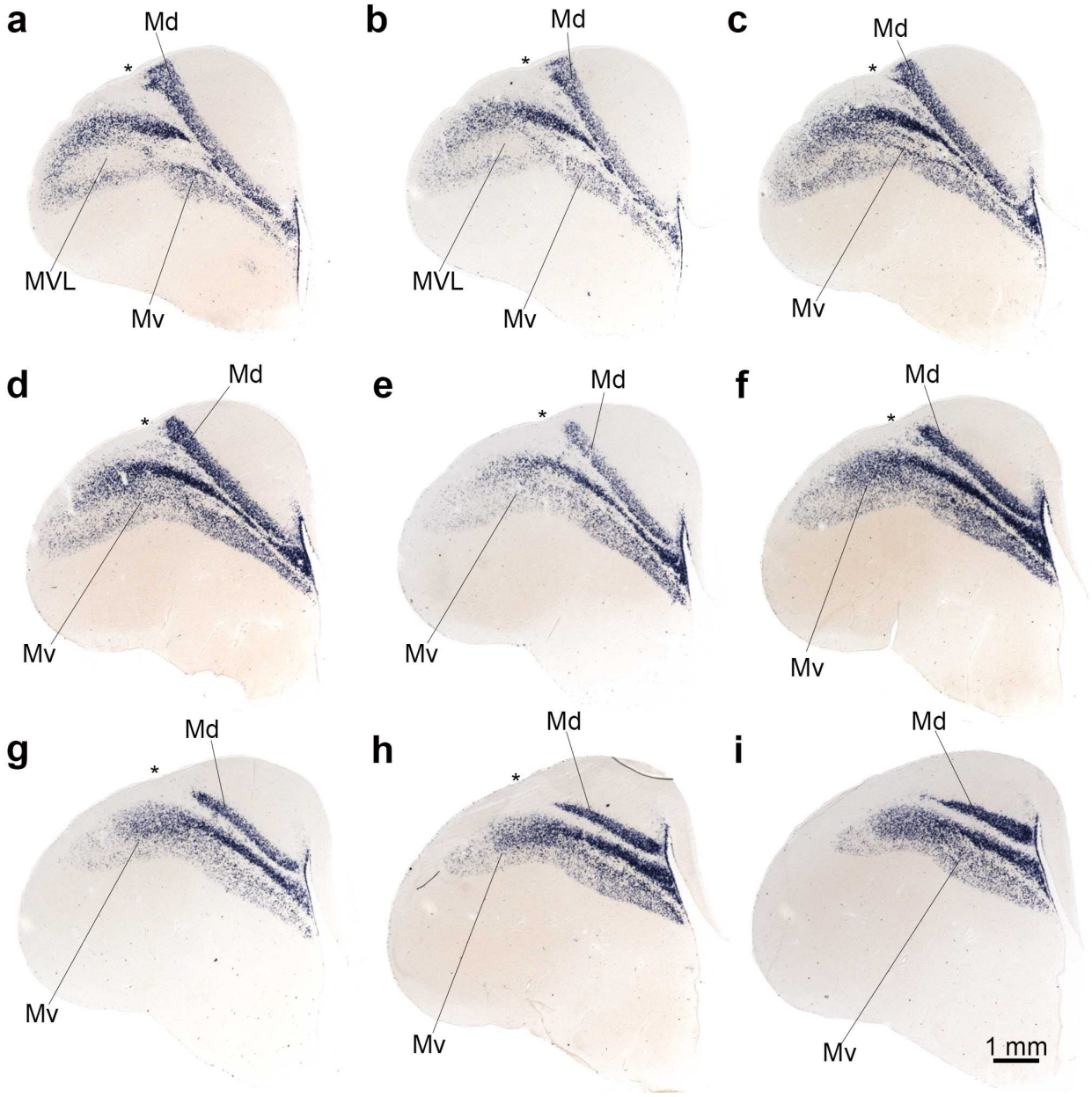

Figure 4.5 *NHLH2* series: Part 2
In situ hybridization for mesopallium candidate #7 *NHLH2* on coronal sections from a single P0 chicken telencephalon. Dorsal mesopallium (Md), ventral mesopallium (Mv), and MVL are labeled. An asterisk notes the location of the vallecula.

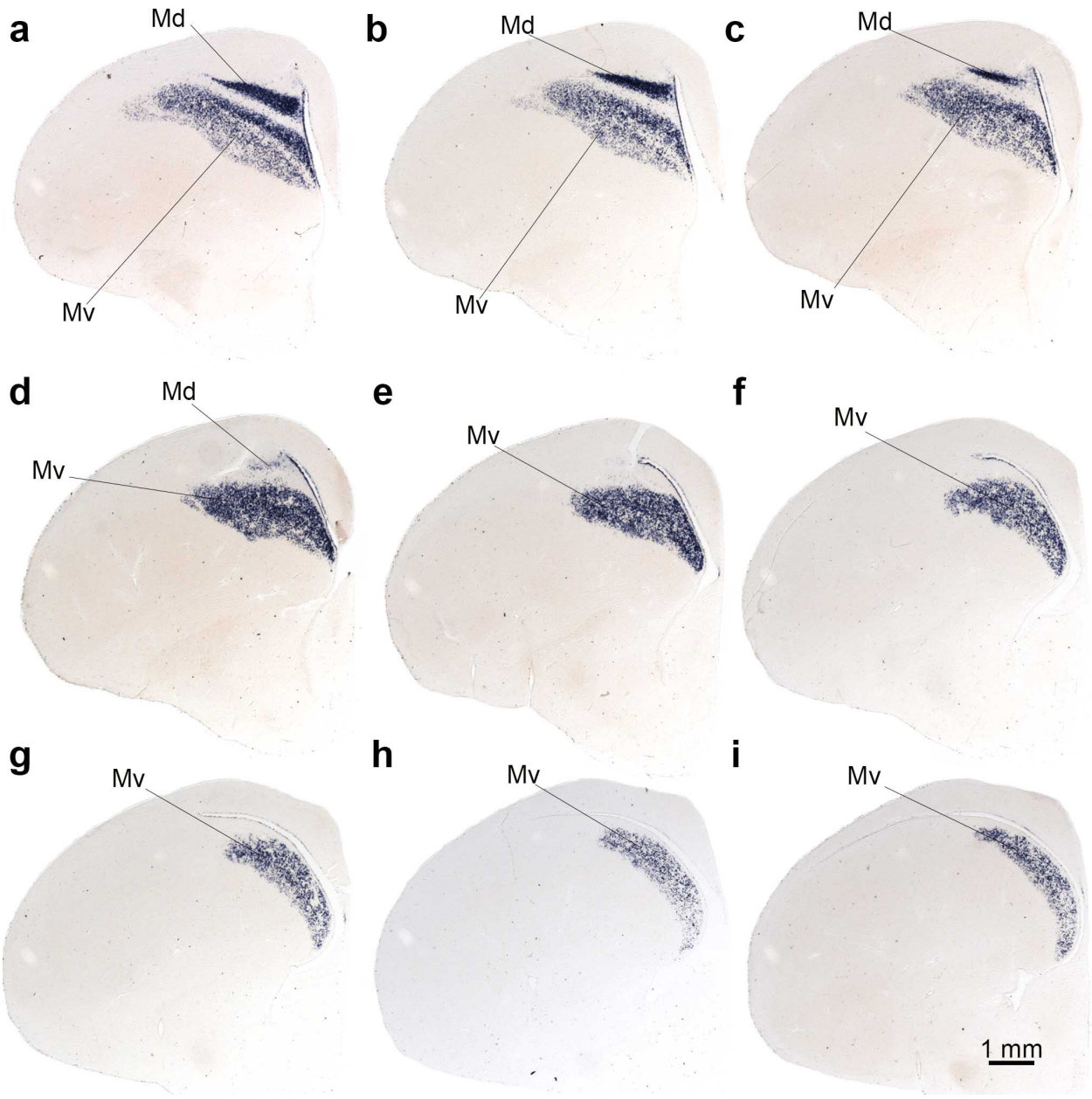

Figure 4.6 *NHLH2* series: Part 3
In situ hybridization for mesopallium candidate #7 *NHLH2* on coronal sections from a single posthatch day zero chicken telencephalon. Dorsal mesopallium (Md) and ventral mesopallium (Mv) are labeled.

Transcription factors enriched in the mesopallium are candidates for identifying mesopallium homologs in non-avian dorsal telencephalon

The previously described comparative studies established that transcription factors are more likely than other classes of molecules to show conservation of expression at the cell-type level (Chapter 3). I focused on transcription factors for comparative purposes in this study.

ID2 (candidate #3) encodes the transcription factor Inhibitor of DNA binding 2, an HLH protein lacking a DNA binding domain. It is a putative dominant-negative regulator of other HLH factors. I found that chicken *ID2* is expressed in Md and Mv at high levels at least as early as E14 (not shown), and continues to label mesopallium at P0 (Figure 4.7a).

SATB2 (#4, special AT-rich sequence binding protein 2) belongs to the CUT class of homeobox factors, a small gene family including *CUX1, CUX2,* and *SATB1,* all of which are expressed in the neocortex (Szemes et al. 2006, Cubelos et al. 2010, Huang et al. 2011, Cubelos et al. 2015). *SATB2* binds DNA at matrix attachment regions (Britanova et al. 2005, Szemes et al. 2006) and induces local chromatin remodeling by recruiting a variety of corepressors and coactivators (Gyorgy et al. 2008). Chicken *SATB2* is intensely expressed at P0 in the mesopallium, as well as the HA and in subsets of the DVR input nuclei Bas, E, and Field L (Figure 4.7b, Bas and L not shown). One previous study reported *SATB2* expression in the embryonic chicken DT (Suzuki et al. 2012).

I was unable to detect candidate #7 *NHLH2* (described in the previous section and Figure 4.7c) in either the mouse neocortex or the alligator DT (data not shown), suggesting a specific role in the avian mesopallium.

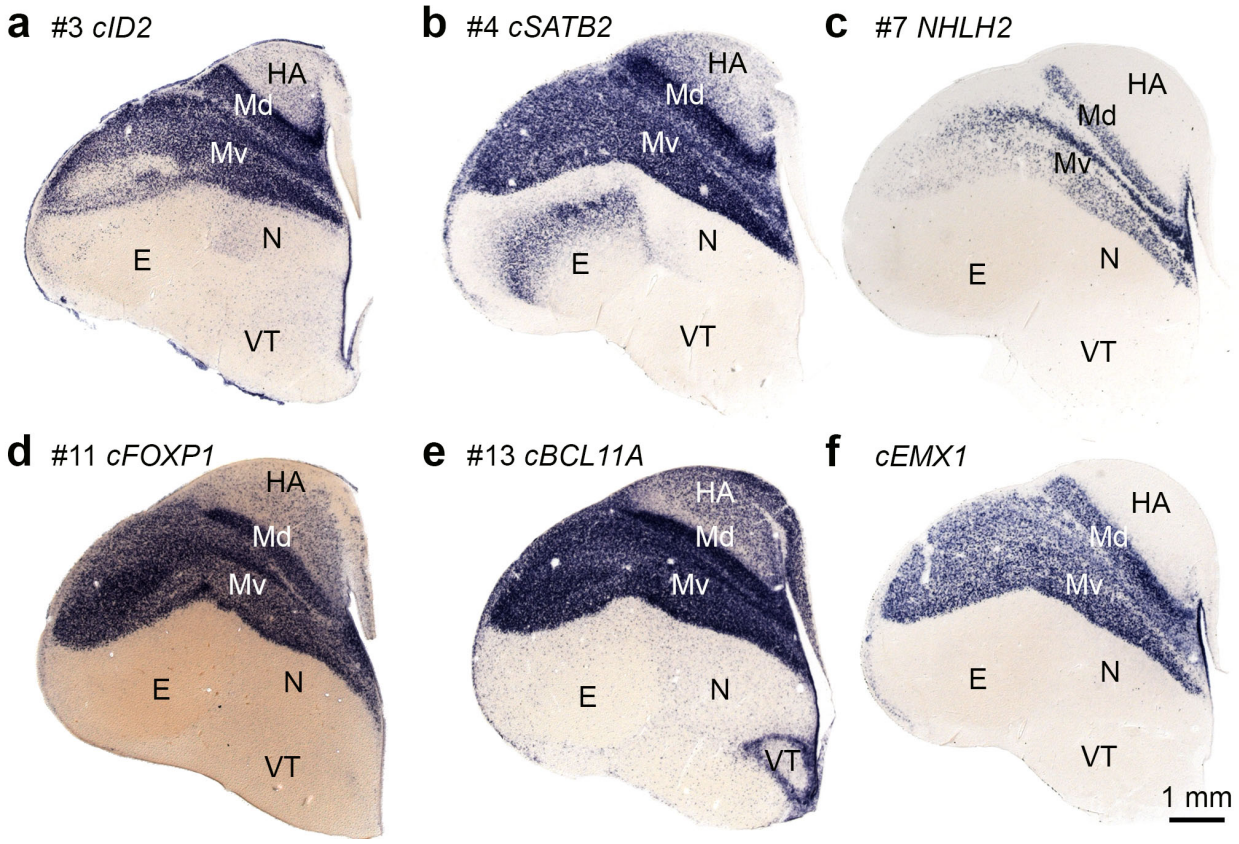

Figure 4.7 Mesopallium transcription factors
Six transcription factors are highly enriched in dorsal (Md) and ventral (Mv) mesopallium: **(a)** #3 *ID2*, **(b)** #4 *SATB2*, **(c)** #7 *NHLH2*, **(d)** #11 *FOXP1*, **(e)** #13 *BCL11A,* and **(f)** *EMX1*. Numbers refer to ranking in Table 4.2. Hyperpallium apicale (HA), entopallium (E), dorsal mesopallium (Md), ventral mesopallium (Mv), nidopallium (N), and ventral telencephalon (VT) are labeled.

FOXP1 (#11, forkhead box P1) encodes a winged helix transcription factor with diverse roles in normal development and oncogenesis, including functions in spinal cord motor neuron specification (Dasen et al. 2008, Adams et al. 2015). Previous studies reported expression in embryonic chicken mesopallium (Suzuki et al. 2012) as well as a variety of adult birds (Jarvis et al. 2013). I confirmed chicken *FOXP1* is expressed highly and specifically at E14 (not shown) and P0 in Md and Mv, as well as in HA (Figure 4.7d).

BCL11A (#13, B-cell CLL/lymphoma 11A) encodes a C2H2-type zinc finger transcription factor paralogous to *BCL11B*. I showed for the first time that chicken *BCL11A* is

expressed in the mesopallium, in addition to scattered expression in HA, olfactory cortex (lateral to E), and ventral telencephalon (Figure 4.7e).

EMX1 encodes a homeodomain-containing transcription factor orthologous to *Drosophila ems* (Simeone et al. 1992a, Simeone et al. 1992b). It was not detected by the HOLT approach due to an additional expression domain in the chicken arcopallium (Table 4.2, bottom of list). However, previous studies reported expression of this gene in mid-gestation chicken pallial neurons and in the pre-neurogenic mouse neural tube (Fernandez et al. 1998, Gorski et al. 2002, Rowell 2013). I found that *EMX1* expression is maintained in the P0 chicken telencephalon (Figure 4.7f): it is expressed with sharp boundaries in Md and Mv, in olfactory cortex, and in arcopallium (not shown).

Other candidates: Transcription factor AP-2-delta (#27 *TFAP2D*) is a sequence-specific DNA-binding molecule with important functions in retina and neural crest development (Van Otterloo et al. 2012, Li et al. 2014). It is highly expressed in mesopallium but shows additional expression in input cells and nidopallium (Figure 4.3d), so will not be considered further. #33 *TLE4* was not examined. Candidate #40 *BHLHE40* shows reasonably specific expression in the mesopallium, in addition to the entopallium belt region (Figure 4.3e), but was not examined in other species. Future studies should test for expression of this gene in the neocortex. #41 *FOSL2* showed extensive non-mesopallium expression in the chicken (data not shown). #45 *ATOH8* was not examined. Chicken expression of #54 *NR4A2* (*NURR1*) was previously reported (Puelles et al. 2016a). It is expressed in medial mesopallium, dorsal corticoid area, and arcopallium. #52 *NR4A3* is expressed in a nearly identical pattern to *NR4A2* (not shown).

I identified five transcription factors (*ID2*, *SATB2*, *FOXP1*, *BCL11A*, and *EMX1*) that together comprise a candidate gene regulatory network for mesopallium cell-type identity. These

five factors will be collectively referred to as the MesoGRN (candidate mesopallium gene regulatory network). The MesoGRN is expressed in two separate but fundamentally similar cell populations: a DVR ventral mesopallium (Mv) and a Wulst dorsal mesopallium (Md).

Mesopallium abuts the IHA in the chicken

I found that the MesoGRN expression domain extends from the Mv into the Wulst, but it is unclear how to relate this territory to anatomy previously described in the literature due to inconsistent nomenclature. Four layer-like territories, or pseudolayers (Medina and Reiner 2000), are traditionally recognized in the Wulst. From medial to lateral, these subdivisions are the HA, IHA, HI, and HD (Reiner et al. 2004a). The classic HD is the lateral-most division of the Wulst, abutting the DVR mesopallium. Previous studies and my data show that expression patterns of most mesopallium genes extend into the Wulst (Chen et al. 2013a, Jarvis et al. 2013). Jarvis et al. (2013) named the mesopallium-like Wulst territory the Md, a name that I adopted in this study. This question then arises: do birds have an HD, an HI, or both that are distinct from the Md? If the Md extends to the IHA, there is no room for a non-mesopallium territory and HD/HI corresponds to Md. If Md does not extend to the IHA, and there is a territory between them, this territory may represent the classic HD or HI.

I performed ISH on serially adjoining sections from E20 chicken telencephalon for the genes *FOXP1* and *KCNH5* (a well-characterized input cell marker expressed in IHA). *FOXP1* labels the Md, which is almost fully contained within the Wulst as indicated by its location dorsal to the vallecula (Figure 4.8a, asterisk). *KCNH5* expression is found a short distance dorsal to the vallecula (Figure 4.8b). Serial section alignment demonstrated that the *FOXP1*(+) and *KCNH5*(+) territories abut, with no intervening *FOXP1*(−)/*KCNH5*(−) zone that could correspond to a separate HD/HI.

I repeated this experiment with a second pair of marker genes, one a transcription factor enriched in the IHA (*NR0B1*, Chapter 3) and the other a g-protein-coupled receptor specific to the mesopallium (*PROKR2*, Figure 4.2e). At P0, when the Wulst and vallecula are sharply defined, *PROKR2* expression (Figure 4.8c) abuts *NR0B1* expression (Figure 4.8d). I conclude that Md extends to IHA in the chicken Wulst.

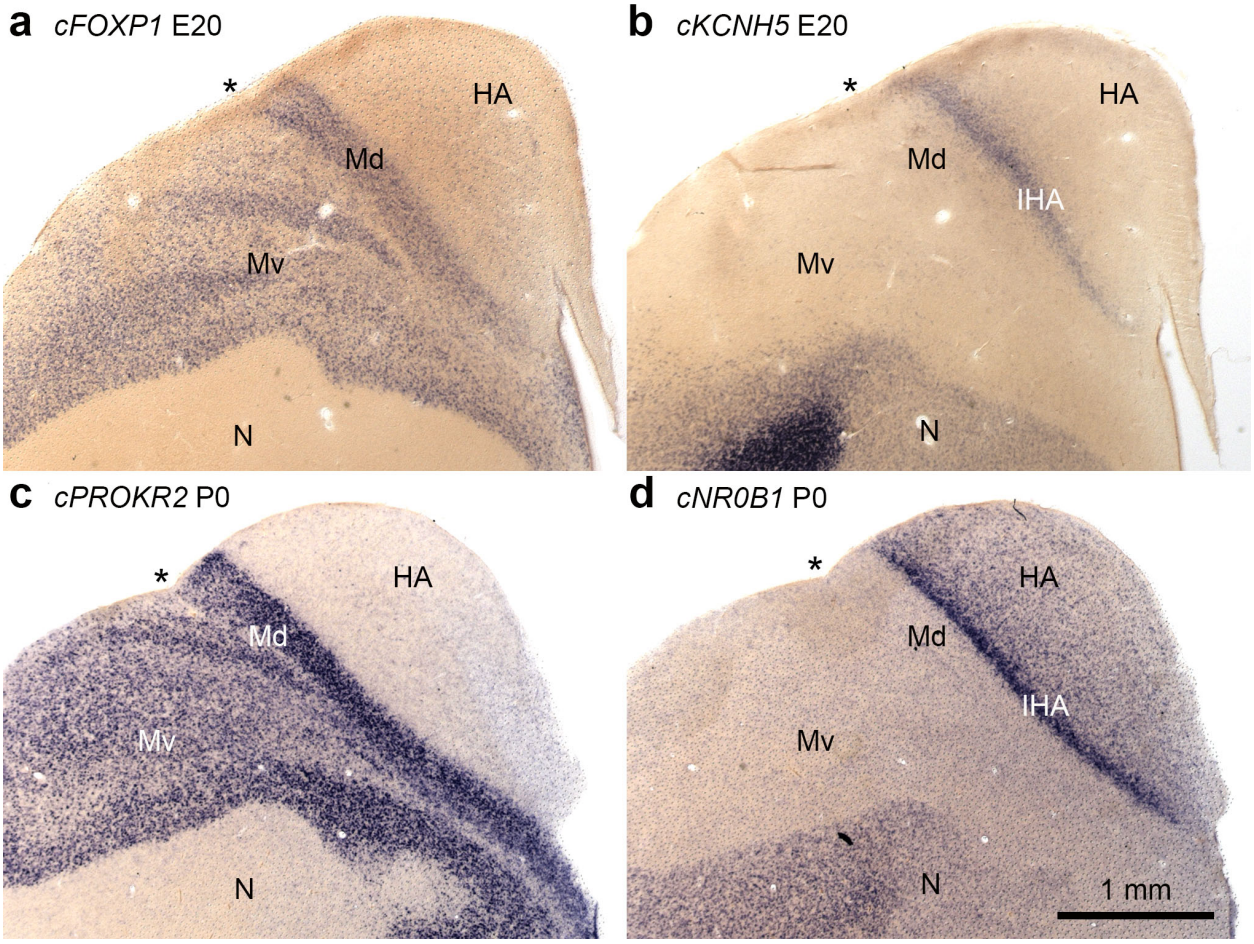

Figure 4.8 Dorsal mesopallium abuts the interstitial nucleus of the HA in the chicken Comparison of mesopallium and IHA markers on serially adjoining sections at **(a, b)** E20 and **(c, d)** P0. **(a)** *FOXP1* expression extends to the IHA, labeled by **(b)** *KCNH5*. **(c)** *PROKR2* expression extends to the IHA, labeled by **(d)** *NR0B1*. Dorsal mesopallium (Md), ventral mesopallium (Mv), IHA, HA, and nidopallium (N) are labeled. An asterisk notes the vallecula.

Mesopallium molecular anatomy and the MesoGRN are conserved across game birds and song birds

The chicken *Gallus gallus* is within a basally branching bird clade, the superorder Galloanserae, along with geese, ducks, quails, and pheasants. Most other extant birds belong to the Neoaves, which diverged from the Galloanserae about 90 million years ago and diversified rapidly and extensively (Jarvis et al. 2014). The absence of HI/HD observed in chicken may be a primitive characteristic, with Neoaves gaining these additional territories later. Alternatively, chickens may have lost HD/HI. To test for these possibilities, I examined *FOXP1* and *KCNH5* expression in the starling *Sturnus vulgaris*. Traits present in the chicken and the starling, a member of the Neoaves, are likely to be ancestral and conserved in all neognath birds.

The starling Wulst, as recognized by the position of the vallecula (Figure 4.9a, asterisk), dominates the anterior DT. I reasoned that the disproportionately large starling Wulst would be a good candidate to harbor an HD/HI territory between the Md and IHA, if such a territory is present in birds. Starling *FOXP1* is expressed in a Wulst Md domain dorsal to the vallecula in addition to a ventral Mv domain (Figure 4.9a). The starling Md extends to the IHA, as labeled by *KCNH5* (Figure 4.9b). Blue dots are *KCNH5*(+) IHA cells clustered along a band of beige discoloration likely corresponding to dense axonal white matter delivering primary sensory information (Figure 4.9b). At middle (Figure 4.9c) and posterior (Figure 4.9d) levels of the telencephalon, starling *BCL11A* identifies both Md and Mv with their characteristic relations to the vallecula and IHA. The starling does not possess an HD or HI separate from a MesoGRN-expressing Md.

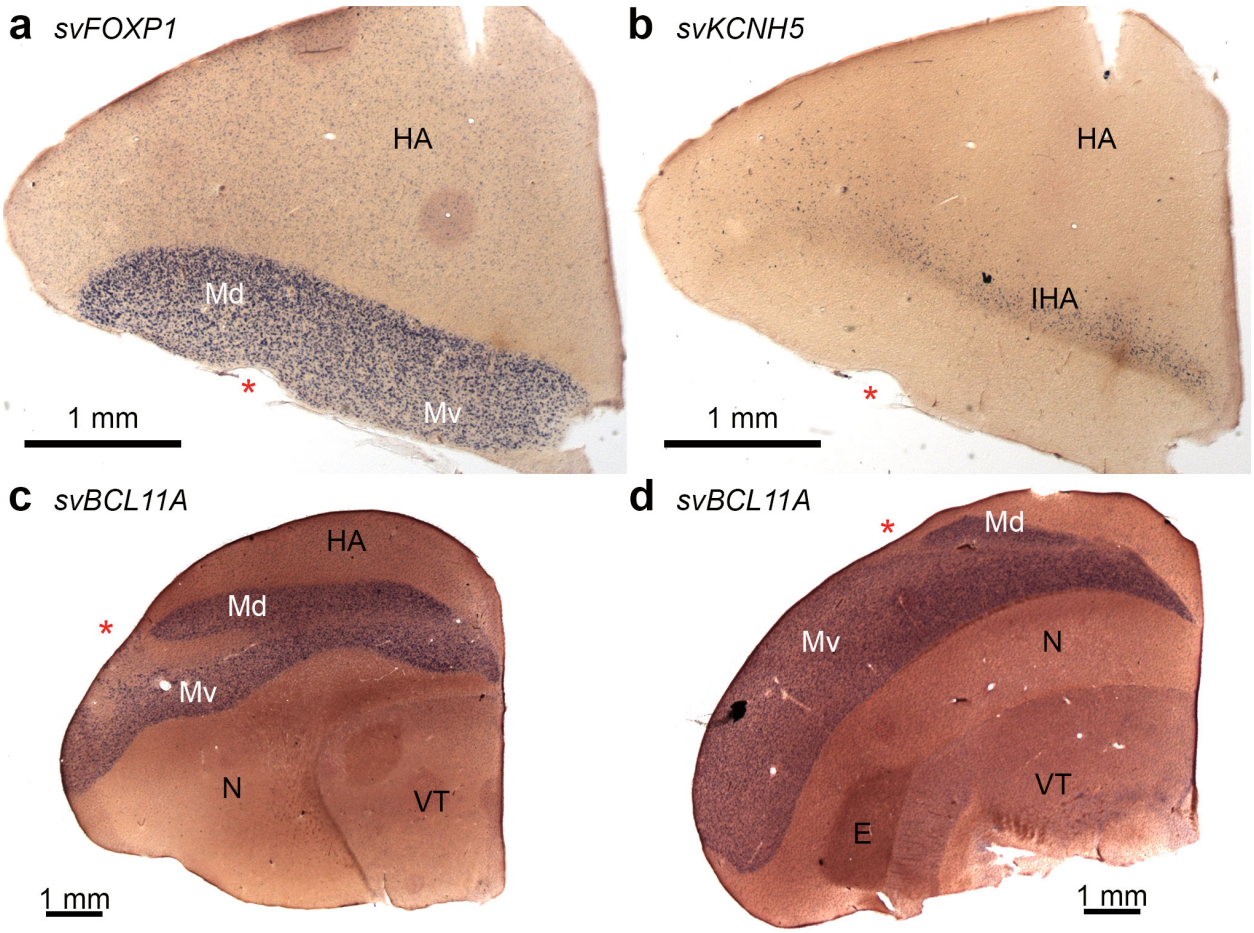

Figure 4.9 Mesopallium organization and transcription factors are conserved across neognath birds
Adjacent sections through anterior telencephalon of an adult starling demonstrate that the **(a)** *FOXP1*-expressing mesopallium extends to the **(b)** *KCNH5*-expressing IHA. Sections through **(c)** middle and **(d)** posterior levels of starling telencephalon demonstrate conserved expression of *BCL11a* in Md and Mv. Entopallium (E), HA, IHA, dorsal mesopallium (Md), ventral mesopallium (Mv), nidopallium (N), and ventral telencephalon (VT) are labeled. An asterisk notes the vallecula.

I conclude that all neognath birds (neoaves and galloanserae) have an Md and Mv, and they share conserved expression of at least two members of the MesoGRN, *FOXP1* and *BCL11A*. I further conclude that the classic HD/HI must correspond to the Md, as previously proposed (Jarvis et al. 2013). It is unclear how previous researchers identified two Wulst structures (HD and HI) where I only identify one (Md): in both chicken and starling, Md appears quite homogenous in staining. Perhaps anatomists believed they had to find an HD and HI based

on a previous authoritative precedent and sought out something to attach those labels to. Chick Mv, for example, does contain internal molecular subdivisions (Figures 4.4–4.6). In some cases, HD or HI may have been assigned to these DVR structures. Another possibility is that some birds do possess species-specific elaborations of Md or IHA into substructures.

The MesoGRN is expressed in mouse neocortex

My data on chickens and starlings, along with alligator gene expression (Chapter 5), indicates that the MesoGRN is conserved across avian and non-avian DT, at least in the archosaurs. I now ask whether the neocortex contains cells similar in gene expression to mesopallium. A neocortical cell population expressing some combination of MesoGRN factors, and with functions and connectivity similar to the mesopallium, would be a strong candidate for a homolog.

I found that mouse orthologs of all five transcription-factor components of the avian MesoGRN are expressed in postnatal mouse neocortex (Figure 4.10a–e). All five MesoGRN genes are expressed in multiple neocortical layers, and each shows a unique pattern with respect to the other four. Notably, all five factors are expressed in the upper neocortical layers L2/3.

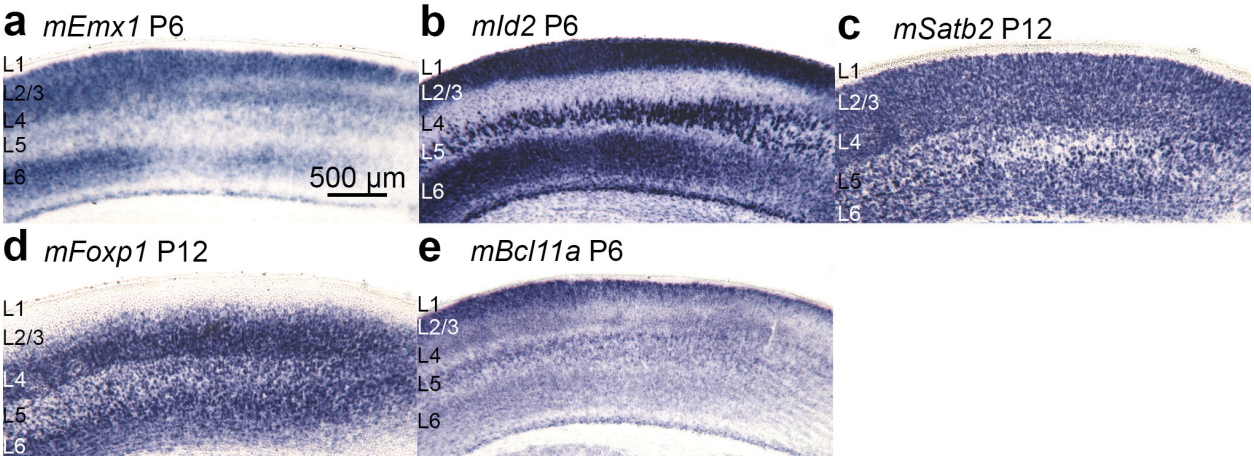

Figure 4.10 MesoGRN transcription factors are expressed in mouse neocortex
Mesopallium-enriched transcription factors **(a)** *Emx1*, **(b)** *Id2*, **(c)** *Satb2*, **(d)** *Foxp1*, and **(e)** *Bcl11a* are expressed in mouse neocortex. *Satb2* and *Foxp1* are expressed too intensely at P6 to discern layers, so P12 sections are shown instead. Neocortical layers L1 through L6 are labeled.

MesoGRN factors are co-expressed in mouse and chicken

Cellular co-expression data on MesoGRN factors could provide further support for a cell-type homology. For example, co-expression would rule out the possibility that MesoGRN factors are expressed in similarly distributed but mutually exclusive cell populations.

Work in the mouse has shown that *Foxp1* (Hisaoka et al. 2010) and *Bcl11a* (Woodworth et al. 2016) are co-expressed with *Satb2*. In addition, where *Foxp1* and *Bcl11a* are expressed in L5, they co-localize with *Satb2* but not with the output cell marker *Bcl11b*. Co-expression data for *Emx1*, *Id2*, or any other combination of MesoGRN factors are currently lacking.

I tested whether MesoGRN factors are co-expressed in the chicken using two-color fluorescent in situ hybridization (FISH). Because Satb2 and Bcl11a are both functionally required for the development of neocortical callosal projection neurons, co-localization of these transcripts in chicken may identify a homologous cell population. I found that chicken *BCL11A* (Figure 4.11a) and *SATB2* (Figure 4.11b) are co-expressed (Figure 4.11c, yellow) in many, but not necessarily all, mesopallium cells.

I also demonstrated using FISH that chicken *ID2* is co-expressed with *SATB2* in mesopallium (Figure 4.11d–f). This result further suggests a conserved gene regulatory network. A comprehensive co-expression analysis in mouse and chicken could provide stronger support for this hypothesis, but is limited by the technical challenges of detecting multiple transcripts simultaneously. Recently developed single-cell RNA sequencing technology may be able to identify cells that express the entire MesoGRN repertoire (Macosko et al. 2015, Ziegenhain et al. 2017).

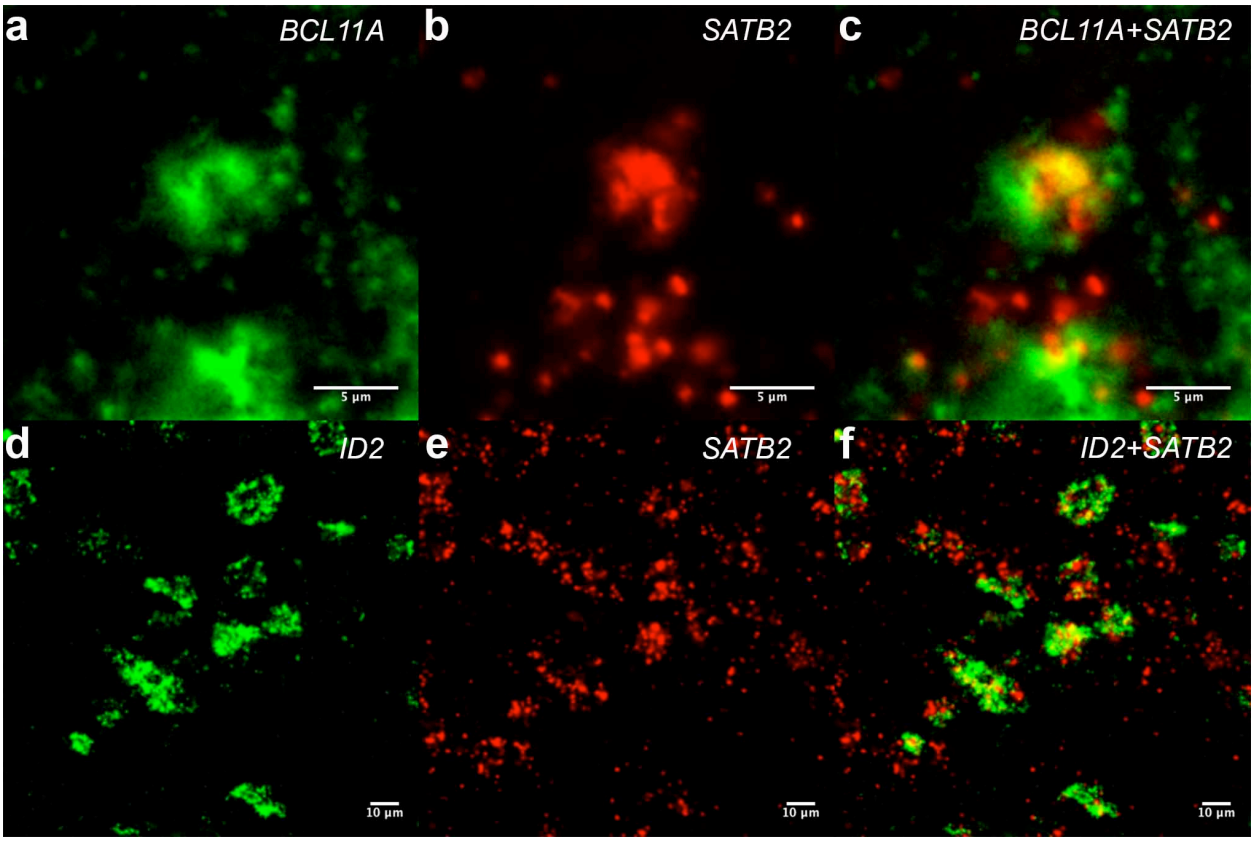

Figure 4.11 Mesopallium transcription factors are co-expressed in chicken
Two color fluorescent in situ hybridization for *BCL11A/SATB2* and *ID2/SATB2* in E20 chicken. Photos from posterior mesopallium. **(a)** *BCL11A* transcript co-localizes with **(b, c)** *SATB2* transcript. **(d)** *ID2* transcript co-localizes with **(e, f)** *SATB2* transcript. Scale bar is 5 µm in **a**–**c** and 10 µm in **d**–**f**.

A fate-restricted dorsal telencephalon territory gives rise to the mesopallium

The mesopallium is a largely homogeneous territory in which cells expressing common transcripts are clustered together and are spatially segregated from other cell types. The mature anatomy of mesopallium raises the possibility that chicken mesopallial cells are born in a dedicated progenitor territory—that is, from a delineated population of progenitor cells giving rise only to mesopallium. If true, this would be a striking divergence from the model for neocortical neurogenesis, in which all major excitatory cell types are generated from all parts of the neocortical primordium.

I performed whole mount ISH for *SATB2* on HH30 chicken embryos, approximately one full day after mesopallium neurogenesis commences (Rowell 2013). Staining reveals a patch of *SATB2*(+) cells located in anterodorsal telencephalon with a sharp posterior boundary (Figure 4.12a). Thus, candidate mesopallium precursors form a coherent territory at the earliest stages they can be detected. At embryonic day eight, *SATB2*(+) cells are densely packed in an anterior territory (4.12b) but are not present in the posterior DVR, which likely corresponds to the nidopallium and arcopallium (4.12c). These gene expression data suggest that mesopallium arises from a restricted territory of the DT ventricular zone.

Gene expression evidence is, however, insufficient for fate mapping through time. These results could be explained by production of mesopallium cells throughout DT that coalescence by migration and then express the mesopallium marker *SATB2*. A second alternative interpretation is that mesopallium cells are born in a dedicated territory that also produces other cell types. In order to test these possibilities, I fate-mapped rostral telencephalon using an indelible genetic label.

To trace the descendants of DT progenitors, I electroporated (Momose et al. 1999) the DNA constructs PBXW-sfGFP and CDV-hypbase into the telencephalon of HH23/24 chicken embryos. PBXW-sfGFP encodes the superfolder GFP molecule, an extremely bright GFP variant (Pedelacq et al. 2006), flanked by PiggyBac transposition sequences. CDV-hypbase encodes the PiggyBac transposase, which randomly inserts sfGFP and its promoter into the genome (Ding et al. 2005). One day after electroporation, I triaged embryos based on reporter fluorescence restricted to the rostral telencephalon. Retained embryos were further incubated and collected at E14 for processing.

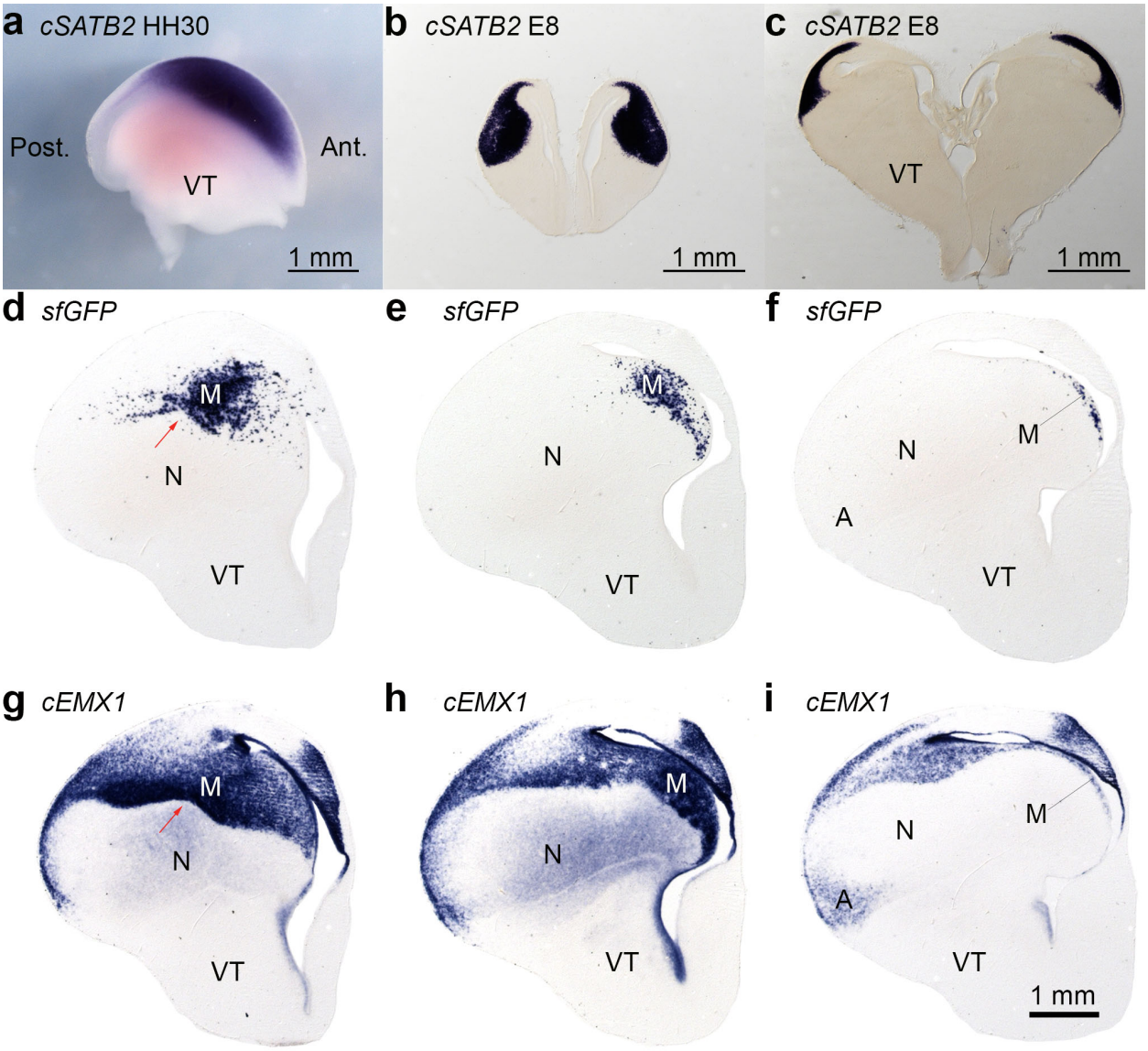

Figure 4.12 A mesopallium-restricted territory in chicken telencephalon
(a) Whole mount in situ hybridization for *SATB2* in HH30 chicken. Only the telencephalon is pictured, lateral view with anterior to right. **(b)** Anterior and **(c)** middle sections from E8 telencephalon labeled for *SATB2*. **(d–f)** Three sections from a single E14 hemisphere electroporated with PBXW-sfGFP and CDV-hypbase plasmids, labeled with a probe for sfGFP. *EMX1*-labeled sections in **g–i** are adjacent to the above sfGFP sections. Arcopallium (A), mesopallium (M), nidopallium (N), and ventral telencephalon (VT) are labeled.

I detected the descendants of electroporated progenitors by performing ISH for the sfGFP transcript. In four cases, I observed labeling restricted to the mesopallium. One case is shown (Figure 4.12d–f). At all three levels of telencephalon shown, labeling is confined to the mesopallium as indicated by *EMX1* staining on serially adjoining sections (Figure 4.12g–i). The

characteristic contours of mesopallium are evident in sfGFP staining by cells distributed along the Mv ventral border. Staining is absent from the nidopallium, entopallium, and arcopallium. This result strongly supports the existence of a fate-restricted territory in rostral DT that gives rise to mesopallium cells, but not to other cell types including input and output cells. Additional experiments, presumably with broader electroporation sites, recovered the mesopallium–nidopallium border but with other labeled cells in the Wulst or nidopallium (not shown).

HOLT analysis of the nidopallium transcriptome

My finding of a candidate MesoGRN raises the question of whether the avian nidopallium possesses a separate GRN and, if so, whether mammalian DT contains nidopallium-homologous cell types.

Fewer filters were applied for the identification of nidopallium-specific transcripts than for mesopallium-specific transcripts. Beginning with all transcripts, I selected those enriched in N compared to M by 2.5 fold. This resulted in 97,261 candidate transcripts. From these, I selected those coding genes expressed at 5 FPKM or higher in N, yielding 145 genes (Table 4.3).

Table 4.3 Progressive HOLT filters for nidopallium-enriched transcripts

Sequential Filters	# of Transcripts
1) All Transcripts	356,804
2) Nidopallium/Mesopallium ≥ 2.5	97,261
3) Abundance ≥ 5 FPKM, Coding	145

I first selected transcripts enriched in N compared to M by 2.5 fold. Then, I ranked transcripts in descending order of expression in N and selected coding transcripts expressed at 5 FPKM or greater.

The top 145 nidopallium HOLT candidates are listed in Table 4.4, with transcriptional regulators bolded. My approach recovered the single known nidopallium marker, the transcription factor *DACH2* (#32) (Szele et al. 2002). I previously examined 16 of these genes

due to their enrichment in the entopallium, a nucleus within the nidopallium (Chapter 3): #4 *CRABP1*, #6 *DCBLD1*, #7 *LINGO3*, #13 *NRXN3*, #14 *ANOS1*, #21 *CDH6*, #23 *KCNH5*, #39 *TMEM196*, #52 *PPP1R1B*, #58 *MOXD1*, #68 *CRHBP*, #78 *NR0B1*, #79 *DIRAS2* #87 *DACH1*, #89 *STK31*, and #101 *MYOM2*. The following 14 candidates were also previously examined by us and others: #3 *NR2F2* (Briscoe), #10 *PCP4* (Dugas-Ford et al. 2012), #19 *RALY* (Briscoe), #37 *STXBP6* (Briscoe), #41 *GFRA4* (Briscoe), #55 *Beta-keratin* (Briscoe), #64 *FEZF2* (Dugas-Ford et al. 2012), #72 *SNCG* (Briscoe), #73 *ROBO2* (Briscoe), #99 *ANKFN1* (Briscoe), #113 *DLX6* (Jarvis et al. 2013), #116 *FOXP2* (Jarvis et al. 2013), #119 *SLITRK3* (Briscoe), and #143 *LHX8*. None of these 30 genes is a marker of the nidopallium in the sense that *DACH2* is, which labels the entire nidopallium between its borders with ventral telencephalon, mesopallium, arcopallium, and the lateral ventricle. The remaining 114 genes are novel candidate nidopallium markers.

Table 4.4 Nidopallium HOLT candidates

The 145 most abundant nidopallium genes are listed by descending levels of expression. Transcriptional regulator genes are bolded.

Rank	Gene	N	M	E	A
1	***MEIS2***	185.69	68.94	143.07	125.62
2	***LBH***	77.38	26.80	74.60	71.99
3	***NR2F2***	71.11	16.66	25.88	59.13
4	*CRABP1*	70.05	26.41	175.31	51.78
5	*CPLX1*	63.72	23.02	55.28	45.68
6	*DCBLD1*	57.57	22.15	163.14	37.45
7	*LINGO3*	56.76	19.08	90.19	31.51
8	*FAM19A2*	49.18	10.29	40.17	55.81
9	*PLPP4*	42.96	7.01	30.15	24.97
10	*PCP4*	41.38	16.30	45.47	22.12
11	*LYPD3*	36.02	12.61	9.76	27.68
12	*ADIRF*	33.71	10.48	3.47	15.93
13	*NRXN3*	31.00	6.51	31.55	23.55
14	*ANOS1*	28.75	8.62	188.43	11.48

Table 4.4, continued

Rank	Gene	N	M	E	A
15	*SEMA3A*	27.97	8.62	40.33	33.05
16	*CDKN1C*	27.65	10.29	12.80	22.84
17	*RD3*	27.06	3.04	24.57	20.10
18	*FAM172A*	26.98	4.01	18.36	18.96
19	*RALY*	25.86	4.25	32.43	13.09
20	*LSP1*	25.12	8.74	12.25	14.69
21	*CDH6*	25.04	6.71	33.85	10.18
22	*EPHA3*	24.45	3.93	19.64	18.42
23	*KCNH5*	24.01	3.06	64.49	12.34
24	*SYNDIG1*	23.79	5.61	22.63	15.02
25	*SPHKAP*	22.86	7.45	40.95	21.22
26	*CAB39L*	22.32	3.94	21.36	15.28
27	*CNTN4*	21.83	4.55	23.67	20.15
28	*VSTM2L*	21.60	7.89	39.53	10.84
29	*SERTM1*	21.41	0.88	29.78	15.00
30	***SIX3***	21.10	0.01	2.06	10.38
31	*KCNIP2*	21.10	5.20	26.94	14.70
32	***DACH2***	20.42	3.77	23.74	11.00
33	*RPRM*	20.09	5.46	7.18	30.32
34	*GAD2*	19.70	6.24	12.96	19.61
35	*IGSF9B*	19.32	3.81	21.44	18.20
36	***PBX3***	19.26	6.16	20.02	16.16
37	*STXBP6*	19.05	7.26	34.12	15.74
38	*TPRKB*	18.95	5.97	24.45	23.94
39	*TMEM196*	18.07	2.23	37.97	9.68
40	*SORCS3*	17.84	7.03	14.35	15.89
41	*GFRA4*	17.53	2.88	15.94	19.97
42	*GRP*	17.10	1.92	22.02	14.73
43	*MYRIP*	17.09	6.40	15.36	18.06
44	*TNR*	16.20	2.70	8.52	15.17
45	*RET*	16.06	3.38	7.66	13.23
46	*AKR1B10*	15.81	3.67	2.72	15.32
47	*CEP128*	15.36	4.24	21.24	6.52
48	*FAM135B*	15.28	4.68	13.13	14.60
49	*AGRN*	15.20	4.86	12.91	8.43
50	*HS3ST2*	15.19	4.79	16.41	9.61
51	*CDH22*	15.10	1.10	17.12	10.50

Table 4.4, continued

Rank	Gene	N	M	E	A
52	*PPP1R1B*	14.49	0.89	12.63	10.95
53	*NOV*	14.41	1.79	2.67	14.93
54	*CACNA2D2*	14.22	5.42	11.40	11.37
55	*BETA-KERATIN*	13.96	0.01	5.02	21.02
56	*CALB2*	13.77	4.02	3.40	10.25
57	*SCN1A*	13.53	2.68	22.38	15.10
58	*MOXD1*	13.45	2.39	31.75	4.75
59	*CORT*	13.37	0.40	8.06	12.97
60	*KCTD12*	13.33	4.43	7.07	7.96
61	***SOX2***	13.32	4.90	8.80	7.27
62	*RGS4*	13.09	4.40	13.57	11.44
63	*SP9*	12.59	3.46	3.18	7.26
64	***FEZF2***	12.39	3.71	10.83	10.34
65	*AKAP12*	12.03	4.30	6.15	11.22
66	*IGSF9B*	11.57	4.57	10.83	10.18
67	*C1QL1*	11.30	3.81	4.46	11.55
68	*CRHBP*	11.18	4.29	38.23	9.97
69	*PMCH*	11.08	0.99	7.36	6.28
70	*EPHB2*	10.90	4.01	8.92	9.56
71	*CECR6*	10.68	2.73	3.68	8.19
72	*SNCG*	10.63	2.55	2.74	11.10
73	*ROBO2*	10.61	3.47	15.04	5.55
74	*UNC5C*	10.59	3.95	9.43	9.90
75	*SPTSSB*	10.44	3.46	8.87	10.68
76	*POF1B*	10.40	1.66	13.08	9.30
77	*FAM84A*	10.31	4.02	7.45	9.61
78	***NR0B1***	10.20	3.46	27.32	4.75
79	*DIRAS2*	10.07	1.79	35.33	8.26
80	*DHRS12*	9.83	0.77	4.67	7.07
81	*CPNE9*	9.79	3.04	16.45	6.53
82	*GRM1*	9.64	3.30	8.95	10.99
83	*TENM4*	9.54	2.95	3.55	7.64
84	*PTPRD*	9.48	2.08	21.10	12.45
85	*ZBTB49*	9.48	3.79	7.96	8.09
86	*SYT10*	9.14	1.47	2.46	8.70
87	***DACH1***	9.02	1.90	14.85	4.55
88	*SLC24A4*	8.91	3.34	4.17	7.14

Table 4.4, continued

Rank	Gene	N	M	E	A
89	*STK31*	8.77	2.25	18.48	6.40
90	*TESC*	8.74	2.61	4.04	8.22
91	*CPNE8*	8.67	0.96	2.69	8.00
92	*FAM20C*	8.65	2.78	6.74	4.61
93	*TESK2*	8.42	3.24	5.16	8.68
94	*COL25A1*	8.37	2.47	7.00	9.75
95	***BCL11B***	8.33	2.99	4.23	4.57
96	*FAM135B*	8.14	1.31	3.82	8.41
97	*RNF223*	8.06	3.00	10.15	7.02
98	*RNF152*	8.04	2.33	4.00	7.34
99	*ANKFN1*	7.96	2.51	16.30	6.94
100	*CXCL12*	7.76	1.35	4.97	11.21
101	*MYOM2*	7.62	0.77	13.40	4.64
102	*MMP17*	7.58	3.02	5.08	10.24
103	*PLXDC1*	7.38	2.71	12.07	7.48
104	*CHODL*	7.35	1.72	3.75	6.46
105	*AKAP2*	7.21	2.11	3.79	4.22
106	*CHRM2*	7.15	0.62	2.97	3.80
107	*CASQ1*	7.14	1.59	1.18	8.61
108	***ARID3B***	7.07	1.98	8.93	4.76
109	*SORCS2*	7.04	2.48	4.36	7.58
110	*PLAU*	6.93	2.51	4.04	7.08
111	*PTGFR*	6.83	1.03	2.97	7.09
112	*SPON2*	6.76	2.61	4.90	7.72
113	***DLX6***	6.71	2.10	1.25	4.91
114	*IGSF9B*	6.61	2.09	5.79	5.04
115	*LINGO2*	6.61	2.40	6.36	6.58
116	***FOXP2***	6.49	0.79	3.06	4.73
117	*FAM196A*	6.45	2.22	3.76	5.18
118	*IPCEF1*	6.45	2.29	2.78	3.89
119	*SLITRK3*	6.43	0.01	0.83	2.92
120	*SPNS3*	6.38	1.20	3.09	9.05
121	*ST3GAL1*	6.31	1.96	2.69	5.63
122	*RNF150*	6.27	2.24	4.71	2.71
123	*SPATA6*	6.26	2.19	5.21	9.00
124	*CSRNP1*	6.12	1.05	1.77	6.81
125	*THSD7A*	6.08	2.39	7.70	6.04

Table 4.4, continued

Rank	Gene	N	M	E	A
126	*C1QTNF3*	6.05	1.73	1.17	5.26
127	*GLRA2*	5.99	2.08	5.62	4.59
128	*TCERG1L*	5.93	0.70	3.40	10.89
129	*VILL*	5.89	1.71	4.60	5.26
130	***FOXP4L***	5.86	1.07	1.76	3.37
131	*NTM*	5.73	1.57	3.25	3.30
132	*BRDT*	5.72	1.93	2.07	3.03
133	*UNC5D*	5.68	0.01	0.01	7.16
134	*FBXL14*	5.55	1.78	3.76	2.87
135	*NOS1*	5.53	1.27	2.00	6.14
136	***ZNF831***	5.51	1.71	4.23	8.76
137	***CUX1***	5.50	0.78	0.70	5.59
138	*SLC5A9*	5.45	2.06	5.03	8.33
139	*PARPBP*	5.39	0.56	3.92	3.14
140	*NDST4*	5.37	1.34	4.03	5.86
141	*R3HDML*	5.26	0.15	0.98	2.84
142	*ADCY7*	5.26	1.62	2.68	4.02
143	***LHX8***	5.17	0.29	1.04	2.76
144	*PARK7*	5.11	1.95	3.25	1.91
145	*NTN1*	5.09	1.94	1.91	4.06

DACH2 is the only known marker of the nidopallium

One transcription factor, *DACH2,* was previously reported in the literature as a nidopallium marker (Szele et al. 2002). *DACH2* and its paralogue *DACH1* are the vertebrate orthologs of *Drosophila dac* (Hammond et al. 1998). Their functions in DT development are unknown. Chicken *DACH2* is expressed in the nidopallium at least as early as E11 (Szele et al. 2002), and by E14 labels an adult-like nidopallium (Figure 4.13a–c). Bas, E, and Field L are included in the *DACH2*(+) territory. *DACH2* also labels the non-input divisions of nidopallium including a territory dorsal to Bas (Figure 4.13a), medial to E (Figure 4.13b), and lateral to Field L (Figure 4.13c). The basic organization of the nidopallium is not significantly different at E20,

but labeling is now visible in the IHA (Figure 4.13d). *DACH2*, then, is not strictly a nidopallium marker but rather a marker of input and non-mesopallium association territories.

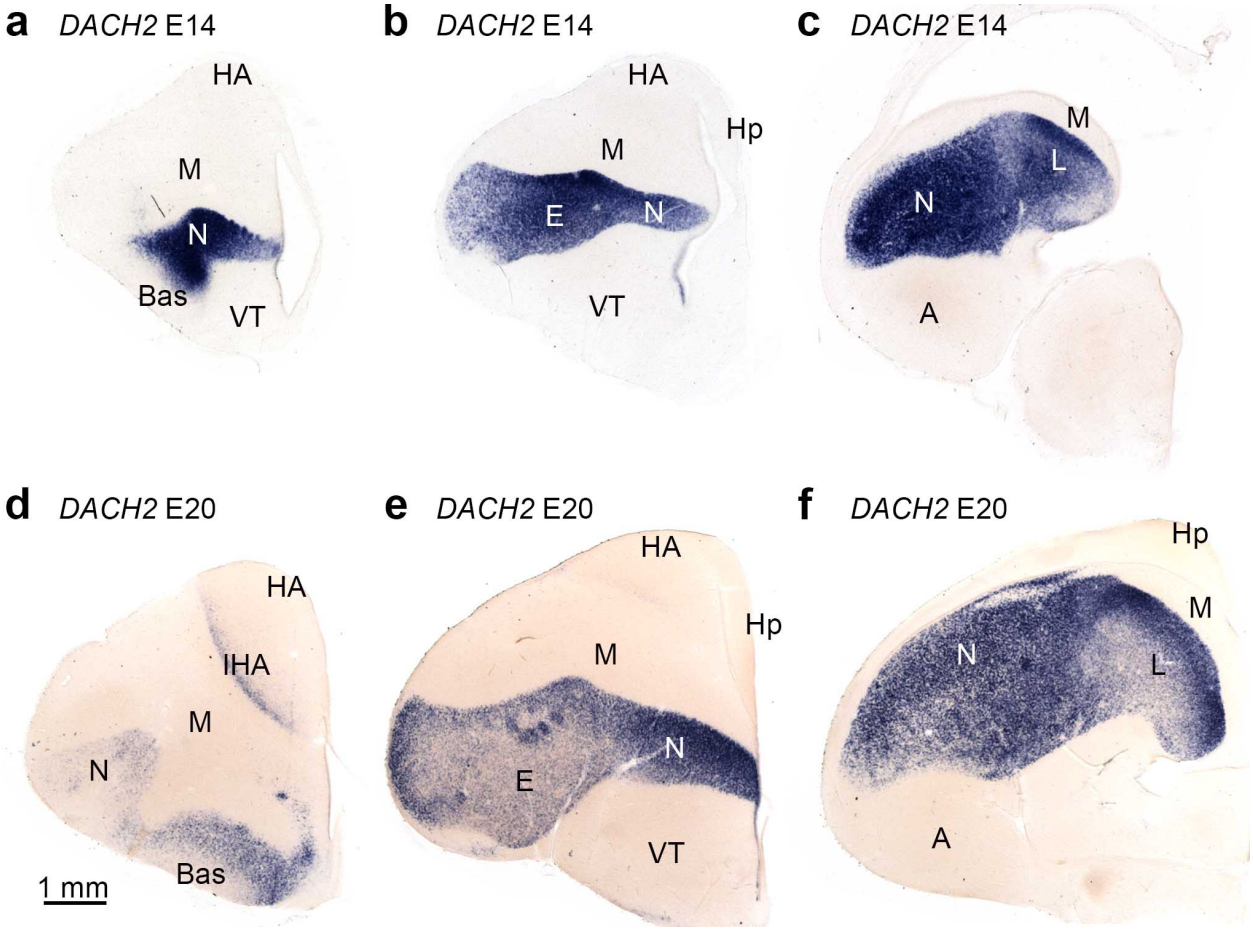

Figure 4.13 Chicken *DACH2* expression identifies the nidopallium
DACH2 staining identifies nidopallium in **(a)** anterior, **(b)** middle, and **(c)** posterior sections from a single E14 hemisphere. *DACH2* identifies nidopallium at E20, in addition to the IHA at anterior levels **(d–f)**. Arcopallium (A), nucleus basorostralis (Bas), entopallium (E), hippocampus (Hp), Field L (L), HA, IHA, mesopallium (M), nidopallium (N), and ventral telencephalon (VT) are labeled.

At least 30 of the top 145 nidopallium HOLT candidates were examined by ISH in this study and others, and none of them recapitulate the expression pattern of *DACH2*. Six sample transcriptional regulators are shown in Figure 4.14 to demonstrate the diversity of expression patterns found. Each is shown at a middle (Figure 4.14, first and third columns) and posterior level of the telencephalon (Figure 4.14, second and fourth columns). The top candidate, #1 *MEIS2*, shows scattered expression across DT territories (Figure 4.14a,b). #2 *LBH* strongly

marks M (Figure 4.14c) and A (Figure 4.14d), but not N. At anterior and middle levels, #3 *NR2F2* labels N and shows a sharp border with M (Figure 4.14e). At posterior levels, however, it is expressed intensely in A (Figure 4.14f). #65 *FEZF2* is most strongly expressed in output territories HA (Figure 4.14g) and A (Figure 4.14h). #101 *BCL11B* is expressed throughout most of the DT (Figure 4.14i,j). #149 *CUX1* is expressed in Bas (not shown), medial N (Figure 4.14k) and Field L (Figure 4.14l). These genes are not useful as nidopallium markers.

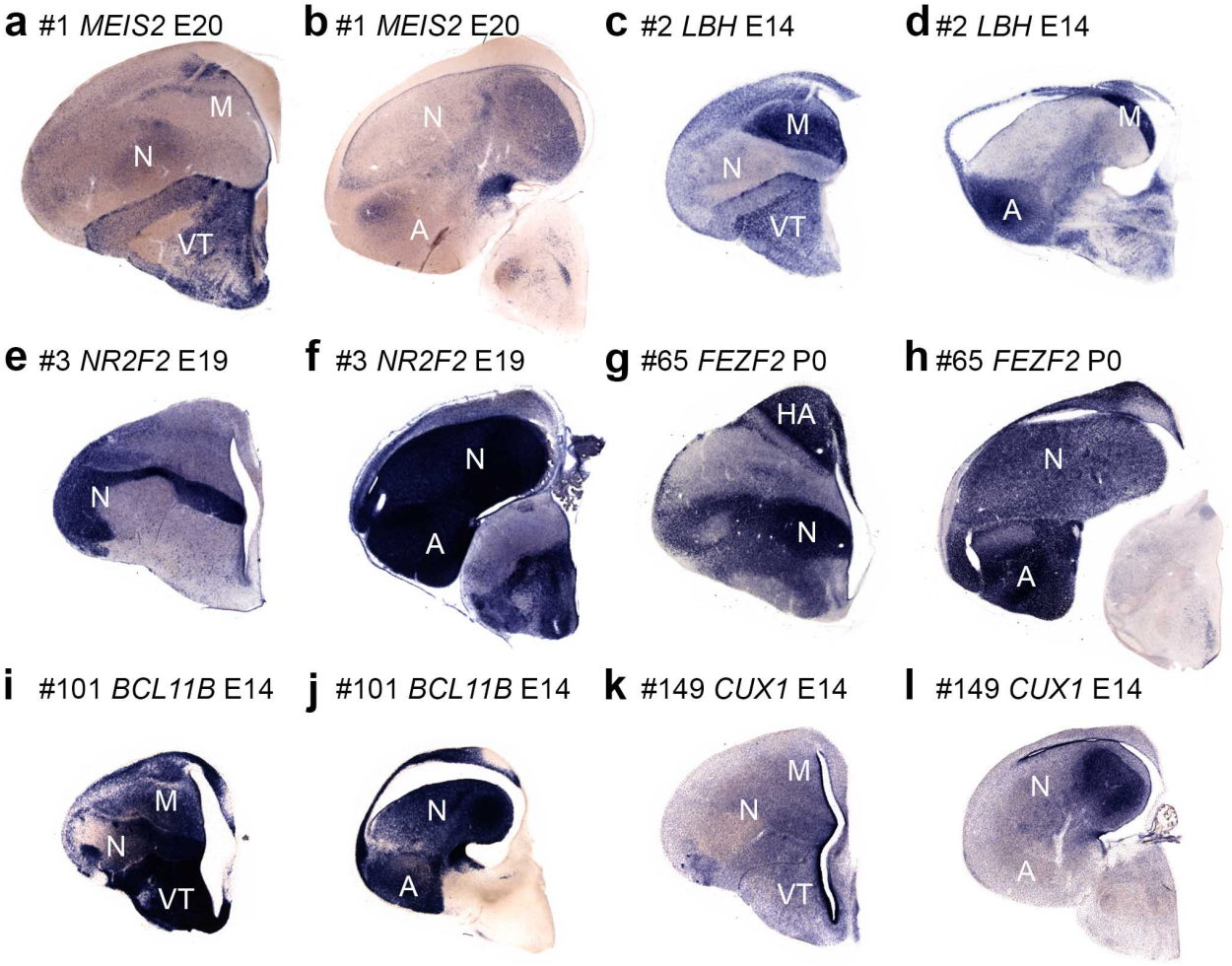

Figure 4.14 No additional nidopallium-specific marker genes were identified
Six transcription factors identified by the HOLT method are shown at a middle (**a**, **c**, **e**, **g**, **i**, **k**) and posterior (**b**, **d**, **f**, **h**, **j**, **l**) sections at various stages of telencephalon development. Arcopallium (A), HA, mesopallium (M), nidopallium (N), and ventral telencephalon are labeled.

Dach2 is thus the only nidopallium transcription factor marker gene available for potentially identifying a mammalian nidopallium homolog. Preliminary mouse ISH experiments determined that mouse *Dach2* is expressed at extremely low levels, yielding only faint labeling after a full week of color development. To increase the signal I prepared two non-overlapping probes of 1.5 kb length for combined use in subsequent ISH experiments. This approach labeled a small cell population distributed in a continuous laminar pattern across the entire neocortex.

Two lines of evidence indicate that *Dach2* is expressed just below L4 at postnatal day six (P6). The somatosensory barrel fields are well formed at P6 and are faintly visible as darkened blobs in L4 situated above the *Dach2*(+) lamina (Figure 4.15a,c). In addition, serially adjoining sections labeled with *Fezf2* probe (Figure 4.15b,d) also indicate that *Dach2*(+) cells are in L5. Notably, *Dach2* staining is found in an upper part of L5 possibly corresponding to L5a. At this time, no conclusions on any nidopallium homology can be drawn from the expression of this single marker.

Interestingly, chicken *DACH1* (#87, also recovered by entopallium HOLT in Chapter 3) appears to be nested within the *DACH2* expression domain (not shown). I employed a similar two-probe approach to identify *Dach1*-expressing cells in the mouse neocortex. Labeled cells appear to be present in a subset of the mouse *Dach2*(+) lamina (data not shown). Previous studies have reported *Dach1*/*Dach2* co-expression and redundant functionality in other developmental contexts (Davis et al. 2001, Davis et al. 2008).

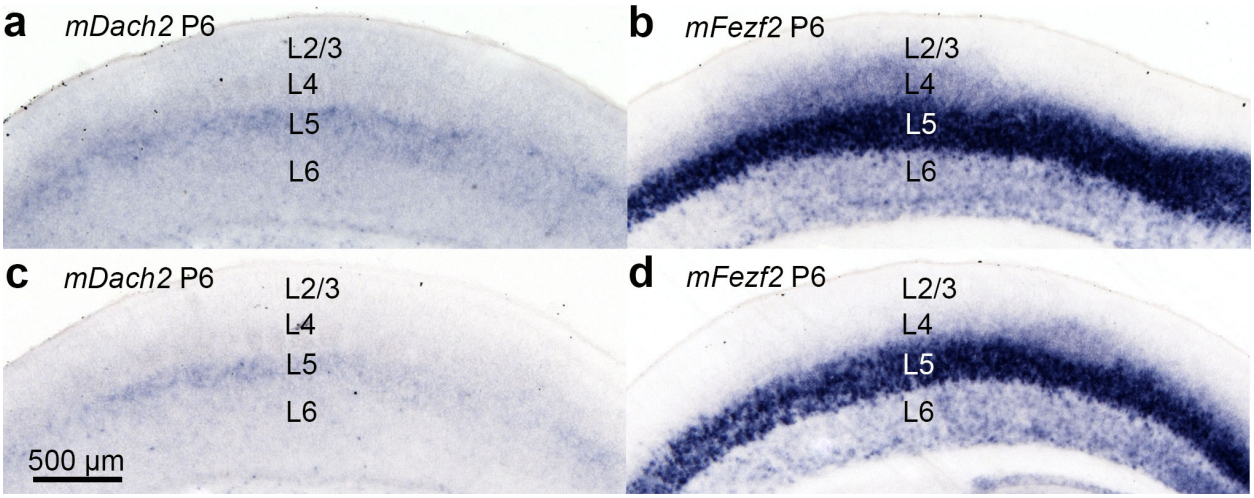

Figure 4.15 Mouse *Dach2* is expressed in a subset of layer 5 cells
(a, c) In situ hybridization for two non-overlapping *Dach2* probes labels cells in mouse neocortical L5 at postnatal day six. **(b, d)** *Fezf2* is an established layer 5 (L5) marker gene. Adjacent sections suggest that *Dach2*(+) cells are in upper L5. Sections in **a** and **b** are anterior to sections in **c** and **d**. The whisker barrels are structures found in the primary somatosensory cortex of rodents. They are faintly visible in **a** and **c**, just above *Dach2* labeling.

DISCUSSION

Gene expression and connections support homology of mesopallium to neocortical intratelencephalic neurons

I found that five transcription factors of the MesoGRN selectively enriched in chicken mesopallium and alligator (Chapter 5) mesopallium are expressed in the mouse neocortex. However, the MesoGRN-expressing cells do not form a coherent territory as in archosaurs. They are instead scattered across multiple neocortical layers. MesoGRN expression therefore does not support homology of the mesopallium with any single neocortical layer.

The MesoGRN factors are not upper layer (L2/3) specific markers, although all of them are expressed in L2/3 (Figure 4.10a–e). L2/3 enriched markers do exist, including *Cux1*, *Cux2* (Cubelos et al. 2010), and *Unc5d* (Rowell et al. 2010). Likewise, none of these three genes are expressed specifically in the chicken mesopallium (Figure 4.14k,l, *CUX2* and *UNC5D* not shown). L2/3 excitatory projection neurons make exclusively IT connections: they receive

information from within the telencephalon and, in turn, send axons to telencephalic targets—most prominently to the contralateral hemisphere via the corpus callosum. Based on connections, L2/3 neurons are an attractive candidate for a mesopallium homolog. However, this homology is not supported by gene expression evidence.

The MesoGRN factors are expressed in the deep layers, but are not restricted to L5, L6, or L5 and L6 in combination. L5 is the source of output projections to brainstem and spinal cord, most prominently through the pyramidal tract (PT). L5 specifically expresses genes including *Fezf2* (Inoue et al. 2004, Molyneaux et al. 2005), *Etv1* (Hevner et al. 2003), and *Cacna1h* (Talley et al. 1999). Chicken orthologs of mouse L5 markers are, as expected, expressed in long-range output neurons found in the HA and A (Dugas-Ford et al. 2012). Mesopallium is unlikely to be homologous to L5 output neurons.

L6 is also a source of cerebral output. L6 axons mainly target the dorsal thalamus to provide feedback inhibition on cortical input and do not extend as far as L5 axons. Interestingly, there is little evidence for avian DT–thalamus projections except as collaterals of brainstem projecting neurons, and therefore no compelling reason to compare mesopallium specifically to L6 cortico-thalamic (CT) neurons. Future studies should address this outstanding question of L6 CT origins.

The data do not support a homology of mesopallium to any neocortical layer in particular. Instead, MesoGRN expression patterns are consistent with the distribution of neocortical IT projection neurons. These neurons form the vast majority of upper layers L2 and L3, but are also intermingled with the connectionally and molecularly distinct output neurons in L5 and L6. MesoGRN factors appear to be expressed less densely in L5 compared with L2/3, consistent with their labeling a subset of L5 cells (Figure 4.10a–e). The trans-laminar distribution

of IT cells raises a critical point: avian DT nuclei are not homologous to neocortical layers. Instead, avian DT cell types, which are clustered into nuclei, are homologous to neocortical cell types that may or may not be found in a single layer. Input, PT, and CT neurons are enriched in L4, L5, and L6, respectively, but IT neurons are present in multiple layers.

Neocortical MesoGRN expression patterns are consistent with homology of mesopallium to IT cells. These cell populations also form several varieties of similar circuitry:

1) Neocortical L4 input neurons project heavily to IT neurons in L2/3 and L5 (Douglas and Martin 2004, Thomson and Lamy 2007, Harris and Shepherd 2015). The neocortical input-IT projection is fundamentally similar to the projections from the avian input nuclei E, Field L, and Bas to mesopallium (Atoji and Wild 2012).

2) Neocortical L2/3 neurons send a major descending projection to L5 output neurons. Likewise, all sensory recipient divisions of the mesopallium in turn issue projections to motor output nuclei of the arcopallium (Atoji and Wild 2012).

3) IT neurons in L2/3 and L5 form reciprocal connections across lamina and areas. L6 IT neurons also send long-range connections within the neocortex and to claustrum (a DT structure). These varieties of intracortical circuitry resemble the projections from mesopallium to nidopallium, and the intra-mesopallial connections from Md (then called “HD”) with Mv (Atoji and Wild 2012).

4) Finally, a critical subclass of corpus callosum-projecting IT cells sends collateral axons to the striatum in ventral telencephalon (Wilson 1987, Reiner et al. 2003, Reiner et al. 2010, Sohur et al. 2014). Similarly, the mesopallium projects to striatum in quail (Bons and Oliver 1986) and pigeon (Veenman et al. 1995, Reiner et al. 2001, Atoji and Wild 2012).

I propose that the avian mesopallium cell type is homologous to mammalian neocortical IT cells of L2, L3, L5, and L6. These cell types form multiple common varieties of IT circuits and share expression of at least five transcription factors. I reject the alternate possibilities that the mesopallium is homologous to upper layers only, or to any particular neocortical area.

The expanded Karten Hypothesis

Harvey Karten's proposal of homologous cell types in the amniote DT provided a crucial conceptual paradigm shift for comparative neuroanatomy (Karten 1969). Previous generations of anatomists carved vertebrate brains into large territories: neocortex, amygdala, Wulst, DVR, and so on. Attempts to compare biology at the level of telencephalic subdivisions bred a great diversity of interpretations with no clear path towards reconciliation (Striedter 2006). Karten recognized that the fundamental unit of brain organization is not a territory, or a developmental field, but rather the individual neuronal cell. In principle, neuronal cell types could be reorganized over evolutionary time into new and barely recognizable structures. Morphology of these neuronal cell types could be transformed from stellate to pyramidal, their assemblies from clustered to laminar, all without changing their fundamental cellular identity and circuitry. Here I add a third conserved cell type to Karten's original concept of input and output cells: the IT cell. I propose that the common ancestor of amniotes, which includes mammals, reptiles, and birds, had input, output, and IT cells in its DT. This hypothesis provides a clear resolution to the enigma of the mesopallium and the possibility of neocortical IT cell homologs in the bird.

I argue that the "IT cell" category is the level of abstraction that best accounts for the available evidence. Most attempts to identify neocortex homologs in sauropsids conceptualized the neocortex in terms of layers. As a result, previous authors were fixated on the question of whether L2/3 homologs exist in birds and reptiles. This approach has led to conflicting

conclusions. On one hand, some authors conclude that upper layers L2 and L3 are a mammalian invention (Cheung et al. 2007, Abdel-Mannan et al. 2008): they were added de novo in early mammals to a "primitive" three-layered reptilian dorsal cortex. This idea is rife with scala naturae thinking. It cannot be assumed that extant animals are frozen in evolutionary time, or that they can be arranged in order of evolutionary development. Moreover, while the question of novelty is a fundamental problem in biology (Wagner 2014), it cannot be assumed that truly novel, complex entities can appear suddenly in phylogeny. Evolution can only tinker with what is already available. A second interpretation is that birds (and by extension, reptiles) do in fact have a homolog of L2/3 in the mesopallium (Suzuki et al. 2012). This idea is not supported by the available gene expression data. It may be partially correct, but is limited by the constructed category of L2/3. I affirm the notion that L2/3 cells are a subset of IT cells, a larger biological category defined by function and gene expression (Harris and Shepherd 2015).

On the diversification of intratelencephalic cells

It is necessary to discuss IT cells as a broad category in order to facilitate cross-species comparisons. It is well established, however, that IT cells comprise many subtypes in both mammals and birds. In mammals, IT cells are found in L2/3, L5, and L6. These cell populations share expression of the MesoGRN, but they are also known to have layer-specific transcriptional differences with likely functional consequences (Molyneaux et al. 2009, Fame et al. 2011, Fame et al. 2016, Fame et al. 2017). For instance, L2/3 IT cells express marker genes that differentiate them from L5 IT cells (Molyneaux et al. 2009). IT subpopulations likely express slightly different combinations of MesoGRN factors, given the differences in their expression patterns (Figure 4.10). There is also a tremendous diversity of connectional properties within this class. IT cells can send long range projections across areas, across layers, to the striatum, to other IT

cells, or to L5/6 output cells. The full diversity of these neurons is not known, and mapping these connection types onto neuronal subtypes is a formidable challenge for the field. Emerging technologies, including high-throughput electron microscopy and tissue-scale fluorescent imaging, may enable the reconstruction of IT neurons and their input and output circuitry (Kasthuri et al. 2015, Kim et al. 2015, Economo et al. 2016).

Our understanding of mesopallium cell-type diversity is lacking. There are at least two major populations located in Md and Mv, respectively. Within the Mv, separate subpopulations receive different types of sensory information from DVR input nuclei (Atoji and Wild 2012). It is unknown whether, for instance, mesopallium cells that receive sensory information are the same as those that project to the nidopallium, arcopallium, or other mesopallium subtypes. Most mesopallium marker genes discussed here label the mesopallium more or less evenly. A deeper analysis, perhaps accomplished by transcriptionally profiling mesopallium subdivisions, would likely uncover intra-class molecular diversity.

There is currently little evidence to support finer homologies than at the level of the IT cell. For example, are subsets of mesopallium homologous to L2/3 or L5 IT cells, respectively? I anticipate that such an approach would not be biologically meaningful. The common ancestor of mammals and birds may have had a small population of IT cells, with relatively few subclasses, which underwent independent diversifications in clade specific ways. The result of this diversification is a large variety of IT subclasses in mammals that are all evolutionarily more closely related to one another than any single subclass is to avian IT cells. Indeed, even within the mammalian superorder euarchontoglires, IT cells are thought to have molecularly diversified independently between rodents and primates (Fame et al. 2017). Similar tree-thinking logic applies to species and to individual genes.

Independent diversifications of IT cells are clearly seen at the connectional level, as well. One significant clade-specific adaptation is the corpus callosum of placental mammals. Reptiles and birds lack this major pathway linking the cerebral hemispheres. Axons of the corpus callosum arise specifically from IT cells of multiple layers. I interpret the evolutionary genesis of the corpus callosum as the addition of a novel connection onto an otherwise pre-existing cell type. A second interesting difference between mammals and birds is the directionality of information flow between input and IT cells. In mammals, L4 input cells are thought to lie strictly upstream in excitatory neocortical networks. L4 projects heavily to L2/3 and L5, but does not receive excitatory connections in return (Feldmeyer 2012, Harris and Shepherd 2015). In contrast, the avian mesopallium forms bidirectional connections with all DVR primary input nuclei (Atoji and Wild 2012). The effects of these differences on DT information processing are unknown.

Mammals and birds also independently expanded their total numbers of IT cells. Mammalian IT cell numbers have been expanded in at least two ways: by increasing total cortical surface area (which might be expected to increase all major types of neurons proportionally) and by increasing the numbers of upper layer neurons through an extended neurogenesis. Both phenomena occurred in primate phylogeny. Upper layers occupy a larger fraction of total cortical depth in primates compared to rodents. Analogous expansions of mesopallium in large-brained birds were noted above. I can now propose that these independent expansions involve homologous associational cell-type populations, a fascinating example of parallel evolution of the neural bases of higher cognitive abilities.

Candidate gene regulatory networks (GRNs) for conserved dorsal telencephalon cell types

My previous comparative studies of input cells established that transcription factors are much more likely to be conserved at the cell-type level than are other classes of molecules. That is, a group of transcription factors is likely to be co-expressed in the same cell population in different species. In previous studies, I identified four transcription factors highly enriched in neocortical L4 and in all avian DT input populations: *RORA*, *RORB*, *NR0B1*, and *SATB1* (Figure 4.16, Input Cell GRN). I conclude the amniote LCA had input cells in its DT that received primary sensory information and expressed all four of these factors. This ancestral cell type diversified into the mammalian neocortical L4 and avian Bas, E, Field L, and IHA (Figure 4.16).

In this study, I focused my attention on transcription factors for species comparisons. I identified six transcription factors that are expressed specifically in avian mesopallium: *NHLH2*, *EMX1*, *ID2*, *SATB2*, *FOXP1*, and *BCL11A*. I found that five of these transcription factors are expressed in neocortical IT cells- a cell class with connections and associational functions fundamentally similar to the mesopallium (Figure 4.16, IT Cell GRN). At least two of these genes, *Satb2* and *Bcl11a*, are known to control the identity of mouse IT (specifically, callosal) cells (Alcamo et al. 2008, Gyorgy et al. 2008, Woodworth et al. 2016).

Satb2 is a critical determinant of callosal neuron identity in the mouse cerebral cortex: in the absence of *Satb2*, would-be callosal neurons misexpress *Bcl11b*, a determinant of output neuron identity (Arlotta et al. 2005), and misroute their axons through ventral telencephalon (Britanova et al. 2008, Gyorgy et al. 2008). A recent study from the Macklis group described a similar role for *Bcl11a* in mouse neocortex development, where its phenotype resembles that of *Satb2* (Woodworth et al. 2016). *Bcl11a* is expressed in *Satb2*(+) neurons extending axons across the corpus callosum, and is mutually exclusive to *Bcl11b*(+) output neurons. Mice mutant for

Bcl11a exhibit defects in corpus callosum development (Woodworth et al. 2016). While *Foxp1* has not been functionally tested in IT cells, it is expressed in *Satb2*(+)/*Bcl11b*(−) excitatory projection neurons in neocortical L3–L6, but not in GABAergic interneurons (Hisaoka et al. 2010). That *SATB2*, *BCL11A*, and *FOXP1* are all expressed together in the mesopallium suggests conserved roles for these factors in the specification of cell-type identity.

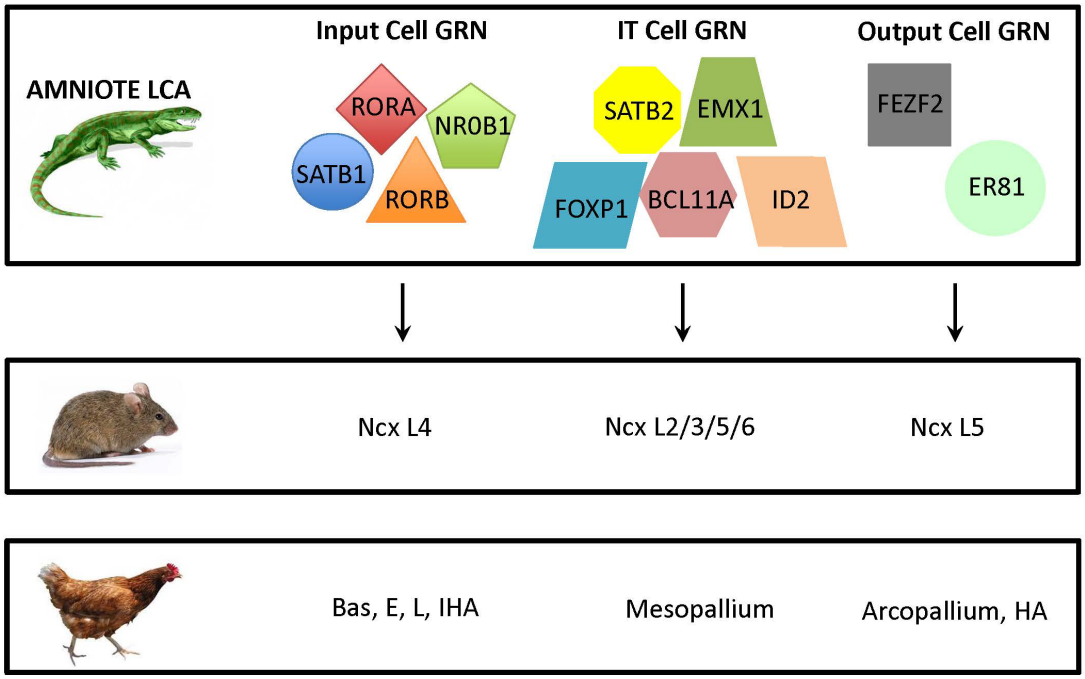

Figure 4.16 Candidate gene regulatory networks for input, intratelencephalic, and output cells

Three non-overlapping sets of conserved transcription factors are hypothesized to control the identity of dorsal telencephalon cell types in amniotes. These sets are referred to as gene regulatory networks (GRNs). Colored shapes represent transcription factor molecules in the cell nucleus. The input includes RORA, RORB, NR0B1, and SATB1. The IT cell GRN includes SATB2, EMX1, FOXP1, BCL11A, and ID2. The output cell GRN includes FEZF2 and ER81. In this model, the last common ancestor of amniotes (hypothetical animal shown) had input, IT, and output cell types expressing the indicated GRNs. The ancestral input cells diversified into neocortical layer 4 in mammals and Bas, E, L, and IHA in birds. The ancestral IT cells diversified into neocortical IT cells of multiple layers in mammals, and mesopallium in birds. The ancestral output cells gave rise to mammalian neocortical layer 5, and arcopallium and HA in birds.

Previous studies reported expression of *Id2* in mouse neocortical L2/3, L5, and L6 (Rubenstein et al. 1999, Zhou et al. 2001, Bishop et al. 2002), but expression of *Emx1* has not been reported in the postnatal or adult neocortex. The functions of these genes in post-mitotic neurons are unknown. *Emx1* in particular is an ancient and highly conserved homeobox-containing gene with well-known roles in neocortex specification and patterning (Simeone et al. 1992a, Simeone et al. 1992b, Fernandez et al. 1998, Bishop et al. 2002, Stocker and O'Leary 2016). It is a highly attractive candidate gene for future manipulation experiments.

I propose that these factors comprise a gene regulatory network for IT cell identity, and that their essential activities are conserved in birds (and non-avian reptiles). Biological conservation over great evolutionary time, such as the 320 million years separating mammals and birds, is a natural experimental test of genetic necessity. If these factors were not required together in the same cell population, one would not expect to find this cohort of genes maintained in such similar cell types in mouse and chicken. This prediction, however, requires extensive further testing. CRISPR technology, only recently developed (Cong et al. 2013), is rapidly becoming easier for more researchers to deploy in more species (Veron et al. 2015, Kalebic et al. 2016). An experimental approach using in utero or in ovo electroporation may allow us to dissect the functions of candidate-gene regulatory networks in mouse and chicken.

Divergence in developmental mechanisms for dorsal telencephalon cell-type specification

Mammalian and avian DT organizations are highly divergent. In the neocortex, each major cell class is found in a thin lamina extending over the entire neocortical surface. Every area of neocortex has the same fundamental cell-type composition, although with variations of relative cell-type abundance, connectivity, and cell morphology. IT cells, for example, are found in every neocortical area. The avian DVR contains territories, each with a single principal cell

type segregated from others. Avian IT cells are collected in the mesopallium, separate from input and output populations. Major divergences in developmental mechanisms have surely accompanied divergence of DT anatomy.

Importantly, cell types can still be homologous across species even if their mode of generation differs. For example, the turtle dorsal cortex contains homologs of neocortical input and output cells (Dugas-Ford et al. 2012), despite the fact that neocortical cells are born in an "inside-out" pattern while turtle dorsal cortex is produced in an inverse "outside-in" pattern (Goffinet et al. 1986). Garcia-Moreno and Molnar recently claimed that chickens do not have a homolog of callosal projection neurons because of differences in neurogenesis and radial glia behavior (Garcia-Moreno and Molnar 2015). I disagree with this interpretation because developmental mechanisms generating a cell type are only one of many potential character traits that should be considered for homology.

I provided strong experimental support for a fate-restricted territory in anterior chicken DT that gives rise only to IT cells. This is a clear and striking difference from neocortical neurogenesis: in the neocortex, all major cell types are thought to be generated sequentially at all points along the neocortical neuroepithelium (Rakic 2009). A key future direction is to elucidate the developmental causes of these differences. One possibility is a difference in the mode of cell-type specification. In the avian DT, the spatial relations of progenitors to neighboring signaling centers may regulate specification of progenitors towards an IT fate. For example, IT fate may be specified by high or prolonged *FGF8* signaling from the anterior neural ridge, analogous to the specification of neocortical area fates in mouse DT (Fukuchi-Shimogori and Grove 2001, Toyoda et al. 2010). Whatever the mechanisms of divergence, it is clear that avian IT progenitors must be distinct from input and output progenitors.

The long-standing model of neocortical neurogenesis postulates that radial glia progenitors sequentially produce all major neural subtypes in turn. Specifically, any given progenitor is competent to produce any neuron type (Guo et al. 2013). However, the nuances of neocortical cell lineages are complex and underexplored experimentally, and many different possibilities formally exist (Greig et al. 2013). Two recent studies challenged this entrenched concept by identifying fate-restricted neocortical progenitors in the mouse. These cells are amplified by symmetric, non-neurogenic divisions during early neurogenesis, and later gave rise to *Satb2*(+) upper layer neurons and a smaller population of *Satb2*(+)/*Bcl11b*(−) deep layer neurons (Franco et al. 2012, Gil-Sanz et al. 2015). That these fate-restricted neocortical progenitors could be homologous to avian mesopallium progenitors is an extremely exciting possibility worthy of future study.

On the nature of nidopallium

Establishing the mesopallium as a territory of neocortical IT-homologous cells highlights the mystery of the avian nidopallium. What is the nidopallium homolog, if not IT cells? The entire nidopallium could be homologous to neocortical L4, but this possibility is currently unsupported because only primary sensory divisions of the nidopallium (Bas, E, and Field L) express L4 marker genes. The nidopallium makes numerous associational connections similar to those of the mesopallium, but does not express any of the described IT markers. This is partly due to a selection bias: I previously sought genes expressed in mesopallium exclusively.

I was unable to identify any nidopallium-specific markers beyond *DACH2*, despite examining more than 30 genes from the transcriptome data. The genes examined proved to be present in nidopallium, but did not label the entire structure. One possible interpretation is that additional nidopallium determinants exist but eluded detection. A second possibility is a

combinatorial GRN that would have been culled through the design of the HOLT method. A third possibility, which I currently favor, is that the nidopallium does not have a consistent molecular identity like the mesopallium. The nidopallium contains input cell populations, but also expresses various markers of output cell identity, including *FEZF2*. Nidopallium also contains IT-like cells of unknown homology. If nidopallium is a complex mixture of cell types with independent developmental and evolutionary histories, it may not be sensible to ask whether nidopallium has a single mammalian homolog. This is analogous to asking whether birds have a single homolog of neocortical L5. Birds have homologs of L5 output neurons in the HA and arcopallium and L5 IT neurons in the mesopallium.

Expression of *Dach2* in the mouse neocortex must not be over-interpreted, as it is only a single gene. Nonetheless, *Dach2* expression in L5a raises some interesting possibilities. L5a contains IT-like cells in receipt of secondary sensory information from L4 and L2/3 (Harris and Shepherd 2015). The L5a population identified by *Dach2* staining may correspond to a poorly understood IT cell variety. L5a may also receive primary sensory information from the thalamus and, consequently, *Dach2* labeling may identify an input cell subtype. L5a is also thought to receive selective input from associational matrix-type thalamic nuclei, distinct from the core-type thalamic nuclei that project most densely to L4 (Harris and Shepherd 2015). Another possibility is that the proximity of *Dach2*(+) cells to input cells is of developmental importance, rather than expression of *Dach2* in input cells per se. The possibility that *Dach2* is an irrelevant red herring also cannot be ruled out at this time. In any case, new approaches are required to study this cell population in mouse because the extreme paucity of expression precludes the co-expression studies necessary for further characterization. The development of mouse *Dach2*-Cre reporter lines may be helpful in this regard.

CHAPTER 5

Molecular anatomy of the alligator dorsal telencephalon

ABSTRACT

The evolutionary relationships of the mammalian neocortex and avian dorsal telencephalon (DT) nuclei have been debated for more than a century. Despite their central importance to this debate, non-avian reptiles remain underexplored using modern molecular techniques. Reptile studies harbor great potential for revealing the changes in DT organization that occurred in the early evolution of amniotes. They may also help to clarify adaptations in the avian DT, which comprises a huge, cell-dense dorsal ventricular ridge (DVR) and a nuclear dorsal-most structure, the Wulst. Even among reptiles, a wide diversity of clade-specific DT structures can be identified. Crocodilians are phylogenetically and anatomically attractive for DT comparative studies: they are the closest living relatives of birds and have a strikingly bird-like DVR, but they also possess a highly differentiated cerebral cortex. I studied the DT of the American alligator, *Alligator mississippiensis*, at late embryonic stages using a panel of molecular marker genes. Gene expression and cytoarchitectonic analyses identified clear homologs of all major avian DVR subdivisions: a mesopallium, an extensive nidopallium containing primary sensory input territories, and an arcopallium. The alligator medial cortex is divided into three components resembling mammalian dentate gyrus, CA fields, and subiculum in gene expression and topology. The alligator dorsal cortex contains putative homologs of neocortical input, output, and intratelencephalic projection neuron subtypes and, most notably, they are organized into sublaminae similar to mammalian neocortical layers. These findings on the molecular anatomy of the crocodilian DT are summarized in an atlas of the alligator telencephalon.

INTRODUCTION

The dorsal telencephalon (DT) is broadly associated with sensory integration, execution of motor commands, and higher cognitive functions. The DT is also the mostly highly divergent of any vertebrate brain region and manifests a staggering diversity of anatomies (Nieuwenhuys et al. 1998, Butler and Hodos 2005). It is clear that DT organization is unusually pliable to the pressures of evolution and adaptation compared with, for example, the basal ganglia, which has changed little in its essentials since the human lineage diverged from that of lamprey (Grillner and Robertson 2016). While presumably beneficial to radiating vertebrates, this pliability has made it notoriously difficult for anatomists to resolve homologies of DT components. In particular, the questions of which DT regions, structures, or cells in reptiles and birds are homologous to the mammalian neocortex have cultivated a multigenerational debate in evolutionary neuroscience (Striedter 2005, Butler et al. 2011, Dugas-Ford and Ragsdale 2015). Progress has undoubtedly been hindered by a lack of reptile gene expression data.

Mammals, reptiles, and birds (together, the extant amniotes) share some relatively noncontroversial DT structures. In all amniotes, information from the olfactory bulbs reaches a thin, lateral territory called the piriform cortex in mammals (Figure 5.1, CPi of cat and mouse) and the lateral cortex in reptiles (Figure 5.1, LC). Birds maintain this sensory pathway despite a secondary reduction in the size of their olfactory bulbs and olfactory cortex (Figure 5.1, CPi of pigeon) (Reiner and Karten 1985, Atoji and Wild 2014). There is widespread agreement that the lateral olfactory-recipient zones are homologous. Likewise, a medial DT territory is designated the hippocampus in mammals and birds (Figure 5.1, Hp of pigeon, not visible in cat and mouse sections) and the medial cortex in reptiles (Figure 5.1, MC). Its basic functions in spatial memory are thought to be a shared feature across amniotes (Striedter 2016). It remains unclear whether

reptiles and birds have specific homologs of dentate gyrus, CA fields, or subiculum, which together constitute the mammalian hippocampal formation (Striedter 2016).

The DT cell populations located between lateral olfactory and medial hippocampal territories are more problematic. In mammals, this space is occupied by the six-layered neocortex (Figure 5.1, Ncx). The neocortex varies greatly in size and folding complexity across species (Figure 5.1, smooth in mouse and folded in cat), but its six-layered architecture (Brodmann 2006), canonical columnar circuitry (Lorente de Nó 1938, Mountcastle 1957, Harris and Shepherd 2015), and tangential organization into sensory and motor areas (Krubitzer 2007) are highly conserved.

Reptiles and birds do not have a six-layered neocortex. Instead, reptiles possess a three-layered dorsal cortex (Figure 5.1, DC). Interpretations of this major species difference vary, but it is commonly thought that reptile dorsal cortex layers correspond to neocortical molecular layer 1 (L1) and the deep layers L5 and L6 (Cheung et al. 2007). The upper neocortical layers L2, L3, and L4 are, in this view, mammalian innovations built upon a primitive reptilian condition. This "deep layer hypothesis" is challenged by the existence of neocortical L4-like connections and gene expression in the turtle dorsal cortex (Hall and Ebner 1970b, Dugas-Ford et al. 2012). The cell-type composition of the dorsal cortex is more complex than previously thought, and the structural and evolutionary relationships of the dorsal cortex to mammalian neocortex are in no sense understood.

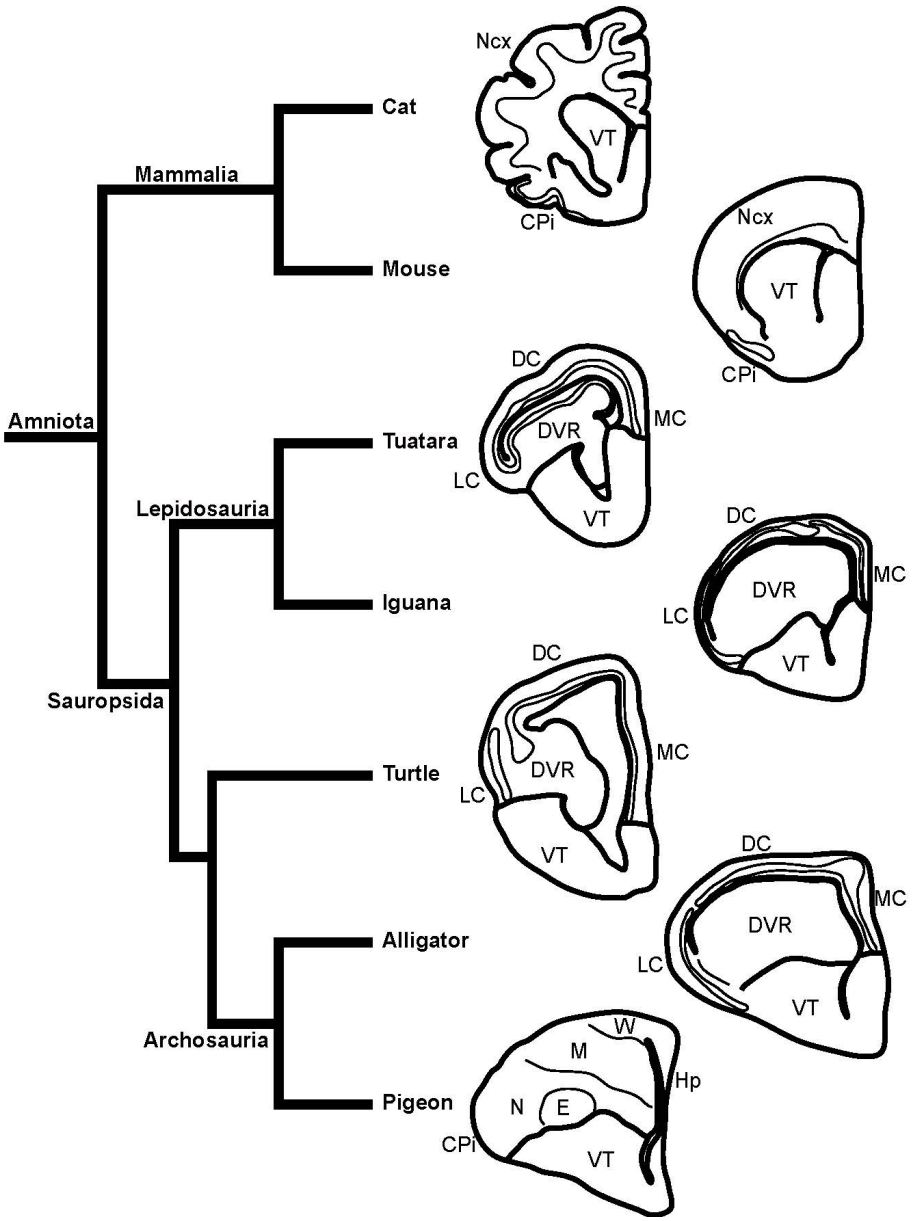

Figure 5.1 Amniote phylogeny and representative telencephalon anatomies
The clade Amniota includes mammalia and sauropsida (reptiles and birds). Snakes, lizards, and the tuatara form a major Sauropsida group called Lepidosauria. The second major Sauropsida group includes turtles and Archosauria (crocodilians and birds). Schematic tracings of telencephalon anatomy for representative amniotes are shown in coronal cross section, with medial to right and dorsal at top. All amniotes have a ventral telencephalon (VT) and dorsal telencephalon. Mammalian dorsal telencephalon includes neocortex (Ncx), piriform cortex (Cpi), hippocampus (not shown), and amygdala (not shown). Reptile dorsal telencephalon includes a cerebral cortex with medial (MC), dorsal (DC), and lateral (LC) divisions, as well as a dorsal ventricular ridge (DVR). Birds have a DVR, but with further internal subdivisions including mesopallium (M), nidopallium (N), entopallium (E), and arcopallium (not shown). Birds have a dorsal Wulst (W), medial hippocampus (Hp), and lateral piriform cortex (CPi). Drawings are not to scale.

Birds have a Wulst in place of a dorsal cortex (Figure 5.1, W), so named because it forms a conspicuous bulge atop the telencephalon (Kalischer 1905). The Wulst contains populations of clustered cells rather than cortical layers, although these closely apposed cell populations have been referred to as pseudolayers to emphasize their organizational similarities to cortex (Medina and Reiner 2000). These cell populations include, from medial to lateral, the hyperpallium apicale (HA), the interstitial nucleus of the hyperpallium apicale (IHA), and the dorsal mesopallium (Md) (Reiner et al. 2004a, Jarvis et al. 2013). Birds almost certainly descended from animals with a dorsal cortex, but it is unknown how the layered dorsal cortex was modified into a Wulst with distinct nuclei.

The reptilian and avian DT contains a second decidedly nonmammalian structure called the dorsal ventricular ridge (Figure 5.1, DVR). (Johnston 1915, Ulinski 1983). The DVR lies below the dorsal cortex or Wulst, but is still within the DT (Reiner et al. 2004a). In many species, it forms a protrusion into the lateral ventricle (Figure 5.1, turtle). The profound challenges in comparing DVR to mammalian DT are well documented (Holmgren 1925, Ariëns Kappers et al. 1936, Karten 1969, Bruce and Neary 1995, Fernandez et al. 1998, Puelles 2001, Dugas-Ford et al. 2012), but the difficulty of comparing this structure across reptiles, or from reptiles to birds, is seldom acknowledged.

DVR organization differs widely across reptile groups. Pleurodiran (or side-necked) turtles have a large nuclear territory in their anterior DT, a trait not apparent in Cryptodiran turtles (Riss et al. 1969). In other groups, like crocodilians, the DVR is densely packed with cells and can be divided into multiple territories with sharp boundaries (Crosby 1917, Riss et al. 1969). In the remarkable brain of the tuatara, the DVR contains a thin cortex-like structure that appears to be continuous with the dorsal cortex at the lateral edge of the DT (Figure 5.1, cortex

outlined within DVR) (Cairney 1926, Durward 1930, Reiner and Northcutt 2000). Reptile DVR is often divided into an anterior ADVR and posterior, or basal, BDVR (Ulinski 1983). Nonetheless, homologies of specific DVR subdivisions across reptiles are poorly understood.

Birds elaborated the DVR by developing novel subdivisions and connections. The avian ADVR is divided into the ventral mesopallium (Figure 5.1, M) and the nidopallium (Figure 5.1, N) (Ulinski 1983, Reiner et al. 2004a). The nidopallium contains primary sensory nuclei including the visual entopallium (Figure 5.1, E). A posterior avian DVR territory called the arcopallium is thought to be homologous to the reptilian BDVR (Ulinski 1983), and itself contains at least four subdivisions with distinct connectional characteristics (Reiner et al. 2004a, Dugas-Ford 2009). As with divisions of the avian Wulst, it is unknown whether reptiles have homologs of mesopallium, nidopallium, or arcopallium subdivisions.

Crocodilians are phylogenetically positioned to address many of these crucial outstanding problems in comparative DT anatomy. They can serve as model reptiles, in that they possess a reptile-typical cerebral cortex with LC, DC, and MC subdivisions (Figure 5.1, alligator). Consistent with their position as the closest living relatives of birds, crocodilians have a large, cell-dense DVR with clear internal subdivisions. Indeed, they have the largest brain of any non-avian reptile, even approaching the relative size of basally branching birds such as *Gallus gallus* (Northcutt 2013). This observation, coupled with the exceptionally slow rate of crocodilian genome evolution (Green et al. 2014), suggests that the crocodilian DVR may closely resemble that of the last common ancestor of birds. Moreover, a molecular study of crocodilian cerebral cortex will allow further comparisons with the avian Wulst and with the mammalian neocortex.

The value of the crocodilian brain to comparative anatomy has been appreciated by many researchers (Rabl-Rückhard 1878, Herrick 1890, Unger 1906, Reese 1915, Crosby 1917, Rose

1923, Huber 1926, Riss et al. 1969, Pritz 1974b, Pritz 1975, Pritz and Northcutt 1977, Ulinski 1983, Clark and Ulinski 1984). I advance the understanding of this important animal by performing a detailed molecular anatomical study of alligator DT, the first such comprehensive effort in any reptile brain. I analyzed the DT of the late-embryonic American alligator, *Alligator mississippiensis*, by performing in situ hybridization with a panel of cell- and region-specific marker genes previously characterized in mouse and chicken. These marker genes often identified differentiated subdivisions of alligator DT, with expression boundaries that coincided with cytoarchitectonic boundaries. When possible, I propose mammalian and avian homologies to alligator DT structures. These findings are documented, in part, by an atlas of the late-embryonic alligator telencephalon.

RESULTS

Orientation and atlas

I examined late-embryonic alligators at Ferguson's stage 25, defined as resembling "a miniature version of a hatchling, with a considerable volume of external yolk and a large umbilical region" (Ferguson 1985). These animals appear fully formed and are within a few days of hatching (Figure 5.2a). The external morphology of the telencephalon is typical of reptiles: elongate, slender, and without any dramatic folds (Figure 5.2b). The olfactory bulb is situated rostrally in the alligator snout, connected to the DT by a long olfactory tract (Figure 5.2b, OB). The olfactory bulb was not examined in this study.

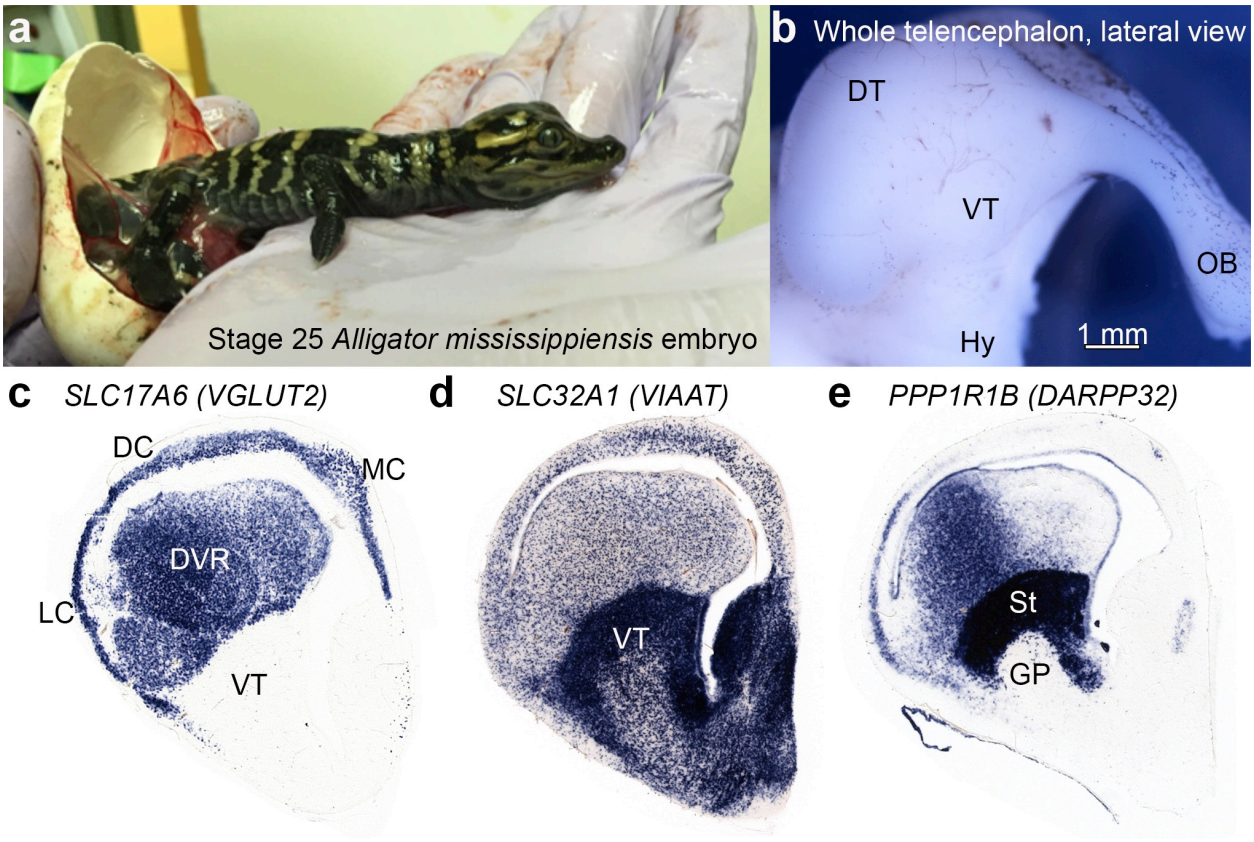

Figure 5.2 Overview of *Alligator mississippiensis* telencephalon
(a) Lateral view of a stage 25 alligator embryo. This animal is a "miniature hatchling." **(b)** Lateral view of a whole alligator telencephalon. Dorsal telencephalon (DT), ventral telencephalon (VT), hypothalamus (a diencephalic structure, Hy), and olfactory bulb (OB) are labeled. **(c)** *SLC17A6* expression labels excitatory neurons of the DT. Medial cortex (MC), dorsal cortex (DC), lateral cortex (LC), and dorsal ventricular ridge (DVR) are labeled. **(d)** *SLC32A1* expression labels ventral telencephalon (VT) and inhibitory interneurons scattered across all DT subdivisions. **(e)** *PPP1R1B* expression strongly labels the striatum (St), a VT subdivision. The internal VT region that does not express *PPP1R1B* is likely homologous to mammalian and avian globus pallidus (GP). Sections correspond approximately to atlas level 8.

Like other studied vertebrates, the alligator has a telencephalon comprising a DT enriched in *SLC17A6*-expressing excitatory neurons (Figure 5.2c), and a ventral telencephalon where *SLC32A1*-expressing inhibitory neurons are concentrated (Figure 5.2d, VT) (Dugas-Ford and Ragsdale 2015). The VT is also the developmental origin of the inhibitory interneurons that populate the DT (Anderson et al. 1997, Marin and Rubenstein 2001, Martinez-de-la-Torre et al. 2011). These cells are scattered across all DT subdivisions in the alligator (Figure 5.2d). The

dorsal-most zone of the VT expresses *PPP1R1B* (*DARPP32*) and is likely the alligator striatum (Figure 5.2e, St) (Ouimet et al. 1992, Reiner et al. 1998, Reiner et al. 2004a).

The alligator DT is divided into cerebral cortex and DVR (Table 5.1). The cerebral cortex is divided into a lateral cortex (LC), dorsal cortex (DC), and medial cortex (MC) (Ulinski 1990a). I do not further subdivide the LC. My data, presented below, establish that the dorsal cortex contains lateral (DCl) and medial (DCm) fields. Furthermore, the medial cortex contains lateral (MCl), intermediate (MCi), and medial (MCm) fields. I show that the DVR is divided into mesopallium (M), nidopallium (N), and arcopallium (A). I do not designate further mesopallium subdivisions, but I do identify an important cell population that demonstrates anatomical continuity between mesopallium and DCl. I name this structure the mesopallial bridge (mb). The nidopallium contains at least three primary sensory input territories identified as nucleus basorostralis (Bas), entopallium (E), and Field L (L), but these three territories only account for a fraction of total nidopallium area. I divide the arcopallium into a dorsolateral nucleus (Adl), a dorsomedial nucleus (Adm), and a ventral nucleus (Av).

The described DT subdivisions are shown in the following atlas, with 12 levels of the right telencephalon placed in anterior to posterior sequence (Figures 5.3–5.14). The atlas is derived from a single cerebral hemisphere sliced coronally at 20 μm thickness. At each level, three serially adjoining sections labeled for *ELAVL4* (panel a), *NEFM* (panel b), and *SLC17A6* (panel c) are shown. A schematic illustrates my interpretation of the anatomy at each level (panel d), produced by tracing the *ELAVL4* section. Gene expression patterns used to define these divisions and support the proposed homologies are described in the following sections. Marker genes employed in this study are listed in Table 5.2.

Table 5.1 Hierarchical organization of alligator telencephalon subdivisions

Telencephalon													
Dorsal Telencephalon (DT)												VT	
Cerebral Cortex							Dorsal Ventricular Ridge (DVR)					St	GP
LC	DC		MC			M	N			A			
	DCl	DCm	MCl	MCi	MCm		Bas	E	L	Adl	Adm	Av	

Telencephalon has dorsal (DT) and ventral (VT) divisions. VT contains striatum (St) and globus pallidus (GP) in addition to other cell populations. DT contains cerebral cortex and dorsal ventricular ridge (DVR). Cerebral cortex contains lateral (LC), dorsal (DC), and medial (MC) fields. DC contains lateral (DCl) and medial (DCm) fields. MC contains lateral (MCl), intermediate (MCi), and medial (MCm) fields. DVR contains mesopallium (M), nidopallium (N), and arcopallium (A). Nidopallium contains nucleus basorostralis (Bas), entopallium (E), and Field L (L). Arcopallium contains dorso-lateral (Adl), dorso-medial (Adm), and ventral (Av) nuclei.

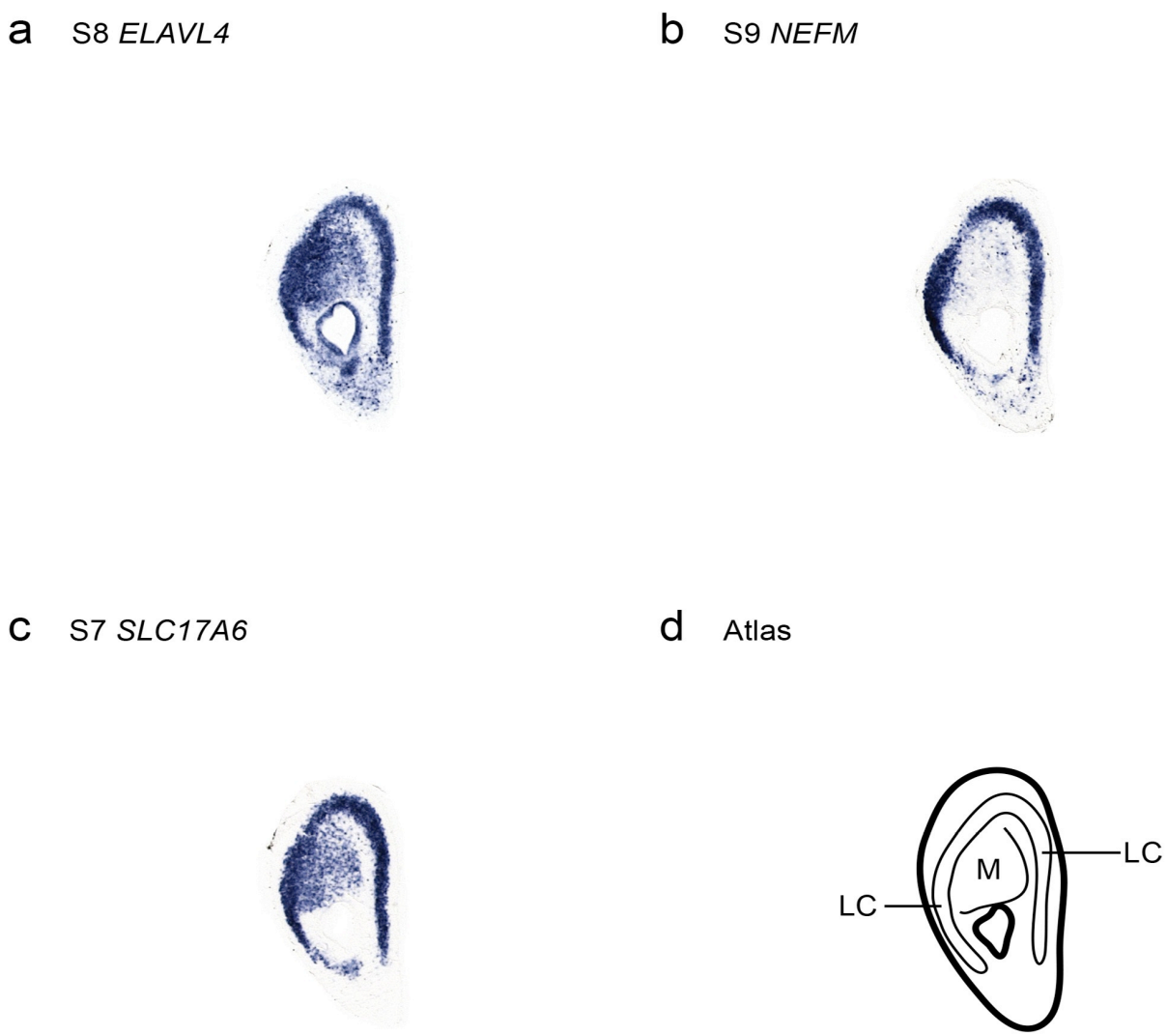

Figure 5.3 Atlas: Level 1
Sections 7–9 are shown. In situ hybridizations for **(a)** *ELAVL4*, **(b)** *NEFM*, and **(c)** *SLC17A6*. **(d)** Schematic illustration.

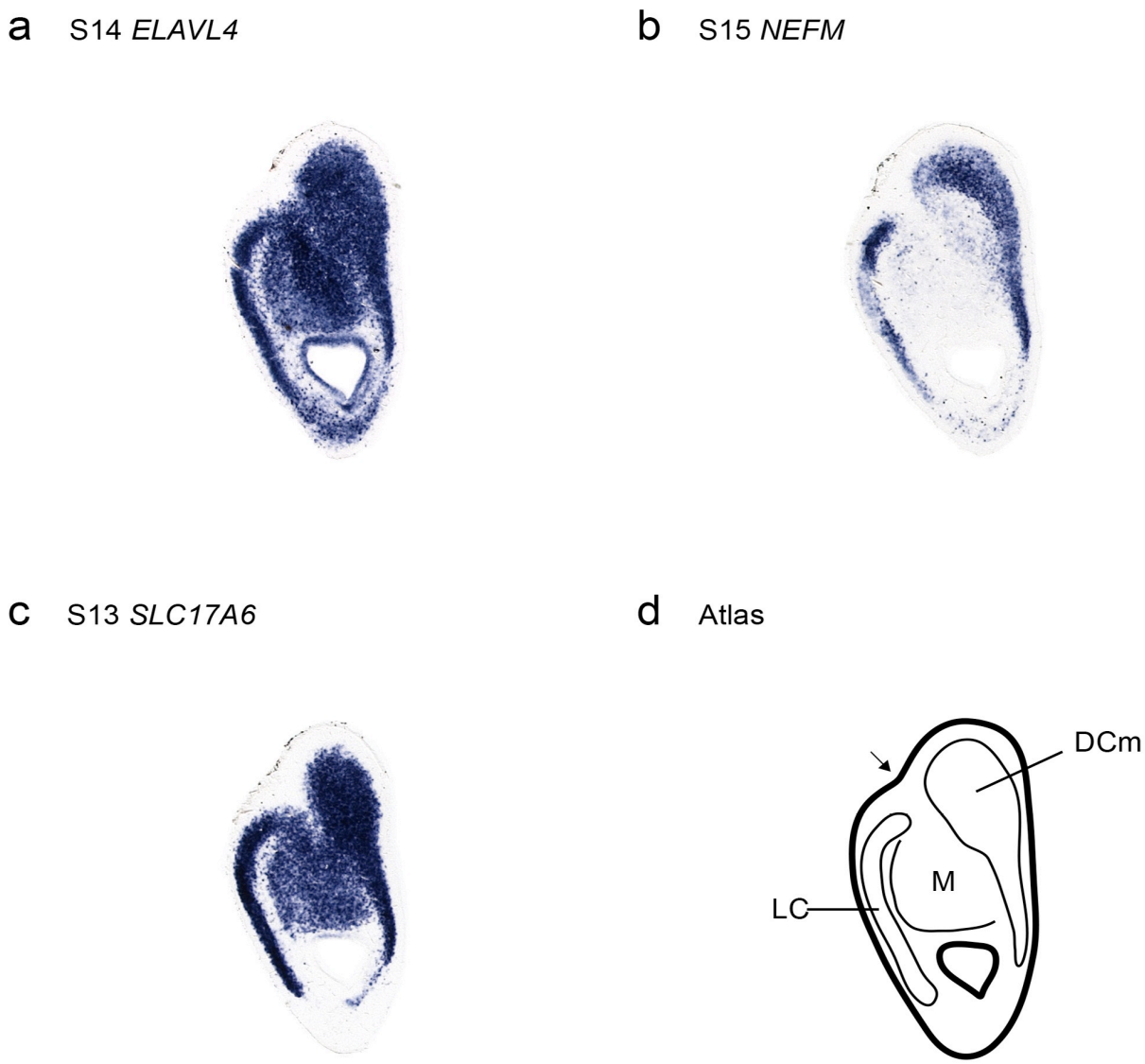

Figure 5.4 Atlas: Level 2
Sections 13–15 are shown. In situ hybridizations for **(a)** *ELAVL4*, **(b)** *NEFM*, and **(c)** *SLC17A6*. **(d)** Schematic illustration. The arrow indicates a shallow sulcus between dorsal cortex and DVR.

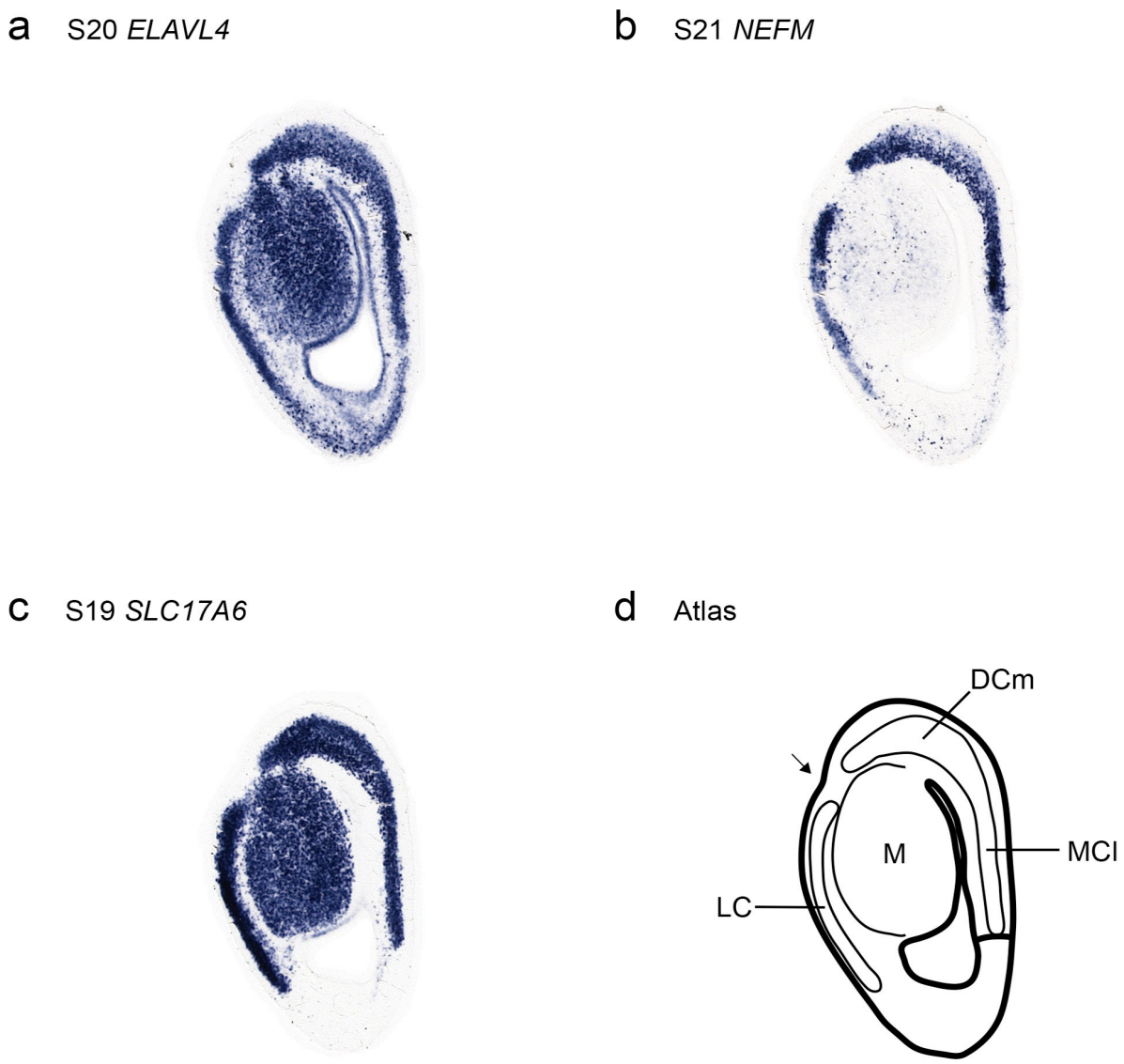

Figure 5.5 Atlas: Level 3
Sections 19–21 are shown. In situ hybridizations for **(a)** *ELAVL4*, **(b)** *NEFM*, and **(c)** *SLC17A6*. **(d)** Schematic illustration. The arrow indicates a shallow sulcus between dorsal cortex and DVR.

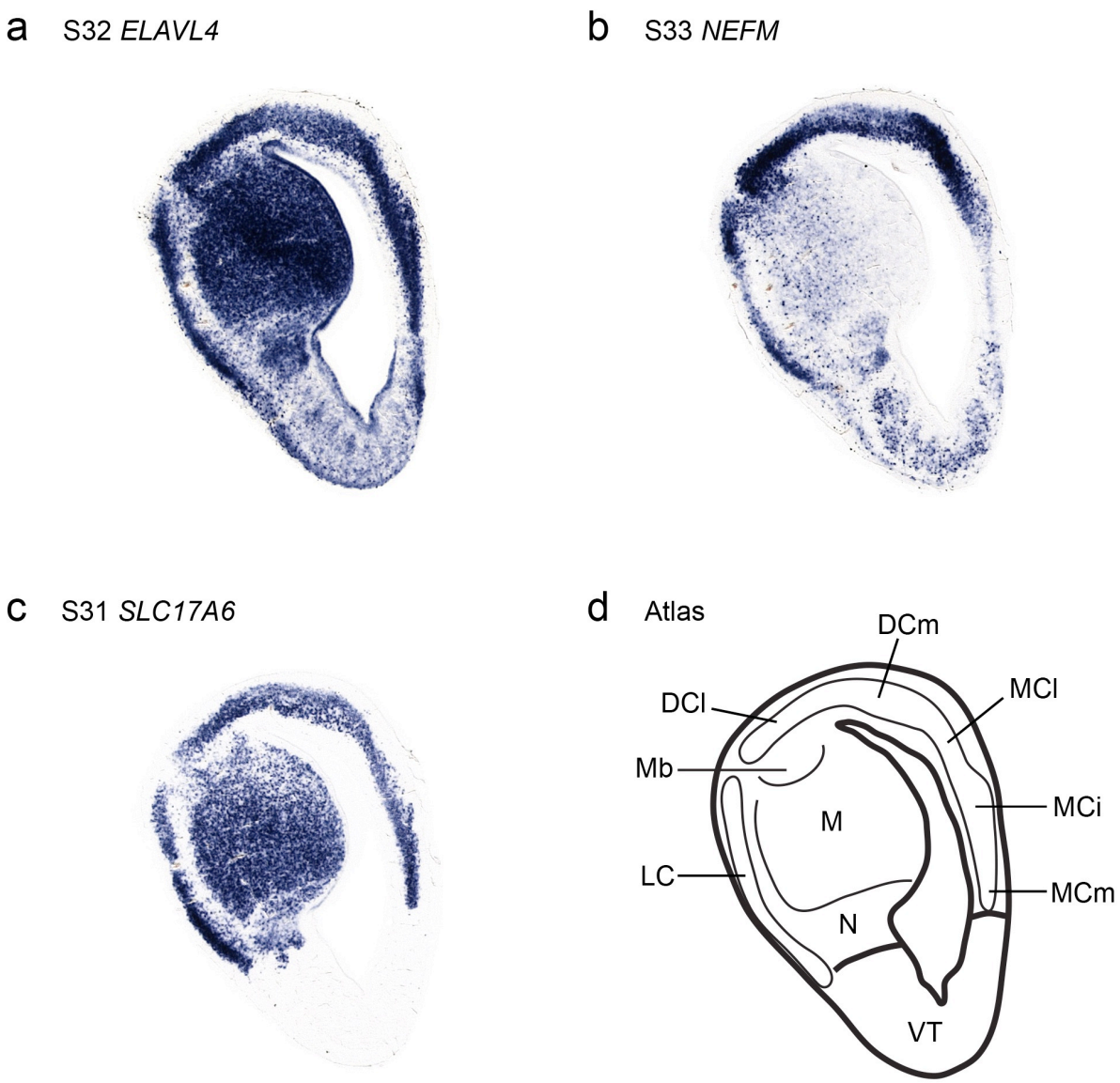

Figure 5.6 Atlas: Level 4
Sections 31–33 are shown. In situ hybridizations for **(a)** *ELAVL4*, **(b)** *NEFM*, and **(c)** *SLC17A6*. **(d)** Schematic illustration.

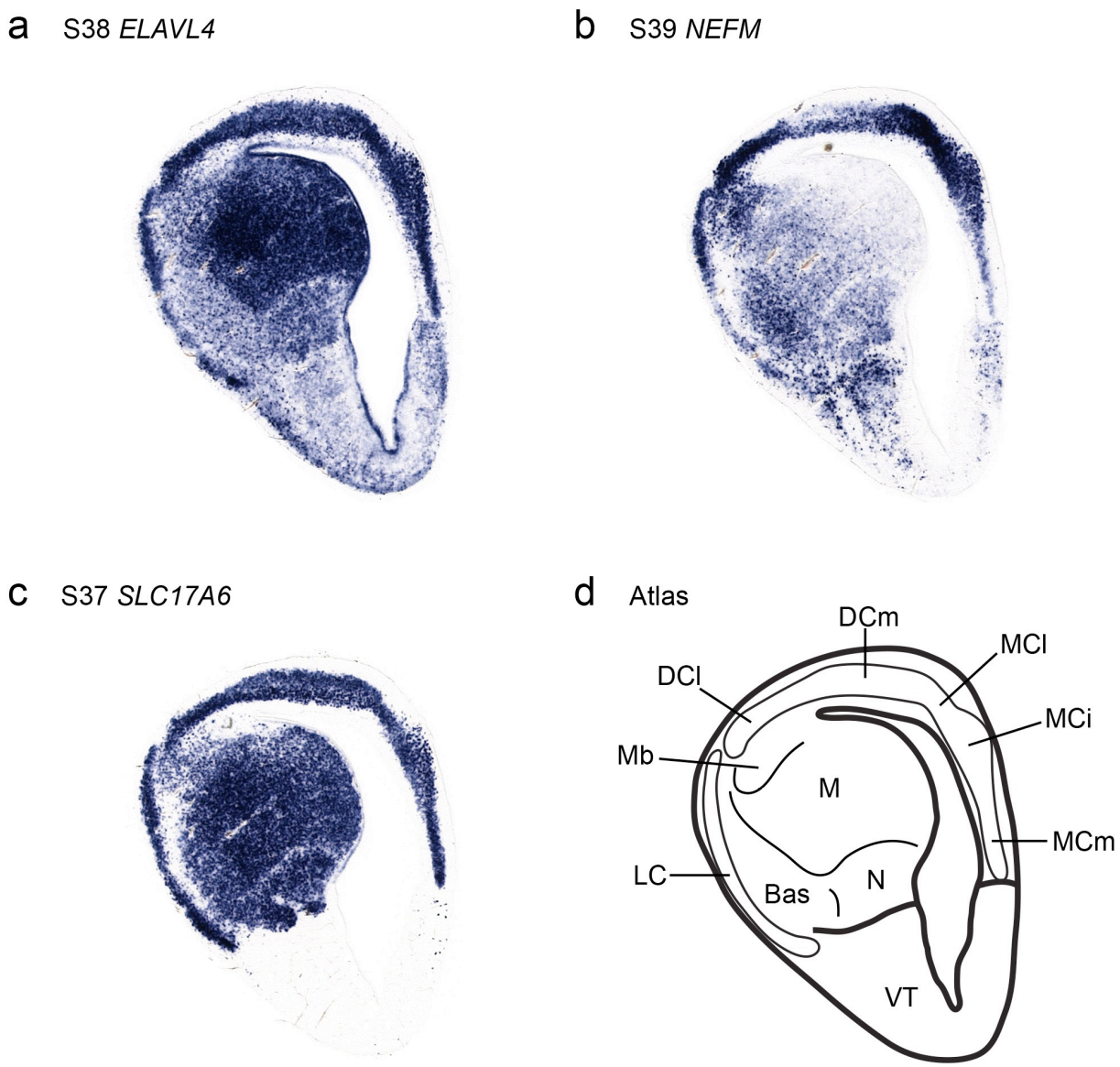

Figure 5.7 Atlas: Level 5
Sections 37–39 are shown. In situ hybridizations for **(a)** *ELAVL4*, **(b)** *NEFM*, and **(c)** *SLC17A6*. **(d)** Schematic illustration.

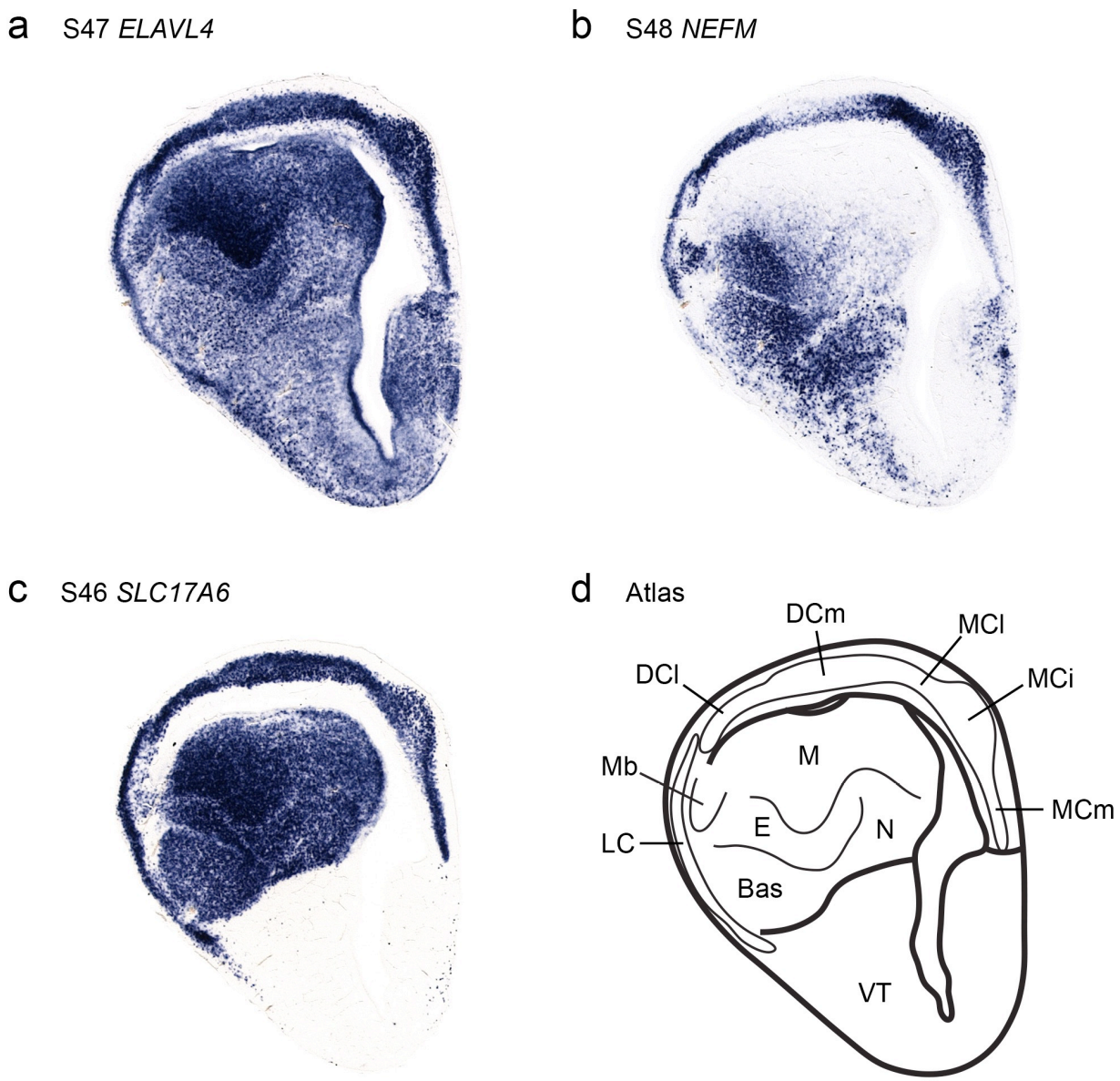

Figure 5.8 Atlas: Level 6
Sections 46–48 are shown. In situ hybridizations for **(a)** *ELAVL4*, **(b)** *NEFM*, and **(c)** *SLC17A6*. **(d)** Schematic illustration.

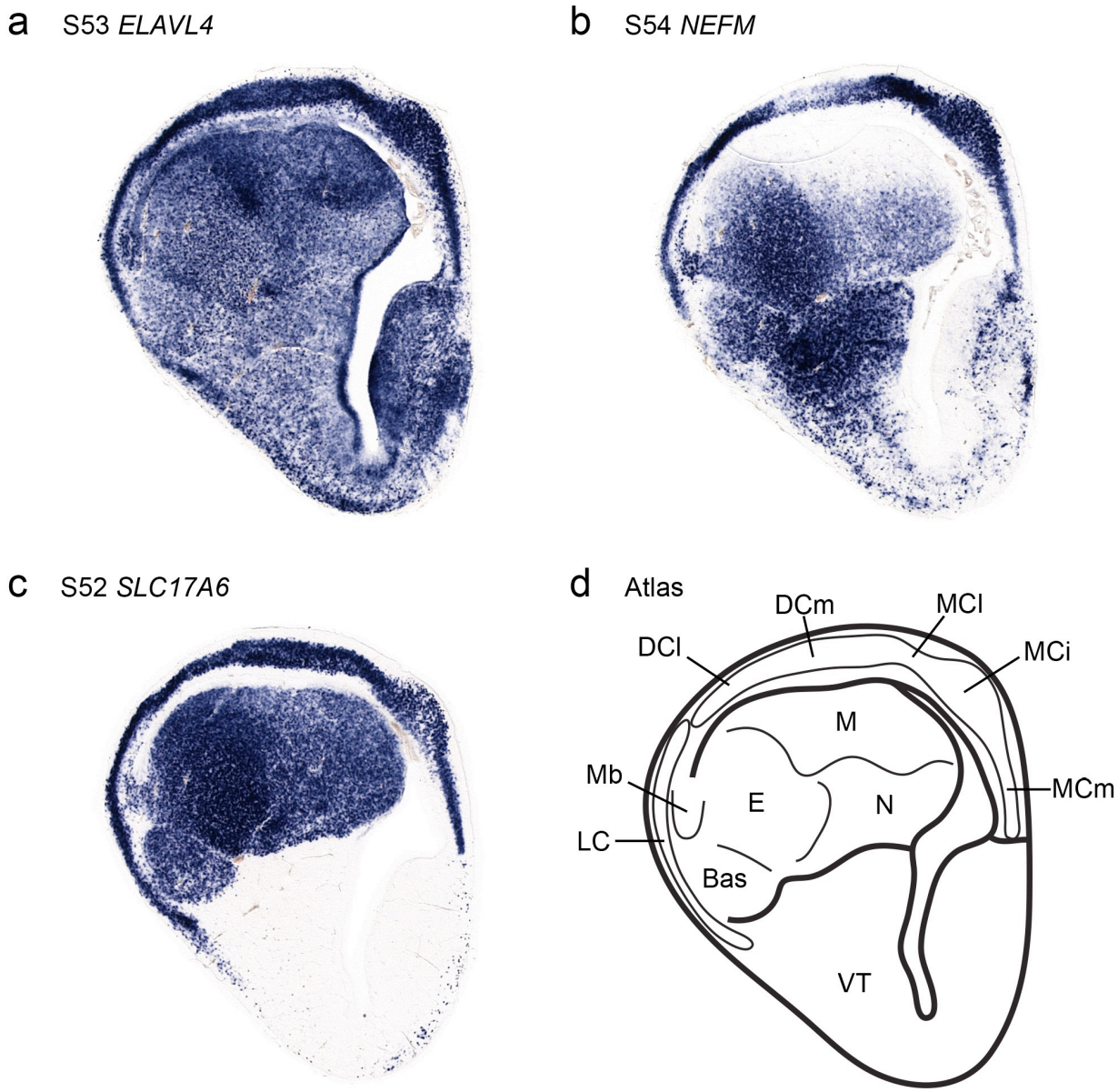

Figure 5.9 Atlas: Level 7
Sections 52–54 are shown. In situ hybridizations for **(a)** *ELAVL4*, **(b)** *NEFM*, and **(c)** *SLC17A6*. **(d)** Schematic illustration.

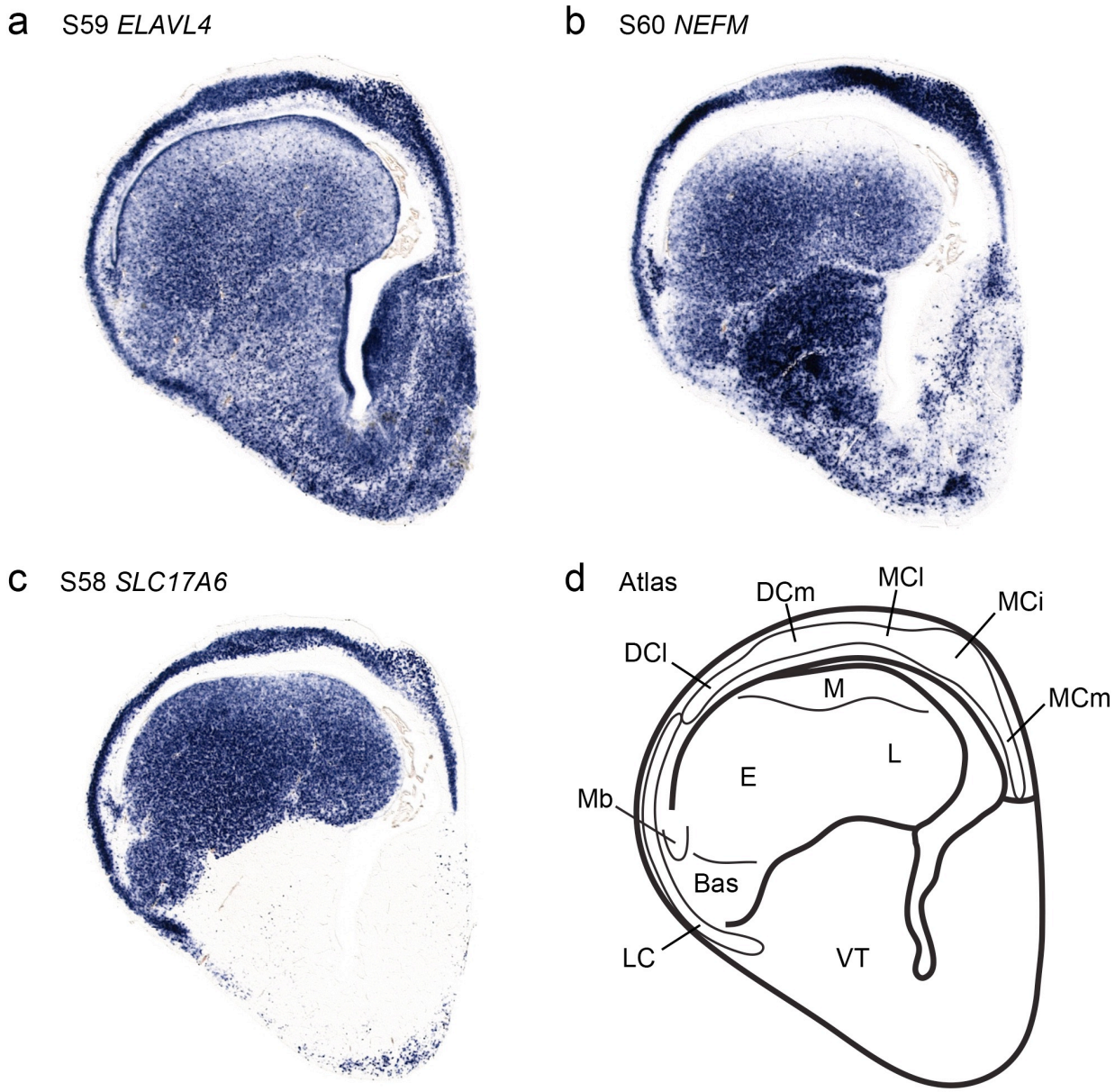

Figure 5.10 Atlas: Level 8
Sections 58–60 are shown. In situ hybridizations for **(a)** *ELAVL4*, **(b)** *NEFM*, and **(c)** *SLC17A6*. **(d)** Schematic illustration.

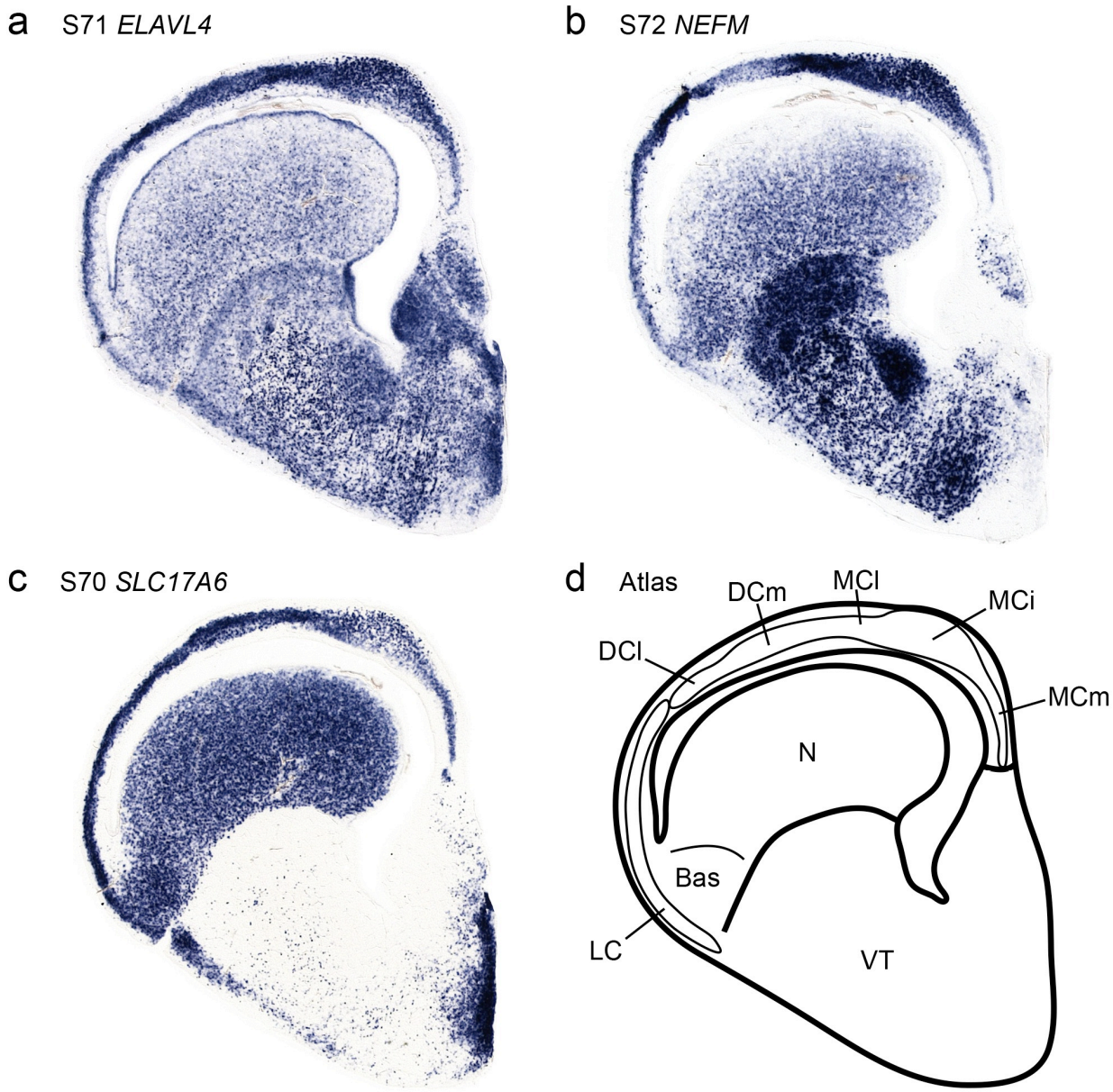

Figure 5.11 Atlas: Level 9
Sections 70–72 are shown. In situ hybridizations for **(a)** *ELAVL4*, **(b)** *NEFM*, and **(c)** *SLC17A6*. **(d)** Schematic illustration.

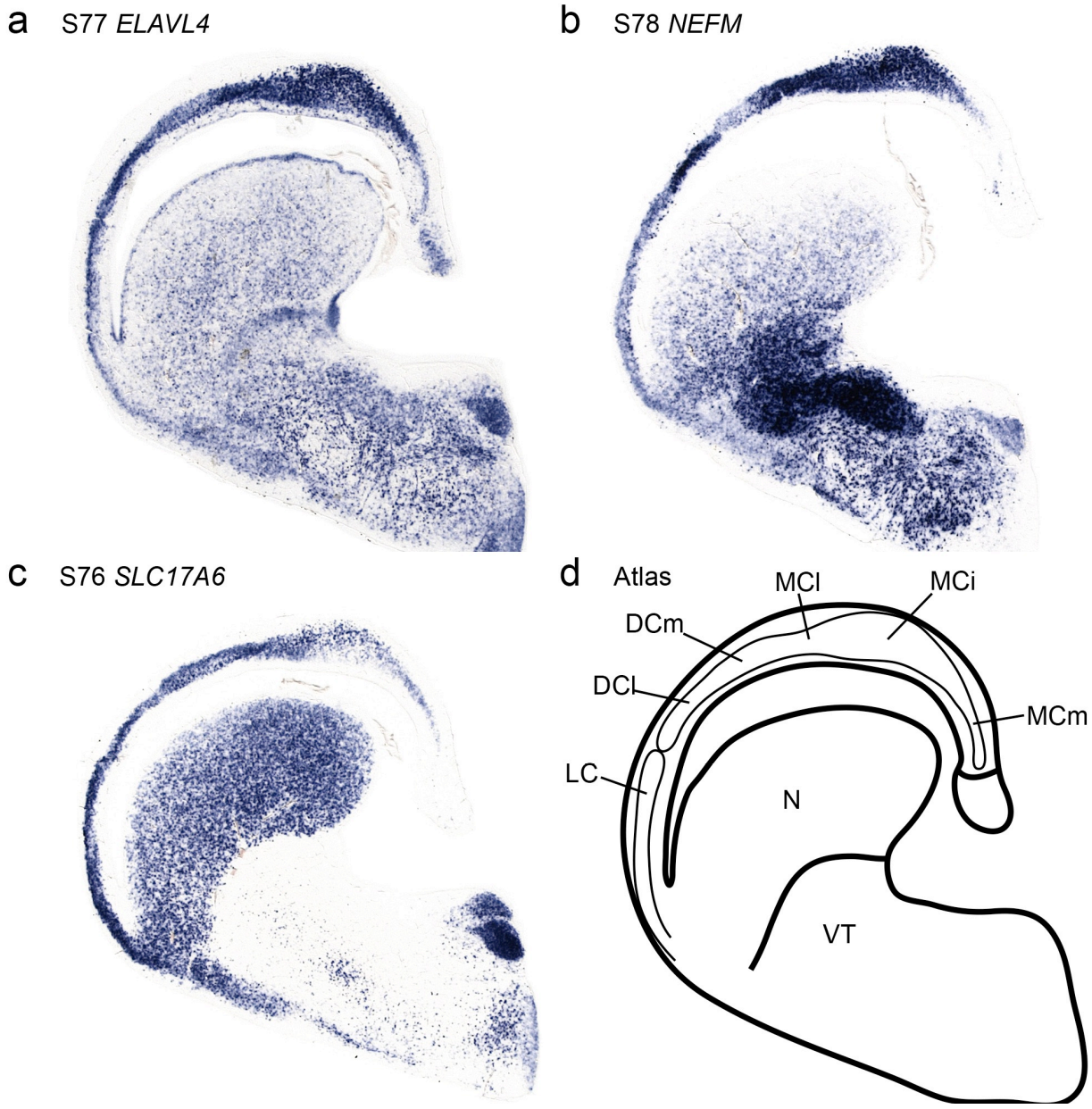

Figure 5.12 Atlas: Level 10
Sections 76–78 are shown. In situ hybridizations for **(a)** *ELAVL4*, **(b)** *NEFM*, and **(c)** *SLC17A6*. **(d)** Schematic illustration.

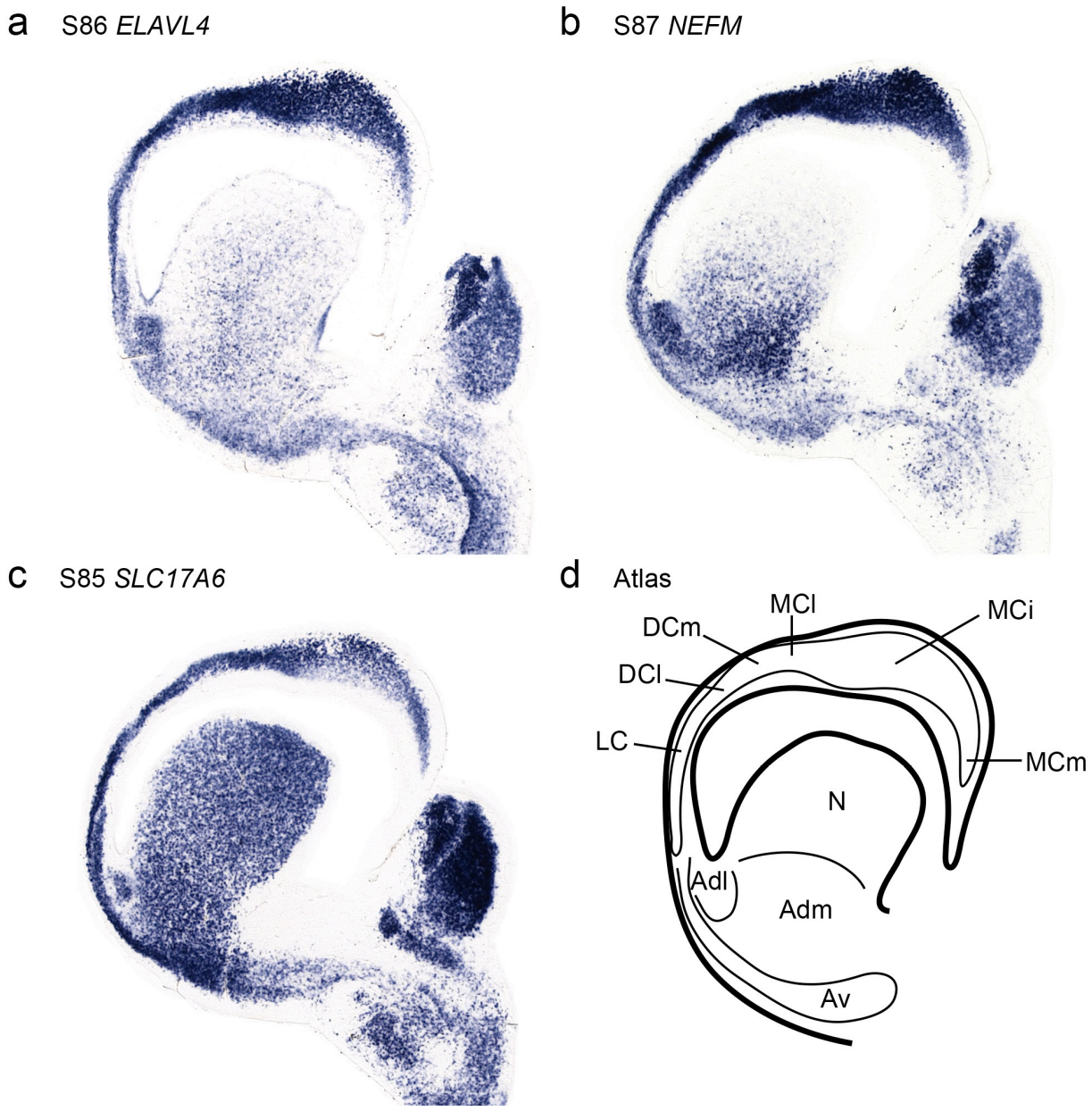

Figure 5.13 Atlas: Level 11
Sections 85–87 are shown. In situ hybridizations for **(a)** *ELAVL4*, **(b)** *NEFM*, and **(c)** *SLC17A6*. **(d)** Schematic illustration.

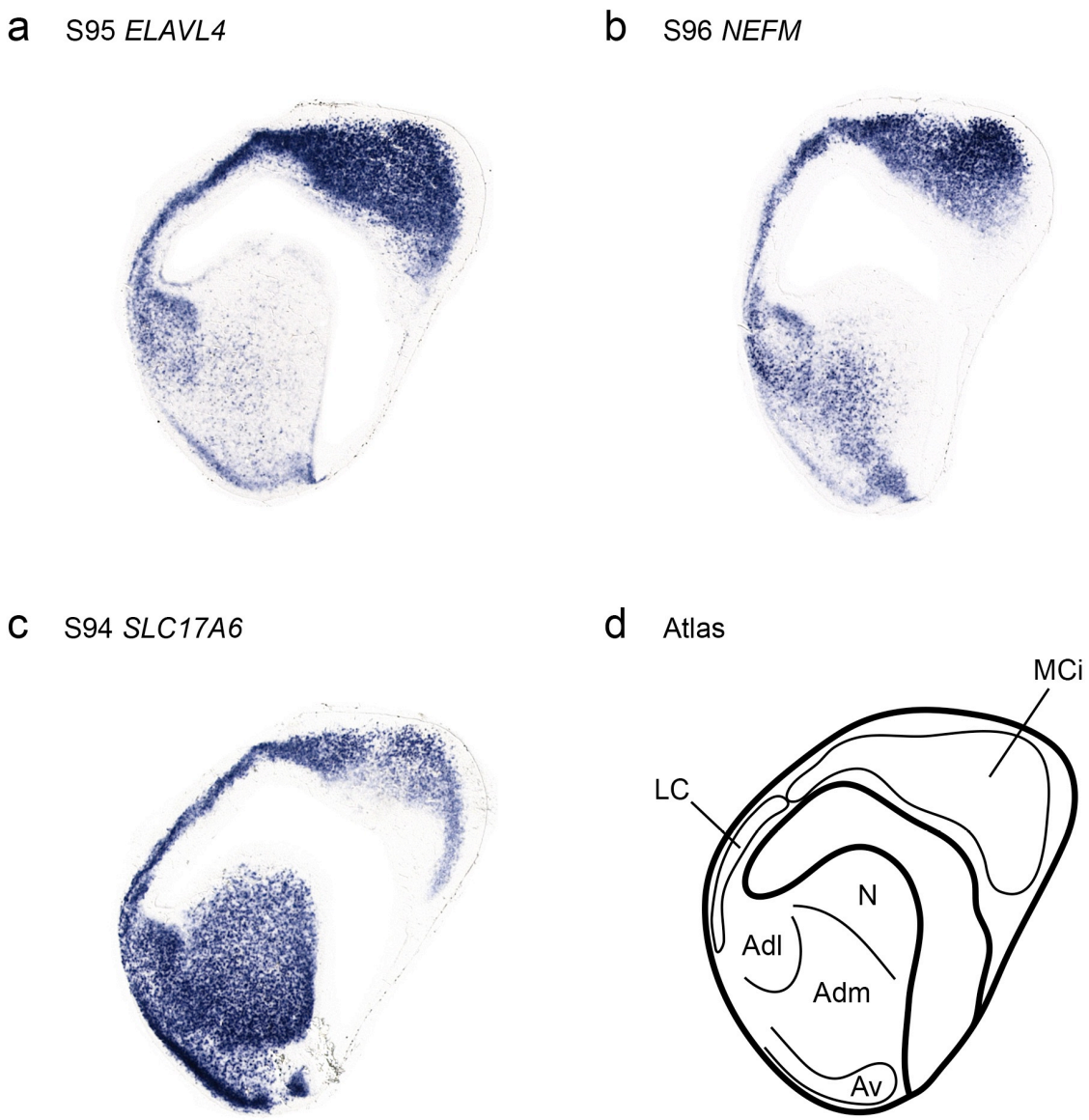

Figure 5.14 Atlas: Level 12
Sections 94–96 are shown. In situ hybridizations for **(a)** *ELAVL4*, **(b)** *NEFM*, and **(c)** *SLC17A6*. **(d)** Schematic illustration.

Table 5.2 Molecular markers for analysis of alligator telencephalon

Alligator cDNAs	Expression Pattern
BCL11A / CTIP1	MCm, MCl, DC, LC, M, VT
CACNA1H	DCm L2b, DCl
DACH2	DCm L2a, N
KCNH5 / EAG2	DCm L2a, Bas, E, L
ELAVL4 / HUD	General neuronal marker
EMX1	MCm, MCi, DCm L2a, DCl, LC, M, Adl
ETV1 / ER81	MCi, MCl, DC
FOXP1	DCm L2b, DCl, M, VT
GRIK3	DCm L2b, DCl, LC, M, VT
ID2	MCm, MCl, DCm L2b, DCl, LC, M, VT
LHX2	Adl
LHX9	Adl
NEFM	General neuronal marker
PPP1R1B / DARPP32	LC, N, St
PROX1	MCm
RORA	Bas, E, L
RORB (not shown)	Bas, E, M
SATB1	MCm, DCm, Bas, E, L
SATB2	DCm, DCl, mb, M
SLC17A6 / VGLUT2	Excitatory neurons
SLC32A1 / VIAAT	Inhibitory neurons
SULF2	DCm L2b
ZBTB20	MCm, MCi

Genes examined in this study are listed at left, along with common names where applicable. Territories labeled by each gene are listed at right. Abbreviations are according to Table 5.1.

Organization of the alligator dorsal ventricular ridge

A note on dorsal ventricular ridge nomenclature

Researchers have generally used a nomenclature for reptile DVR distinct from bird nomenclature. Ulinski, for example, divided reptile DVR into ADVR and BDVR (Ulinski 1983). Few have ventured to use avian nomenclature for reptile anatomy, even for territories highly likely to be homologous (such as the DVR target of ascending visual information from thalamic

nucleus rotundus, see below). The alligator DVR, however, bears a compelling resemblance to bird DVR. I break from tradition by using several avian terms that are explicit proposals of homology.

Sensory input domains and nidopallium

In all amniotes studied, the DT receives ascending visual, auditory, and somatosensory information from the dorsal thalamus. Sensory input first reaches neocortical L4 of primary sensory cortices in mammals. In birds, sensory input targets a trio of distinct DVR nuclei: Bas (somatosensory, auditory, and vestibular), E (visual), and Field L (auditory). I first sought to molecularly identify the targets of primary sensory thalamic axons in the alligator DT.

Harvey Karten (1969) first proposed that the primary sensory input cells of mammalian and avian DT are homologous at the cell-type level. The Ragsdale laboratory provided support for Karten's cell-type homology hypothesis by identifying the ion channel gene *KCNH5* (also known as *EAG2*) and the transcription factor *RORB* as conserved molecular markers of DT input cells (Dugas-Ford et al. 2012). My previous work adds the transcription factors *RORA* and *SATB1* to this list of conserved input cell marker genes (Chapter 3). I examined the expression patterns of these four genes in the alligator DVR.

In birds, the thalamic nucleus rotundus receives visual information from the optic tectum (Braford 1972). Rotundus projects in turn to the avian E within DVR. Michael Pritz identified a comparable projection from rotundus to lateral DVR in the alligator (Pritz 1975). A charting of this projection pattern appears in Figure 5.15a. *KCNH5*, *SATB1*, *RORA* (Figure 5.15b–d), and *RORB* (not shown) probes strongly label this territory, closely following the nuclear position and contours that Pritz described. I designate this nucleus the alligator entopallium (E).

KCNH5 (Figure 5.15b) and *SATB1* (Figure 5.15c) are expressed in an additional nucleus ventrolateral to E. *RORA* strongly labels this structure at more anterior levels (not shown). This nucleus resembles the avian Bas, which in chickens expresses the same input markers and is located in a similar topological position (Chapter 3).

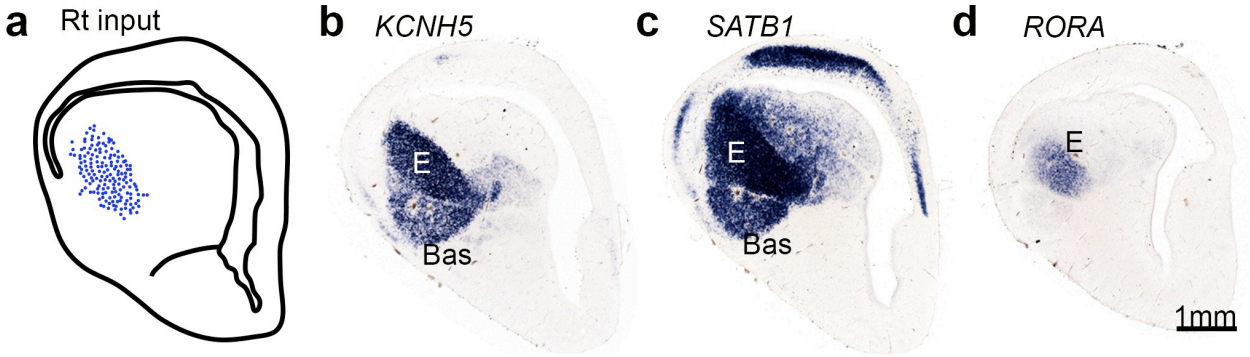

Figure 5.15 Conserved input cell markers label a crocodilian entopallium and nucleus basorostralis
(a) A schematic illustration adapted from Pritz (1975) shows the DVR target of ascending visual information from the thalamic nucleus rotundus. Blue stippling represents axon terminals. **(b)** *KCNH5* probe labels entopallium (E) and nucleus basorostralis (Bas). **(c)** *SATB1* probe labels E and Bas. Dorsal cortex labeling is discussed later in the context of cerebral cortex. **(d)** *RORA* probe labels E. *RORA* weakly labels Bas at this level, but labels it strongly in more anterior sections (not shown). Sections correspond approximately to atlas level 7.

Auditory information in the avian brain is relayed from the midbrain to the thalamic nucleus ovoidalis before reaching Field L in the medial DVR. Alligators have a thalamic auditory relay nucleus, the nucleus reuniens, which receives information from the midbrain and projects to the medial DVR (Pritz 1974a, Pritz 1974b). The DVR target of this projection is reproduced in Figure 5.16a. *KCNH5*, *SATB1*, and *RORA* are expressed in a territory likely corresponding to the site of auditory input (Figure 5.16b–d). I name this zone the alligator Field L. Unlike the entopallium and the avian Field L, the alligator Field L does not form a clearly delineated nucleus.

In alligators, somatosensory information originating in spinal cord and dorsal column nuclei is relayed through the thalamic nucleus medialis and reaches central ADVR (Pritz and

Northcutt 1980). This thalamic projection to DVR likely terminates between E and L. Input cell marker gene expression is consistent with described somatosensory projections (Figure 5.16b–d). No cytoarchitectonic specializations are obvious here and I do not provide a name for this area.

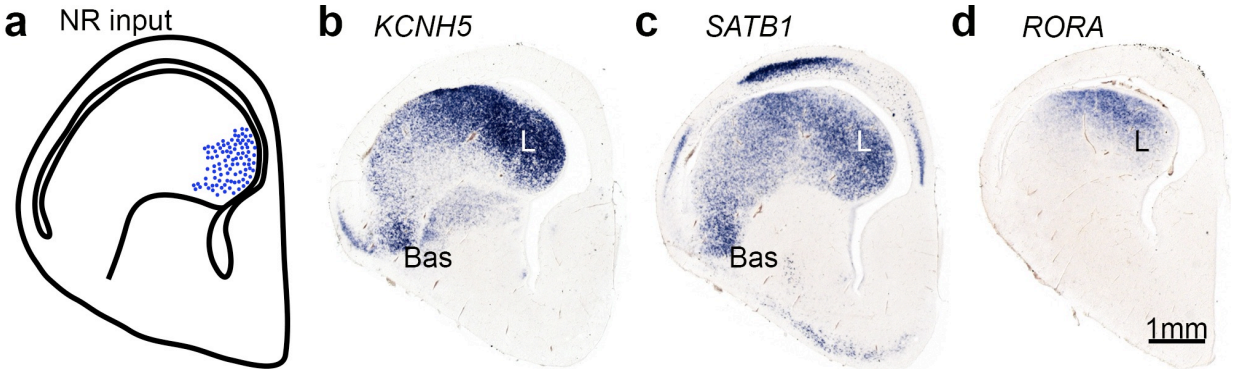

Figure 5.16 Conserved input cell markers label a crocodilian Field L
(a) A schematic illustration adapted from Pritz (1974b) shows the DVR target of ascending auditory information from the thalamic nucleus reuniens. Blue stippling represents axon terminals. **(b)** *KCNH5*, **(c)** *SATB1*, and **(d)** *RORA* probes label Field L (L). These three genes are also expressed in a more lateral/central territory (not named) that may receive somatosensory information from the thalamic nucleus medialis. **(b)** *KCNH5* and **(c)** *SATB1* label the posterior end of Bas at this level. Sections correspond approximately to atlas level 8.

Avian Bas, E, and Field L are subdivisions of a larger DVR territory named the nidopallium (Reiner et al. 2004a). The nidopallium is a complex territory of unknown homology. Non-primary input zones of the avian nidopallium form associational connections implicated in avian cognitive functions (Atoji and Wild 2009). The transcription factor *DACH2* is the only known marker gene that specifically labels the entire avian nidopallium (Szele et al. 2002, Rowell and Ragsdale 2012). I found that alligator *DACH2* labels a massive territory similar in organization to the avian nidopallium. A series of six sections from a single cerebral hemisphere are shown to demonstrate the overall organization of alligator nidopallium (Figure 5.17a–f). Alligator *DACH2* labels a contiguous DVR territory that includes the previously described input zones in addition to a frontal area (Figure 5.17a), areas medial to Bas and E (Figure 5.17b,c), and a large caudal area (Figure 5.17e,f). I do not provide names for these nidopallium territories in

order to avoid implying avian homologies. Dorsal cortex expression of *DACH2* (Figure 5.17), *KCNH5*, and *SATB1* (Figures 5.15 and 5.16) is discussed in the section on cerebral cortex.

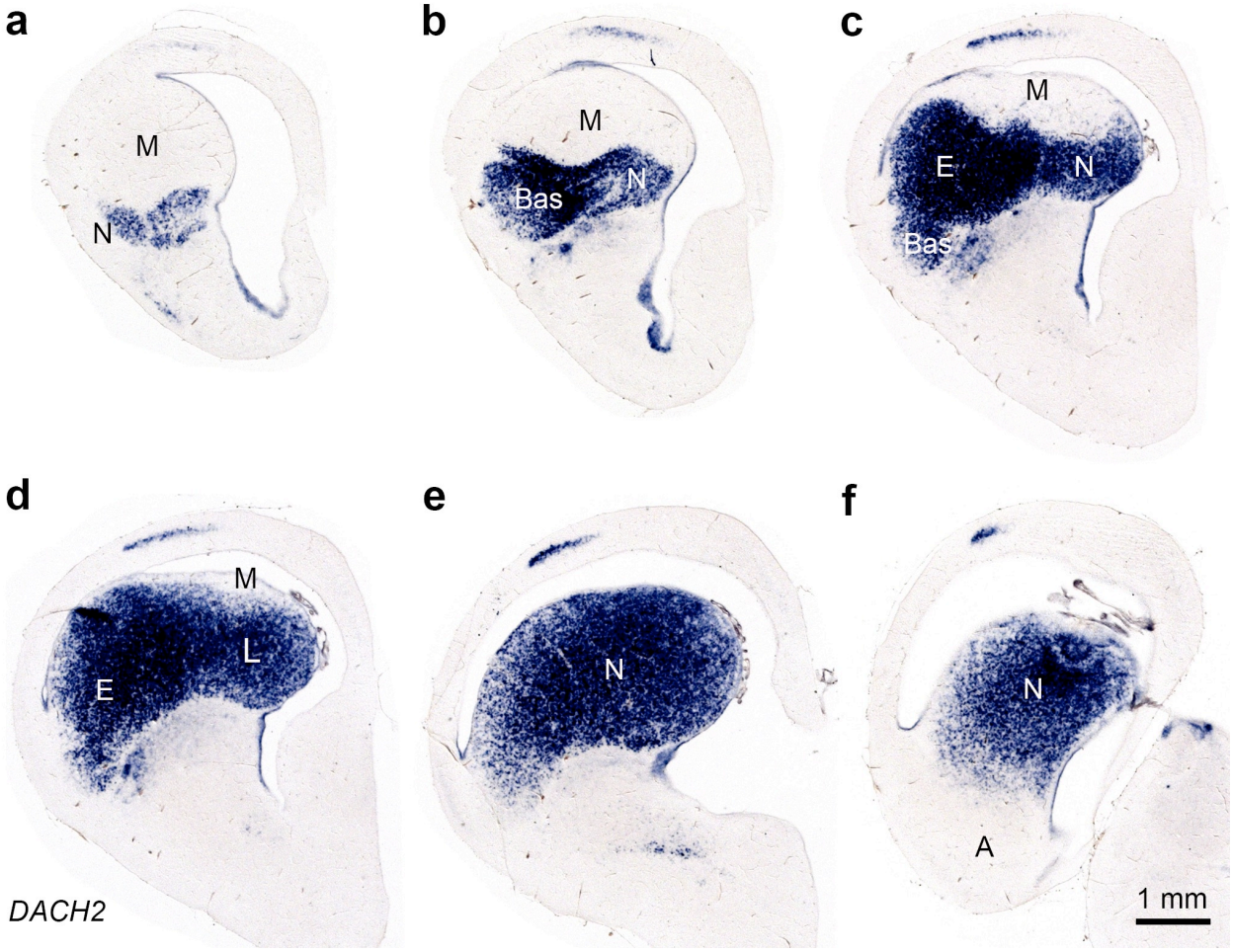

Figure 5.17 Alligator *DACH2* expression identifies the nidopallium and a dorsal cortex cell population
An anteroposterior series of sections from a single cerebral hemisphere labeled with *DACH2* probe. Primary sensory input nuclei are contained within nidopallium (N): Bas is present in **b**, **c**, and possibly in **d**. E is present in **c** and **d**. L is likely present in **d**, but is difficult to identify with cytoarchitectonics. Territories labeled as N are non-primary input parts of the nidopallium. The *DACH2*(−) territory in dorsal DVR is the mesopallium (M). The *DACH2*(−) territory in ventroposterior DVR is the arcopallium (A). A thin dorsal cortex domain is labeled by *DACH2* across most of the anteroposterior axis of the telencephalon.

Mesopallium

Birds have a large DT associational territory called the mesopallium (Reiner et al. 2004a, Atoji and Wild 2012). Avian mesopallium is a target for secondary sensory information from the primary sensory nuclei Bas, E, Field L, and IHA (Atoji and Wild 2012). Clarifications to mesopallium nomenclature denote a ventral mesopallium (Mv) located in the avian DVR and a dorsal mesopallium (Md) located in the avian Wulst (Sun and Reiner 2000, Reiner et al. 2004a, Jarvis et al. 2013). RNA-sequencing and gene expression studies identified a collection of six transcription factors (*EMX1*, *SATB2*, *ID2*, *FOXP1*, *BCL11A*, and *NHLH2*) highly enriched in avian Mv/Md. I further showed that five of these six transcription factors (the exception being *NHLH2*) are expressed in mammalian neocortical intratelencephalic (IT) association neurons, which in placental mammals include projection neurons of the corpus callosum. I proposed that avian mesopallium (Mv/Md) and mammalian IT neurons are homologous at the cell-type level (Chapter 4). The common ancestor of mammals and birds also gave rise to all extant reptiles, so I expected to find these transcription factors expressed together in alligator DT.

I examined the expression of five IT-specific transcription factors and the mesopallium-specific ion channel gene *GRIK3* (Jarvis et al. 2013) (Chapter 4) in the alligator DT. These six genes identify the *DACH2*(−) dorsal DVR (Figure 5.18a–f). All six genes are also expressed in the dorsal cortex. There are, therefore, two distinct alligator DT territories expressing conserved IT/mesopallium marker genes: a dorsal cortex domain and a DVR domain. Dorsal cortex expression patterns will be described in more detail below. These two alligator domains form a continuous cell population laterally. This continuity is most obvious in Figure 5.18b, where SATB2-expressing cells curve around the lateral ventricle to link the dorsal cortex to

mesopallium. I name this domain the mesopallial bridge (mb). I do not propose any specific mammalian or avian homolog for the alligator mb.

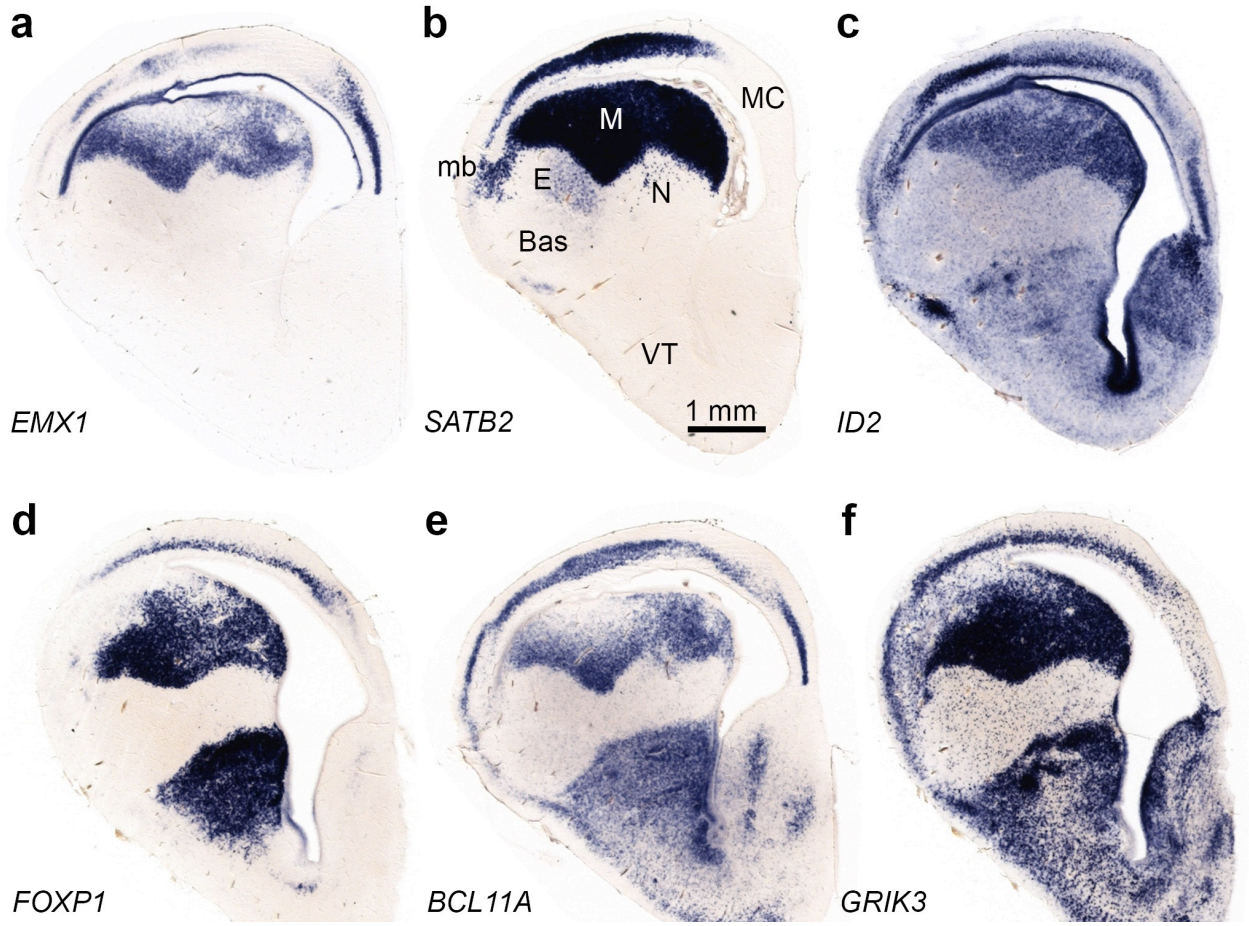

Figure 5.18 Conserved intratelencephalic projection neuron markers are expressed in a dorsal ventricular ridge mesopallium and cerebral cortex cell populations
In situ hybridization for five intratelencephalic (IT) projection neuron-specific transcription factors, and the mesopallium-specific ion channel gene *GRIK3*. **(a)** *EMX1*, **(b)** *SATB2*, **(c)** *ID2*, **(d)** *FOXP1*, **(e)** *BCL11a*, and **(f)** *GRIK3* label the mesopallium (M) in dorsal DVR. All six genes are also expressed in dorsal cortex. **(b)** *SATB2* labeling connects mesopallium to dorsal cortex around the lateral ventricle. I name the *SATB2*(+) cell population at the apex of the lateral ventricle the mesopallial bridge (mb). Other IT-specific genes label mb more strongly at anterior levels (not shown). Sections correspond approximately to atlas level 6.

To better demonstrate the anatomy of mesopallium and nidopallium, I performed in situ hybridization for *EMX1* and *DACH2* on serially adjoining sagittal sections (Figure 5.19). Sections are oriented with anterior to the left and dorsal at top. *EMX1*- and *DACH2*-expressing territories are complementary in the DVR, but overlap in DC. At the medial-most level (Figure

5.19a,d), mesopallium extends to the anterior pole of DVR while nidopallium occupies the posterior pole. At lateral levels (Figure 5.19c,f), the mesopallium is limited to anterior DT but the nidopallium is more extensive. Arcopallium (Figure 5.19c,f, A) is identified as the *DACH2*(−)/*EMX1*(+) domain in posterolateral DT.

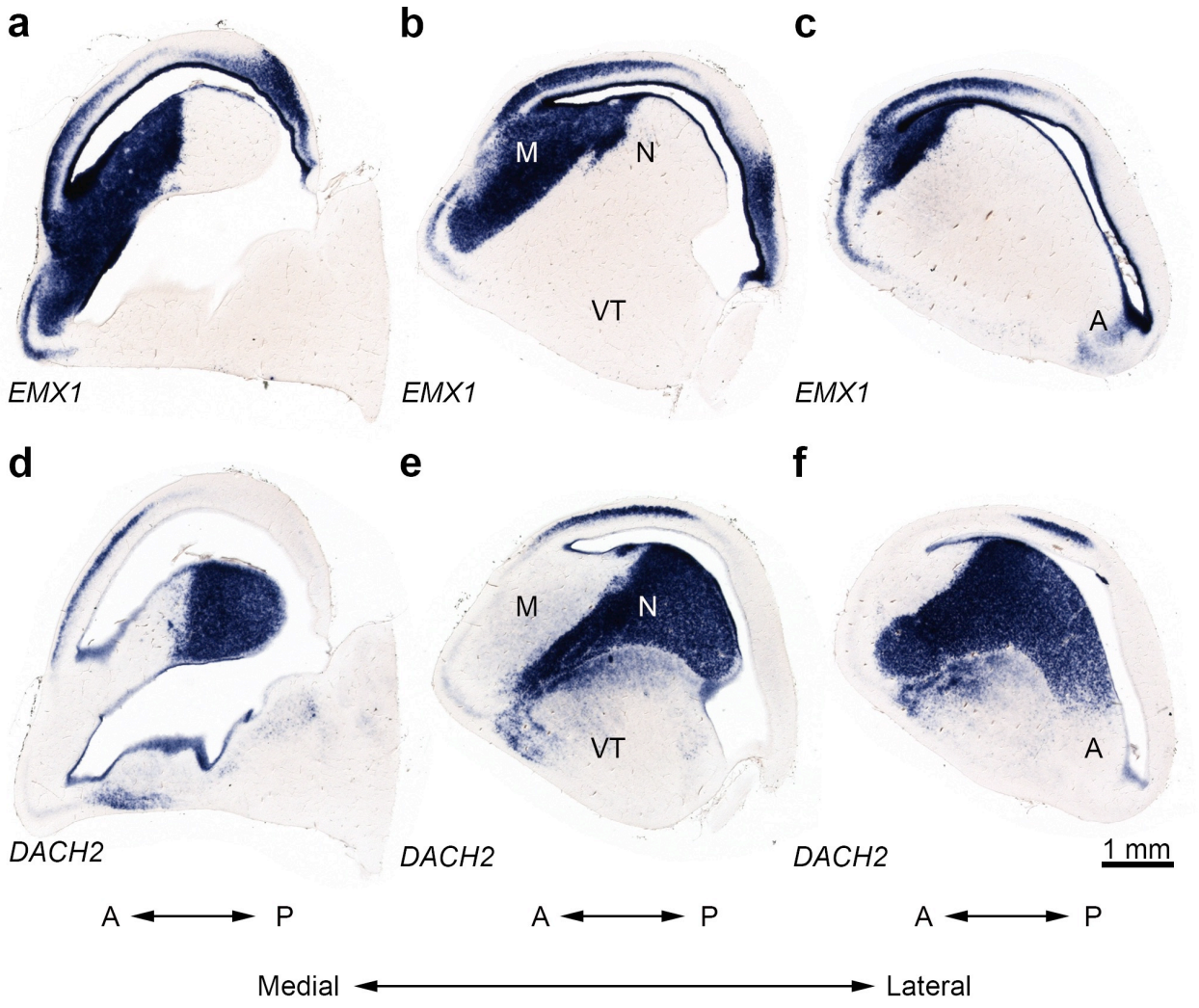

Figure 5.19 *EMX1* and *DACH2* in sagittal view
Six sagittal sections from the same cerebral hemisphere labeled with **(a–c)** *EMX1* or **(d–f)** *DACH2* probes. Anterior is orientated to left and dorsal at top. **a**/**d**, **b**/**e**, and **c**/**f** are serially adjoining pairs progressing from medial to lateral. *EMX1*(+) mesopallium (M) and *DACH2*(+) nidopallium (N) are complementary territories in DVR. Arcopallium (A) is visible in posterolateral DT (**c**, **f**).

Arcopallium

Alligator arcopallium is a relatively small territory in posterolateral DT, defined in part by the absence of *DACH2* staining. The *DACH2*-expressing nidopallium extends to the posterior pole of DVR, and includes nearly all of the DVR territory that bulges into the ventricle (e.g., Figure 5.14). I used cytoarchitectonic criteria to define a cell-dense dorsolateral nucleus (Adl), a cell-diffuse dorsomedial nucleus (Adm), and a thin, superficial ventral arcopallium (Av) (Figures 5.13, 5.14, 5.20). I identified very few markers for specific alligator arcopallium nuclei. The exception is Adl, which is visible in *NEFM* staining (Figure 5.20a) and expresses the transcription factors *EMX1* (Figure 5.20b), *LHX9* (Figure 5.20c), and *LHX2* (Figure 5.20d). Future studies may reveal further molecular subdivisions in alligator arcopallium. I do not propose specific avian homologs of alligator Adl, Adm, or Av.

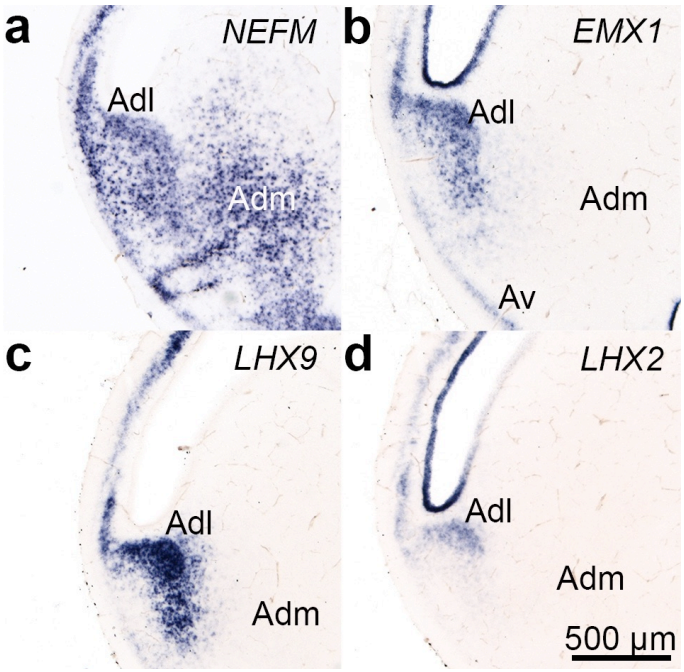

Figure 5.20 Alligator arcopallium contains Adl, Adm, and Av subdivisions
(a) *NEFM* staining demonstrates a cell-dense dorsolateral arcopallium (Adl) and a cell-diffuse dorsomedial arcopallium (Adm). Adl is labeled by probes for the transcription factors **(b)** *EMX1*, **(c)** *LHX9*, and **(d)** *LHX2*. I did not identify molecular markers for Adm. A thin, superficial ventral arcopallium (Av) is lightly stained by *EMX1* probe. Av can be seen more fully in the atlas. Sections correspond approximately to atlas level 12.

Organization of the alligator cerebral cortex

A note on cerebral cortex nomenclature

Previous researchers studied the cerebral cortex in a variety of reptiles with differing cerebral anatomies. Consequently, a confusing array of nomenclatures has developed (Nieuwenhuys et al. 1998). Most researchers, however, agree that the reptile cerebral cortex contains three layers and can be divided into medial, dorsal, and lateral cortices (Ulinski 1990a, Naumann 2017). Some confidently named the medial cortex "hippocampus" and the lateral cortex "piriform cortex" (Johnston 1915, Crosby 1917, Cairney 1926, Nieuwenhuys et al. 1998). I opt for the more commonly used topographic, evolutionarily neutral terms MC, DC, and LC and explore possible homologies with gene expression analyses.

Dorsal cortex

ELAVL4 is used as a general marker of neurons in metazoans (Shigeno et al. 2015). *ELAVL4* staining in the alligator dorsal cortex demonstrates the canonical division into three layers (Figure 5.21a). An upper L1, closest to the pial surface, contains only a few, scattered neuronal cell bodies. A thicker L2 forms the principal cellular layer and is densely packed with cell bodies. An inner L3, closest to the ventricle, contains loosely arranged neurons.

SLC17A6 encodes the vesicular glutamate transporter 2 (*VGLUT2*) and is expressed in glutamatergic excitatory neurons. *SLC17A6*-expressing cell bodies are confined to the principal cellular layer, L2 (Figure 5.21b). *SLC32A1* encodes the vesicular inhibitory amino acid transporter (*VIAAT*) and is expressed in GABAergic and glycinergic inhibitory interneurons. *SLC32A1*-expessing cell bodies are scattered from the pial surface to the ventricular surface, in all three dorsal cortex layers (Figure 5.21c). These staining patterns suggest that nearly all neurons in L1 and L3 are inhibitory interneurons born in VT, while L2 contains a mixture of

interneurons and DT-derived excitatory neurons. This result is consistent with the distribution of neurons described in turtle (Shen and Kriegstein 1986, Blanton et al. 1987) and lizard cortices (Schwerdtfeger and Lorente 1988).

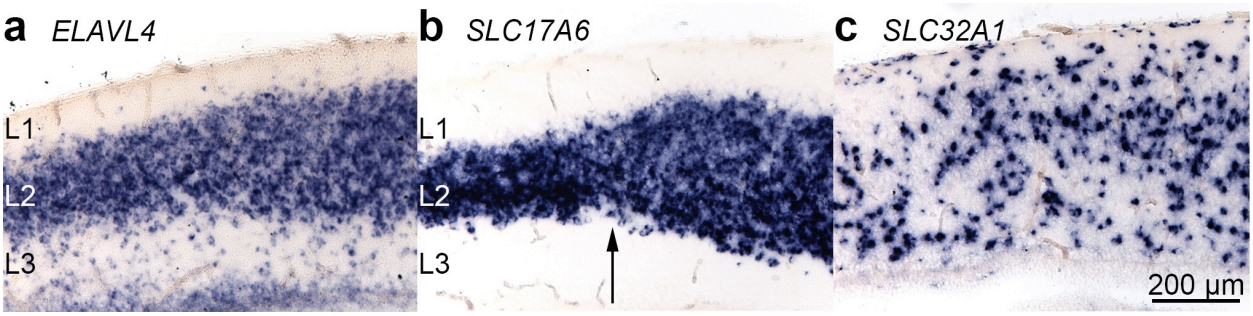

Figure 5.21 Neuronal distribution in alligator dorsal cortex
A magnified view of central dorsal cortex is shown with medial to the right. The general neuronal marker **(a)** *ELAVL4* demonstrates the three principal cellular layers in dorsal cortex, labeled L1, L2, and L3. **(b)** The excitatory neuron marker *SLC17A6* is restricted to the middle cellular layer, L2. **(c)** The inhibitory neuron marker *SLC32A1* labels cells in all three dorsal cortex layers. The arrow in **b** indicates a transition from a thin lateral L2 to a thicker medial L2. The sections in **b** and **c** are serially adjoining, **a** is from a separate telencephalon. Sections correspond approximately to atlas level 7.

The sections in Figure 5.21 are shown at a transition zone where the relatively thin lateral L2 broadens to a thicker L2 medially (Figure 5.21b, arrow). The thinner lateral territory (DCl) and thicker medial territory (DCm) are dissociated by gene expression. *SATB2* labels lateral dorsal cortex (DCl) and medial dorsal cortex (DCm), with an expression cutoff point that coincides with the medial boundary of DCm (Figure 5.22a, arrow). *SATB1* is a conserved marker of primary sensory input zones. Its expression is restricted to DCm (Figure 5.22b). Thus, I can molecularly define the DCl as *SATB1*(−)/*SATB2*(+) and DCm as *SATB1*(+)/*SATB2*(+). The transcription factor *ID2* is robustly expressed in DCl (Figure 5.22c). Within DCm, *ID2* is weakly expressed in an upper territory and more strongly expressed in a lower territory (Figure 5.22c). *SATB1* is more strongly expressed in upper DCm (Figure 5.22b). *SATB1* and *ID2* expression indicate that DCm contains molecularly distinct sublaminae. I name the upper DCm sublamina L2a and the lower DCm sublamina L2b.

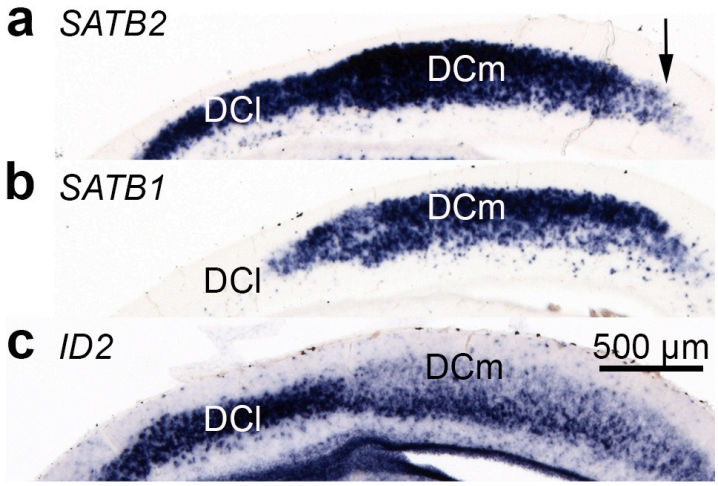

Figure 5.22 Alligator dorsal cortex contains medial and lateral fields
Alligator dorsal cortex can be divided into medial dorsal cortex (DCm) and lateral dorsal cortex (DCl). DCm expresses both **(a)** *SATB2* and **(b)** *SATB1*. DCl expresses **(a)** *SATB2*, but not **(b)** *SATB1*. **(c)** *ID2* strongly labels DCl, and labels lower DCm more strongly than upper DCm. *SATB1* shows the opposite pattern: it is expressed more strongly in **(b)** upper DCm. The sections in **a** and **b** are serially adjoining, **c** is from a separate telencephalon. The arrow in **a** indicates the medial boundary of DCm. Sections correspond approximately to atlas level 7.

NEFM encodes the middle-weight neurofilament, which, like *ELAVL4*, is used as a general neuronal marker gene (Ding et al. 2016). *NEFM* strongly labels DCl, weakly labels DCm L2a, and strongly labels DCm L2b (Figure 5.23a). *DACH2* is expressed in a stripe along the anteroposterior axis of the dorsal cortex (Figure 5.17a–f, Figure 5.23b). The sections shown in Figure 5.23a and Figure 5.23b are serially adjoining: *DACH2*-expressing cell bodies are located in the *NEFM*-weak L2a sublamina along its entire extent. *NEFM* and *DACH2* show opposing expression gradients, with *NEFM* expressed more strongly in medial L2a and *DACH2* expressed more strongly laterally (Figure 5.23a,b). *KCNH5*, a conserved marker of DT input cells (Dugas-Ford et al. 2012), is expressed in a small domain in lateral L2a (Figure 5.23d, also visible in Figure 5.15b). The IT cell marker *FOXP1* is expressed in a band of consistent thickness in DCl L2 and DCm L2b (Figure 5.23c), a pattern similar to *GRIK3* (Figure 5.18f).

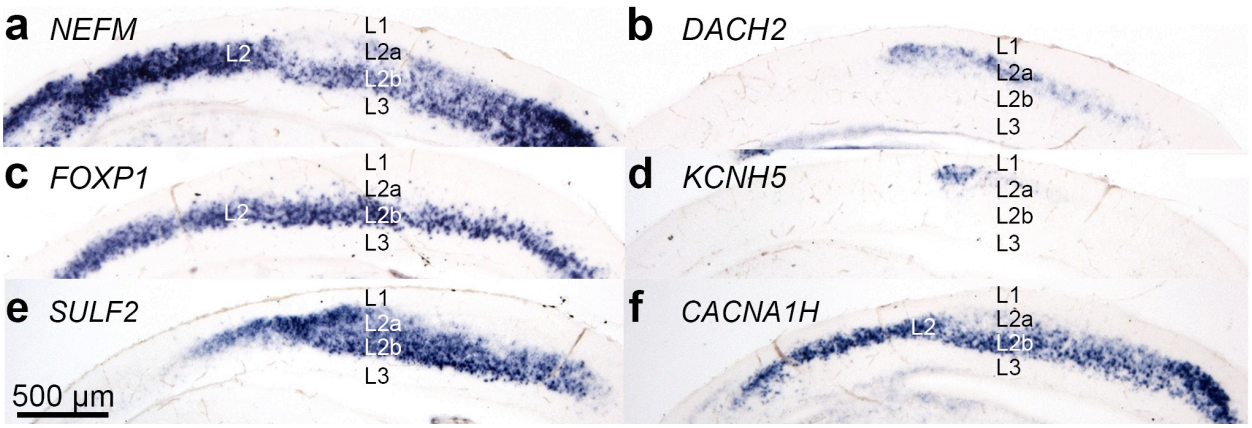

Figure 5.23 Medial dorsal cortex (DCm) contains molecularly distinct sublaminae
(a) Within DCm, *NEFM* weakly labels an upper layer (L2a) and more strongly labels a lower layer (L2b). **(b)** *DACH2* expression is specific to L2a. **(c)** IT cell marker *FOXP1* is expressed in DCl L2 and DCm L2b. **(d)** Input cell marker *KCNH5* is expressed in a lateral subset of L2a cells. **(e)** Output cell marker *SULF2* is most strongly expressed in DCm L2b. **(f)** Output cell marker CACNA1H is expressed in DCl L2 and DCm L2b. The sections in **a** and **b** are serially adjoining, other sections are from separate telencephala. Sections correspond approximately to atlas level 7.

The mammalian neocortex contains primary sensory input neurons in L4 and long-range output neurons in L5. Output neurons project to motor-related targets in brainstem and spinal cord, most prominently through the pyramidal tract. Karten proposed that neocortical output cells are homologous to the long-range projection neurons in the avian HA and arcopallium (Karten 1969), a prediction supported by comparative gene expression studies (Rowell et al. 2010, Dugas-Ford et al. 2012). I tested whether the alligator dorsal cortex expresses conserved marker genes for DT output neurons. Two such markers, *SULF2* and *CACNA1H*, are expressed in L2b of alligator DCm (Figure 5.23e,f). These expression patterns raise the possibility that alligator input cells are found in a cortical layer directly above output cells, a pattern reminiscent of the organization in the mammalian neocortex. It is unknown whether alligator dorsal cortex projects to brainstem motor centers, but previous studies reported projections from reptile DC to visual thalamus (dorsal lateral geniculate nucleus and nucleus rotundus) and optic tectum (Ulinski 1990a).

The five IT-cell transcription factors expressed in the mesopallium are also found in the alligator dorsal cortex (Figure 5.18a–e). All five genes are expressed in DCl L2, a region depleted of the input markers *KCNH5* and *SATB1*. These gene expression patterns suggest that DCl will be found in future studies to be an IT association territory similar to the avian mesopallium (Atoji and Wild 2012).

DCm and mesopallium first appear at a more anterior level than DCl. The *SATB1*(+)/*SATB2*(+) DCm is first seen as a nub-like structure in Figure 5.4, adjacent to anterior mesopallium. The *SATB1*(−)/*SATB2*(+) DCl appears at a more posterior level shown in Figure 5.6. I suggest that anterior mesopallium is indistinguishable from, or equivalent to, anterior DCl (Figure 5.4). Posteriorly, the mesopallium separates into the dorsal DCl and the ventral DVR mesopallium domains by the intervening ventricle. DCl and DVR continuity is reflected by the mesopallial bridge (mb), visible in Figures 5.6 through 5.10.

Medial cortex

The six-layered mammalian neocortex transitions medially to a three-layered hippocampal formation, which features three highly conserved subdivisions. From medial to lateral, these subdivisions are the *Prox1*(+)/*Zbtb20*(+) dentate gyrus, the *Prox1*(−)/*Zbtb20*(+) CA fields, and the *Prox1*(−)/*Zbtb20*(−) subiculum (Pleasure et al. 2000, Mitchelmore et al. 2002, Nielsen et al. 2007). There is a long-standing consensus that reptile medial cortex contains a homolog of mammalian hippocampus (Ariëns Kappers et al. 1936). However, these conclusions are based on regional topography and differ significantly as to whether reptiles have homologs of individual hippocampal subdivisions (Hevner 2016, Striedter 2016). I examined expression of the well-characterized marker genes *PROX1* and *ZBTB20* in alligator medial cortex.

NEFM staining demonstrates three differentiated subdivisions in alligator medial cortex (Figure 5.24a). The ventral and medial-most territory (MCm) contains densely packed neurons in a tight tri-laminal configuration. The main cellular layer is broader and less densely packed in an intermediate territory (MCi). A narrow and more densely packed lateral territory (MCl) separates MCi from DCm (Figure 5.24a, also see Figure 5.25). Alligator *PROX1* is expressed specifically in MCm (Figure 5.24b). *ZBTB20* expression encompasses both MCm and MCi (Figure 5.24c).

The third and lateral-most division of medial cortex (MCl) does not express *PROX1* or *ZBTB20* (Figure 5.24b,c). It does, however, strongly express *ETV1* (Figure 5.24d), a trait shared with rodent and ferret subiculum (Dugas-Ford et al. 2012). No unique marker genes of mammalian subiculum or alligator MCl are presently known. I therefore distinguish the alligator MCl as the territory between the *SATB2*(+) DCm and the *ZBTB20*(+) MCi (Figure 5.25a, MCl between arrows). I similarly found that the mouse subiculum is a *Satb2*(−) zone separating the neocortex from CA fields (Figure 5.25b, Sub between arrows). Mouse *Satb2* is also expressed in the CA fields, which I interpret as a species difference in light of the remaining similarities of molecular topology (Table 5.3).

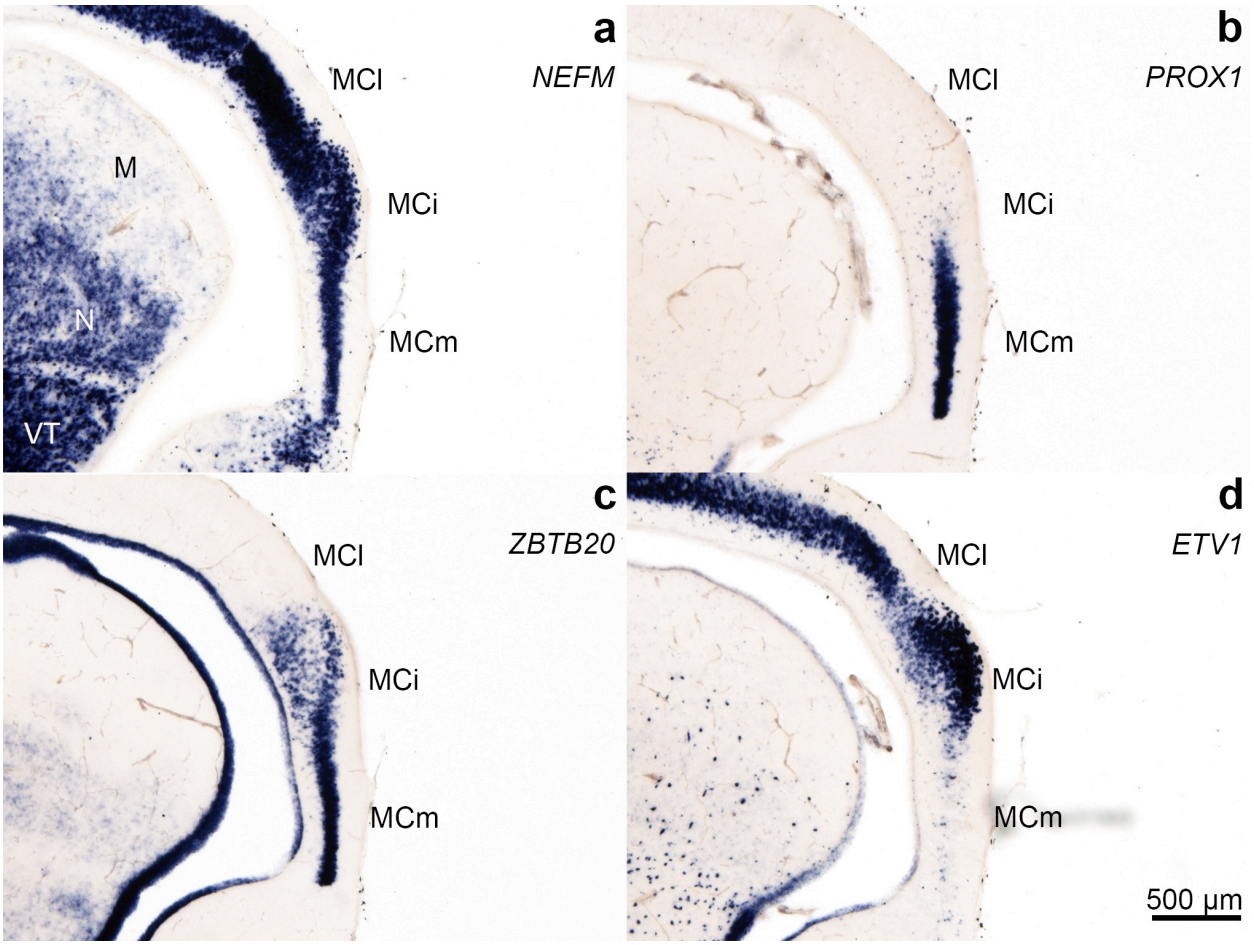

Figure 5.24 Medial cortex contains three fields and expresses conserved hippocampal marker genes

(a) *NEFM* identifies three fields within the medial cortex: medial medial cortex (MCm), intermediate medial cortex (MCi), and lateral medial cortex (MCl). **(b)** The dentate gyrus-specific transcription factor *PROX1* is expressed only in MCm. **(c)** Mouse *Zbtb20* labels dentate gyrus and CA fields. Alligator *ZBTB20* is expressed in MCm and MCi. **(d)** *ETV1* is expressed in MCl and MCi, but is nearly absent from MCm. Four serially adjoining sections from the same telencephalon are shown. Sections correspond approximately to atlas level 6.

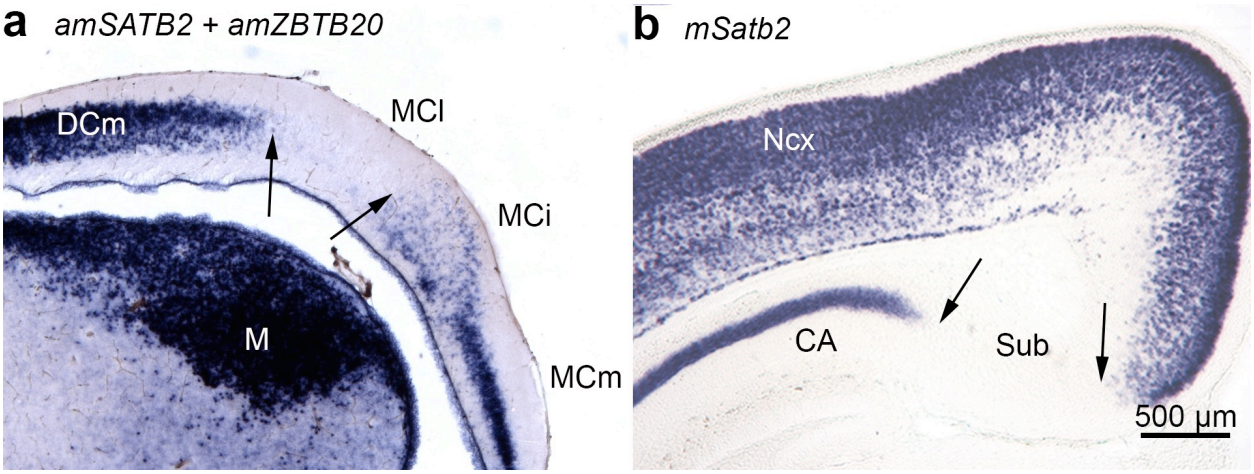

Figure 5.25 A subiculum-like domain separates alligator intermediate medial cortex and medial dorsal cortex

(a) A two-probe, single-color in situ hybridization experiment for *SATB2* and *ZBTB20*. *SATB2* has an expression boundary at the medial edge of medial dorsal cortex (DCm, left arrow). *ZBTB20* has an expression boundary at the lateral edge of intermediate medial cortex (MCi, right arrow). I define the space between them as the lateral-most division of medial cortex (MCl). **(b)** The subiculum is a *Satb2*(−) zone separating the neocortex from CA fields in postnatal day 6 mouse (white space between arrows). *Satb2* is also expressed in CA fields.

Table 5.3 A conserved molecular code for hippocampal subdivisions

	Alligator mississippiensis				***Mus musculus***			
Gene	**DCm**	**MCl**	**Mci**	**MCm**	**Ncx**	**Sub**	**CA**	**DG**
SATB2	+				+		+	
ETV1	+	+	+		+	+	+	
ZBTB20			+	+			+	+
PROX1				+				+

The transcription factors *SATB2*, *ETV1*, *ZBTB20*, and *PROX1* are expressed in a similar topological pattern in alligator and mouse. Medial medial cortex (MCm) is comparable to dentate gyrus (DG). Intermediate medial cortex (MCi) is comparable to CA fields (CA). Lateral medial cortex (MCl) is comparable to subiculum (Sub). *SATB2* expression shows a medial boundary in medial dorsal cortex (DCm) and neocortex (Ncx). *Satb2* expression in mouse CA fields is a possible deviation from this otherwise conserved molecular organization.

Lateral cortex

Crocodilians have a large olfactory-recipient lateral cortex (Scalia et al. 1969). In the anterior-most atlas level (Figure 5.3), I interpret all visible cortex as a circumferential LC. This region does not express markers of DC including either *SATB1* or *SATB2* (not shown). Consistent with this molecular observation, olfactory tracing studies in *Caiman sklerops* demonstrated circumferential olfactory input in anterior sections (Scalia et al. 1969). From the level in Figure 5.4 onward, LC is restricted to the lateral DT surface. At the levels in Figure 5.5 through Figure 5.10, the dorsal boundary of LC is discontinuous with lateral DC. Beyond this point, LC appears to merge with DC and it becomes increasingly difficult to discern dorsal and ventral LC boundaries based on cytoarchitecture. Interestingly, LC and DC merge at approximately the posterior boundary of the mesopallial bridge. Scalia et al. did not observe olfactory projections to ventroposterior DT in *Caiman* (Scalia et al. 1969), suggesting that arcopallium does not contain olfactory cortex (Figures 5.13 and 5.14).

I did not identify any LC-specific marker genes, nor did I identify any genes that label the entire LC. I identified three transcription factors expressed in anterior alligator LC and in mouse piriform cortex: *BCL11A* (Figure 5.26a,d), *ID2* (Figure 5.26b,e), and *EMX1* (Figure 5.26c,f). Expression of these markers was weaker or absent at posterior levels (e.g., Figure 5.18a), indicating molecular heterogeneity across the LC. I note that while these three genes are also mesopallium/IT cell markers, LC does not express *SATB2* or *FOXP1* (Figure 5.18b,d). These gene expression data supplement existing topological and connectional data and provide some additional support for the homology of alligator LC to mammalian piriform cortex.

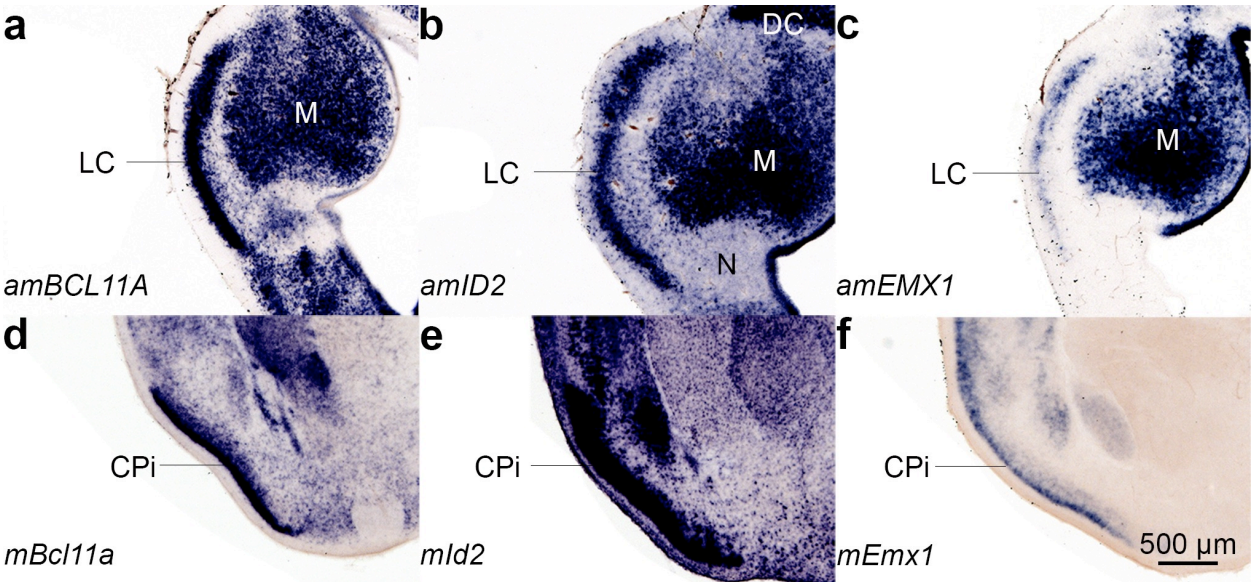

Figure 5.26 Alligator lateral cortex expresses transcription factor markers of mouse piriform cortex
Anterior alligator lateral cortex (LC) expresses the transcription factors **(a)** *BCL11A*, **(b)** *ID2*, and **(c)** *EMX1*. Mouse piriform cortex (Cpi) expresses the same combination of genes **(d–f)**. Sections correspond approximately to atlas level 4.

DISCUSSION

"The relative simplicity and the primitive character of the brain of the alligator seemed to make it a fit subject for comparison with that of [mammals]. The important position occupied by these reptiles with relation to their own class and the Sauropsida generally…and especially their resemblance to birds in very important structural points, adds importance to otherwise trivial details. It soon appeared that, entirely aside from the problems in the interest of which the investigation was made, the intrinsic importance of the subject warranted a more detailed treatment than at first expected."

-C.L. Herrick (Herrick 1890)

Alligator dorsal telencephalon in relation to birds

Alligator dorsal cortex and avian Wulst

The most dramatic difference between the DT of reptiles and the DT of birds is that reptiles have a prominent cortical structure and birds do not (Figure 5.1). The avian Wulst is organized into nuclei and lacks the defining characteristics of cortex including either an outer fiber-rich layer or principal neurons with layer-spanning dendrites oriented perpendicular to the brain surface (Nauta and Feirtag 1986). Despite these differences, some classic authors surmised that the avian Wulst is an elaborated and expanded, although greatly modified, form of reptile dorsal cortex (Huber 1929). Molecular data support this interpretation and suggests homologies of the alligator dorsal cortex cell populations to cells within avian Wulst nuclei.

The avian Wulst contains input, output, and IT cells organized into three separate territories. The IHA is a thin domain intercalated between the HA medially and Md laterally. The IHA is a primary sensory input territory in receipt of somatosensory and visual information from the dorsal thalamus (Karten et al. 1973). Consistent with connections, the IHA expresses conserved marker genes of mammalian neocortical L4 including *KCNH5* and *SATB1* (Dugas-Ford et al. 2012). It is also labeled strongly by *DACH2*. The medial HA is an output population that extends axons to brainstem motor centers and spinal cord (Karten 1971). HA expresses output markers of mammalian neocortical L5 (Dugas-Ford et al. 2012). The ventrolateral Wulst division, Md, is an intratelencephalic relay territory and expresses markers of mesopallium/neocortical IT cells.

I propose the upper layer of alligator medial dorsal cortex is homologous at the level of cell type to the avian IHA. Alligator DCm L2a expresses *KCNH5* (Figure 5.23d), *SATB1* (Figure 5.22b), and *DACH2* (Figure 5.23b), and runs along the anteroposterior axis in a stripe-like

configuration (Figure 5.17a–f). These characteristics are notably similar to the three-dimensional architecture of the avian IHA. L2a is a strong candidate for a primary sensory input zone of alligator DC. It is not known whether these connections exist: previous experiments have recorded evoked potentials to visual and somatic stimulation in the alligator dorsal cortex, but lesion studies failed to identify retrogradely degenerated cells in the thalamus (Kruger and Berkowitz 1960). *KCNH5* identifies a small subset of L2a cells. This may indicate that the primary input zone is very small, and relatively few thalamic projection fibers would be affected in lesion studies. On the other hand, this may simply reflect immaturity of the brain at the stage examined. In the chicken, for example, *KCNH5* expression does not become robust in the IHA until fairly late in gestation (Rowell 2013).

Output cell markers *SULF2* and *CACNA1H* are both expressed in DCm L2b (Figure 5.23e,f). These data suggest that L2b is an output-like territory in alligator cortex, but there is to date no evidence for projections from alligator dorsal cortex to the brainstem (Ulinski 1990b). Still, HA neurons may be homologous to candidate output cells of alligator L2b. Bird-specific elaborations in the breadth of HA projections may have been acquired after their divergence from non-avian reptiles.

I propose, again at the level of cell type, that the lateral part of the alligator dorsal cortex, DCl, is homologous to the avian dorsal mesopallium (Md). Alligator DCl expresses five transcription factors characteristic of mesopallium (Figure 5.18), and forms a continuous cell population with mesopallium (Figure 5.18b). Avian Md is similarly found at the ventrolateral margin of the Wulst. The Md abuts the DVR mesopallium anteriorly and, at more posterior levels in some avian species, is separated from the DVR mesopallium by the intervening ventricle (Chen et al. 2013a, Jarvis et al. 2013). Connections of alligator DCl are not known.

Previous studies reported association projections running anteroposteriorly within the cortex of lizards (Lohman and Mentink 1972). Alligator DCl may form association connections, either rostrocaudally within DCl or across cerebral cortex subdivisions. In the anterior alligator DT, a shallow sulcus separates dorsal cortex from the DVR (Figures 5.4 and 5.5, arrow). I speculate this sulcus could even be homologous as an anatomical landmark to the avian vallecula separating Wulst from DVR.

Despite the potential homologies of cell populations described above (L2a to IHA, L2b to HA, and DCl to Md), dorsal cortex and Wulst are organized in strikingly different ways (see Figure 6.1 in Chapter 6). The avian IHA is not orientated parallel to the brain surface like L2a, but is instead roughly orthogonal to the brain surface. Moreover, IHA is not superficial as is alligator L2a, but is buried beneath the HA. Alligator L2a is separated from DCl in the plane of the cortical sheet. In birds, the IHA is stacked atop the Md. The developmental mechanisms of DT morphogenesis underlying these differences are an important future research direction.

Likely in order to adapt to their behavioral and ecological niches, birds expanded total cell numbers in their DT, even mirroring primate numbers when corrected for brain size (Olkowicz et al. 2016). A simple mediolateral tangential expansion of an alligator dorsal cortex would separate DCm cell populations from relays in DCl. This effect could be countered by reorganizing dorsal cortex cell types into a Wulst-like organization. Stacking IHA, HA, and Md may be a more efficient way to build circuitry between input, output, and IT cells: an IHA input neuron or HA output neuron does not need to extend an axon very far to reach Md IT neurons for associative functions. Mammals independently evolved a similar, but distinct, system in the form of the columnar neocortical circuit linking input, IT, and output cell types. Cell-type layering like that present in the neocortex and in the Wulst might also provide computational benefits by

bringing multiple distinct cell-type populations into topographical alignment. Such an alignment may facilitate the generation of map-like representations of sensory information, and the coherent propagation of maps through multiple stages of information processing.

Alligator DVR and avian DVR

The bird DVR is large, cell-dense, and contains many internal subdivisions. The evolutionary origin of these subdivisions, and in particular the origin of the avian mesopallium and nidopallium, has been very uncertain. I report here that the alligator has clear molecular homologs of mesopallium, nidopallium (including Bas, E, and Field L), and arcopallium. Of particular note is the presence of a putative nucleus basorostralis (Bas) in alligator DVR.

The unusual avian nucleus Bas receives trigeminal somatosensory information via a direct projection from the hindbrain principal trigeminal sensory nucleus, which travels through the quintofronal tract without an intervening synapse in the thalamus (Dubbeldam et al. 1981). It also receives auditory input from the nucleus of the lateral lemniscus, as well as vestibular input (Arends and Zeigler 1986, Wild and Farabaugh 1996, Wild et al. 2001). Although not formally demonstrated, previous studies provided evidence for similar projections in turtle (Kunzle 1985) and a lizard (Ten Donkelaar and De Boer-Van Huizen 1981). Clark and Ulinski (Clark and Ulinski 1984) noted that this territory in alligator does not receive sensory input from any thalamic nuclei studied to date, and suggested that it may correspond to the avian Bas. The available molecular data support this homology and moves the evolutionary origin of this DT sensory input nucleus to at least the common ancestor of birds and non-avian reptiles. Whether the sensory projections to Bas are homologous to any mammalian pathways is an interesting outstanding question.

The afferent and efferent connections of alligator mesopallium (M), nidopallium (N), and arcopallium are not known. If they accord with what is known in birds, alligator M and N would receive secondary sensory information from Bas, E, and Field L; M and N would interconnect with one another; and M and N would send efferents to arcopallium.

The alligator arcopallium deserves special attention, as it appears considerably smaller and less differentiated than its avian homolog. Avian arcopallium can be divided into two broad divisions based on function and connectivity. A dorsal somatomotor region receives sensory information from intermediate relays in the nidopallium and mesopallium, and projects to brainstem nuclei. A more ventral "limbic" division forms connections with hypothalamus (Zeier and Karten 1971). Connections of reptile BDVR are generally poorly understood, and this is especially true in alligator. Without tracing studies in alligator it is premature to propose homologies with either somatomotor or limbic avian arcopallium. However, connections resembling the long-distance motor output of avian arcopallium have not yet been reported in reptiles. Moreover, output cell markers *SULF2* and *CACNA1H* are expressed in chicken arcopallium (Dugas-Ford et al. 2012), but I did not detect their expression in alligator arcopallium. It is possible that a somatomotor district of the crocodilian arcopallium is small or even absent.

Alligator dorsal telencephalon in relation to mammals

Alligator medial cortex and mammalian hippocampus

Hippocampus is thought to be "functionally homologous" across amniotes despite substantial variations in architecture (Colombo and Broadbent 2000). In mammals, the hippocampal formation comprises the dentate gyrus, CA fields, and subiculum. There is presently no consensus on whether reptiles and birds have specific homologs of these three

divisions. I provided evidence for a highly conserved tri-partite molecular organization present in the hippocampus of the mouse and the medial cortex of a reptile.

Alligator dorsal cortex, alligator DVR, and mammalian neocortex

Non-avian reptiles are, along with mammals, the only known vertebrates with a multilayered cerebral cortex. That the reptile three-layered dorsal cortex must in some character feature be homologous to the mammalian six-layered neocortex has never been controversial. The nature of this homology, however, has not been resolved.

One hypothesis proposes that reptile dorsal cortex resembles the ancestral mammalian condition. In this view, dorsal cortex L1, L2, and L3 are homologous to neocortical L1, L5, and L6. The dorsal cortex was elaborated into the neocortex by adding the upper neocortical layers L2, L3, and L4 (Ebner 1976, Reiner 1991, Cheung et al. 2007). This "deep-layer hypothesis" is no longer tenable; reptiles have homologs of neocortical L4 input cells. Tracing studies demonstrated nearly 50 years ago that turtle dorsal cortex receives visual information from the LGN of dorsal thalamus (Hall and Ebner 1970b). Although visual projections could have terminated on the apical dendrites of L5-like cells, it is now known that visual input zones of turtle dorsal cortex express neocortical L4 marker genes (Dugas-Ford et al. 2012). In this report, I provided molecular evidence that alligator DVR and dorsal cortex contain homologs of neocortical IT cells, which form the greater part of neocortical L2 and L3.

Dorsal cortex and neocortex contain a similar set of neuronal cell types, but their organizations are divergent. Alligator DCl may consist almost entirely of IT cells, while putative input and output cells are layered in alligator DCm. DCl and DCm form longitudinal bands along the anteroposterior axis. In contrast, the cell-type composition of the neocortex is relatively homogenous. Every neocortical area is thought to contain the same fundamental set of cell types

in the same basic laminar organization: deep layers L5 and L6 contain output and IT cells, L4 contains input cells, and L2 and L3 contain IT cells. The only core neocortical cell type that may be absent from crocodilian dorsal cortex is the cortico-thalamic cell, neurons located in L6 that project from neocortex to thalamus but not beyond. These cells have not yet been formally demonstrated in the dorsal telencephalon of any nonmammalian amniote.

I argue that alligator dorsal cortex cannot be homologous to any particular neocortical area, such as primary visual cortex, as an "area" comprises the full complement of neocortical cell types. The DCm and DCl divisions of alligator dorsal cortex should best not be compared directly to mammalian neocortical areas. I instead apply the term cortical "field." A field in this sense contains a subset of the cell-type repertoire present in a neocortical area or in the dorsal cortex as a whole.

Both alligator dorsal cortex and DVR contain homologs of three core neocortical cell types. It is easy to imagine how the reptile dorsal cortex could be remodeled into a six-layered neocortex in phylogeny, but less so for the DVR. This effect of DVR appearance on human intuition contributed to early mischaracterizations of the DVR as a ventral telencephalic structure (Ariëns Kappers et al. 1936, Reiner et al. 2004a). The very question of how the dorsal cortex or DVR could be modified into the neocortex is, however, misguided. The phylogenetic distribution of DT structures implies that there is no more reason to think the dorsal cortex and DVR are ancestral to mammals than to think the neocortex is ancestral to extant reptiles. More likely, the neocortex, DVR, and dorsal cortex were derived from a simple evolutionary antecedent that did not closely resemble any of its complex modern descendants. The hypothetical ancestral structure contained input, output, and IT cells. It may, for example, have architecturally resembled the cortex found in tuatara (Figure 5.1) (Reiner and Northcutt 2000).

Alligator dorsal telencephalon in relation to other reptiles

Comparative anatomy of reptile cerebral cortex

Cerebral cortex shows marked variation across non-avian reptiles, as reflected in the diverse nomenclatures developed for medial and dorsal cortices (Nieuwenhuys et al. 1998, Striedter 2016). It is not known whether snakes, lizards, turtles, and tuataras have homologs of alligator MCm, MCi, MCl, DCm, or DCl. In particular, some lizards and snakes have a discontinuous cerebral cortex where ends of opposing cortices can overlap to form a short segment of "five-layered" cortex (Figure 5.1, Iguana) (Ulinski 1990a). The molecular tools presented in this report could, with the exception of the endangered tuatara, readily address these outstanding questions.

The striking conservation of molecular topology in mouse hippocampus and alligator medial cortex strongly suggests that the same fields, molecularly defined, are present in all amniotes. Previous authors recognized three fields in turtle medial cortex: a medial small-celled cortex ("2"), an intermediate large-celled diffuse cortex ("3"), and a lateral cell-dense cortex ("4") (Riss et al. 1969). These are strong candidate homologs of the MCm, MCi, and MCl, respectively. Riss et al. were convinced of this possibility and designated three medial fields in crocodile by the same nomenclature (Riss et al. 1969). Combinatorial expression of *PROX1*, *ZBTB20*, and *SATB2* may be sufficient to test for this tripartite organization in other reptiles and birds. At least in the chicken, *PROX1* and *ETV1* pick out non-overlapping territories in most medial DT (Dugas-Ford et al. 2012).

Whether cell-type layering in alligator DCm is ancestral or derived is an important outstanding question requiring further comparative study. Such a layering scheme has not been described in any other reptile. It also has not been described in the numerous previous studies of

adult crocodilian telencephalon. The relative thickness of DCm compared to DCl is hard to miss in the presented embryonic specimens, but the cortex appears thin and uniform in available images of adult alligator and crocodile (Crosby 1917, Riss et al. 1969). It is possible that the embryonic layers flatten to an unknown arrangement after hatching. Late-stage embryos and adults should therefore be examined in other reptiles. If reptiles inherited and subsequently simplified a multilayered dorsal cortex, it would be an ironic reversal of the common conception that mammals elaborated the "simple" reptile cortex.

Comparative anatomy of reptile DVR

I identified an alligator DVR mesopallium and propose it is homologous to avian ventral mesopallium (Mv). Alligator mesopallium and avian Mv have similar organizations and share expression of five transcription factor markers. This conservation across more than 240 million years of divergence (Green et al. 2014) raises the possibility that a mesopallium may exist in other reptilian species.

Pleurodiran turtles have a large nuclear territory in rostral dorsal cortex that appears to continue into rostral DVR. This territory strongly resembles the alligator mesopallium in topology and morphology. Indeed, Riss et al. designated the Pleurodiran structure and the crocodilian mesopallium as zone "5" (Riss et al. 1969). If Pleurodirans have a mesopallium, the brain morphology of Cryptodirans can be interpreted as a secondary simplification. The "pallial thickening" in these turtles, a lateral continuation of dorsal cortex into rostral DVR, may be a vestigial mesopallium (Riss et al. 1969).

My previous studies on the chicken nidopallium transcriptome failed to identify any specific nidopallium markers beyond the transcription factor *DACH2* (Chapter 4). Alligator *DACH2* labels a strikingly bird-like nidopallium containing multiple primary sensory nuclei.

This marker gene may be useful for identifying nidopallium, mesopallium, and arcopallium in other reptiles. The function of *DACH2* in DT is not known, but conservation of expression across archosaurs suggests that it is an important cellular determinant. Future studies of *DACH2* in the experimentally tractable chicken and mouse systems may help to answer the crucial outstanding question of nidopallium origins.

CHAPTER 6

The evolutionary history of neocortical cell types

ABSTRACT

The six-layered mammalian neocortex is essential for higher-order sensory processing and cognition, yet its evolutionary origins remain controversial. The quest to identify neocortical homologs in nonmammals has proven to be exceptionally difficult because the dorsal telencephalon (DT) takes on dramatically different forms in reptiles and birds. In my view, the neuronal cell type within a neural circuit is the unit of brain organization most informative for cross-species comparisons, rather than cellular assemblies or developmental fields. My comparative molecular data and decades of connectional studies strongly suggest that the last common ancestor of amniotes possessed precursors to neocortical input, output, and intratelencephalic cell types. Reptiles and birds therefore evolved divergent DT structures based on the same fundamental DT cell types and circuits as those found in the mammalian neocortex. The identification of homologous cell types is a crucially important step toward understanding neocortex origins. The next and arguably more exciting challenge is to identify the developmental mechanisms that reorganize existing cell types into genuine neuroanatomical novelties. The variation within and across extant DT character states (mammalian, reptilian, avian) offers some clues, namely that quantitative variation within a state is common but transitions to new states are infrequent and likely require major developmental innovations. I propose a model for the evolutionary history of neocortical cell types from the amniote common ancestor to their various present-day incarnations.

INTRODUCTION

The evolutionary origins of the six-layered mammalian neocortex have been debated for more than a century (Striedter 1997). The question of whether nonmammals have neocortical homologs persists because it is at the center of a perfect storm of conceptual problems in biology: how to compare structures bearing little anatomical resemblance, how to select units of biological organization for cross-species comparisons, and the meaning of homology itself. Progress has awaited refinement of evolutionary thought and the development of molecular tools to probe the genetic makeup of morphological characters.

It was readily apparent to the earliest comparative neuroanatomists that all, and only, mammals have a neocortex in their dorsal telencephalon (DT) (Edinger et al. 1899). The neocortex was thus an attractive evolutionary and anatomical substrate for the cognitive abilities thought to be unique to mammals. Early anatomists implicitly selected the whole neocortex as the biological unit for species comparisons. Mammals have a neocortex, nonmammals do not, and it is therefore an evolutionary novelty built atop a primitive reptilian brain. This perspective is inadequate if we wish to understand the origins of the neocortex. Instead, it is essential to recognize that the neocortex is a complex entity built of numerous components at multiple levels of biological organization including molecules, cell types, circuits, and structures. Some of these components may be evolutionarily older than the neocortex itself, and might be present in nonmammals. Modern researchers disagree on which of these units should be compared across distantly related species in order to establish homologies.

A contemporary evolutionary developmental perspective advocated most forcefully by Günter Wagner highlights the importance of cell types to discussions of homology (Wagner 2007, Wagner 2014, Arendt et al. 2016). The key claims of this view are that 1) cell types are a

fundamental unit of animal organization, 2) cell type is specified in development by evolutionary stable collections of transcription factors, 3) homologous cell types can exist in very distantly related animals, and 4) cell types can acquire species-specific states through modifications that do not compromise their essential identities. From this view, in order to understand neocortex origins, we must break down the neocortex into its constituent cell-type populations.

I elaborated earlier the cell-type homology hypothesis (Karten 1969) by proposing that reptiles and birds have homologs of neocortical input, output, and intratelencephalic (IT) cell types (Chapter 4) (Dugas-Ford et al. 2012). These three basic cell types have maintained their defining connectional and molecular properties for more than 300 million years of evolution, likely because they are essential to telencephalon function and amniote behavior. Other properties of these conserved cell types are far more flexible, especially their organization into tissue-scale architectures.

Homologous cell types: Input, output, and intratelencephalic cells

The mammalian neocortex is an elaborately layered neuronal structure in which layers serve to organize neocortical cell types and their circuitry. Cortical layers are distinguished by criteria including cell morphology, cell packing density, connections, and gene expression. Early anatomists recognized varying numbers of layers in different contexts, but for decades neuroscience has settled on Brodmann's six-layer convention (Brodmann 2006).

The neocortex is foremost a sensory processing organ. Primary visual, somatosensory, and auditory information enters the neocortex predominantly through synapses on neurons in layer 4 (L4) of primary sensory areas (Figure 6.1, green "input" cells). Neurons in neocortical L5 extend long axons out of the telencephalon to deliver motor output to brainstem and spinal cord (Figure 6.1, red "output" cells) (Gilbert and Kelly 1975, Lund et al. 1975, Jones and Wise 1977).

IT association neurons are most abundant in L2 and L3, but are also found in deep layers L5 and L6 (Figure 6.1, blue "IT" cells) (Harris and Shepherd 2015). IT neurons serve as a relay between input cells and output cells within a neocortical column, but additionally send axons across the corpus callosum and to other neocortical areas.

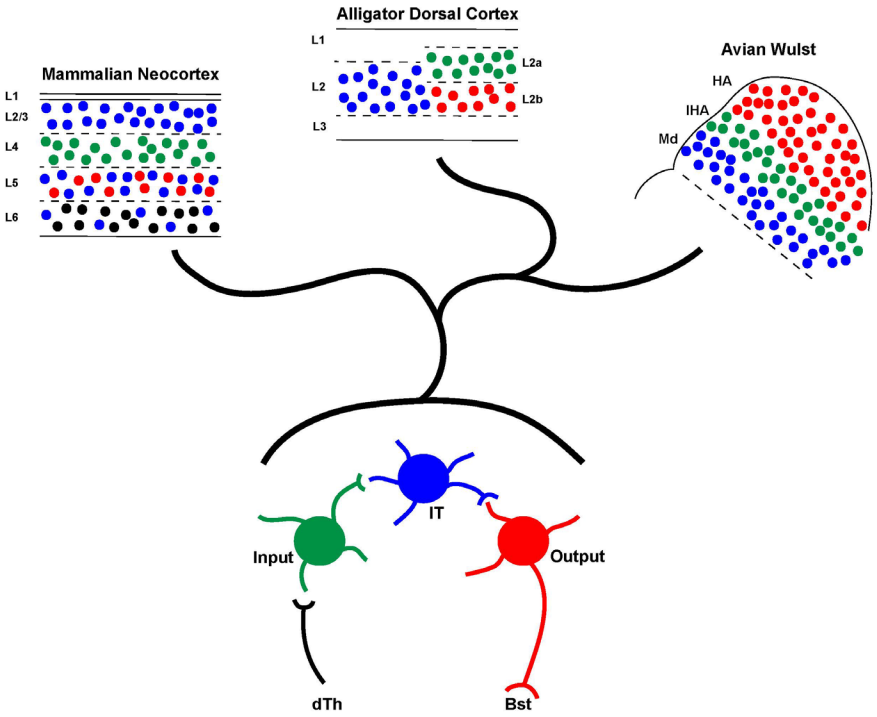

Figure 6.1 Evolution of neocortical input, output, and intratelencephalic cells
The common ancestor of amniotes had input (green), output (red), and intratelencephalic (IT, blue) cells in its dorsal telencephalon (DT). Input cells received primary sensory information from dorsal thalamus (dTh), while output cells extended axons to brainstem (Bst). IT cells served as a relay between input and output cells. These three principal DT cell types were reorganized into dramatically different architectures in extant mammals, reptiles, and birds, but nonetheless maintained their defining connection types and gene expression patterns.

The bulk of the sauropsid (reptiles and birds) DT comprises a nuclear territory called the dorsal ventricular ridge (DVR) (Ulinski 1983, Reiner et al. 2004a). Above the DVR, non-avian reptiles have a three-layered dorsal cortex (Ulinski 1990a, Naumann 2017). The dorsal cortex is not a neocortex, nor is it, in my view, simply a primitive neocortex. In place of a dorsal cortex, birds have a nuclear territory called the Wulst. This structure is likely a derived dorsal cortex that secondarily lost cortical lamination. All modern researchers agree that dorsal cortex and Wulst

are homologous in some way to neocortex (Medina and Reiner 2000), but DVR is a source of significant controversy.

Birds possess sensory projections from the thalamus to DT that resemble mammalian projections from thalamus to L4 of primary sensory areas (Jarvis et al. 2013). To review briefly an extensive connectional literature, lemniscal somatosensory and visual pathways target the interstitial nucleus of the HA (IHA) in the avian Wulst while tectofugal visual and lemniscal auditory pathways target the DVR nuclei entopallium (E) and Field L, respectively (Wild et al. 1993, Shimizu et al. 1995, Krutzfeldt and Wild 2005, Dugas-Ford and Ragsdale 2015). These four separate sensory channels are strikingly similar to mammalian lemniscal pathways to primary somatosensory, visual, and auditory cortex, and the tectofugal pathway to secondary visual cortex. Karten noted that it would be unparsimonious to suppose that these pathways evolved independently in (relatively) close animal clades. It is more likely that these pathways, including their DT targets, are homologous by descent in mammals and birds. More specifically, Karten proposed that the sensory input neurons located in avian IHA, E, and L are homologous as cell types to mammalian neocortical sensory input cells in L4 (Karten 1969). Long-distance projections from avian HA (in the Wulst, Figure 6.1) and arcopallium (in the DVR) to the brainstem were discovered subsequently (Zeier and Karten 1971, Wild and Williams 2000). Karten further proposed that these output cells are homologous to neocortical L5 cells (Karten 1997, Butler et al. 2011).

If input and output cells of mammals and birds are homologous, they may share expression of specific marker genes that reflect their common evolutionary history. In other words, there may be evolutionarily indispensable genes specifically required for the development and function of DT cell types. The Ragsdale laboratory tested this prediction with comparative

gene expression studies. They first identified neocortical L4/input and L5/output marker genes conserved across mammals (Rowell et al. 2010), then tested where avian orthologs of these genes are expressed in DT. In short, the conserved neocortex L4 markers *KCHN5* and *RORB* are highly enriched in avian IHA, E, and Field L, as predicted (Dugas-Ford et al. 2012). Conserved L5 markers, including *ETV1*, *PCP4*, *SULF2*, and *FEZF2*, are expressed in the avian output nuclei HA and arcopallium (Dugas-Ford et al. 2012). These gene expression data provide compelling support for Karten's hypothesis of homologous cell types. It is unlikely that the projection patterns evolved independently, and it is independently unlikely that these cells would also acquire the same patterns of cell-type-specific gene expression.

To understand the extent of molecular conservation better, I performed a forward screen for conservation of L4/input cell marker genes. The avian input nuclei E, Field L, and a variety of outgroup nuclei were collected by dissection. I sequenced their transcriptomes and identified the most abundant coding transcripts enriched in avian input cells. I then tested whether genes enriched in avian input cells are, in turn, selectively expressed (i.e. conserved) in mouse neocortical L4.

I identified three additional transcription factor genes, *NR0B1*, *RORA,* and *SATB1*, that are highly enriched in mouse L4 and chicken input populations. These data provide further support for homology of amniote input cells. However, almost all other molecular marker genes were divergent (Chapter 3). Importantly, this result in no way falsifies the cell-type homology hypothesis, as homology is based on similarity only. Homology is, in a sense, the question of whether similarity is due to common ancestry or convergence—species differences are universal. The key lesson from this study is that transcription factors are much more likely to be co-expressed in common neuronal cell types across species than are other classes of molecules. The

widespread divergence of input cell transcriptomes is not surprising given the great divergence of input cell organization between the mammalian neocortical layers and the nuclei of the avian Wulst and DVR.

My findings on the evolution of the amniote DT input cell transcriptome are largely concordant with emerging views in evolutionary developmental biology (Wagner 2007, Arendt 2008, Pennisi 2015, Arendt et al. 2016). This view emphasizes cell types as fundamental units of metazoan organization. Cell types are a more direct manifestation of genetic information than are, say, multicellular structures like organs and appendages, because cell types are the things that express genes. Structures like brain nuclei or layered cortices can be built from numerous distinct cell types in cooperation to perform an emergent function. For example, the neocortex, as a structure, is no older than mammals. However, the neocortex is built from excitatory cell types, inhibitory cell types, glia, and endothelial cells that have independent evolutionary histories and may be far more ancient than the neocortex. Homologous cell types can sometimes be recognized in distantly related animals, sometimes contained within highly divergent structures, by the expression of conserved gene regulatory networks comprising transcription factor molecules. Much of the remaining cellular transcriptome is free to diverge and contribute to species-specific functions. I predict that a conserved network of transcription factors (NR0B1, RORA, SATB1, and previously known RORB) regulates the identity of DT input cells in amniotes.

I applied the key lesson from the input cell study—that cell-type features are predicted to be controlled by transcription factor networks—to the identification of a novel class of conserved DT neurons. The avian mesopallium is a large territory of disputed homology. Recent molecular studies have securely established that mesopallium contains two conserved subdivisions: a dorsal

mesopallium (Md) in the Wulst and a ventral mesopallium (Mv) in the DVR (Chapter 4) (Jarvis et al. 2013). Both Md and Mv form intratelencephalic connections as an intermediate between primary input cells and other DT cell types. Previous studies proposed that mesopallium is homologous to neocortical L2 and L3, but the markers employed did not support the comparison (Suzuki et al. 2012, Atoji and Karim 2014). Rather than test whether mammalian upper layer markers are expressed in mesopallium, I identified mesopallium-specific transcription factors and investigated where they are expressed in mouse neocortex (Chapter 4).

I identified a panel of six transcription factor genes (*EMX1*, *SATB2*, *BCL11A*, *ID2*, *FOXP1,* and *NHLH2*) that are highly enriched in chicken mesopallium. I found that mouse orthologs of five of these transcription factors are expressed in the neocortex (Chapter 4). None of these genes is an L2/3-specific marker. Instead, they are expressed in multiple layers in patterns consistent with the distribution of neocortical IT cells. IT cells comprise a broader class of neurons that includes but is not restricted to L2/3 neurons (Harris and Shepherd 2015). Two of the transcription factor genes (*Satb2* and *Bcl11a*) were previously shown to be required for the specification of neocortical IT (specifically, callosal) cells in mouse (Alcamo et al. 2008, Britanova et al. 2008, Woodworth et al. 2016). I proposed the novel hypothesis that a third major class of neocortical neurons, the IT cells, is conserved across amniotes (Chapter 4). The ancestral IT cells likely expressed the five described transcription factors and diversified into mammalian neocortical IT cells and the avian mesopallium (Figure 6.1, blue cells). These findings again accord with the view that cell types are regulated by conserved networks of transcription factors, and that DT cell types form conserved neural circuits.

Any character present in mammals and birds is predicted to be present in non-avian reptiles (barring secondary loss) because the common ancestor of mammals and birds also gave

rise to all extant reptiles. Comparative studies of mammals and birds suggest that input, output, and IT cells form functionally essential circuitry in the amniote DT. All three cell types are present in cortical layers throughout the neocortex. In birds, I found that input, output, and IT cells are present in the Wulst in the IHA, HA, and Md, respectively. All three types are also present in distinct DVR nuclei. It is a natural question whether reptiles have representatives of these three core DT cell types in both the dorsal cortex and the DVR.

I studied the expression of conserved marker genes for input, output, and IT cells in the American alligator, *Alligator mississippiensis* (Chapter 5). All five IT-specific transcription factors are expressed in two distinct alligator territories: a DVR mesopallium and a lateral part of dorsal cortex (DCl). I proposed that alligator mesopallium and DCl are homologous, both at the level of principal DT cell type and at the level of an IT-cell structure, to avian ventral mesopallium (Mv) and dorsal mesopallium (Md), respectively. Alligator mesopallium and DCl form a continuous cell population around the lateral ventricle with possible implications for the evolution of IT cell distribution (see below). The input cell marker genes *KCNH5*, *SATB1*, *RORA*, and *RORB* are expressed in ascending sensory input populations in alligator DVR. These molecular data, together with the tracing data of Pritz (Pritz 1974b, Pritz 1975), allow us to securely identify a crocodilian entopallium and Field L. *KCNH5*, *SATB1*, and *DACH2* (an avian nidopallium and IHA marker) are expressed in a dorsal cortex territory that I propose is homologous at the cell type level to the lemniscal-recipient avian IHA. The output cell markers *SULF2* and *CACNA1H* are expressed in a dorsal cortex cell population possibly homologous to the output neurons in avian HA.

Candidate alligator input and output cells are organized into cortical layers in a medial subdivision of dorsal cortex (DCm). The alligator lamination is neocortex-like, with input cells

directly above output cells. This is the only demonstration to date of molecular sublaminae in a reptile cortex, and it is an important outstanding question whether aspects of this organization are ancestral to amniotes. I conclude the alligator dorsal cortex contains homologs of input, output, and IT cells in an organization distinct from both mammalian neocortex and avian Wulst (Figure 6.1). The available molecular evidence falsifies the long-standing hypothesis that neocortex evolved from dorsal cortex by de novo addition of the upper cortico-cortical layers L2-4 (Ebner 1976, Cheung et al. 2007).

Extant DT structures including neocortex, DVR, dorsal cortex, and Wulst are evolutionary novelties. They are shared-derived characteristics of separate animal clades without obvious precedents outside of amniotes. However, evolution is not thought to pull novelties out of a hat, but rather builds them through innovation from pre-existing components. My central claim is that amniote DT structures are built from the same basic repertoire of cell types present in their last common ancestor (LCA), which have been reorganized in species-specific ways to produce emergent anatomical novelties. A major challenge for the field is to identify the developmental mechanisms underlying evolutionary novelty in DT organization. From the perspective of conserved cell types, the question of DT evolution becomes the question of how cell-type specification and tissue morphogenesis are differentially regulated across species. Because major reorganizations of DT cell types have apparently only occurred a few times throughout amniote evolution, I speculate that major developmental innovations differentiate the DT of amniote groups.

Themes and variations of dorsal telencephalon organization

The neocortex varies dramatically in size across mammalian species while maintaining its basic internal organization. The human neocortical surface area is more than four orders of

magnitude larger than that of a mouse. It is clear that neocortex size is incredibly plastic because multiple independent radiations of mammals (including monotremes, marsupials, and eutherians) have representatives with either smooth or folded neocortices, indicating numerous independent modifications and increases or decreases in neocortical surface area (Lui et al. 2011). It is likely that the number of neocortical neurons and their overall organization are regulated by distinct developmental mechanisms. For instance, the human lineage, after diverging from other great apes, acquired unique genes that dramatically increase neuron number without obviously changing the identity of cells or their layering scheme (Florio et al. 2015, Florio et al. 2016, Florio et al. 2017). The basic columnar circuitry including input, output, and IT cells is highly conserved across mammals (Harris and Shepherd 2015). All mammals have a conserved set of primary sensory areas that share the same relative topology: the lemniscal visual area in the back, the lemniscal somatosensory area in front, and tectofugal visual and lemniscal auditory areas located laterally (Krubitzer and Seelke 2012).

Analogous patterns of variation are present within reptiles and birds. All known reptiles have a cerebral cortex and a DVR. All birds have a Wulst (instead of a cerebral cortex) and a DVR. The relative proportions of internal DT subdivisions, as well as total DT size, can vary greatly across birds (Iwaniuk et al. 2005). However, no known reptile or bird exhibits a fundamental departure from the DT organization characteristic of its group. These patterns of variation suggest that mammals, non-avian reptiles, and birds have distinct "DT types" with inherent biological differences.

The dorsal telencephalon is a character with unambiguous homology in all amniotes. The three principal amniote DT types represent distinct character states, each of which internally varies quantitatively while adhering to a basic structural plan. Günter Wagner introduced the

term “variational modalities” to describe this type of variation (Wagner 2014, Love 2015). “Two or more sets of character states of the same character (homolog) are called variational modalities if they are non-overlapping and if transitions among character states within each mode are much more frequent than between modalities” (Wagner 2014). In other words, the amniote DT types are variational modalities because they are stable attractor states that infrequently transform into a new stable state. The prediction is that major developmental differences distinguish variational modalities, while intense selective pressure due to developmental constraint and evolutionary exigencies maintains variation within a modality.

A second example of variational modalities is found in vertebrate paired limbs. The fins of fish and the limbs of tetrapods are homologous as limbs. However, they are very distinct limb character states. Fish fins and tetrapod limbs each come in a great variety of shapes and sizes, but we can easily recognize that they are so structurally consistent within each group that we can meaningfully say there is a “fish limb” and a “tetrapod limb.” A major developmental innovation is thought to have accompanied the transition from a fish-like limb to an early tetrapod limb, namely the innovation of autopodial digits comprised of endochondral bone (Nakamura et al. 2016).

Obviously, transitions across DT variational modalities occur because multiple types exist. These transitions, however, are extremely rare and have apparently occurred only a few times over the course of amniote DT evolution. As an analogy, a hypothetical molecule may exist in one of two stable states that are separated by enormous activation energy. Each of the two stable states possesses some degrees of freedom, as atoms can rotate around the axis of a chemical bond. However, a transition between states involves the breakage and formation of chemical bonds and occurs only in the presence of an appropriate catalyst. In the following

section, I will speculate on the mechanisms of anatomical transitions across amniote DT types. Later I will discuss the hypothesis that these transitions co-occur with other major evolutionary transitions. The selective pressures driving these transitions may be thought of as catalysts.

A model of evolutionary transformations to amniote dorsal telencephalon organization

There is no fossil record for the internal organization of vertebrate brains. To propose anatomical transformations, we can only construct models of the ancestral DT anatomy by comparing extant forms. The results described in this thesis support an argument that the amniote LCA had input, output, IT cells, and a medial hippocampal territory (Figure 6.2, green, red, blue, and orange cells, respectively). My model of anatomical transformations is based on these results and makes two key assumptions: 1) the DT anatomy of the amniote LCA was much simpler than extant DT types, and 2) the topological distribution of cell types resembled that of extant sauropsids more than it resembled that of mammals.

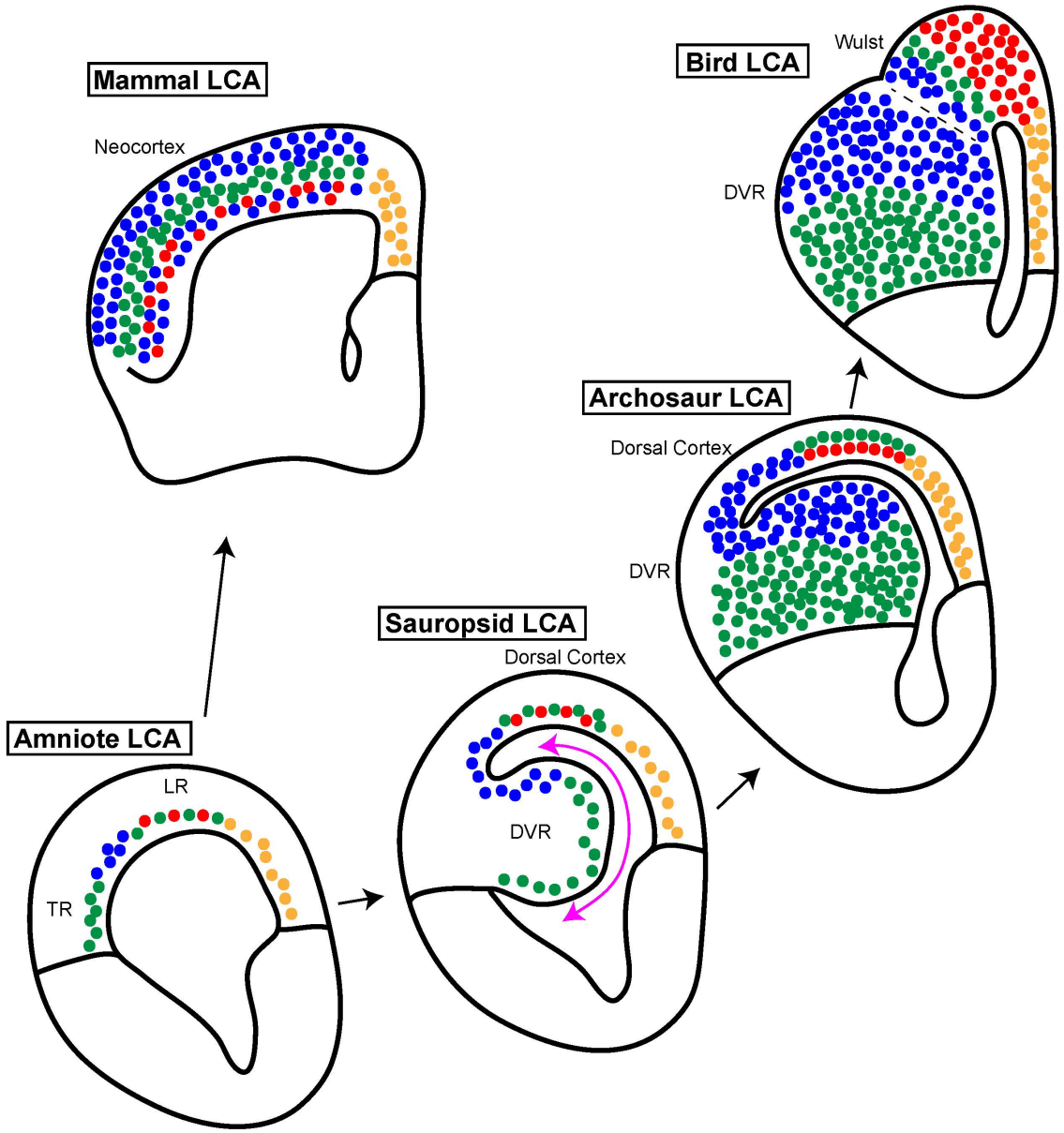

Figure 6.2 Anatomical transformations during the phylogenetic diversification of amniote dorsal telencephala

I propose the amniote last common ancestor (LCA) had an architecturally simple dorsal telencephalon (DT) resembling that of modern amphibians, which contained input (green), output (red), intratelencephalic (blue), and hippocampal (orange) cells. A dorsal population of input cells received lemniscal visual and somatosensory information (lemniscal-recipient, LR). A ventrolateral group of input cells received mixed lemniscal and transtectal sensory information (TR). This simple, ancestral DT underwent independent evolutionary transformations to give rise to mammalian neocortex and sauropsid dorsal ventricular ridge (DVR), dorsal cortex, and Wulst. See text for details.

The amniote LCA. Amphibia is the closest living outgroup to amniotes. The amphibian DT (including both anurans and urodeles) is extremely simple in its morphology (Nieuwenhuys et al. 1998). The overall shape of the telencephalon is a smooth oval. There is no DVR. The neurons are loosely distributed next to the ventricle with structural specializations into possible nuclei only in a few clades (Northcutt 1974). I suggest that the DT of the amniote LCA resembled the impoverished architecture of the amphibian DT (Figure 6.2, Amniote LCA).

All extant amniotes receive lemniscal somatosensory and visual information in dorsal DT and tectofugal visual and lemniscal auditory information in lateral DT. The model amniote LCA has two populations of input cells: a lemniscal recipient dorsal group (Figure 6.2, LR) and a mixed transtectal and lemniscal-recipient lateral group (Figure 6.2, TR). The dorsal group gave rise to input cells in the sauropsid dorsal cortex and Wulst. The lateral group gave rise to input populations in the DVR, including entopallium and Field L. I speculate that in the LCA a population of IT cells was intercalated between the dorsal and lateral input groups, much as the IT cell population separates dorsal and lateral input cell groups in birds and alligators (Chapters 4 and 5). Output cells are found in the avian Wulst and reptile dorsal cortex, so I suggest that output cells were intermingled at least with the dorsal input cell groups (Figure 6.2, red cells).

The sauropsid LCA. The first major developmental transformation was likely the acquisition of the DVR in the sauropsid lineage. At this transition, the targets of the dorsal and lateral ascending sensory pathways became individualized into morphologically distinct territories: a dorsal cortex-like structure and a lateral DVR. The two territories may have acquired unique sets of transcription factors that permitted them to acquire separate patterns of gene expression and to pursue very different modes of development, but these differentiating factors have not been identified. The dorsal and lateral developmental dichotomy is in contrast

with the mammalian DT, where dorsal and lateral ascending sensory pathways both target a uniform morphological structure, the neocortex.

The sauropsid LCA may have resembled the modern tuatara *Sphenodon punctatus*, which has a fairly uniform cortex-like structure extending from "dorsal cortex" through the DVR (Figure 6.2, Sauropsid LCA). I suggest that a population of IT cells spanned the territory between the dorsal cortex and DVR much as the mesopallium bridge connects dorsal cortex to mesopallium in *Alligator mississippiensis* (Chapter 5). The origin of the DVR may have been accomplished in part by an expansion of ventricular zone progenitors analogous to expansion of neocortical progenitors in mammals (Figure 6.2, pink arrow). This expansion may have resulted in more neurons and more neural processing power for the laterally targeted sensory channels. The acquisition of the DVR, through unknown developmental innovations, can be considered an irreversible transformation across DT types because all known extant sauropsids have a DVR.

The archosaur LCA. The basic plan of sauropsid DT cell-type organization is in place after the transition to the sauropsid LCA. Much of the ensuing variation across reptiles appears to be quantitative, but molecular data on squamate (snakes and lizards) DT organization is lacking. I suggest that the archosaur LCA closely resembled modern alligators in its DT morphology (Figure 6.2, Archosaur LCA). The archosaur LCA differs from the sauropsid LCA mainly by possessing many more neurons that pack the DVR from the ventricle to the pial surface. There was likely an increase in dorsal cortex cell number, as *Alligator mississippiensis* appears to have a more cell-rich cortex than turtles and other extant reptiles (Chapter 5). It is unknown when alligator DC cell-type sub-lamination might have arisen, but I propose that it was present at least in the archosaur LCA (Figure 6.2, stacked green and red cells in the Archosaur LCA).

The bird LCA. The transition from an alligator-like, archosaur DT to the LCA of birds involved a second major transformation across variational modalities, or across DT types. This transition entailed the modification of the tri- or tetra-laminar dorsal cortex into the nuclear Wulst. Dorsal cortex and Wulst contain the same core set of cell types, but they are organized into very different structures (Figure 6.1). Alligator dorsal cortex input cells form a superficial cortical layer. In birds, the input IHA is sandwiched between the Md ventrally and the HA dorsally (Figure 6.1). Alligator input cells are oriented in a layer parallel to the ventricle and to the brain surface, while the avian IHA runs in an orthogonal stripe from ventricle to brain surface. The developmental mechanistic causes of these differences in cell-type organization are wholly unknown.

Some differences between Wulst and dorsal cortex could be elegantly explained by a developmental fusion of the ventricle separating an alligator-like dorsal cortex from DVR. Such a fusion would stack the DCl (the Md equivalent) atop the DVR mesopallium (the Mv equivalent), and would cause an apparent change in the orientation of IHA relative to the brain surface. It would also explain why Md and Mv territories are separated by a lamina despite their extensive molecular similarities (Figures 6.1 and 6.2, dotted line). Notably, the Jarvis group claimed to observe such a fusion event during zebra finch embryogenesis (Chen et al. 2013a). Unfortunately, little evidence was provided to support this claim, and I have seen no trace of this ventricular fusion in the development of the chicken.

The mammal LCA. Historical attempts to describe neocortex origins imagined the transformation of a reptile- or avian-like DT into the neocortex (Edinger et al. 1899, Ariëns Kappers et al. 1936). Harvey Karten, for instance, sought to explain the transformation of a DVR-like structure into neocortex by hypothesizing extensive tangential cellular migrations from

a ventrolateral domain into a dorsal domain (Karten 1969). However, mammals are not thought to have evolved from animals resembling modern sauropsids. The transformations leading to the mammalian neocortex need to be considered in the context of the amniote LCA, and not the sauropsid lineage. The amniote LCA may not have had a morphological DVR or neocortex, but was instead independently adapted into both.

I propose the amniote LCA underwent an independent transition across modalities to the mammalian neocortex. Cell-type distribution throughout the tangential extent of neocortex is highly consistent. In the neocortex, major cell classes are distributed in thin laminae extending over the entire neocortical surface (Figure 6.2, Mammal LCA). In sauropsid DVR, DT cell types are found in spatially segregated nuclei of consistent internal cellular identity. For example, the avian entopallium is a large nucleus that contains input cells while the mesopallium contains IT cells. These anatomical differences suggest fundamental differences in the mechanisms of cell-type specification in mammals and sauropsids. Specifically, sauropsid DT cell types may be specified by spatial information and arise from fate-restricted progenitors. In contrast, neocortical progenitors at all locations are thought to generate all neocortical cell types sequentially in the well-known inside-out pattern.

I explored this idea in the chicken telencephalon. Using in ovo electroporation of PiggyBac transposition vectors, I fate-mapped anterior chicken DT and identified a field of progenitors that gave rise to mesopallium but not to input or output cell types (Chapter 4). This result suggests that a spatially contiguous subset of progenitors is fated to produce IT cells, but other populations of progenitors give rise to input or output cells (Figure 6.3, light-blue IT progenitors segregated from light-red output progenitors). Recent fate-mapping studies in mouse neocortex provide an interesting parallel to these mesopallium observations. The long-standing

model of neocortical neurogenesis states that all radial glia progenitors are competent to produce all major neocortical cell types in sequence (Rakic 2009, Guo et al. 2013). The Müller lab challenged this concept by providing evidence for fate-restricted neocortical progenitors that give rise to *Satb2*(+) IT cells of upper and lower layers, but not to *Bcl11b*(+) output cells (Franco et al. 2012, Franco and Muller 2013, Gil-Sanz et al. 2015). These fate-restricted progenitors were found intermixed with other progenitor types across the neocortical ventricular zone (Figure 6.3, light-blue IT-restricted progenitors intermixed with light-red output progenitors).

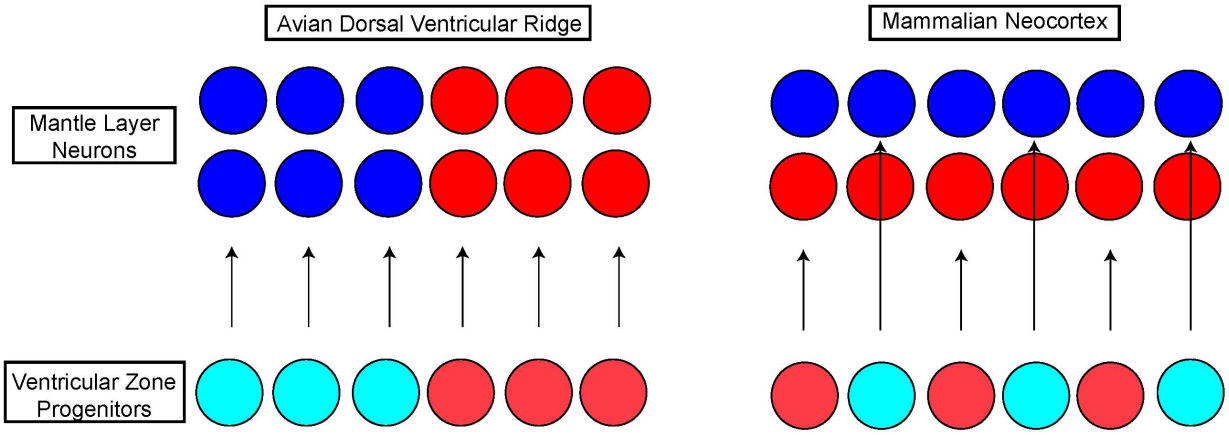

Figure 6.3 Evolution of dorsal telencephalon cell-type progenitor zones
Fate-mapping experiments establish that avian mesopallium intratelencephalic (IT) cells arise from a coherent territory of fate-restricted progenitor cells in anterior dorsal telencephalon (DT). Output cells must arise from a separate field of progenitors. The avian progenitor organization differs from that of mammalian neocortex. However, neocortex may contain a population of homologous IT-restricted progenitors intermixed with other cell populations. These differences may account for much of the divergence of DT anatomy across mammals and birds.

I suggest that IT-restricted progenitors may be homologous across mammals and birds, but the inductive signals that specify them may be deployed in different ways. Divergence in the signals that dictate when and where DT cell types are specified may be a means by which neocortex anatomy diverged from sauropsid DT. The developmental changes culminating in neocortical cell-type distribution and lamination were apparently permanent, as no extant mammal has deviated from the basic plan since. Some large-brained mammals such as humans,

elephants, and whales have gone to great lengths to fold an enormously expanded neocortex into their skulls, but otherwise seem to be stuck with its six-layered architecture.

Mammals and sauropsids may possess distinct DT types, or variational modalities, that differ from one another by virtue of significant developmental innovations. The hypothetical changes to the mode of cell-type specification I described might qualify as "significant developmental innovations." These changes set apart mammalian and sauropsid DT organizations such that they now explore non-overlapping subsets of morphological space.

A critique of the tetrapartite pallium model

The major alternative interpretation of amniote DT homologies proposes that the DVR is not homologous to neocortex, but is instead homologous, as a field, to subcortical nuclei in the mammalian piriform lobe (including claustrum, endopiriform nucleus, and the basolateral complex of the amygdala). This idea is sometimes referred to as the piriform lobe hypothesis or claustroamygdalar hypothesis (Butler et al. 2011, Dugas-Ford and Ragsdale 2015). This hypothesis does not invoke cell-type homologies and selects very different units of biological organization, namely developmental fields and their adult derivatives.

The most widely adopted version of this idea was developed by Luis Puelles and colleagues (Puelles et al. 1999, Puelles et al. 2000, Puelles et al. 2016a, Puelles et al. 2016b, Watson and Puelles 2017). These authors consider relative location of a character within a nervous system Bauplan to be the dominant, if not the sole, criterion for homology. In this view, the nervous system is divided into a grid-like series of territories, or developmental fields (also referred to as morphogenetic fields), along anteroposterior and mediolateral coordinates. Fate of adult structures is specified within these fields by highly conserved transcription factor codes regulated by spatial information. Each field gives rise to a specific set of neural cell populations

and structures. Importantly, the authors propose that all vertebrates have exactly the same set of developmental fields in an "invariant" relative organization (Puelles et al. 2016b). As the most crucial claim, Puelles et al. argue that the adult derivatives of the same (or homologous) developmental field in different species are homologous (as a field) (Puelles and Medina 2002).

In this scheme, the embryonic dorsal telencephalon (or pallium) contains four conserved mediolateral subdivisions named medial, dorsal, lateral, and ventral pallium. The authors refer to this model as the Tetrapartite Pallium Model, which I will abbreviate as the TPM (Puelles et al. 2016b). The medial pallium gives rise to mammalian hippocampus and its sauropsid homologs. The notion that hippocampus is homologous across amniotes is not currently controversial (Striedter 2016), even if the theoretical underpinnings of the TPM are problematic (see below). The dorsal pallium gives rise to the avian Wulst, reptilian dorsal cortex, and the entire mammalian neocortex. The lateral pallium gives rise to avian mesopallium, turtle pallial thickening (other reptiles have not been studied by relevant criteria), and mammalian claustrum and insular cortex. The ventral pallium gives rise to avian nidopallium and arcopallium, possibly the entire reptilian DVR, mammalian amygdala, and in all clades the olfactory cortex.

The TPM proposes a very different set of homologies from the cell-type homology hypothesis, largely as a result of selecting different organizational units, or "levels," for homology (Dugas-Ford and Ragsdale 2015). I argue that the conclusions of the TPM depend upon a number of logical fallacies.

1) Not every character can have a homolog. Because all vertebrates have the same set of fields, and the derivatives of the same field are always homologous, the TPM leads to the extreme conclusion that every adult neural character has a homolog in every other vertebrate. In other words, there can be no true evolutionary innovations. It is true that no biological character

can evolve from nothing, but this idea should not be conflated with the notion that every structure must have a homolog. Every character must have a beginning, and these beginnings are marked by developmental innovation. Glen Northcutt suggested that hypotheses of field homology for complex entities involve character comparisons at an inappropriate level of biological organization (Northcutt 1999). The neocortex, as a structure, is a mammalian innovation. To understand neocortex evolution, we must instead seek to identify homologs at the level of its principal components—the DT cell types.

The evolutionary history of IT cells illustrates how novel DT structures can arise but lack specific homologs. The amniote LCA may have possessed a limited ancestral stock of IT cell sub-types (Figure 6.2, Amniote LCA blue cells). In the avian lineage these IT cells diversified into dorsal mesopallium (Md) and ventral mesopallium (Mv) subpopulations. The mammalian IT cells followed a separate, independent evolutionary history to diversify into cells of different cortical layers with differing connections and gene expression (Fame et al. 2017). In this scenario, cells in avian Md and Mv are more closely related to each other than either cell population is to any IT cell in the neocortex, and so do not have separate mammalian homologs. The TPM, however, places Md in dorsal pallium and Mv in lateral pallium, which demands that Md is homologous as (part of) a field to neocortex while Mv is homologous to claustrum and insula. The mesopallium cannot be homologous to the neocortex or to any neocortical area because it contains IT cells but not input or output cells. Likewise, the neocortex is not homologous to any particular structure in the sauropsid DT.

Proponents of the TPM may object that they do not, in fact, propose strict one to one homologies for every entity in the nervous system. Instead, the adult derivatives of a developmental field in one species are collectively homologous to the derivatives of the same

field in a separate species. The concept of field homology is questionable, however, because it assumes that the derivatives of a field are: 1) always more closely related to one another than any is to the derivatives of another field, and 2) have historically always arisen from the same field. Experimental support for these assumptions is absent.

The TPM is problematic because, as a matter of definition, it is impossible to identify any adult structure without homology in all other vertebrates. This is also true of the developmental fields from which the adult structures arise, because all vertebrates have the same fields in an invariant topology. Evolution can simplify organisms and cause the loss of characters, but the TPM rules out loss of developmental fields. The TPM is thus a form of evolutionary preformationism in that it stipulates that every extant vertebrate has an identical, and highly complex, nervous system Bauplan that can be traced unchanged into deep evolutionary time. If developmental fields exist, then surely they can arise through evolutionary innovation. The TPM implies the unlikely scenario that all nervous system developmental fields originated before the vertebrate LCA, but no further changes were allowed to occur over the subsequent 500 million years that witnessed the evolution of lampreys, lungfish, and rhinoceros. The TPM is unfair to evolution and its powers of creation.

2) The foundation of the TPM is a series of unsupported assertions. The TPM can be unpacked into several strong assertions. The homology conclusions of the model are only warranted if all of the underlying premises are true. First, the DT of every extant vertebrate contains four identical and homologous morphogenetic fields. Second, each field gives rise to a specific set of known adult derivatives. Third, the adult derivatives of the same field in different species are homologous as a field.

A morphogenetic field is a quasi-autonomous self-regulating field of uncommitted progenitor cells that responds to signals from nearby signaling centers, often but not always located at its boundaries. There is no experimental evidence to suggest that the medial, dorsal, lateral, and ventral pallium domains meet these criteria in a single vertebrate, let alone all of them. No signaling centers have been discovered to lie within the DT at the boundaries of these domains. No ablation experiments have been performed to test whether the proposed fields can self-regulate to give rise to normally patterned derivatives. Specific markers of different fields have not been identified in order to unambiguously resolve whether the same fields are present in different species. The entire DT, however, is a candidate morphogenetic field. The DT possesses distinct signaling centers at its medial edge (the hem), its lateral edge (the antihem), and at its rostromedial pole (the anterior neural ridge) (Grove et al. 1998, Fukuchi-Shimogori and Grove 2001, Assimacopoulos et al. 2003, Rash and Grove 2006, Assimacopoulos et al. 2012, Caronia-Brown et al. 2014). The DT gives rise to many structures and cell types, but there is no requirement that distinct structures each have their own field of origin. Finally, there is no evidence to suggest lineal restriction, or compartmentalization, of neural progenitors in the proposed DT fields. If progenitors can freely move across fields, there is little sense in which the fields are differentially fated territories.

The derivatives of the proposed DT fields have not been established with fate mapping techniques. The vast majority of data to support the TPM derives from comparative gene expression studies, which are fundamentally insufficient for fate mapping. Gene expression is dynamic during development, and therefore cannot be used to follow cell populations from their birth through their migration to an adult structure. Importantly, DT structures are assembled from diverse cell types that can arise from different progenitor populations. No DT structure can be a

derivative of any single DT progenitor field because, for example, all DT structures contain inhibitory interneurons derived from the ventral telencephalon. All DT structures also contain glial cells from multiple disparate telencephalic origins (Rowitch and Kriegstein 2010). Only a recognition of cell types as biological units can resolve this problem.

The third premise, that adult derivatives of the same developmental field in different species are homologous, is possibly the most problematic. I can perceive no logical, biological, or experimental reason to accept the idea that development from equivalent topological origins necessitates homology of derivatives. To my knowledge, such a narrow definition of homology has not been accepted with consensus in any field of evolutionary biology. Progenitor cells and differentiated neural cell types are different things, which express different genes, have different identities, and can have independent evolutionary histories. In other words, they are different characters. Homology of one does not depend upon the other, nor does homology critically depend on a lineal relationship of characters. The developmental origin of a character is just one of many potential, and evolutionarily labile, character traits to be weighed in order to infer homology (Dugas-Ford and Ragsdale 2015).

3) The TPM ignores neural connections and function. The avian nidopallium contains cell populations that receive primary sensory input and express conserved markers (*KCNH5*, *RORA*, *RORB*, and *SATB1*) of neocortical L4. I argue that these data support homology of primary sensory input cells. Proponents of the TPM, however, dismiss these data because "similarity of connections is irrelevant with regard to homology" (Puelles et al. 2016b). The TPM proposes that nidopallium is homologous to amygdala, meaning that similar sensory input connections evolved independently or were otherwise relocated across conserved DT sectors. This interpretation is not only unparsimonious, but is a fundamental misunderstanding of the

meaning of homology. Connections are not irrelevant to homology because no character trait is irrelevant to homology. Character traits are homologous if they are recognizably inherited from the same thing in their last common ancestor. Sensory input projections to DT are either homologous, or they are not. To state that they are irrelevant is to ignore the question entirely.

Organisms are selected for based upon whether they survive and reproduce. Gene expression patterns and progenitor domains are invisible to natural selection, which acts proximally upon behavior and indirectly upon the biological means of behavior production. We can imagine, as an analogy, a car selected for based upon its ability to continuously drive. We could hypothetically switch out individual components of the car in a piecemeal fashion so long as the car continuously maintains its ability to move. We can repaint the exterior, swap out seats, and install a new stereo. Over great evolutionary time, the car may barely resemble its ancestor. However, we may never be able to remove, even temporarily, essential engine components without stalling the car. I suggest that sensory pathways to the DT are essential components of the vertebrate engine. The telencephalon cannot do much without them, and neither can the animal. They evolved once, at least as early as the amniote LCA, and they were never lost. Far from irrelevant, connections are critical clues to the homology of brain parts because they create the behaviors visible to natural selection.

4) The TPM has limited explanatory power. The TPM is an excessively simplistic view of nervous system evolution that flattens the nuance of evolution and development into an arbitrary standard. A model that purports to solve all vertebrate brain homologies simultaneously may further have the harmful effect of inhibiting the formulation of productive questions for further research. By ignoring cell types and circuitries, the TPM fails to explain the striking similarities of amniote DT cell-type composition described throughout this thesis. The TPM

ignores the possibility of developmental innovation and fails to offer any explanation for the existence of distinct DT types and their patterns of variation.

I argued above that natural selection preserves brain organization only indirectly by selecting for adaptive behaviors. If connections and function are irrelevant to homology, as the authors of the TPM claim, it is unclear how natural selection could preserve, with absolute fidelity, the complete developmental Bauplan of every vertebrate. It is unclear why adult neural derivatives should evolve at all, or even be constrained, if natural selection "does not care" about the functional and behavioral output of the nervous system.

5) Gene expression data often do not support claims of the TPM. The four DT subdivisions of the TPM are defined by topological relationships and the conserved expression of several transcription factors. The transcription factor *EMX1* plays a crucial definitional role in the TPM. The ventral pallium, located intermediate to the lateral pallium and ventral telencephalon, is defined in part by its absence of *EMX1* expression (Fernandez et al. 1998). The ventral pallium is believed to include the mammalian amygdala, the avian nidopallium and arcopallium, the reptilian DVR, and olfactory cortex in all amniotes. Contrary to this claim, I demonstrated that olfactory cortex in mouse and alligator expresses *EMX1* (Chapter 5). As expected from mammalian and reptilian expression, avian olfactory cortex also expresses *EMX1* (Chapter 4, Figure 4.12) (Puelles et al. 2016b). Alligator arcopallium (Chapter 5) and avian arcopallium (Puelles et al. 2016b) express *EMX1* in some subnuclei. As pointed out previously (Dugas-Ford and Ragsdale 2015), fate mapping experiments in mouse show that nearly all DT excitatory neurons, including those in amygdala, are derived from *Emx1*(+) progenitors (Gorski et al. 2002). *DACH2* is the only known specific marker of nidopallium, and I determined that

mouse *Dach2* is expressed in the neocortex (Chapter 4). These data do not support the existence of a conserved ventral pallium developmental field.

Chicken *NR4A2* is similarly problematic. This gene was claimed to mark specifically the avian mesopallium and the mammalian claustrum/insula to support their homology as derivatives of lateral pallium (Puelles et al. 2016a). *Nr4a2* is not specific to mammalian claustrum, but is additionally expressed throughout deep layers of the neocortex (Puelles et al. 2016a). Likewise, chicken *NR4A2* is not specifically expressed in mesopallium. Instead, it marks a restricted subset of ventral mesopallium in addition to strong labeling in HA and other superficial DT cell populations of unknown homology (Puelles et al. 2016a). These complex expression patterns make *NR4A2* expression all but uninterpretable across species. Moreover, no single marker gene should ever be used to make such far-reaching conclusions. Chicken *NR4A2* expression is quite unlike the expression patterns of dozens of other mesopallium-specific genes described by us (Chapter 4) and by the Jarvis group (Jarvis et al. 2013). These genes are expressed throughout the entire mesopallium including both Md and Mv, and support the characterization of Md and Mv as containing a similar major cell type. *NR4A2* expression does not support the existence of a conserved lateral pallium developmental field.

The origin of dorsal telencephalon types

Mammals, reptiles, and birds each possess a distinct DT type. There could have been many possible DT types distributed across extant amniotes. Nonetheless, only a few DT types exist and they align with major radiations of extant amniotes defined by criteria completely independent of brain organization. Why, and how, do separate amniote groups have their own unique DT types? Classic neuroanatomists certainly recognized that vertebrate classes have distinct DT types. They approached this question by invoking the scala naturae: each group of

vertebrates has a DT type because the types represent stages of development leading to the human neocortex (Edinger et al. 1899). The scala naturae has been rejected by modern evolutionary science. However, the puzzle of DT types and their correlation with "vertebrate types" has not, to my knowledge, been given extensive consideration in modern comparative anatomical literature.

I argued above that selective pressure due to developmental constraints maintains quantitative variation within DT types (i.e. variational modalities). Only very rarely do major developmental innovations overcome these constraints to create a new, evolutionarily stable DT type. These events appear to have coincided with major evolutionary transitions leading to modern amniote groups. Rare transitions to new vertebrate classes may be the catalysts necessary to break free of the developmental constraints on DT organization. I propose the hypothesis that DT anatomy types are adaptations to the behavioral requirements of dramatically new anatomies and ecological niches that arise during major evolutionary transitions.

As the most structurally divergent part of the vertebrate brain, the DT is likely to contribute to species- or clade-specific behaviors. Major vertebrate transitions probably involved comprehensive changes to many aspects of behavior including predator/prey interactions, foraging, mating strategies, parenting, and other intraspecific social interactions. During great behavioral transitions, animals may need to process sensory information in novel ways in order to adaptively respond to their environment. Vertebrates often evolve ways to collect new types of information—such as electric sense in platypus, magnetoreception in birds, or infrared sense in snakes (Krubitzer 1998, Güntürkün 2017). Somatic innovations including tetrapod-type limbs and their later alteration to bird-type wings changed the way that animals move through the world. These new locomotor devices likely require very different neural control mechanisms

than their ancestral forms. New limb types may have required cascading changes throughout the nervous system to coordinate muscle groups for walking, running, or for flight. However, adaptation to radically new niches is clearly insufficient stimulus for the generation of novel DT types, as cetaceans (dolphins and whales) and chiroptera (bats) have secondarily adapted to marine and aerial environments without the loss of the neocortex. There is something exceptional, although presently undefined, about the developmental and genomic events that occurred during the origins of vertebrate classes.

The conceptual framework of topological relationships within a Bauplan may be useful for comparing the brains of closely related species, such as mammals to other mammals. However, the Bauplan, like everything else in biology, evolves. I argued that developmental innovations rearrange old DT cell types, resulting in new DT structural types, or new DT Bauplans. Homologies do not exist for many mammalian and avian DT structures; instead, we must recognize cell types and their circuitries as a more fundamental unit of organization. The evolutionary origins of the core DT cell types are unknown. DT cell types and the gene regulatory networks that control them have certainly been assembled over evolutionary time. Future studies will seek to identify these cell types in ever more distantly related animals, and they may not be present. Instead, we may only be able to recognize homologies at even lower levels of biological organization, such as fragments of gene regulatory networks or individual genes. The origin and diversification of vertebrate neuronal cell types is an underexplored biological and conceptual problem for future research.

Final comments

The goal of neuroscience is to understand how the brain creates behavior. In this light, the state of modern comparative neuroscience is primitive. So far, we know that different groups of vertebrates have dorsal telencephala with very different internal organizations. This thesis is a molecular exploration of the cell types and organization of the amniote dorsal telencephalon. I am interested in the telencephalon because it contributes to higher cognitive function. Some themes emerge from this and related comparative analyses: 1) amniotes have a common set of sensory pathways that target conserved DT input cells (Chapter 3); 2) sensory information of multiple distinct modalities is processed by conserved DT intratelencephalic cells (Chapter 4); and 3) the DT influences behavior through the action of conserved motor output cells (Dugas-Ford et al. 2012). I argued in Chapter 4 that the evolution of advanced cognitive abilities in large-brained mammals and birds correlates with selective expansion of homologous associational DT cell populations. In Chapter 5, I studied the alligator DT as an outgroup to mammals and to birds in order to form hypotheses about how DT cell types have been reorganized in independent amniote lineages. In Chapter 6, I argued that important remaining challenges include identifying the developmental mechanisms of DT anatomical innovation, and ascertaining how divergent neural architectures contribute to species-specific behavior, cognition, and adaptation.

REFERENCES

Abdel-Mannan, O., A. F. Cheung, and Z. Molnar (2008). "Evolution of cortical neurogenesis." Brain Res Bull **75**(2–4): 398–404.

Achermann, J. C., J. J. Meeks, and J. L. Jameson (2001). "Phenotypic spectrum of mutations in DAX-1 and SF-1." Mol Cell Endocrinol **185**(1–2): 17–25.

Adams, K. L., D. L. Rousso, J. A. Umbach, and B. G. Novitch (2015). "Foxp1-mediated programming of limb-innervating motor neurons from mouse and human embryonic stem cells." Nat Commun **6**: 6778.

Agarwala, S., T. A. Sanders, and C. W. Ragsdale (2001). "Sonic hedgehog control of size and shape in midbrain pattern formation." Science **291**(5511): 2147–2150.

Akashi, M. and T. Takumi (2005). "The orphan nuclear receptor RORalpha regulates circadian transcription of the mammalian core-clock Bmal1." Nat Struct Mol Biol **12**(5): 441–448.

Alcamo, E. A., L. Chirivella, M. Dautzenberg, G. Dobreva, I. Farinas, R. Grosschedl, and S. K. McConnell (2008). "Satb2 regulates callosal projection neuron identity in the developing cerebral cortex." Neuron **57**(3): 364–377.

Altman, J. and M. B. Carpenter (1961). "Fiber projections of the superior colliculus in the cat." J Comp Neurol **116**: 157–177.

Amamoto, R. and P. Arlotta (2013). "Reshaping the brain: direct lineage conversion in the nervous system." F1000Prime Rep **5**: 33.

Anderson, S. A., D. D. Eisenstat, L. Shi, and J. L. Rubenstein (1997). "Interneuron migration from basal forebrain to neocortex: Dependence on Dlx genes." Science **278**(5337): 474–476.

Arends, J. J. and H. P. Zeigler (1986). "Anatomical identification of an auditory pathway from a nucleus of the lateral lemniscal system to the frontal telencephalon (nucleus basalis) of the pigeon." Brain Res **398**(2): 375–381.

Arendt, D. (2008). "The evolution of cell types in animals: emerging principles from molecular studies." Nat Rev Genet **9**(11): 868–882.

Arendt, D., J. M. Musser, C. V. Baker, A. Bergman, C. Cepko, D. H. Erwin, M. Pavlicev, G. Schlosser, S. Widder, M. D. Laubichler, and G. P. Wagner (2016). "The origin and evolution of cell types." Nat Rev Genet **17**(12): 744–757.

Ariëns Kappers, C. U., G. C. Huber, and E. C. Crosby (1936). The comparative anatomy of the nervous system of vertebrates, including man. New York: Macmillan.

Arlotta, P. and O. Hobert (2015). "Homeotic transformations of neuronal cell identities." Trends Neurosci **38**(12): 751–762.

Arlotta, P., B. J. Molyneaux, J. Chen, J. Inoue, R. Kominami, and J. D. Macklis (2005). "Neuronal subtype-specific genes that control corticospinal motor neuron development in vivo." Neuron **45**(2): 207–221.

Assimacopoulos, S., E. A. Grove, and C. W. Ragsdale (2003). "Identification of a Pax6-dependent epidermal growth factor family signaling source at the lateral edge of the embryonic cerebral cortex." J Neurosci **23**(16): 6399–6403.

Assimacopoulos, S., T. Kao, N. P. Issa, and E. A. Grove (2012). "Fibroblast growth factor 8 organizes the neocortical area map and regulates sensory map topography." J Neurosci **32**(21): 7191–7201.

Atoji, Y. and M. R. Karim (2014). "Homology of the mesopallium in the adult chicken identified by gene expression of the neocortical marker cholecystokinin." Neurosci Lett **562**: 85–89.

Atoji, Y. and J. M. Wild (2009). "Afferent and efferent projections of the central caudal nidopallium in the pigeon (Columba livia)." J Comp Neurol **517**(3): 350–370.

Atoji, Y. and J. M. Wild (2012). "Afferent and efferent projections of the mesopallium in the pigeon (Columba livia)." J Comp Neurol **520**(4): 717–741.

Atoji, Y. and J. M. Wild (2014). "Efferent and afferent connections of the olfactory bulb and prepiriform cortex in the pigeon (Columba livia)." J Comp Neurol **522**(8): 1728–1752.

Auersperg, A. M., B. Szabo, A. M. von Bayern, and A. Kacelnik (2012). "Spontaneous innovation in tool manufacture and use in a Goffin's cockatoo." Curr Biol **22**(21): R903–904.

Balaban, C. D. (1978). "Structure of anterior dorsal ventricular ridge in a turtle (Pseudemys scripta elegans)." J Morphol **158**(3): 291–322.

Balakhonov, D. and J. Rose (2017). "Crows rival monkeys in cognitive capacity." Sci Rep **7**(1): 8809.

Balamotis, M. A., N. Tamberg, Y. J. Woo, J. Li, B. Davy, T. Kohwi-Shigematsu, and Y. Kohwi (2012). "Satb1 ablation alters temporal expression of immediate early genes and reduces dendritic spine density during postnatal brain development." Mol Cell Biol **32**(2): 333–347.

Bates, L. A., J. H. Poole, and R. W. Byrne (2008). "Elephant cognition." Curr Biol **18**(13): R544–546.

Belgard, T. G., J. F. Montiel, W. Z. Wang, F. Garcia-Moreno, E. H. Margulies, C. P. Ponting, and Z. Molnar (2013). "Adult pallium transcriptomes surprise in not reflecting predicted homologies across diverse chicken and mouse pallial sectors." Proc Natl Acad Sci U S A **110**(32): 13150–13155.

Bishop, K. M., J. L. Rubenstein, and D. D. O'Leary (2002). "Distinct actions of Emx1, Emx2, and Pax6 in regulating the specification of areas in the developing neocortex." J Neurosci **22**(17): 7627–7638.

Blanton, M. G., J. M. Shen, and A. R. Kriegstein (1987). "Evidence for the inhibitory neurotransmitter gamma-aminobutyric acid in aspiny and sparsely spiny nonpyramidal neurons of the turtle dorsal cortex." J Comp Neurol **259**(2): 277–297.

Blinkov, S. M. l. and I. a. I. Glezer (1968). The human brain in figures and tables: A quantitative handbook. New York: Basic Books.

Bolger, A. M., M. Lohse, and B. Usadel (2014). "Trimmomatic: A flexible trimmer for Illumina sequence data." Bioinformatics **30**(15): 2114–2120.

Bonke, B. A., D. Bonke, and H. Scheich (1979). "Connectivity of the auditory forebrain nuclei in the guinea fowl (Numida meleagris)." Cell Tissue Res **200**(1): 101–121.

Bons, N. and J. Oliver (1986). "Origin of the afferent connections to the parolfactory lobe in quail shown by retrograde labelling with a fluorescent neuron tracer." Exp Brain Res **63**(1): 125–134.

Boord, R. L. (1965). "Efferent projections of cochlear nuclei in the pigeon." Amer Zool **5**: 669.

Boukhtouche, F., M. Doulazmi, F. Frederic, I. Dusart, B. Brugg, and J. Mariani (2006a). "RORalpha, a pivotal nuclear receptor for Purkinje neuron survival and differentiation: From development to ageing." Cerebellum **5**(2): 97–104.

Boukhtouche, F., S. Janmaat, G. Vodjdani, V. Gautheron, J. Mallet, I. Dusart, and J. Mariani (2006b). "Retinoid-related orphan receptor alpha controls the early steps of Purkinje cell dendritic differentiation." J Neurosci **26**(5): 1531–1538.

Braford, M. R., Jr. (1972). "Ascending efferent tectal projections in the South American spectacled caiman." Anat Rec **172**: 275–276.

Brauth, S. E. and C. M. McHale (1988). "Auditory pathways in the budgerigar. II. Intratelencephalic pathways." Brain Behav Evol **32**(4): 193–207.

Britanova, O., S. Akopov, S. Lukyanov, P. Gruss, and V. Tarabykin (2005). "Novel transcription factor Satb2 interacts with matrix attachment region DNA elements in a tissue-specific manner and demonstrates cell-type-dependent expression in the developing mouse CNS." Eur J Neurosci **21**(3): 658–668.

Britanova, O., C. de Juan Romero, A. Cheung, K. Y. Kwan, M. Schwark, A. Gyorgy, T. Vogel, S. Akopov, M. Mitkovski, D. Agoston, N. Sestan, Z. Molnar, and V. Tarabykin (2008). "Satb2 is a postmitotic determinant for upper-layer neuron specification in the neocortex." Neuron **57**(3): 378–392.

Brodmann, K. a. G., L. J. (2006). Brodmann's localisation in the cerebral cortex. New York: Springer.

Bruce, L. L. and T. J. Neary (1995). "The limbic system of tetrapods: a comparative analysis of cortical and amygdalar populations." Brain Behav Evol **46**(4–5): 224–234.

Brusatte, S. L., J. K. O'Connor, and E. D. Jarvis (2015). "The Origin and Diversification of Birds." Curr Biol **25**(19): R888–898.

Butler, A. B. and W. Hodos (2005). Comparative vertebrate neuroanatomy: Evolution and adaptation. Hoboken, NJ: Wiley-Interscience.

Butler, A. B., A. Reiner, and H. J. Karten (2011). "Evolution of the amniote pallium and the origins of mammalian neocortex." Ann N Y Acad Sci **1225**: 14–27.

Butti, C., C. M. Janeway, C. Townshend, B. A. Wicinski, J. S. Reidenberg, S. H. Ridgway, C. C. Sherwood, P. R. Hof, and B. Jacobs (2015). "The neocortex of cetartiodactyls: I. A comparative Golgi analysis of neuronal morphology in the bottlenose dolphin (Tursiops truncatus), the minke whale (Balaenoptera acutorostrata), and the humpback whale (Megaptera novaeangliae)." Brain Struct Funct **220**(6): 3339–3368.

Cai, S., H. J. Han, and T. Kohwi-Shigematsu (2003). "Tissue-specific nuclear architecture and gene expression regulated by SATB1." Nat Genet **34**(1): 42–51.

Cai, S., C. C. Lee, and T. Kohwi-Shigematsu (2006). "SATB1 packages densely looped, transcriptionally active chromatin for coordinated expression of cytokine genes." Nat Genet **38**(11): 1278–1288.

Cairney, J. (1926). "A general survey of the forebrain of *Sphenodon punctatum*." J Comp Neurol **42**(2): 255–348.

Caronia-Brown, G., M. Yoshida, F. Gulden, S. Assimacopoulos, and E. A. Grove (2014). "The cortical hem regulates the size and patterning of neocortex." Development **141**(14): 2855–2865.

Carroll, S. B. (2008). "Evo-devo and an expanding evolutionary synthesis: A genetic theory of morphological evolution." Cell **134**(1): 25–36.

Chen, C. C., C. M. Winkler, A. R. Pfenning, and E. D. Jarvis (2013a). "Molecular profiling of the developing avian telencephalon: Regional timing and brain subdivision continuities." J Comp Neurol **521**(16): 3666–3701.

Chen, X. R., N. Heck, A. M. Lohof, C. Rochefort, M. P. Morel, R. Wehrle, M. Doulazmi, S. Marty, V. Cannaya, H. X. Avci, J. Mariani, L. Rondi-Reig, G. Vodjdani, R. M. Sherrard, C. Sotelo, and I. Dusart (2013b). "Mature Purkinje cells require the retinoic acid-related orphan receptor-alpha (RORalpha) to maintain climbing fiber mono-innervation and other adult characteristics." J Neurosci **33**(22): 9546–9562.

Cheung, A. F., A. A. Pollen, A. Tavare, J. DeProto, and Z. Molnar (2007). "Comparative aspects of cortical neurogenesis in vertebrates." J Anat **211**(2): 164–176.

Clark, J. M. and P. S. Ulinski (1984). "A Golgi study of the anterior dorsal ventricular ridge in the alligator, *Alligator mississippiensis*." J Morphol **179**: 153–174.

Close, J., H. Xu, N. De Marco Garcia, R. Batista-Brito, E. Rossignol, B. Rudy, and G. Fishell (2012). "Satb1 is an activity-modulated transcription factor required for the terminal differentiation and connectivity of medial ganglionic eminence-derived cortical interneurons." J Neurosci **32**(49): 17690–17705.

Colombo, M. and N. Broadbent (2000). "Is the avian hippocampus a functional homologue of the mammalian hippocampus?" Neurosci Biobehav Rev **24**(4): 465–484.

Cong, L., F. A. Ran, D. Cox, S. Lin, R. Barretto, N. Habib, P. D. Hsu, X. Wu, W. Jiang, L. A. Marraffini, and F. Zhang (2013). "Multiplex genome engineering using CRISPR/Cas systems." Science **339**(6121): 819–823.

Connors, B. W. and A. R. Kriegstein (1986). "Cellular physiology of the turtle visual cortex: Distinctive properties of pyramidal and stellate neurons." J Neurosci **6**(1): 164–177.

Cowan, W. M., L. Adamson, and T. P. Powell (1961). "An experimental study of the avian visual system." J Anat **95**: 545–563.

Crosby, E. C. (1917). "The forebrain of *Alligator mississippiensis*." J Comp Neurol **27**(3): 325–403.

Cubelos, B., C. G. Briz, G. M. Esteban-Ortega, and M. Nieto (2015). "Cux1 and Cux2 selectively target basal and apical dendritic compartments of layer II-III cortical neurons." Dev Neurobiol **75**(2): 163–172.

Cubelos, B., A. Sebastian-Serrano, L. Beccari, M. E. Calcagnotto, E. Cisneros, S. Kim, A. Dopazo, M. Alvarez-Dolado, J. M. Redondo, P. Bovolenta, C. A. Walsh, and M. Nieto (2010). "Cux1 and Cux2 regulate dendritic branching, spine morphology, and synapses of the upper layer neurons of the cortex." Neuron **66**(4): 523–535.

Darwin, C. (1859). On the origin of species by means of natural selection. London: J. Murray.

Darwin, C. (1871). The descent of man, and selection in relation to sex. London: J. Murray.

Dasen, J. S., A. De Camilli, B. Wang, P. W. Tucker, and T. M. Jessell (2008). "Hox repertoires for motor neuron diversity and connectivity gated by a single accessory factor, FoxP1." Cell **134**(2): 304–316.

Davidson, E. H. (2006). The regulatory genome: Gene regulatory networks in development and evolution. Burlington, MA: Academic.

Davis, R. J., M. Harding, Y. Moayedi, and G. Mardon (2008). "Mouse Dach1 and Dach2 are redundantly required for Mullerian duct development." Genesis **46**(4): 205–213.

Davis, R. J., W. Shen, Y. I. Sandler, T. A. Heanue, and G. Mardon (2001). "Characterization of mouse Dach2, a homologue of Drosophila dachshund." Mech Dev **102**(1-2): 169–179.

De la Rossa, A., C. Bellone, B. Golding, I. Vitali, J. Moss, N. Toni, C. Luscher, and D. Jabaudon (2013). "In vivo reprogramming of circuit connectivity in postmitotic neocortical neurons." Nat Neurosci **16**(2): 193–200.

Denaxa, M., M. Kalaitzidou, A. Garefalaki, A. Achimastou, R. Lasrado, T. Maes, and V. Pachnis (2012). "Maturation-promoting activity of SATB1 in MGE-derived cortical interneurons." Cell Rep **2**(5): 1351–1362.

Desan, P. H. (1988). "The organization of the cerebral cortex of the pond turtle, Pseudemys scripta elegans." PhD Dissertation, Harvard University.

Devanna, P. and S. C. Vernes (2014). "A direct molecular link between the autism candidate gene RORa and the schizophrenia candidate MIR137." Sci Rep **4**: 3994.

Diamond, I. T., M. Snyder, H. Killackey, J. Jane, and W. C. Hall (1970). "Thalamo-cortical projections in the tree shrew (Tupaia glis)." J Comp Neurol **139**(3): 273–306.

Ding, S., X. Wu, G. Li, M. Han, Y. Zhuang, and T. Xu (2005). "Efficient transposition of the piggyBac (PB) transposon in mammalian cells and mice." Cell **122**(3): 473–483.

Ding, S. L., J. J. Royall, S. M. Sunkin, L. Ng, B. A. Facer, P. Lesnar, A. Guillozet-Bongaarts, B. McMurray, A. Szafer, T. A. Dolbeare, A. Stevens, L. Tirrell, T. Benner, S. Caldejon, R. A. Dalley, N. Dee, C. Lau, J. Nyhus, M. Reding, Z. L. Riley, D. Sandman, E. Shen, A. van der Kouwe, A. Varjabedian, M. Write, L. Zollei, C. Dang, J. A. Knowles, C. Koch, J. W. Phillips, N. Sestan, P. Wohnoutka, H. R. Zielke, J. G. Hohmann, A. R. Jones, A. Bernard, M. J. Hawrylycz, P. R. Hof, B. Fischl, and E. S. Lein (2016). "Comprehensive cellular-resolution atlas of the adult human brain." J Comp Neurol **524**(16): 3127–3481.

Douglas, R. J. and K. A. Martin (2004). "Neuronal circuits of the neocortex." Annu Rev Neurosci **27**: 419–451.

Dubbeldam, J. L., C. S. Brauch, and A. Don (1981). "Studies on the somatotopy of the trigeminal system in the mallard, Anas platyrhynchos L. III. Afferents and organization of the nucleus basalis." J Comp Neurol **196**(3): 391–405.

Dubbeldam, J. L. and A. M. Visser (1987). "The organization of the nucleus basalis-neostriatum complex of the mallard (Anas platyrhynchos L.) and its connections with the archistriatum and the paleostriatum complex." Neuroscience **21**(2): 487–517.

Dugas-Ford, J. (2009). "A comparative molecular study of the amniote dorsal telencephalon." PhD Dissertation, University of Chicago.

Dugas-Ford, J. and C. W. Ragsdale (2015). "Levels of homology and the problem of neocortex." Annu Rev Neurosci **38**: 351–368.

Dugas-Ford, J., J. J. Rowell, and C. W. Ragsdale (2012). "Cell-type homologies and the origins of the neocortex." Proc Natl Acad Sci U S A **109**(42): 16974–16979.

Durward, A. (1930). "The cell masses in the forebrain of Sphenodon punctatum." J Anat **65**: 8–44.

Dussault, I., D. Fawcett, A. Matthyssen, J. A. Bader, and V. Giguere (1998). "Orphan nuclear receptor ROR alpha-deficient mice display the cerebellar defects of staggerer." Mech Dev **70**(1–2): 147–153.

Ebner, F. F. (1976). "The forebrain of reptiles and mammals." In Evolution of brain and behavior in vertebrates, edited by R. B. Masterton, M. E. Bitterman, C. B. G. Campbell, and N. Hotton, 147–167. New York: Wiley.

Economo, C. and L. C. Triarhou (2009). Cellular structure of the human cerebral cortex. Basel, Switzerland: Karger.

Economo, M. N., N. G. Clack, L. D. Lavis, C. R. Gerfen, K. Svoboda, E. W. Myers, and J. Chandrashekar (2016). "A platform for brain-wide imaging and reconstruction of individual neurons." Elife **5**: e10566.

Edinger, L., W. S. Hall, P. L. Holland, and E. P. Carlton (1899). The anatomy of the central nervous system of man and of vertebrates in general. Philadelphia: F.A. Davis Co.

Edinger, L., Wallenberg,. A., Holmes, G. (1903). "5. Das Vorderhirn der Vögel." In Untersuchungen über die vergleichende Anatomie des Gehirns.

Erzurumlu, R. S. and P. C. Kind (2001). "Neural activity: sculptor of 'barrels' in the neocortex." Trends Neurosci **24**(10): 589–595.

Fame, R. M., C. Dehay, H. Kennedy, and J. D. Macklis (2017). "Subtype-specific genes that characterize subpopulations of callosal projection neurons in mouse identify molecularly homologous populations in macaque cortex." Cereb Cortex **27**(3): 1817–1830.

Fame, R. M., J. L. MacDonald, S. L. Dunwoodie, E. Takahashi, and J. D. Macklis (2016). "Cited2 regulates neocortical layer II/III generation and somatosensory callosal projection neuron development and connectivity." J Neurosci **36**(24): 6403–6419.

Fame, R. M., J. L. MacDonald, and J. D. Macklis (2011). "Development, specification, and diversity of callosal projection neurons." Trends Neurosci **34**(1): 41–50.

Feldmeyer, D. (2012). "Excitatory neuronal connectivity in the barrel cortex." Front Neuroanat **6**: 24.

Ferguson, M. W. J. (1985). "Reproductive biology and embryology of the crocodilians." In Biology of the reptilia, edited by C. Gans, F. Billett, and P. F. A. Maderson, 329-492. New York: Wiley.

Fernandez, A. S., C. Pieau, J. Reperant, E. Boncinelli, and M. Wassef (1998). "Expression of the Emx-1 and Dlx-1 homeobox genes define three molecularly distinct domains in the telencephalon of mouse, chick, turtle and frog embryos: Implications for the evolution of telencephalic subdivisions in amniotes." Development **125**(11): 2099–2111.

Fitch, W. M. (2000). "Homology a personal view on some of the problems." Trends Genet **16**(5): 227–231.

Flechsig, P. (1901). "Developmental (myelogenetic) localisation of the cerebral cortex in the human subject." Lancet **2**: 1027–1029.

Florio, M., M. Albert, E. Taverna, T. Namba, H. Brandl, E. Lewitus, C. Haffner, A. Sykes, F. K. Wong, J. Peters, E. Guhr, S. Klemroth, K. Prufer, J. Kelso, R. Naumann, I. Nusslein, A. Dahl, R. Lachmann, S. Paabo, and W. B. Huttner (2015). "Human-specific gene ARHGAP11B promotes basal progenitor amplification and neocortex expansion." Science **347**(6229): 1465–1470.

Florio, M., V. Borrell, and W. B. Huttner (2017). "Human-specific genomic signatures of neocortical expansion." Curr Opin Neurobiol **42**: 33–44.

Florio, M., T. Namba, S. Paabo, M. Hiller, and W. B. Huttner (2016). "A single splice site mutation in human-specific ARHGAP11B causes basal progenitor amplification." Sci Adv **2**(12): e1601941.

Franco, S. J., C. Gil-Sanz, I. Martinez-Garay, A. Espinosa, S. R. Harkins-Perry, C. Ramos, and U. Muller (2012). "Fate-restricted neural progenitors in the mammalian cerebral cortex." Science **337**(6095): 746–749.

Franco, S. J. and U. Muller (2013). "Shaping our minds: stem and progenitor cell diversity in the mammalian neocortex." Neuron **77**(1): 19–34.

Fukuchi-Shimogori, T. and E. A. Grove (2001). "Neocortex patterning by the secreted signaling molecule FGF8." Science **294**(5544): 1071–1074.

Funke, K. (1989a). "Somatosensory areas in the telencephalon of the pigeon. I. Response characteristics." Exp Brain Res **76**(3): 603–619.

Funke, K. (1989b). "Somatosensory areas in the telencephalon of the pigeon. II. Spinal pathways and afferent connections." Exp Brain Res **76**(3): 620–638.

Garcia-Moreno, F. and Z. Molnar (2015). "Subset of early radial glial progenitors that contribute to the development of callosal neurons is absent from avian brain." Proc Natl Acad Sci U S A **112**(36): E5058–5067.

Gehrke, A. R. and N. H. Shubin (2016). "Cis-regulatory programs in the development and evolution of vertebrate paired appendages." Semin Cell Dev Biol **57**: 31–39.

Gil-Sanz, C., A. Espinosa, S. P. Fregoso, K. K. Bluske, C. L. Cunningham, I. Martinez-Garay, H. Zeng, S. J. Franco, and U. Muller (2015). "Lineage Tracing Using Cux2-Cre and Cux2-CreERT2 Mice." Neuron **86**(4): 1091–1099.

Gilbert, C. D. and J. P. Kelly (1975). "The projections of cells in different layers of the cat's visual cortex." J Comp Neurol **163**(1): 81–105.

Gilbert, S. F. and M. J. F. Barresi (2016). Developmental biology. Sunderland, Massachusetts: Sinauer Associates, Inc.

Goffinet, A. M., C. Daumerie, B. Langerwerf, and C. Pieau (1986). "Neurogenesis in reptilian cortical structures: 3H-thymidine autoradiographic analysis." J Comp Neurol **243**(1): 106–116.

Gorski, J. A., T. Talley, M. Qiu, L. Puelles, J. L. Rubenstein, and K. R. Jones (2002). "Cortical excitatory neurons and glia, but not GABAergic neurons, are produced in the Emx1-expressing lineage." J Neurosci **22**(15): 6309–6314.

Green, R. E., E. L. Braun, J. Armstrong, D. Earl, N. Nguyen, G. Hickey, M. W. Vandewege, J. A. St John, S. Capella-Gutierrez, T. A. Castoe, C. Kern, M. K. Fujita, J. C. Opazo, J. Jurka, K. K. Kojima, J. Caballero, R. M. Hubley, A. F. Smit, R. N. Platt, C. A. Lavoie, M. P. Ramakodi, J. W. Finger, Jr., A. Suh, S. R. Isberg, L. Miles, A. Y. Chong, W. Jaratlerdsiri, J. Gongora, C. Moran, A. Iriarte, J. McCormack, S. C. Burgess, S. V. Edwards, E. Lyons, C. Williams, M. Breen, J. T. Howard, C. R. Gresham, D. G. Peterson, J. Schmitz, D. D. Pollock, D. Haussler, E. W. Triplett, G. Zhang, N. Irie, E. D. Jarvis, C. A. Brochu, C. J. Schmidt, F. M. McCarthy, B. C. Faircloth, F. G. Hoffmann, T. C. Glenn, T. Gabaldon, B. Paten, and D. A. Ray (2014). "Three crocodilian genomes reveal ancestral patterns of evolution among archosaurs." Science **346**(6215): 1254449.

Greig, L. C., M. B. Woodworth, M. J. Galazo, H. Padmanabhan, and J. D. Macklis (2013). "Molecular logic of neocortical projection neuron specification, development and diversity." Nat Rev Neurosci **14**(11): 755–769.

Grillner, S. and B. Robertson (2016). "The basal ganglia over 500 million years." Curr Biol **26**(20): R1088–R1100.

Grove, E. A., S. Tole, J. Limon, L. Yip, and C. W. Ragsdale (1998). "The hem of the embryonic cerebral cortex is defined by the expression of multiple Wnt genes and is compromised in Gli3-deficient mice." Development **125**(12): 2315–2325.

Güntürkün, O., Stacho, M., Ströckens, F. (2017). "The brains of reptiles and birds." In Evolution of nervous systems, edited by J. Kaas. Oxford, UK: Elsevier.

Guo, C., M. J. Eckler, W. L. McKenna, G. L. McKinsey, J. L. Rubenstein, and B. Chen (2013). "Fezf2 expression identifies a multipotent progenitor for neocortical projection neurons, astrocytes, and oligodendrocytes." Neuron **80**(5): 1167–1174.

Gyorgy, A. B., M. Szemes, C. de Juan Romero, V. Tarabykin, and D. V. Agoston (2008). "SATB2 interacts with chromatin-remodeling molecules in differentiating cortical neurons." Eur J Neurosci **27**(4): 865–873.

Haas, B. J., A. Papanicolaou, M. Yassour, M. Grabherr, P. D. Blood, J. Bowden, M. B. Couger, D. Eccles, B. Li, M. Lieber, M. D. MacManes, M. Ott, J. Orvis, N. Pochet, F. Strozzi, N. Weeks, R. Westerman, T. William, C. N. Dewey, R. Henschel, R. D. LeDuc, N. Friedman, and A. Regev (2013). "De novo transcript sequence reconstruction from RNA-seq using the Trinity platform for reference generation and analysis." Nat Protoc **8**(8): 1494–1512.

Hall, W. C. and F. F. Ebner (1970a). "Parallels in the visual afferent projections of the thalamus in the hedgehog (Paraechinus hypomelas) and the turtle (Pseudemys scripta)." Brain Behav Evol **3**(1): 135–154.

Hall, W. C. and F. F. Ebner (1970b). "Thalamotelencephalic projections in the turtle (Pseudemys scripta)." J Comp Neurol **140**(1): 101–122.

Hammond, K. L., I. M. Hanson, A. G. Brown, L. A. Lettice, and R. E. Hill (1998). "Mammalian and Drosophila dachshund genes are related to the Ski proto-oncogene and are expressed in eye and limb." Mech Dev **74**(1-2): 121–131.

Harris, J. A., K. E. Hirokawa, S. A. Sorensen, H. Gu, M. Mills, L. L. Ng, P. Bohn, M. Mortrud, B. Ouellette, J. Kidney, K. A. Smith, C. Dang, S. Sunkin, A. Bernard, S. W. Oh, L. Madisen, and H. Zeng (2014). "Anatomical characterization of Cre driver mice for neural circuit mapping and manipulation." Front Neural Circuits **8**: 76.

Harris, K. D. and G. M. Shepherd (2015). "The neocortical circuit: Themes and variations." Nat Neurosci **18**(2): 170–181.

Hasan, K. B., S. Agarwala, and C. W. Ragsdale (2010). "PHOX2A regulation of oculomotor complex nucleogenesis." Development **137**(7): 1205–1213.

Herculano-Houzel, S. (2016). The human advantage: A new understanding of how our brain became remarkable. Cambridge, MA: MIT Press.

Herculano-Houzel, S., K. Catania, P. R. Manger, and J. H. Kaas (2015). "Mammalian brains are made of these: A dataset of the numbers and densities of neuronal and nonneuronal cells in the brain of glires, primates, scandentia, eulipotyphlans, afrotherians and artiodactyls, and their relationship with body mass." Brain, Behavior and Evolution **86**(3–4): 145–163.

Herkenham, M. (1980). "Laminar organization of thalamic projections to the rat neocortex." Science **207**(4430): 532–535.

Herrick, C. L. (1890). "Notes upon the brain of the alligator." J Cincinnati Soc Nat Hist **12**: 129–162.

Hevner, R. F. (2016). "Evolution of the mammalian dentate gyrus." J Comp Neurol **524**(3): 578–594.

Hevner, R. F., R. A. Daza, J. L. Rubenstein, H. Stunnenberg, J. F. Olavarria, and C. Englund (2003). "Beyond laminar fate: Toward a molecular classification of cortical projection/pyramidal neurons." Dev Neurosci **25**(2–4): 139–151.

Hisaoka, T., Y. Nakamura, E. Senba, and Y. Morikawa (2010). "The forkhead transcription factors, Foxp1 and Foxp2, identify different subpopulations of projection neurons in the mouse cerebral cortex." Neuroscience **166**(2): 551–563.

Hobert, O. (2008). "Regulatory logic of neuronal diversity: Terminal selector genes and selector motifs." Proc Natl Acad Sci U S A **105**(51): 20067–20071.

Hobert, O. (2011). "Regulation of terminal differentiation programs in the nervous system." Annu Rev Cell Dev Biol **27**: 681–696.

Hobert, O. (2016). "Terminal selectors of neuronal identity." Curr Top Dev Biol **116**: 455–475.

Holmgren, N. (1925). "Points of view concerning forebrain morphology in higher vertebrates." Acta Zool **6**(3): 413–459.

Horn, G. (1985). Memory, imprinting, and the brain: An inquiry into mechanisms. Oxford, UK: Clarendon Press.

Hoyle, C., V. Narvaez, G. Alldus, R. Lovell-Badge, and A. Swain (2002). "Dax1 expression is dependent on steroidogenic factor 1 in the developing gonad." Mol Endocrinol **16**(4): 747–756.

Hu, V. W., T. Sarachana, R. M. Sherrard, and K. M. Kocher (2015). "Investigation of sex differences in the expression of RORA and its transcriptional targets in the brain as a potential contributor to the sex bias in autism." Mol Autism **6**: 7.

Huang, Y., L. Zhang, N. N. Song, Z. L. Hu, J. Y. Chen, and Y. Q. Ding (2011). "Distribution of Satb1 in the central nervous system of adult mice." Neurosci Res **71**(1): 12–21.

Huber, G. C., Crosby, E.C. (1926). "On thalamic and tectal nuclei and fiber paths in the brain of the American alligator." J Comp Neurol **40**(1): 97–227.

Huber, G. C., Crosby, E.C. (1929). "The nuclei and fiber paths of the avian diencephalon, with consideration of telencephalic and certain mesencephalic centers and connections." J Comp Neurol **48**(1): 1–225.

Inoue, K., T. Terashima, T. Nishikawa, and T. Takumi (2004). "Fez1 is layer-specifically expressed in the adult mouse neocortex." Eur J Neurosci **20**(11): 2909–2916.

Iwaniuk, A. N., K. M. Dean, and J. E. Nelson (2005). "Interspecific allometry of the brain and brain regions in parrots (psittaciformes): Comparisons with other birds and primates." Brain Behav Evol **65**(1): 40–59.

Jabaudon, D., S. J. Shnider, D. J. Tischfield, M. J. Galazo, and J. D. Macklis (2012). "RORβ induces barrel-like neuronal clusters in the developing neocortex." Cereb Cortex **22**(5): 996–1006.

Jacobs, B., J. Lubs, M. Hannan, K. Anderson, C. Butti, C. C. Sherwood, P. R. Hof, and P. R. Manger (2011). "Neuronal morphology in the African elephant (Loxodonta africana) neocortex." Brain Struct Funct **215**(3–4): 273–298.

Jarvis, E. D. (2004). "Learned birdsong and the neurobiology of human language." Ann N Y Acad Sci **1016**: 749–777.

Jarvis, E. D. and C. V. Mello (2000). "Molecular mapping of brain areas involved in parrot vocal communication." J Comp Neurol **419**(1): 1–31.

Jarvis, E. D., S. Mirarab, A. J. Aberer, B. Li, P. Houde, C. Li, S. Y. Ho, B. C. Faircloth, B. Nabholz, J. T. Howard, A. Suh, C. C. Weber, R. R. da Fonseca, J. Li, F. Zhang, H. Li, L. Zhou, N. Narula, L. Liu, G. Ganapathy, B. Boussau, M. S. Bayzid, V. Zavidovych, S. Subramanian, T. Gabaldon, S. Capella-Gutierrez, J. Huerta-Cepas, B. Rekepalli, K. Munch, M. Schierup, B. Lindow, W. C. Warren, D. Ray, R. E. Green, M. W. Bruford, X. Zhan, A. Dixon, S. Li, N. Li, Y. Huang, E. P. Derryberry, M. F. Bertelsen, F. H. Sheldon, R. T. Brumfield, C. V. Mello, P. V. Lovell, M. Wirthlin, M. P. Schneider, F. Prosdocimi, J. A. Samaniego, A. M. Vargas Velazquez, A. Alfaro-Nunez, P. F. Campos, B. Petersen, T. Sicheritz-Ponten, A. Pas, T. Bailey, P. Scofield, M. Bunce, D. M. Lambert, Q. Zhou, P. Perelman, A. C. Driskell, B. Shapiro, Z. Xiong, Y. Zeng, S. Liu, Z. Li, B. Liu, K. Wu, J. Xiao, X. Yinqi, Q. Zheng, Y. Zhang, H. Yang, J. Wang, L. Smeds, F. E. Rheindt, M. Braun, J. Fjeldsa, L. Orlando, F. K. Barker, K. A. Jonsson, W. Johnson, K. P. Koepfli, S. O'Brien, D. Haussler, O. A. Ryder, C. Rahbek, E. Willerslev, G. R. Graves, T. C. Glenn, J. McCormack, D. Burt, H. Ellegren, P. Alstrom, S. V. Edwards, A. Stamatakis, D. P. Mindell, J. Cracraft, E. L. Braun, T. Warnow, W. Jun, M. T. Gilbert and G. Zhang (2014). "Whole-genome analyses resolve early branches in the tree of life of modern birds." Science **346**(6215): 1320–1331.

Jarvis, E. D., J. Yu, M. V. Rivas, H. Horita, G. Feenders, O. Whitney, S. C. Jarvis, E. R. Jarvis, L. Kubikova, A. E. Puck, C. Siang-Bakshi, S. Martin, M. McElroy, E. Hara, J. Howard, A. Pfenning, H. Mouritsen, C. C. Chen, and K. Wada (2013). "Global view of the functional molecular organization of the avian cerebrum: Mirror images and functional columns." J Comp Neurol **521**(16): 3614–3665.

Jetten, A. M., S. Kurebayashi, and E. Ueda (2001). "The ROR nuclear orphan receptor subfamily: Critical regulators of multiple biological processes." Prog Nucleic Acid Res Mol Biol **69**: 205–247.

Johnson, M. H. and G. Horn (1987). "The role of a restricted region of the chick forebrain in the recognition of individual conspecifics." Behav Brain Res **23**(3): 269–275.

Johnston, J. B. (1915). "The cell masses in the forebrain of the turtle, Cistudo carolina." J Comp Neurol **25**(5): 393–468.

Jones, E. G. and S. P. Wise (1977). "Size, laminar and columnar distribution of efferent cells in the sensory-motor cortex of monkeys." J Comp Neurol **175**(4): 391–438.

Kalebic, N., E. Taverna, S. Tavano, F. K. Wong, D. Suchold, S. Winkler, W. B. Huttner, and M. Sarov (2016). "CRISPR/Cas9-induced disruption of gene expression in mouse embryonic brain and single neural stem cells in vivo." EMBO Rep **17**(3): 338–348.

Kalischer, O. (1905). Das Grosshirn der Papageien in anatomischer und physiologischer Beziehung. Berlin: Akad. d. Wissensch.

Kandel, E. R. (2013). Principles of neural science. New York: McGraw-Hill.

Karten, H. J. (1967). "The organization of the ascending auditory pathway in the pigeon (Columba livia). I. Diencephalic projections of the inferior colliculus (nucleus mesencephali lateralis, pars dorsalis)." Brain Res **6**(3): 409–427.

Karten, H. J. (1968). "The ascending auditory pathway in the pigeon (Columba livia). II. Telencephalic projections of the nucleus ovoidalis thalami." Brain Res **11**(1): 134–153.

Karten, H. J. (1969). "The organization of the avian telencephalon and some speculations on the phylogeny of the amniote telencephalon." Ann N Y Acad Sci **167**: 164–179.

Karten, H. J. (1971). "Efferent projections of the Wulst of the owl." Anat Rec **169**: 353.

Karten, H. J. (1997). "Evolutionary developmental biology meets the brain: The origins of mammalian cortex." Proc Natl Acad Sci U S A **94**(7): 2800–2804.

Karten, H. J. (2015). "Vertebrate brains and evolutionary connectomics: On the origins of the mammalian 'neocortex'." Philos Trans R Soc Lond B Biol Sci **370**(1684).

Karten, H. J. and W. Hodos (1970). "Telencephalic projections of the nucleus rotundus in the pigeon (Columba livia)." J Comp Neurol **140**(1): 35–51.

Karten, H. J., W. Hodos, W. J. Nauta, and A. M. Revzin (1973). "Neural connections of the "visual wulst" of the avian telencephalon. Experimental studies in the piegon (Columba livia) and owl (Speotyto cunicularia)." J Comp Neurol **150**(3): 253–278.

Karten, H. J. and A. M. Revzin (1966). "The afferent connections of the nucleus rotundus in the pigeon." Brain Res **2**(4): 368–377.

Kasthuri, N., K. J. Hayworth, D. R. Berger, R. L. Schalek, J. A. Conchello, S. Knowles-Barley, D. Lee, A. Vazquez-Reina, V. Kaynig, T. R. Jones, M. Roberts, J. L. Morgan, J. C. Tapia, H. S. Seung, W. G. Roncal, J. T. Vogelstein, R. Burns, D. L. Sussman, C. E. Priebe, H. Pfister, and J. W. Lichtman (2015). "Saturated reconstruction of a volume of neocortex." Cell **162**(3): 648–661.

Kim, E. J., A. L. Juavinett, E. M. Kyubwa, M. W. Jacobs, and E. M. Callaway (2015). "Three types of cortical layer 5 neurons that differ in brain-wide connectivity and function." Neuron **88**(6): 1253–1267.

Kiritooshi, N., T. Yorimitsu, T. Shirai, O. R. Puli, A. Singh, and H. Nakagoshi (2014). "A vertex specific dorsal selector Dve represses the ventral appendage identity in Drosophila head." Mech Dev **133**: 54–63.

Kirsch, J. A., O. Gunturkun, and J. Rose (2008). "Insight without cortex: :essons from the avian brain." Conscious Cogn **17**(2): 475–483.

Kohwi-Shigematsu, T., Y. Kohwi, K. Takahashi, H. W. Richards, S. D. Ayers, H. J. Han, and S. Cai (2012). "SATB1-mediated functional packaging of chromatin into loops." Methods **58**(3): 243–254.

Korzeniewska, E. and O. Gunturkun (1990). "Sensory properties and afferents of the N. dorsolateralis posterior thalami of the pigeon." J Comp Neurol **292**(3): 457–479.

Kratsios, P., A. Stolfi, M. Levine, and O. Hobert (2011). "Coordinated regulation of cholinergic motor neuron traits through a conserved terminal selector gene." Nat Neurosci **15**(2): 205–214.

Krubitzer, L. (1998). "What can monotremes tell us about brain evolution?" Philos Trans R Soc Lond B Biol Sci **353**(1372): 1127–1146.

Krubitzer, L. (2007). "The magnificent compromise: Cortical field evolution in mammals." Neuron **56**(2): 201–208.

Krubitzer, L. A. and A. M. Seelke (2012). "Cortical evolution in mammals: The bane and beauty of phenotypic variability." Proc Natl Acad Sci U S A **109 Suppl 1**: 10647–10654.

Kruger, L. and E. C. Berkowitz (1960). "The main afferent connections of the reptilian telencephalon as determined by degeneration and electrophysiological methods." J Comp Neurol **115**: 125–141.

Krutzfeldt, N. O. and J. M. Wild (2004). "Definition and connections of the entopallium in the zebra finch (Taeniopygia guttata)." J Comp Neurol **468**(3): 452–465.

Krutzfeldt, N. O. and J. M. Wild (2005). "Definition and novel connections of the entopallium in the pigeon (Columba livia)." J Comp Neurol **490**(1): 40–56.

Kunzle, H. (1985). "The cerebellar and vestibular nuclear complexes in the turtle. II. Projections to the prosencephalon." J Comp Neurol **242**(1): 122–133.

Li, X., E. A. Monckton, and R. Godbout (2014). "Ectopic expression of transcription factor AP-2delta in developing retina: Effect on PSA-NCAM and axon routing." J Neurochem **129**(1): 72–84.

Logue, M. W., C. Baldwin, G. Guffanti, E. Melista, E. J. Wolf, A. F. Reardon, M. Uddin, D. Wildman, S. Galea, K. C. Koenen, and M. W. Miller (2013). "A genome-wide association study of post-traumatic stress disorder identifies the retinoid-related orphan receptor alpha (RORA) gene as a significant risk locus." Mol Psychiatry **18**(8): 937–942.

Lohman, A. H. and G. M. Mentink (1972). "Some cortical connections of the Tegu lizard (Tupinambis teguixin)." Brain Res **45**(2): 325–344.

Lorente de Nó, R. (1922). "La corteza cereral del ratón." Trabajos Cajal Madrid **20**: 41–80.

Lorente de Nó, R. (1938). "Architectonics and structure of the cerebral cortex." In Physiology of the nervous system, edited by J. F. Fulton, 291–330. London: Oxford University Press.

Love, A. C. (2015). "ChINs, swarms, and variational modalities: concepts in the service of an evolutionary research program." Biology & Philosophy **30**(6): 873–888.

Lowe, S. R., J. L. Meyers, S. Galea, A. E. Aiello, M. Uddin, D. E. Wildman, and K. C. Koenen (2015). "RORA and posttraumatic stress trajectories: Main effects and interactions with childhood physical abuse history." Brain Behav **5**(4): e00323.

Lui, J. H., D. V. Hansen, and A. R. Kriegstein (2011). "Development and evolution of the human neocortex." Cell **146**(1): 18–36.

Lund, J. S., R. D. Lund, A. E. Hendrickson, A. H. Bunt, and A. F. Fuchs (1975). "The origin of efferent pathways from the primary visual cortex, area 17, of the macaque monkey as shown by retrograde transport of horseradish peroxidase." J Comp Neurol **164**(3): 287–303.

Macosko, E. Z., A. Basu, R. Satija, J. Nemesh, K. Shekhar, M. Goldman, I. Tirosh, A. R. Bialas, N. Kamitaki, E. M. Martersteck, J. J. Trombetta, D. A. Weitz, J. R. Sanes, A. K. Shalek, A. Regev, and S. A. McCarroll (2015). "Highly parallel genome-wide expression profiling of individual cells using nanoliter droplets." Cell **161**(5): 1202–1214.

Marin, O. and J. L. Rubenstein (2001). "A long, remarkable journey: Tangential migration in the telencephalon." Nat Rev Neurosci **2**(11): 780–790.

Marino, L. (2004). "Dolphin cognition." Curr Biol **14**(21): R910–911.

Marner, L., J. R. Nyengaard, Y. Tang, and B. Pakkenberg (2003). "Marked loss of myelinated nerve fibers in the human brain with age." J Comp Neurol **462**(2): 144–152.

Martinez-de-la-Torre, M., M. A. Pombal, and L. Puelles (2011). "Distal-less-like protein distribution in the larval lamprey forebrain." Neuroscience **178**: 270–284.

McCorrison, J. M., P. Venepally, I. Singh, D. E. Fouts, R. S. Lasken, and B. A. Methe (2014). "NeatFreq: Reference-free data reduction and coverage normalization for De Novo sequence assembly." BMC Bioinformatics **15**: 357.

Medina, L., A. Abellan, and E. Desfilis (2013). "A never-ending search for the evolutionary origin of the neocortex: Rethinking the homology concept." Brain Behav Evol **81**(3): 150–153.

Medina, L. and A. Reiner (2000). "Do birds possess homologues of mammalian primary visual, somatosensory and motor cortices?" Trends Neurosci **23**(1): 1–12.

Mi, H., X. Huang, A. Muruganujan, H. Tang, C. Mills, D. Kang, and P. D. Thomas (2017). "PANTHER version 11: Expanded annotation data from gene ontology and reactome pathways, and data analysis tool enhancements." Nucleic Acids Res **45**(D1): D183–D189.

Minami, R., M. Wakabayashi, S. Sugimori, K. Taniguchi, A. Kokuryo, T. Imano, T. Adachi-Yamada, N. Watanabe, and H. Nakagoshi (2012). "The homeodomain protein defective proventriculus is essential for male accessory gland development to enhance fecundity in Drosophila." PLoS One **7**(3): e32302.

Mitchelmore, C., K. M. Kjaerulff, H. C. Pedersen, J. V. Nielsen, T. E. Rasmussen, M. F. Fisker, B. Finsen, K. M. Pedersen, and N. A. Jensen (2002). "Characterization of two novel nuclear BTB/POZ domain zinc finger isoforms. Association with differentiation of hippocampal neurons, cerebellar granule cells, and macroglia." J Biol Chem **277**(9): 7598–7609.

Molnar, Z. and A. Pollen (2014). "How unique is the human neocortex?" Development **141**(1): 11–16.

Molyneaux, B. J., P. Arlotta, R. M. Fame, J. L. MacDonald, K. L. MacQuarrie, and J. D. Macklis (2009). "Novel subtype-specific genes identify distinct subpopulations of callosal projection neurons." J Neurosci **29**(39): 12343–12354.

Molyneaux, B. J., P. Arlotta, T. Hirata, M. Hibi, and J. D. Macklis (2005). "Fezl is required for the birth and specification of corticospinal motor neurons." Neuron **47**(6): 817–831.

Momose, T., A. Tonegawa, J. Takeuchi, H. Ogawa, K. Umesono, and K. Yasuda (1999). "Efficient targeting of gene expression in chick embryos by microelectroporation." Dev Growth Differ **41**(3): 335–344.

Mountcastle, V. B. (1957). "Modality and topographic properties of single neurons of cat's somatic sensory cortex." J Neurophysiol **20**(4): 408–434.

Mouritsen, H., G. Feenders, M. Liedvogel, K. Wada, and E. D. Jarvis (2005). "Night-vision brain area in migratory songbirds." Proc Natl Acad Sci U S A **102**(23): 8339–8344.

Nakagawa, Y. and D. D. O'Leary (2003). "Dynamic patterned expression of orphan nuclear receptor genes RORα and RORβ in developing mouse forebrain." Dev Neurosci **25**(2-4): 234–244.

Nakamori, T., K. Sato, Y. Atoji, T. Kanamatsu, K. Tanaka, and H. Ohki-Hamazaki (2010). "Demonstration of a neural circuit critical for imprinting behavior in chicks." J Neurosci **30**(12): 4467–4480.

Nakamura, T., A. R. Gehrke, J. Lemberg, J. Szymaszek, and N. H. Shubin (2016). "Digits and fin rays share common developmental histories." Nature **537**(7619): 225–228.

Naumann, R. K. a. L., G. (2017). "Function and evolution of the reptilian cerebral cortex." In Evolution of nervous systems, edited by J. H. Kaas. Oxford, UK: Elsevier Inc.

Nauta, W. J. H. and M. Feirtag (1986). Fundamental neuroanatomy. New York: W.H. Freeman.

Nielsen, J. V., F. H. Nielsen, R. Ismail, J. Noraberg, and N. A. Jensen (2007). "Hippocampus-like corticoneurogenesis induced by two isoforms of the BTB-zinc finger gene Zbtb20 in mice." Development **134**(6): 1133–1140.

Nieuwenhuys, R., H. J. t. Donkelaar, and C. Nicholson (1998). The central nervous system of vertebrates. New York: Springer.

Nieuwenhuys, R., J. Voogd, and C. v. Huijzen (2008). The human central nervous system. New York: Springer.

Nishimura, M., S. Suzuki, T. Satoh, and S. Naito (2009). "Tissue-specific mRNA expression profiles of human solute carrier 35 transporters." Drug Metab Pharmacokinet **24**(1): 91–99.

Northcutt, R. G. (1974). "Some histochemical observations on the telencephalon of the bullfrog, Rana catesbeiana Shaw." J Comp Neurol **157**(4): 379–389.

Northcutt, R. G. (1999). "Field homology: A meaningless concept." Eur J Morphol **37**(2-3): 95–99.

Northcutt, R. G. (2013). "Variation in reptilian brains and cognition." Brain Behav Evol **82**(1): 45–54.

Olkowicz, S., M. Kocourek, R. K. Lucan, M. Portes, W. T. Fitch, S. Herculano-Houzel, and P. Nemec (2016). "Birds have primate-like numbers of neurons in the forebrain." Proc Natl Acad Sci U S A **113**(26): 7255–7260.

Ouimet, C. C., A. S. LaMantia, P. Goldman-Rakic, P. Rakic, and P. Greengard (1992). "Immunocytochemical localization of DARPP-32, a dopamine and cyclic-AMP-regulated phosphoprotein, in the primate brain." J Comp Neurol **323**(2): 209–218.

Papez, J. W. (1936). "Evolution of the medial geniculate body." J. Comp. Neurol. **64**: 41–61.

Park, S. Y., J. J. Meeks, G. Raverot, L. E. Pfaff, J. Weiss, G. D. Hammer, and J. L. Jameson (2005). "Nuclear receptors Sf1 and Dax1 function cooperatively to mediate somatic cell differentiation during testis development." Development **132**(10): 2415–2423.

Patel, M. V., I. A. McKay, and J. M. Burrin (2001). "Transcriptional regulators of steroidogenesis, DAX-1 and SF-1, are expressed in human skin." J Invest Dermatol **117**(6): 1559–1565.

Pedelacq, J. D., S. Cabantous, T. Tran, T. C. Terwilliger, and G. S. Waldo (2006). "Engineering and characterization of a superfolder green fluorescent protein." Nat Biotechnol **24**(1): 79–88.

Pennisi, E. (2015). "Using evolution to better identify cell types." Science **350**(6261): 618–619.

Pepperberg, I. M. (1999). The Alex studies: Cognitive and communicative abilities of grey parrots. Cambridge, MA: Harvard University Press.

Pleasure, S. J., A. E. Collins, and D. H. Lowenstein (2000). "Unique expression patterns of cell fate molecules delineate sequential stages of dentate gyrus development." J Neurosci **20**(16): 6095–6105.

Prior, H., A. Schwarz, and O. Gunturkun (2008). "Mirror-induced behavior in the magpie (Pica pica): evidence of self-recognition." PLoS Biol **6**(8): e202.

Pritz, M. B. (1974a). "Ascending connections of a midbrain auditory area in a crocodile, Caiman crocodilus." J Comp Neurol **153**(2): 179–197.

Pritz, M. B. (1974b). "Ascending connections of a thalamic auditory area in a crocodile, caiman crocodilus." J Comp Neurol **153**(2): 199–213.

Pritz, M. B. (1975). "Anatomical identification of a telencephalic visual area in crocodiles: Ascending connections of nucleus rotundus in Caiman crocodilus." J Comp Neurol **164**(3): 323–338.

Pritz, M. B. and R. G. Northcutt (1977). "Succinate dehydrogenase activity in the telencephalon of crocodiles correlates with the projection areas of sensory thalamic nuclei." Brain Res **124**(2): 357–360.

Pritz, M. B. and R. G. Northcutt (1980). "Anatomical evidence for an ascending somatosensory pathway to the telencephalon in crocodiles, Caiman crocodilus." Exp Brain Res **40**(3): 342–345.

Puelles, L. (2001). "Thoughts on the development, structure and evolution of the mammalian and avian telencephalic pallium." Philos Trans R Soc Lond B Biol Sci **356**(1414): 1583–1598.

Puelles, L. (2007). The chick brain in stereotaxic coordinates: An atlas featuring neuromeric subdivisions and mammalian homologies. Boston, MA: Academic Press.

Puelles, L., A. Ayad, A. Alonso, J. E. Sandoval, M. MartInez-de-la-Torre, L. Medina, and J. L. Ferran (2016a). "Selective early expression of the orphan nuclear receptor Nr4a2 identifies the claustrum homolog in the avian mesopallium: Impact on sauropsidian/mammalian pallium comparisons." J Comp Neurol **524**(3): 665–703.

Puelles, L., E. Kuwana, E. Puelles, A. Bulfone, K. Shimamura, J. Keleher, S. Smiga, and J. L. Rubenstein (2000). "Pallial and subpallial derivatives in the embryonic chick and mouse telencephalon, traced by the expression of the genes Dlx-2, Emx-1, Nkx-2.1, Pax-6, and Tbr-1." J Comp Neurol **424**(3): 409–438.

Puelles, L., E. Kuwana, E. Puelles, and J. L. Rubenstein (1999). "Comparison of the mammalian and avian telencephalon from the perspective of gene expression data." Eur J Morphol **37**(2–3): 139–150.

Puelles, L. and L. Medina (2002). "Field homology as a way to reconcile genetic and developmental variability with adult homology." Brain Research Bulletin **57**(3): 243–255.

Puelles, L., J. E. Sandoval, A. Ayad, R. del Corral, A. Alonso, J. L. Ferran, and M. Martinez-de-la-Torre (2016b). "The pallium in reptiles and birds in the light of the updated tetrapartite pallium model." In Evolution of nervous systems, edited by J. Kaas. Oxford, UK: Elsevier Inc.

Rabl-Rückhard (1878). "Das centralnervensystem des alligators." Zeitsch wiss Zool **30**: 336–373.

Rakic, P. (2009). "Evolution of the neocortex: A perspective from developmental biology." Nat Rev Neurosci **10**(10): 724–735.

Rash, B. G. and E. A. Grove (2006). "Area and layer patterning in the developing cerebral cortex." Curr Opin Neurobiol **16**(1): 25–34.

Reese, A. M. (1915). The alligator and its allies. New York: Putnam.

Rehkamper, G., H. D. Frahm, and K. Zilles (1991). "Quantitative development of brain and brain structures in birds (galliformes and passeriformes) compared to that in mammals (insectivores and primates)." Brain Behav Evol **37**(3): 125–143.

Reiner, A. (1991). "A comparison of neurotransmitter-specific and neuropeptide-specific neuronal cell types present in the dorsal cortex in turtles with those present in the isocortex in mammals: Implications for the evolution of isocortex." Brain Behav Evol **38**(2–3): 53–91.

Reiner, A. (2013). "You are who you talk with--a commentary on Dugas-Ford et al. PNAS, 2012." Brain Behav Evol **81**(3): 146–149.

Reiner, A., N. M. Hart, W. Lei, and Y. Deng (2010). "Corticostriatal projection neurons - dichotomous types and dichotomous functions." Front Neuroanat **4**: 142.

Reiner, A., Y. Jiao, N. Del Mar, A. V. Laverghetta, and W. L. Lei (2003). "Differential morphology of pyramidal tract-type and intratelencephalically projecting-type corticostriatal neurons and their intrastriatal terminals in rats." J Comp Neurol **457**(4): 420–440.

Reiner, A. and H. J. Karten (1985). "Comparison of olfactory bulb projections in pigeons and turtles." Brain Behav Evol **27**(1): 11–27.

Reiner, A. and R. G. Northcutt (2000). "Succinic dehydrogenase histochemistry reveals the location of the putative primary visual and auditory areas within the dorsal ventricular ridge of Sphenodon punctatus." Brain Behav Evol **55**(1): 26–36.

Reiner, A., M. Perera, R. Paullus, and L. Medina (1998). "Immunohistochemical localization of DARPP32 in striatal projection neurons and striatal interneurons in pigeons." J Chem Neuroanat **16**(1): 17–33.

Reiner, A., D. J. Perkel, L. L. Bruce, A. B. Butler, A. Csillag, W. Kuenzel, L. Medina, G. Paxinos, T. Shimizu, G. Striedter, M. Wild, G. F. Ball, S. Durand, O. Gunturkun, D. W. Lee, C. V. Mello, A. Powers, S. A. White, G. Hough, L. Kubikova, T. V. Smulders, K. Wada, J. Dugas-Ford, S. Husband, K. Yamamoto, J. Yu, C. Siang, and E. D. Jarvis (2004a). "Revised nomenclature for avian telencephalon and some related brainstem nuclei." J Comp Neurol **473**(3): 377–414.

Reiner, A., D. J. Perkel, L. L. Bruce, A. B. Butler, A. Csillag, W. Kuenzel, L. Medina, G. Paxinos, T. Shimizu, G. Striedter, M. Wild, G. F. Ball, S. Durand, O. Guturkun, D. W. Lee, C. V. Mello, A. Powers, S. A. White, G. Hough, L. Kubikova, T. V. Smulders, K. Wada, J. Dugas-Ford, S. Husband, K. Yamamoto, J. Yu, C. Siang, and E. D. Jarvis (2004b). "The avian brain nomenclature forum: Terminology for a new century in comparative neuroanatomy." J Comp Neurol **473**: E1–E6.

Reiner, A., E. A. Stern, and C. J. Wilson (2001). "Physiology and morphology of intratelencephalically projecting corticostriatal-type neurons in pigeons as revealed by intracellular recording and cell filling." Brain Behav Evol **58**(2): 101–114.

Reiner, A., K. Yamamoto, and H. J. Karten (2005). "Organization and evolution of the avian forebrain." Anat Rec A Discov Mol Cell Evol Biol **287**(1): 1080–1102.

Reiner, A., M. Yang, M. C. Cagle, and M. G. Honig (2011). "Localization of cerebellin-2 in late embryonic chicken brain: Implications for a role in synapse formation and for brain evolution." J Comp Neurol **519**(11): 2225–2251.

Riss, W., M. Halpern, and F. Scalia (1969). "The quest for clues to forebrain evolution - The study of reptiles." Brain Behav Evol **2**: 1–50.

Rose, M. (1923). "Histologische Lokalisation des Vorderhirns der Reptilien." J Psychol Neurol **29**: 219–272.

Roth, G. (2015). "Convergent evolution of complex brains and high intelligence." Philos Trans R Soc Lond B Biol Sci **370**(1684).

Rouaux, C. and P. Arlotta (2010). "Fezf2 directs the differentiation of corticofugal neurons from striatal progenitors in vivo." Nat Neurosci **13**(11): 1345–1347.

Rouaux, C. and P. Arlotta (2013). "Direct lineage reprogramming of post-mitotic callosal neurons into corticofugal neurons in vivo." Nat Cell Biol **15**(2): 214–221.

Rowell, J. J. (2013). "The evolution and development of neocortical neurons." PhD, University of Chicago.

Rowell, J. J., A. K. Mallik, J. Dugas-Ford, and C. W. Ragsdale (2010). "Molecular analysis of neocortical layer structure in the ferret." J Comp Neurol **518**(16): 3272–3289.

Rowell, J. J. and C. W. Ragsdale (2012). "BrdU birth dating can produce errors in cell fate specification in chick brain development." J Histochem Cytochem **60**(11): 801–810.

Rowitch, D. H. and A. R. Kriegstein (2010). "Developmental genetics of vertebrate glial-cell specification." Nature **468**(7321): 214–222.

Rubenstein, J. L., S. Anderson, L. Shi, E. Miyashita-Lin, A. Bulfone, and R. Hevner (1999). "Genetic control of cortical regionalization and connectivity." Cereb Cortex **9**(6): 524–532.

Salzen, E. A., D. M. Parker, and A. J. Williamson (1975). "A forebrain lesion preventing imprinting in domestic chicks." Exp Brain Res **24**(2): 145–157.

Salzen, E. A., A. J. Williamson, and D. M. Parker (1979). "The effects of forebrain lesions on innate and imprinted colour, brightness and shape preferences in domestic chicks." Behav Processes **4**(4): 295–313.

Sarachana, T., M. Xu, R. C. Wu, and V. W. Hu (2011). "Sex hormones in autism: Androgens and estrogens differentially and reciprocally regulate RORA, a novel candidate gene for autism." PLoS One **6**(2): e17116.

Sato, T. K., S. Panda, L. J. Miraglia, T. M. Reyes, R. D. Rudic, P. McNamara, K. A. Naik, G. A. FitzGerald, S. A. Kay, and J. B. Hogenesch (2004). "A functional genomics strategy reveals RORA as a component of the mammalian circadian clock." Neuron **43**(4): 527–537.

Savarese, F., A. Davila, R. Nechanitzky, I. De La Rosa-Velazquez, C. F. Pereira, R. Engelke, K. Takahashi, T. Jenuwein, T. Kohwi-Shigematsu, A. G. Fisher, and R. Grosschedl (2009). "Satb1 and Satb2 regulate embryonic stem cell differentiation and Nanog expression." Genes Dev **23**(22): 2625–2638.

Scalia, F., M. Halpern, and W. Riss (1969). "Olfactory bulb projections in the south american caiman." Brain Behav Evol **2**: 238–262.

Schwerdtfeger, W. K. and M. J. Lorente (1988). "Laminar distribution and morphology of gamma-aminobutyric acid (GABA)-immunoreactive neurons in the medial and dorsomedial areas of the cerebral cortex of the lizard Podarcis hispanica." J Comp Neurol **278**(4): 473–485.

Shen, J. M. and A. R. Kriegstein (1986). "Turtle hippocampal cortex contains distinct cell types, burst-firing neurons, and an epileptogenic subfield." J Neurophysiol **56**(6): 1626–1649.

Shigeno, S., R. Parnaik, C. B. Albertin, and C. W. Ragsdale (2015). "Evidence for a cordal, not ganglionic, pattern of cephalopod brain neurogenesis." Zoological Lett **1**: 26.

Shimizu, T., K. Cox, and H. J. Karten (1995). "Intratelencephalic projections of the visual wulst in pigeons (Columba livia)." J Comp Neurol **359**(4): 551–572.

Shirai, T., T. Yorimitsu, N. Kiritooshi, F. Matsuzaki, and H. Nakagoshi (2007). "Notch signaling relieves the joint-suppressive activity of Defective proventriculus in the Drosophila leg." Dev Biol **312**(1): 147–156.

Shubin, N., C. Tabin, and S. Carroll (2009). "Deep homology and the origins of evolutionary novelty." Nature **457**(7231): 818–823.

Silbereis, J. C., S. Pochareddy, Y. Zhu, M. Li, and N. Sestan (2016). "The cellular and molecular landscapes of the developing human central nervous system." Neuron **89**(2): 248–268.

Simeone, A., D. Acampora, M. Gulisano, A. Stornaiuolo, and E. Boncinelli (1992a). "Nested expression domains of four homeobox genes in developing rostral brain." Nature **358**(6388): 687–690.

Simeone, A., M. Gulisano, D. Acampora, A. Stornaiuolo, M. Rambaldi, and E. Boncinelli (1992b). "Two vertebrate homeobox genes related to the Drosophila empty spiracles gene are expressed in the embryonic cerebral cortex." EMBO J **11**(7): 2541–2550.

Sohur, U. S., H. K. Padmanabhan, I. S. Kotchetkov, J. R. Menezes, and J. D. Macklis (2014). "Anatomic and molecular development of corticostriatal projection neurons in mice." Cereb Cortex **24**(2): 293–303.

Sousa, A. M. M., K. A. Meyer, G. Santpere, F. O. Gulden, and N. Sestan (2017). "Evolution of the human nervous system function, structure, and development." Cell **170**(2): 226–247.

Soussi-Yanicostas, N., J. P. Hardelin, M. M. Arroyo-Jimenez, O. Ardouin, R. Legouis, J. Levilliers, F. Traincard, J. M. Betton, L. Cabanie, and C. Petit (1996). "Initial characterization of anosmin-1, a putative extracellular matrix protein synthesized by definite neuronal cell populations in the central nervous system." J Cell Sci **109**(Pt 7): 1749–1757.

Stephan, H., H. Frahm, and G. Baron (1981). "New and revised data on volumes of brain structures in insectivores and primates." Folia Primatol (Basel) **35**(1): 1–29.

Stickels, R., K. Clark, T. N. Heider, D. M. Mattiske, M. B. Renfree, and A. J. Pask (2015). "DAX1/NR0B1 was expressed during mammalian gonadal development and gametogenesis before it was recruited to the eutherian X chromosome." Biol Reprod **92**(1): 22.

Stocker, A. M. and D. D. O'Leary (2016). "Emx1 is required for neocortical area patterning." PLoS One **11**(2): e0149900.

Striedter, G. F. (1997). "The telencephalon of tetrapods in evolution." Brain Behav Evol **49**(4): 179–213.

Striedter, G. F. (2005). Principles of brain evolution. Sunderland, MA: Sinauer Associates.

Striedter, G. F. (2006). "Precis of principles of brain evolution." Behav Brain Sci **29**(1): 1–12; discussion 12–36.

Striedter, G. F. (2016). "Evolution of the hippocampus in reptiles and birds." J Comp Neurol **524**(3): 496–517.

Sun, Z. and A. Reiner (2000). "Localization of dopamine D1A and D1B receptor mRNAs in the forebrain and midbrain of the domestic chick." J Chem Neuroanat **19**(4): 211–224.

Suzuki, I. K. and T. Hirata (2012). "Evolutionary conservation of neocortical neurogenetic program in the mammals and birds." Bioarchitecture **2**(4): 124–129.

Suzuki, I. K. and T. Hirata (2013). "Neocortical neurogenesis is not really "neo": A new evolutionary model derived from a comparative study of chick pallial development." Dev Growth Differ **55**(1): 173–187.

Suzuki, I. K., T. Kawasaki, T. Gojobori, and T. Hirata (2012). "The temporal sequence of the mammalian neocortical neurogenetic program drives mediolateral pattern in the chick pallium." Dev Cell **22**(4): 863–870.

Szele, F. G., H. K. Chin, M. A. Rowlson, and C. L. Cepko (2002). "Sox-9 and cDachsund-2 expression in the developing chick telencephalon." Mech Dev **112**(1–2): 179–182.

Szemes, M., A. Gyorgy, C. Paweletz, A. Dobi, and D. V. Agoston (2006). "Isolation and characterization of SATB2, a novel AT-rich DNA binding protein expressed in development- and cell-specific manner in the rat brain." Neurochem Res **31**(2): 237–246.

Talley, E. M., L. L. Cribbs, J. H. Lee, A. Daud, E. Perez-Reyes, and D. A. Bayliss (1999). "Differential distribution of three members of a gene family encoding low voltage-activated (T-type) calcium channels." J Neurosci **19**(6): 1895–1911.

Tarazona, O. A., L. A. Slota, D. H. Lopez, G. Zhang, and M. J. Cohn (2016). "The genetic program for cartilage development has deep homology within Bilateria." Nature **533**(7601): 86–89.

Tarlov, E. C. and R. Y. Moore (1966). "The tecto-thalamic connections in the brain of the rabbit." J Comp Neurol **126**(3): 403–435.

Ten Donkelaar, H. J. and R. De Boer-Van Huizen (1981). "Ascending projections of the brain stem reticular formation in a nonmammalian vertebrate (the lizard Varanus exanthematicus), with notes on the afferent connections of the forebrain." J Comp Neurol **200**(4): 501–528.

Thomson, A. M. and C. Lamy (2007). "Functional maps of neocortical local circuitry." Front Neurosci **1**(1): 19–42.

Toyoda, R., S. Assimacopoulos, J. Wilcoxon, A. Taylor, P. Feldman, A. Suzuki-Hirano, T. Shimogori, and E. A. Grove (2010). "FGF8 acts as a classic diffusible morphogen to pattern the neocortex." Development **137**(20): 3439–3448.

Trapnell, C., A. Roberts, L. Goff, G. Pertea, D. Kim, D. R. Kelley, H. Pimentel, S. L. Salzberg, J. L. Rinn, and L. Pachter (2012). "Differential gene and transcript expression analysis of RNA-seq experiments with TopHat and Cufflinks." Nat Protoc **7**(3): 562–578.

Ulinski, P. S. (1983). Dorsal ventricular ridge: A treatise on forebrain organization in reptiles and birds. New York: Wiley.

Ulinski, P. S. (1990a). "The cerebral cortex of reptiles." In Cerebral cortex, edited by E. G. Jones, Peters, A., 139–216. New York: Plenum Press.

Ulinski, P. S., Margoliash, D. (1990b). "Neurobiology of the reptile-bird transition." In Cerebral cortex, edited by E. G. Jones, Peters, A. New York: Plenum Press.

Unger, L. (1906). "Untersuchungun über die Morphologie und Faserung des Reptiliengehirns. II. Das Vorderhirn des Alligators." Sitzb. k. Akad. Wien.

Van Otterloo, E., W. Li, A. Garnett, M. Cattell, D. M. Medeiros, and R. A. Cornell (2012). "Novel Tfap2-mediated control of soxE expression facilitated the evolutionary emergence of the neural crest." Development **139**(4): 720–730.

Veenman, C. L. and K. M. Gottschaldt (1986). "The nucleus basalis-neostriatum complex in the goose (Anser anser L.)." Adv Anat Embryol Cell Biol **96**: 1–85.

Veenman, C. L., J. M. Wild, and A. Reiner (1995). "Organization of the avian "corticostriatal" projection system: A retrograde and anterograde pathway tracing study in pigeons." J Comp Neurol **354**(1): 87–126.

Veron, N., Z. Qu, P. A. Kipen, C. E. Hirst, and C. Marcelle (2015). "CRISPR mediated somatic cell genome engineering in the chicken." Dev Biol **407**(1): 68–74.

Wagner, G. n. P. (2014). Homology, genes, and evolutionary innovation. Princeton, NJ: Princeton University Press.

Wagner, G. P. (2007). "The developmental genetics of homology." Nat Rev Genet **8**(6): 473–479.

Wang, Z., M. Gerstein, and M. Snyder (2009). "RNA-Seq: A revolutionary tool for transcriptomics." Nat Rev Genet **10**(1): 57–63.

Watson, C. and L. Puelles (2017). "Developmental gene expression in the mouse clarifies the organization of the claustrum and related endopiriform nuclei." J Comp Neurol **525**(6): 1499–1508.

Weir, A. A., J. Chappell, and A. Kacelnik (2002). "Shaping of hooks in New Caledonian crows." Science **297**(5583): 981.

Wild, J. M. (1989). "Avian somatosensory system: II. Ascending projections of the dorsal column and external cuneate nuclei in the pigeon." J Comp Neurol **287**(1): 1–18.

Wild, J. M. (1997). "The avian somatosensory system: The pathway from wing to Wulst in a passerine (Chloris chloris)." Brain Res **759**(1): 122–134.

Wild, J. M. and S. M. Farabaugh (1996). "Organization of afferent and efferent projections of the nucleus basalis prosencephali in a passerine, Taeniopygia guttata." J Comp Neurol **365**(2): 306–328.

Wild, J. M., H. J. Karten, and B. J. Frost (1993). "Connections of the auditory forebrain in the pigeon (Columba livia)." J Comp Neurol **337**(1): 32–62.

Wild, J. M., M. F. Kubke, and C. E. Carr (2001). "Tonotopic and somatotopic representation in the nucleus basalis of the barn owl, Tyto alba." Brain Behav Evol **57**(1): 39–62.

Wild, J. M. and M. N. Williams (2000). "Rostral wulst in passerine birds. I. Origin, course, and terminations of an avian pyramidal tract." J Comp Neurol **416**(4): 429–450.

Wilson, C. J. (1987). "Morphology and synaptic connections of crossed corticostriatal neurons in the rat." J Comp Neurol **263**(4): 567–580.

Woodworth, M. B., L. C. Greig, K. X. Liu, G. C. Ippolito, H. O. Tucker, and J. D. Macklis (2016). "Ctip1 regulates the balance between specification of distinct projection neuron subtypes in deep cortical layers." Cell Rep **15**(5): 999–1012.

Wu, L. Q. and J. D. Dickman (2011). "Magnetoreception in an avian brain in part mediated by inner ear lagena." Curr Biol **21**(5): 418–423.

Yamasaki, K., T. Akiba, T. Yamasaki, and K. Harata (2007). "Structural basis for recognition of the matrix attachment region of DNA by transcription factor SATB1." Nucleic Acids Res **35**(15): 5073–5084.

Yamawaki, N., K. Borges, B. A. Suter, K. D. Harris, and G. M. Shepherd (2014). "A genuine layer 4 in motor cortex with prototypical synaptic circuit connectivity." Elife **3**: e05422.

Yasui, D., M. Miyano, S. Cai, P. Varga-Weisz, and T. Kohwi-Shigematsu (2002). "SATB1 targets chromatin remodelling to regulate genes over long distances." Nature **419**(6907): 641–645.

Zeier, H. and H. J. Karten (1971). "The archistriatum of the pigeon: organization of afferent and efferent connections." Brain Res **31**(2): 313–326.

Zhang, G., C. Li, Q. Li, B. Li, D. M. Larkin, C. Lee, J. F. Storz, A. Antunes, M. J. Greenwold, R. W. Meredith, A. Odeen, J. Cui, Q. Zhou, L. Xu, H. Pan, Z. Wang, L. Jin, P. Zhang, H. Hu, W. Yang, J. Hu, J. Xiao, Z. Yang, Y. Liu, Q. Xie, H. Yu, J. Lian, P. Wen, F. Zhang, H. Li, Y. Zeng, Z. Xiong, S. Liu, L. Zhou, Z. Huang, N. An, J. Wang, Q. Zheng, Y. Xiong, G. Wang, B. Wang, J. Wang, Y. Fan, R. R. da Fonseca, A. Alfaro-Nunez, M. Schubert, L. Orlando, T. Mourier, J. T. Howard, G. Ganapathy, A. Pfenning, O. Whitney, M. V. Rivas, E. Hara, J. Smith, M. Farre, J. Narayan, G. Slavov, M. N. Romanov, R. Borges, J. P. Machado, I. Khan, M. S. Springer, J. Gatesy, F. G. Hoffmann, J. C. Opazo, O. Hastad, R. H. Sawyer, H. Kim, K. W. Kim, H. J. Kim, S. Cho, N. Li, Y. Huang, M. W. Bruford, X. Zhan, A. Dixon, M. F. Bertelsen, E. Derryberry, W. Warren, R. K. Wilson, S. Li, D. A. Ray, R. E. Green, S. J. O'Brien, D. Griffin, W. E. Johnson, D. Haussler, O. A. Ryder, E. Willerslev, G. R. Graves, P. Alstrom, J. Fjeldsa, D. P. Mindell, S. V. Edwards, E. L. Braun, C. Rahbek, D. W. Burt, P. Houde, Y. Zhang, H. Yang, J. Wang, C. Avian Genome, E. D. Jarvis, M. T. Gilbert and J. Wang (2014). "Comparative genomics reveals insights into avian genome evolution and adaptation." Science **346**(6215): 1311–1320.

Zhou, C., S. Y. Tsai, and M. J. Tsai (2001). "COUP-TFI: an intrinsic factor for early regionalization of the neocortex." Genes Dev **15**(16): 2054–2059.

Ziegenhain, C., B. Vieth, S. Parekh, B. Reinius, A. Guillaumet-Adkins, M. Smets, H. Leonhardt, H. Heyn, I. Hellmann, and W. Enard (2017). "Comparative analysis of single-cell RNA sequencing methods." Mol Cell **65**(4): 631–643 e634.